BUILDING BRIDGES



molecular regulation of endothelial junctions for the vascular barrier

Rianne Schoon

Building bridges:

molecular regulation of endothelial junctions for the vascular barrier

Rianne Mirjam Schoon

BUILDING BRIDGES
Molecular regulation of endothelial junctions for the vascular barrier

Doctoral thesis, University of Amsterdam, Amsterdam, The Netherlands

Author: Rianne M. Schoon
Cover: Rianne M. Schoon
Layout and design: Rianne M. Schoon
Printing: ProefschriftMaken

ISBN: 978-94-6534-453-9

Copyright © Rianne M. Schoon, 2026, The Netherlands.
All rights reserved. No parts of this thesis may be reproduced, distributed, stored in a retrieval system, or transmitted, in any form or by any means without the prior written permission of the author, or when appropriate, of the publishers.

Building bridges: molecular regulation of endothelial junctions for the vascular barrier

ACADEMISCH PROEFSCHRIFT

ter verkrijging van de graad van doctor
aan de Universiteit van Amsterdam
op gezag van de Rector Magnificus
prof. dr. ir. P.P.C.C. Verbeek
ten overstaan van een door het College voor Promoties ingestelde commissie,
in het openbaar te verdedigen in de Agnietenkapel
op woensdag 1 juli 2026, te 10.00 uur

door Rianne Mirjam Schoon
geboren te Alkmaar

Promotiecommissie

Promotor:	dr. S. Huveneers	AMC-UvA
Copromotor:	prof. dr. J.D. van Buul	AMC-UvA
Overige leden:	prof. dr. C.J.M. de Vries	AMC-UvA
	prof. dr. E.T. van Bavel	AMC-UvA
	dr. J. Kroon	AMC-UvA
	prof. dr. P.H.A. Quax	Universiteit Leiden
	dr. ing. C.E. van den Brom	Vrije Universiteit Amsterdam

Faculteit der Geneeskunde

Contents

Chapter 1 8
General introduction and scope of the thesis

Chapter 2 22
VE-cadherin interaction proteomics identifies ARVCF as stabilizer of endothelial adherens junctions (*iScience, 2026*)

Chapter 3 60
Characterization of the role of identified VE-cadherin interactors

Chapter 4 84
VE-cadherin RGD motifs are dispensable for cell-cell junctions, endothelial barrier function and monocyte extravasation (*Tissue Barriers, 2025*)

Chapter 5 100
Vinculin strengthens the endothelial barrier during vascular development (*Vascular Biology, 2023*)

Chapter 6 112
Breaking barriers in inflammation: Mechano-transduction at the leukocyte-endothelial interface

Chapter 7 140
General discussion

Appendices 150
English summary
Nederlandse lekenintroductie en inhoud
Nederlandse samenvatting
List of publications
PhD portfolio
Curriculum vitae
Closing credits



Chapter 1

General introduction and scope of the thesis

General introduction

The vasculature reaches everywhere

The vasculature is an important transport system for blood that reaches the outer ends of every limb and organ in vertebrate animals. It is organized as a well-connected network of blood vessels: large arteries bring blood rich in oxygen and nutrients to the organs, where smaller capillary vessels deliver the cargo to tissues at the cellular level. In turn, waste products from tissues and oxygen-poor blood are carried into veins that return the blood to the heart, completing the systemic circulation. Continuous blood flow through the vasculature ensures that all tissues receive what they need and that waste is efficiently removed. Beyond its transport function, the vasculature plays critical roles in tissue homeostasis, immune surveillance, and organ development.

Vessels are lined by endothelium

The inside of every vessel in the vasculature is lined with endothelium: a thin, single layer of endothelial cells that is in direct contact with blood and which separates blood from the surrounding tissue. This cellular lining is called the endothelial monolayer and is a remarkable multifunctional and dynamic tissue. The endothelium not only acts as a physical barrier, but it also actively controls what enters and exits the bloodstream. As gatekeepers, the endothelial cells manage the migration of immune cells, and the exchange of molecules like oxygen or solutes like glucose between blood and tissue [1]. Both the barrier and permeability functions are dependent on the connections between the individual endothelial cells. The cell-cell contacts are a fascinating place where form and function must be stably yet flexibly coordinated for vascular integrity [2,3]. When these cell-cell contacts don't function properly, resulting problems could include edema (swelling when fluids from the blood stream enter and stay in other tissue, often in legs and feet), or chronic inflammation (when the body keeps sending immune cells to fight an infection that isn't there, which leads to pain and fatigue) [4,5].

VE-cadherin forming a cell-cell bridge

The structural connections between endothelial cells are formed by a class of calcium-dependent adhesion molecules called cadherins . Endothelial cells express different types of cadherins, vascular endothelial cadherin (VE-cadherin) being, as the name suggests, their most characteristic and specific one [6]. VE-cadherin is a transmembrane protein that sticks out of endothelial cells. Two VE-cadherin molecules on neighboring cells couple their heads in the intercellular space, while their intracellular tails can both link to the cytoskeleton and partake in cytosolic signal transduction. In simpler terms, VE-cadherin forms the molecular bridge between endothelial cells, which communicates signals into the cell interior. Through these properties VE-cadherin enables endothelial cells to sense and respond to the vascular environment.

VE-cadherin as a central signaling intersection

VE-cadherin plays a key role in a wide range of endothelial functions. It maintains barrier integrity across different types of blood vessels, where local mechanical environments can vary greatly (imagine cells in the aorta wall experiencing more blood pressure than in a distal vein in your foot) [7-10]. VE-cadherin-based cell-cell connections are called adherens junctions (often shortened to AJ) and need to adapt when the vessel wall encounters inflammatory signals, so that immune cells recruited from the blood stream can pass through the endothelium into the affected inflamed tissue [11,12]. VE-cadherin is also crucial in supporting new blood vessel growth during development and wound healing [13,14]. In these remodeling settings, VE-cadherin must be tightly regulated, turning adhesion on to strengthen cell-cell contacts in newly formed vessels, or turning it off to loosen contacts when cells migrate. The on/off switching is controlled by recruiting specific molecular interactors to VE-cadherin when needed [14]. In recent years, the proteins regulating VE-cadherin itself, as well as the proteins recruited to the cell-cell contact interface have been extensively studied. Scientific methods for biochemical analysis and imaging techniques advance towards ever better spatiotemporal resolution. Yet, despite increasing insight into the molecular components of adherens junctions, the full biochemical landscape of VE-cadherin-associated complexes remains incompletely defined. Specifically, how VE-cadherin connections are dynamically regulated in response to mechanical forces, developmental cues, or immune signals, remains an active area of investigation.

Molecular architecture and regulation of VE-cadherin-based adherens junctions

Understanding how VE-cadherin combines mechanical coupling and signal transduction requires examining the molecular organization and regulation of the AJ complex. The following section outlines the current framework and discusses structural architecture, post-translational regulation, and signaling pathways that make VE-cadherin the key molecule in controlling vascular integrity.

Structural organization of VE-cadherin complexes

Structurally, VE-cadherin is a 784 amino acid protein with 5 extracellular cadherin domains, a transmembrane region, and an intracellular tail containing conserved binding motifs for catenin family proteins [15]. It does not possess intrinsic enzymatic or catalytic domains, but is itself subject to posttranslational modifications: tyrosine- or serine phosphorylation, glycosylation, ubiquitination, and proteolytic cleavage [16-18]. The VE-cadherin protein folds into a crescent-shaped conformation stabilized by calcium ions, and the homophilic adhesion that occurs at the apical-lateral interface between neighboring cells is also calcium-dependent: a conserved tryptophan residue in the EC1 domain of one cadherin inserts into a hydrophobic pocket of its partner on the opposing membrane [19-21]. These trans-interactions are further stabilized by lateral cis-clustering of cadherins on the same membrane [22], resulting in adhesive assemblies that increase avidity and provide the basis for AJ architecture.

The canonical cadherin-catenin complex

Besides these cadherin couplings outside the cell, the AJ structure is intracellularly anchored to the actin cytoskeleton to increase adhesion stability [23]. The canonical AJ complex associated with VE-cadherin's cytoplasmic regions consists of three main proteins. p120- and β-catenin bind directly to VE-cadherin and function, respectively, to ensure VE-cadherin membrane localization and to connect to α-catenin, which in turn links the AJ structure to the cytoskeleton [24-27]. Junctional maturation involves force-dependent conformational changes of α-catenin and its dimerization, allowing cytoskeletal linkage and actin bundling [28]. Mechanical tension, generated either internally or by the pushing and pulling of neighboring cells, reinforces this coupling and promotes recruitment of additional stabilizing proteins to the core complex [24]. Thus, endothelial AJs are both strong adhesions and mechanosensitive assemblies that adapt to local forces.

Beyond the canonical complex: signaling and cytoskeletal coupling

Beyond this canonical cadherin-catenin complex are a plethora of other proteins and structures associated with the AJ. For instance, VE-cadherin participates in larger transmembrane signaling assemblies. It forms complexes with VEGFR2 and VEGFR3 through intramembrane associations: upon VEGF stimulation, its receptor (VEGFR2) transiently associates with VE-cadherin at junctions [29]. Phosphorylation of VEGFR2 at Y951 enables recruitment of the adaptor TSAd, which binds c-Src and facilitates localized actin reorganization and junction remodeling [30]. VE-cadherin thus acts not merely as a passive adhesion molecule but as a scaffold that spatially organizes growth factor signaling at cell-cell contacts. For these functions, VE-cadherin membrane retention is vital, for which an additional membrane retention mechanism independent of p120-catenin is employed via AnkyrinG that binds to a membrane-proximal region of VE-cadherin and selectively inhibits internalization of cis-dimerized VE-cadherin [31,32]. Another example of VE-cadherin-interaction diversity is that VE-cadherin is not only linked to F-actin, but also interacts with other cytoskeletal factors such as spectrin and cortical actin [33-35]. Additionally, VE-cadherin-catenin complexes including α-catenin, PECAM1, and vinculin are physically coupled to cortical actomyosin, so force on the junction changes their conformation and binding properties [36,37]. Altogether, the take-away message is that all these interactions contribute to junctional organization and secure anchoring of cell adhesions. These signaling assemblies integrate with actomyosin-generated junctional tension, thereby linking receptor activation to mechanical remodeling of adherens junctions.

Phosphorylation-dependent VE-cadherin regulation

Phosphorylation of specific residues within the VE-cadherin cytoplasmic tail is a central regulatory mechanism to dynamically adapt junction stability [38]. Three tyrosine (Y) residues (658, 685, and 731) and one serine residue (S665) function as regulatory switches for VE-cadherin membrane retention,

endocytosis, and AJ-cytoskeletal coupling [39,40]. These modifications are primarily mediated by Src family kinases, including Yes, and occur in a context-dependent manner [41,42]. Under basal flow conditions *in vivo*, venous endothelium exhibits constitutive phosphorylation of Y658 and Y685, as flow activates Src, whereas these residues remain largely unphosphorylated in arteries [43]. Consequently, arterial junctions are comparatively stable at rest, while venous junctions exist in a more dynamic and permissive state, particularly in the postcapillary venules where immune cell extravasation occurs [44-46].

Mechanistically, Y658 lies within VE-cadherin's p120-binding region; its phosphorylation recruits LGN to bind and displace p120-catenin [47,48], reducing VE-cadherin membrane retention and promoting clathrin-mediated internalization and junctional turnover [49]. Y685 phosphorylation is also regulated by flow but as a direct target of Src kinase downstream of inflammation and VEGF signaling [40] that induce VE-cadherin ubiquitination and internalization [17,43]. In contrast to these sites that primarily regulate general vascular permeability, Y731 responds to inflammatory signaling and leukocyte extravasation through the AJs [38,50]. Leukocyte-generated tension induces both actomyosin remodeling of the VE-cadherin-catenin complex and activation of phosphatase SHP2 to bind directly to VE-cadherin and enables Y731 dephosphorylation [51]. In addition to tyrosine phosphorylation, VEGF-induced Src signaling promotes serine phosphorylation of VE-cadherin at S665 via Rac1 and PAK activation, leading to β-arrestin recruitment further enhancing clathrin turnover [40,52,53]. Hence, serine and tyrosine phosphorylation provide parallel pathways for junction remodeling. Lastly, phosphorylation of other AJ complex members than VE-cadherin, such as β-catenin, similarly modulates their affinity for VE-cadherin and affects AJ stability [39]. These kinase-driven events are counterbalanced by phosphatases such as VE-PTP, DEP1, PTPμ, and SHP2, which can all directly associate with VE-cadherin except SHP2 that binds β-catenin, to influence junctional stability [54-59]. Together, this reversible phosphorylation network tunes endothelial barriers to be regionally specialized and rapidly adaptable in response to mechanical and inflammatory demands.

Cytoskeletal regulation and Rho GTPases and actomyosin contractility

While phosphorylation effectively regulates VE-cadherin complex composition and turnover, junction stability is equally determined by the cytoskeletal forces acting on these complexes [23,60,61]. AJs are surrounded by regulatory networks of small GTPases that connect junctional to cytoskeletal dynamics [62,63]. The Rac1-specific guanine nucleotide exchange factor (GEF) Trio associates selectively with VE-cadherin, particularly at nascent or remodeling junctions [64]. Trio-mediated Rac1 activation promotes actin reorganization necessary for adherens junction reassembly without displacing β-catenin [65,66]. Other GEFs than TRIO, such as Tiam1, Syx and TEM4, have been shown to localize at endothelial cell-cell junctions or to co-immunoprecipitate with VE-cadherin or one of the

complex members and influence the barrier via Rho and actomyosin contractility [67-70]. Rap1 signaling enhances VE-cadherin adhesive strength and barrier integrity [71,72]. VE-cadherin recruits MAGI1 and PDZ-GEF1, linking junctional complexes to Rap1 activation [73]. Conversely, RhoA-ROCK-mediated contractility can increase junctional tension and, depending on context, reinforce or disrupt barrier function [74]. Together, the partially overlapping yet diverse functions of small GTPase pathways enable spatiotemporal coordination between signaling, cytoskeletal tension, and adhesion [75].

Mechanotransduction and force-dependent reinforcement

To adapt junction adhesion strength, these mechanical forces generated by GTPase signaling are sensed and processed by the VE-cadherin complex itself: tension across VE-cadherin induces conformational changes in α-catenin, exposing a binding site for vinculin [76,77]. Vinculin recruitment strengthens linkage to F-actin and enhances junctional resilience [13,78]. Mechanical stimuli such as shear stress or pressure can further modulate junction stability through pathways involving Piezo1 and calpain-mediated cleavage of junctional components [79-82]. Thus, endothelial junctions integrate biochemical and mechanical cues to maintain vascular integrity across diverse hemodynamic environments.

Junction remodeling in homeostasis and inflammation

Maintaining barrier integrity requires continuous spatially controlled turnover of VE-cadherin: even in homeostasis, clathrin-mediated endocytosis, regulated by phosphorylation and adaptor proteins, manages junctional plasticity [83]. Ankyrin-G inhibits VE-cadherin endocytosis when AJ complexes are dimerized, independently of p120-catenin binding [31,32], whereas proteins such as PACSIN2, MICAL-L1, and EHD4 regulate local trafficking and recycling [14,84]. Ubiquitin ligases of the MARCH family further modulate VE-cadherin surface levels and junction organization, through crosstalk with VEGF signaling [15,85]. Extracellular cleavage by proteases released during inflammation or tumor invasion represents an additional mechanism of barrier disruption through proteases that cleave the VE-cadherin ectodomain or by removing the β-catenin-binding region [18]. Following local disengagement during leukocyte transmigration, rapid reassembly of VE-cadherin complexes restores barrier integrity, highlighting the reversibility of junctional opening [12]. Together, these mechanisms regulating VE-cadherin turnover prevent overstabilization of the junction, enabling rapid responses to flow, inflammation, and leukocyte transmigration events.

Knowledge gap: the incomplete VE-cadherin interactome

Collectively, these findings depict VE-cadherin-based adherens junctions as modular, heterogeneous signaling platforms rather than uniform adhesive structures. Distinct molecular assemblies that are defined by specific binding partners, phosphorylation states, and mechanical context confer functional specialization to different junctional microdomains. Despite substantial progress in identifying individual interactors, the full biochemical landscape of VE-cadherin complexes and their context-dependent organization remains incompletely understood. This gap provided the rationale for the work presented in this thesis, which aims to further define and functionally characterize novel VE-cadherin-binding proteins and to uncover new principles governing endothelial junction stability.

Scope of the thesis

The incomplete understanding of which proteins regulate VE-cadherin motivated the research presented in this thesis. In this PhD project, we set out to identify and characterize which proteins bind to VE-cadherin and how these interactions contribute to vascular function. We hypothesized that VE-cadherin engages in defined protein associations and that partners may change depending on the biological context. Using a combination of biochemical experiments, mechanobiological approaches, and high spatiotemporal resolution imaging, we identified new VE-cadherin-binding partners: ARVCF, KEAP1, ARHGAP23, and NGLY1. Several of these targets were further studied for their influence on VE-cadherin and the AJ. In addition, we investigated the role of VE-cadherin extracellular adhesion to immune cells, and the function of a protein that stabilizes VE-cadherin during blood vessel formation in development. Together, this thesis presents new insights that help explain how endothelial junctions are regulated during processes such as collective cell migration, leukocyte transmigration, and mechanotransduction.

In **Chapter 1** a general overview of blood vessels was provided. VE-cadherin is introduced as a central molecular bridge that mediates cell-to-cell adhesion for endothelial and vascular integrity. The molecular organization of the AJ complex and its regulatory mechanisms are then discussed in the context of vascular integrity. Together, this chapter provides a foundation for understanding how VE-cadherin acts as a signaling platform at endothelial junctions and sets the stage for the novel interactors studied in the following experimental chapters.

Chapter 2 presents the experimental discovery and characterization of novel VE-cadherin-binding proteins. We used proteomics to uncover a core VE-cadherin interactome that includes several known junctional components and we present four novel interactors of VE-cadherin: ARVCF, KEAP1, ARHGAP23, and NGLY1. One of these proteins, ARVCF, is studied in further detail in this chapter: we unravel the molecular mechanism by which ARVCF associates with a distinct pool of VE-cadherin proteins and demonstrate its functional relevance for junction maturation, endothelial barrier stability, and collective cell migration. These findings expand our understanding of the VE-cadherin complex and introduce a new layer of regulation at the junctions.

Chapter 3 continues the analysis of the newly discovered VE-cadherin-binding proteins identified in chapter 2. We dive deeper into VE-cadherin regulation by exploring the roles of ARHGAP23, PKP4, and KEAP1 in endothelial cell connections. Although these proteins were less amenable to in-depth mechanistic studies, the performed experiments revealed that these proteins do contribute to the stability and organization of VE-cadherin-based cell-cell contacts. Together with the previous chapter, these findings provide complementary insights into the network of proteins, and their function, associated with the VE-cadherin complex.

Chapter 4 shifts the focus from intracellular regulators of VE-cadherin to its extracellular domain. Sticking outside of the endothelial cell membrane, this part of the protein contains two so-called RGD motifs, which are well-known integrin-binding sequences mediating adhesion, but their importance had never been studied on VE-cadherin. In our experiments we made non-functional variants and investigated their effects on junction formation, barrier integrity, and leukocyte passage. We found that the RGD motifs are not needed for any of these key endothelial cell functions, effectively resolving an open question and helping to refine future research to focus on the most functionally relevant regions of VE-cadherin.

Chapter 5 continues on the role of force sensitive proteins in maintaining vascular integrity. In this chapter, we investigate how vinculin, a protein that does not directly bind VE-cadherin but is recruited to junctions under mechanical tension, contributes to endothelial function during blood vessel development. By using both cell culture and a zebrafish model, we show that vinculin supports stable endothelial cell-cell contacts and helps prevent vascular leakage in newly forming vessels. These findings highlight the importance of mechanical reinforcement at adherens junctions and add a developmental perspective to the regulation of endothelial barrier function.

Chapter 6 reviews a broader perspective on the theme of mechanical regulation at endothelial adherens junctions, exploring how endothelial cells respond to mechanical cues during inflammation, particularly in the context of immune cell interactions. Quantitative research is presented on how T-cells, an important immune cell type, engage with and influence endothelial membranes and junctional structures during their journey from circulation, through the junctions, into the tissue, and how mechanotransduction pathways and proteins shape this process. By examining current concepts and molecular players, this chapter offers an integrated view of the dynamic mechanical crosstalk between immune cells and the vascular wall.

Chapter 7 summarizes our findings in this thesis and places them in the broader context of the vascular biology and disease field. Moreover, read this chapter to discover the new questions and hypotheses that our experimental work has given rise to! Altogether, this thesis has brought insight, although there are still plenty innovative ideas and concepts to be explored, experimented, and discussed.

References

1. Cahill, P.A., and Redmond, E.M. (2016). Vascular endothelium - Gatekeeper of vessel health. Atherosclerosis *248*, 97–109. 10.1016/j.atherosclerosis.2016.03.007.
2. Schimmel, L., and Gordon, E. (2018). The precise molecular signals that control endothelial cell-cell adhesion within the vessel wall. Biochem Soc Trans *46*, 1673–1680. 10.1042/BST20180377.
3. Dejana, E., and Giampietro, C. (2012). Vascular endothelial-cadherin and vascular stability. Curr Opin Hematol *19*, 218–223. 10.1097/MOH.0b013e3283523e1c.
4. Schulte, D., Kuppers, V., Dartsch, N., Broermann, A., Li, H., Zarbock, A., Kamenyeva, O., Kiefer, F., Khandoga, A., Massberg, S., and Vestweber, D. (2011). Stabilizing the VE-cadherin-catenin complex blocks leukocyte extravasation and vascular permeability. EMBO J *30*, 4157–4170. 10.1038/emboj.2011.304.
5. Dejana, E., Tournier-Lasserve, E., and Weinstein, B.M. (2009). The control of vascular integrity by endothelial cell junctions: molecular basis and pathological implications. Dev Cell *16*, 209–221. 10.1016/j.devcel.2009.01.004.
6. Colas-Algora, N., and Millan, J. (2019). How many cadherins do human endothelial cells express? Cell Mol Life Sci *76*, 1299–1317. 10.1007/s00018-018-2991-9.
7. Zhou, M., Yu, Y., Chen, R., Liu, X., Hu, Y., Ma, Z., Gao, L., Jian, W., and Wang, L. (2023). Wall shear stress and its role in atherosclerosis. Front Cardiovasc Med *10*, 1083547. 10.3389/fcvm.2023.1083547.
8. Koutsiaris, A.G., Tachmitzi, S.V., Batis, N., Kotoula, M.G., Karabatsas, C.H., Tsironi, E., and Chatzoulis, D.Z. (2007). Volume flow and wall shear stress quantification in the human conjunctival capillaries and post-capillary venules in vivo. Biorheology *44*, 375–386.
9. Mo, F.E. (2021). Shear-Regulated Extracellular Microenvironments and Endothelial Cell Surface Integrin Receptors Intertwine in Atherosclerosis. Front Cell Dev Biol *9*, 640781. 10.3389/fcell.2021.640781.
10. Shirakura, K., Baluk, P., Nottebaum, A.F., Ipe, U., Peters, K.G., McDonald, D.M., and Vestweber, D. (2023). Shear stress control of vascular leaks and atheromas through Tie2 activation by VE-PTP sequestration. EMBO Mol Med *15*, e16128. 10.15252/emmm.202216128.
11. Grönloh, M.L.B., Arts, J.J.G., and van Buul, J.D. (2021). Neutrophil transendothelial migration hotspots - mechanisms and implications. J Cell Sci *134*. 10.1242/jcs.255653.
12. van der Meer, W.J., van Steen, A.C.I., Mahlandt, E., Rolas, L., Wang, H., Arts, J.J.G., Kempers, L., Grönloh, M.L.B., Schoon, R.M., Driessen, A., et al. (2025). Leukocytes use endothelial membrane tunnels to extravasate the vasculature. Cell Rep *44*, 116242. 10.1016/j.celrep.2025.116242.
13. van der Stoel, M.M., Kotini, M.P., Schoon, R.M., Affolter, M., Belting, H.G., and Huveneers, S. (2023). Vinculin strengthens the endothelial barrier during vascular development. Vasc Biol *5*. 10.1530/VB-22-0012.
14. Malinova, T.S., Angulo-Urarte, A., Nuchel, J., Tauber, M., van der Stoel, M.M., Janssen, V., de Haan, A., Groenen, A.G., Tebbens, M., Graupera, M., et al. (2021). A junctional PACSIN2/EHD4/MICAL-L1 complex coordinates VE-cadherin trafficking for endothelial migration and angiogenesis. Nat Commun *12*, 2610. 10.1038/s41467-021-22873-y.
15. Seo, T., Lowery, A.M., Xu, H., Giang, W., Troyanovsky, S.M., Vincent, P.A., and Kowalczyk, A.P. (2024). MARCH family E3 ubiquitin ligases selectively target and degrade cadherin family proteins. PLoS One *19*, e0290485. 10.1371/journal.pone.0290485.
16. Zhang, L., Ma, L., Li, J., Lei, J., Chen, J., and Yu, C. (2021). VE-cadherin N-glycosylation modified by N-acetylglucosaminyltransferase V regulates VE-cadherin-beta-catenin interaction and monocyte adhesion. Exp Physiol *106*, 1869–1877. 10.1113/EP089617.
17. Wilkens, M., Holtermann, L., Stahl, A.K., Stegmeyer, R.I., Nottebaum, A.F., and Vestweber, D. (2024). Ubiquitination of VE-cadherin regulates inflammation-induced vascular permeability in vivo. EMBO Rep *25*, 4013–4032. 10.1038/s44319-024-00221-7.
18. Su, W., and Kowalczyk, A.P. (2017). The VE-cadherin cytoplasmic domain undergoes proteolytic processing during endocytosis. Mol Biol Cell *28*, 76–84. 10.1091/mbc.E16-09-0658.
19. Legrand, P., Bibert, S., Jaquinod, M., Ebel, C., Hewat, E., Vincent, F., Vanbelle, C., Concord, E., Vernet, T., and Gulino, D. (2001). Self-assembly of the vascular endothelial cadherin ectodomain in a Ca2+-dependent hexameric structure. J Biol Chem *276*, 3581–3588. 10.1074/jbc.M002667200.
20. <Boggon, ... Gumbiner, Shapiro (2002) C-cadherin ectodomain structure and implications for cell adhesion mechanisms.pdf>.
21. Boggon, T.J., Murray, J., Chappuis-Flament, S., Wong, E., Gumbiner, B.M., and Shapiro, L. (2002). C-cadherin ectodomain structure and implications for cell adhesion mechanisms. Science *296*, 1308–1313. 10.1126/science.1071559.
22. Brasch, J., Harrison, O.J., Ahlsen, G., Carnally, S.M., Henderson, R.M., Honig, B., and Shapiro, L. (2011). Structure and binding mechanism of vascular endothelial cadherin: a divergent classical cadherin. J Mol Biol *408*, 57–73. 10.1016/j.jmb.2011.01.031.
23. Hartsock, A., and Nelson, W.J. (2008). Adherens and tight junctions: structure, function and connections to the actin cytoskeleton. Biochim Biophys Acta *1778*, 660–669. 10.1016/j.bbamem.2007.07.012.
24. Angulo-Urarte, A., van der Wal, T., and Huveneers, S. (2020). Cell-cell junctions as sensors and transducers of mechanical forces. Biochim Biophys Acta Biomembr *1862*, 183316. 10.1016/j.bbamem.2020.183316.
25. Garrett, J.P., Lowery, A.M., Adam, A.P., Kowalczyk, A.P., and Vincent, P.A. (2017). Regulation of endothelial barrier function by p120-catenin·VE-cadherin interaction. Mol Biol Cell *28*, 85–97. 10.1091/mbc.E16-08-0616.

26. Fang, X., Ji, H., Kim, S.W., Park, J.I., Vaught, T.G., Anastasiadis, P.Z., Ciesiolka, M., and McCrea, P.D. (2004). Vertebrate development requires ARVCF and p120 catenins and their interplay with RhoA and Rac. J Cell Biol *165*, 87–98. 10.1083/jcb.200307109.
27. Kim, Y.M., Krantz, S., Jambusaria, A., Toth, P.T., Moon, H.G., Gunarathna, I., Park, G.Y., and Rehman, J. (2021). Mitofusin-2 stabilizes adherens junctions and suppresses endothelial inflammation via modulation of beta-catenin signaling. Nat Commun *12*, 2736. 10.1038/s41467-021-23047-6.
28. Windgasse, L., and Grashoff, C. (2025). A conformational change in α-catenin's actin-binding domain governs adherens junction maturation. Commun Biol *8*, 1325. 10.1038/s42003-025-08785-3.
29. Coon, B.G., Baeyens, N., Han, J., Budatha, M., Ross, T.D., Fang, J.S., Yun, S., Thomas, J.L., and Schwartz, M.A. (2015). Intramembrane binding of VE-cadherin to VEGFR2 and VEGFR3 assembles the endothelial mechanosensory complex. J Cell Biol *208*, 975–986. 10.1083/jcb.201408103.
30. Sun, Z., Li, X., Massena, S., Kutschera, S., Padhan, N., Gualandi, L., Sundvold-Gjerstad, V., Gustafsson, K., Choy, W.W., Zang, G., et al. (2012). VEGFR2 induces c-Src signaling and vascular permeability in vivo via the adaptor protein TSAd. J Exp Med *209*, 1363–1377. 10.1084/jem.20111343.
31. Cadwell, C.M., Jenkins, P.M., Bennett, V., and Kowalczyk, A.P. (2016). Ankyrin-G Inhibits Endocytosis of Cadherin Dimers. J Biol Chem *291*, 691–704. 10.1074/jbc.M115.648386.
32. Jenkins, P.M., Vasavda, C., Hostettler, J., Davis, J.Q., Abdi, K., and Bennett, V. (2013). E-cadherin polarity is determined by a multifunction motif mediating lateral membrane retention through ankyrin-G and apical-lateral transcytosis through clathrin. J Biol Chem *288*, 14018–14031. 10.1074/jbc.M113.454439.
33. Nelson, C.M., Pirone, D.M., Tan, J.L., and Chen, C.S. (2004). Vascular endothelial-cadherin regulates cytoskeletal tension, cell spreading, and focal adhesions by stimulating RhoA. Mol Biol Cell *15*, 2943–2953. 10.1091/mbc.e03-10-0745.
34. Hiepen, C., Mendez, P.L., and Knaus, P. (2020). It Takes Two to Tango: Endothelial TGFβ/BMP Signaling Crosstalk with Mechanobiology. Cells *9*. 10.3390/cells9091965.
35. Machnicka, B., Grochowalska, R., Bogusławska, D.M., and Sikorski, A.F. (2019). The role of spectrin in cell adhesion and cell-cell contact. Exp Biol Med (Maywood) *244*, 1303–1312. 10.1177/1535370219859003.
36. Favarin, A., Said, R., Wang, H., Zeine, E., Pierrard, A., Pernier, J., Narassimprakash, H., Roméro, S., Gautreau, A.M., Mège, R.M., and Le Clainche, C. (2026). Actomyosin-dependent assembly of the mechanosensitive machinery from adherens junctions triggers actin polymerization and organization. Sci Adv *12*, eady4863. 10.1126/sciadv.ady4863.
37. Dorland, Y.L., and Huveneers, S. (2017). Cell-cell junctional mechanotransduction in endothelial remodeling. Cell Mol Life Sci *74*, 279–292. 10.1007/s00018-016-2325-8.
38. Holtermann, L., Rivera-Galdos, R., Nottebaum, A.F., Wessel, F., Ipe, U., and Vestweber, D. (2025). Distinct VE-cadherin serine and tyrosine phosphorylation sites and their role for inflammation-induced vascular permeability in vivo. Cell Mol Life Sci *82*, 223. 10.1007/s00018-025-05753-2.
39. Potter, M.D., Barbero, S., and Cheresh, D.A. (2005). Tyrosine phosphorylation of VE-cadherin prevents binding of p120- and beta-catenin and maintains the cellular mesenchymal state. J Biol Chem *280*, 31906–31912. 10.1074/jbc.M505568200.
40. Wallez, Y., Cand, F., Cruzalegui, F., Wernstedt, C., Souchelnytskyi, S., Vilgrain, I., and Huber, P. (2007). Src kinase phosphorylates vascular endothelial-cadherin in response to vascular endothelial growth factor: identification of tyrosine 685 as the unique target site. Oncogene *26*, 1067–1077. 10.1038/sj.onc.1209855.
41. Jin, Y., Ding, Y., Richards, M., Kaakinen, M., Giese, W., Baumann, E., Szymborska, A., Rosa, A., Nordling, S., Schimmel, L., et al. (2022). Tyrosine-protein kinase Yes controls endothelial junctional plasticity and barrier integrity by regulating VE-cadherin phosphorylation and endocytosis. Nat Cardiovasc Res *1*, 1156–1173. 10.1038/s44161-022-00172-z.
42. Zanetti, A., Lampugnani, M.G., Balconi, G., Breviario, F., Corada, M., Lanfrancone, L., and Dejana, E. (2002). Vascular endothelial growth factor induces SHC association with vascular endothelial cadherin: a potential feedback mechanism to control vascular endothelial growth factor receptor-2 signaling. Arterioscler Thromb Vasc Biol *22*, 617–622. 10.1161/01.atv.0000012268.84961.ad.
43. Orsenigo, F., Giampietro, C., Ferrari, A., Corada, M., Galaup, A., Sigismund, S., Ristagno, G., Maddaluno, L., Koh, G.Y., Franco, D., et al. (2012). Phosphorylation of VE-cadherin is modulated by haemodynamic forces and contributes to the regulation of vascular permeability in vivo. Nat Commun *3*, 1208. 10.1038/ncomms2199.
44. Benson, B.L., Li, L., Myers, J.T., Dorand, R.D., Gurkan, U.A., Huang, A.Y., and Ransohoff, R.M. (2018). Biomimetic post-capillary venule expansions for leukocyte adhesion studies. Sci Rep *8*, 9328. 10.1038/s41598-018-27566-z.
45. Blanchard, L., and Girard, J.P. (2021). High endothelial venules (HEVs) in immunity, inflammation and cancer. Angiogenesis *24*, 719–753. 10.1007/s10456-021-09792-8.
46. Sawada, J., Perrot, C.Y., Chen, L., Fournier-Goss, A.E., Oyer, J., Copik, A., and Komatsu, M. (2021). High Endothelial Venules Accelerate Naive T Cell Recruitment by Tumor Necrosis Factor-Mediated R-Ras Upregulation. Am J Pathol *191*, 396–414. 10.1016/j.ajpath.2020.10.009.
47. Conway, D.E., Coon, B.G., Budatha, M., Arsenovic, P.T., Orsenigo, F., Wessel, F., Zhang, J., Zhuang, Z., Dejana, E., Vestweber, D., and Schwartz, M.A. (2017). VE-Cadherin Phosphorylation Regulates Endothelial Fluid Shear Stress Responses through the Polarity Protein LGN. Curr Biol *27*, 2219–2225.e2215. 10.1016/j.cub.2017.06.020.

48. Hatanaka, K., Simons, M., and Murakami, M. (2011). Phosphorylation of VE-cadherin controls endothelial phenotypes via p120-catenin coupling and Rac1 activation. Am J Physiol Heart Circ Physiol *300*, H162–172. 10.1152/ajpheart.00650.2010.
49. Nanes, B.A., Chiasson-MacKenzie, C., Lowery, A.M., Ishiyama, N., Faundez, V., Ikura, M., Vincent, P.A., and Kowalczyk, A.P. (2012). p120-catenin binding masks an endocytic signal conserved in classical cadherins. J Cell Biol *199*, 365–380. 10.1083/jcb.201205029.
50. Wessel, F., Winderlich, M., Holm, M., Frye, M., Rivera-Galdos, R., Vockel, M., Linnepe, R., Ipe, U., Stadtmann, A., Zarbock, A., et al. (2014). Leukocyte extravasation and vascular permeability are each controlled in vivo by different tyrosine residues of VE-cadherin. Nat Immunol *15*, 223–230. 10.1038/ni.2824.
51. Arif, N., Zinnhardt, M., Nyamay'Antu, A., Teber, D., Bruckner, R., Schaefer, K., Li, Y.T., Trappmann, B., Grashoff, C., and Vestweber, D. (2021). PECAM-1 supports leukocyte diapedesis by tension-dependent dephosphorylation of VE-cadherin. EMBO J *40*, e106113. 10.15252/embj.2020106113.
52. Gavard, J., and Gutkind, J.S. (2006). VEGF controls endothelial-cell permeability by promoting the beta-arrestin-dependent endocytosis of VE-cadherin. Nat Cell Biol *8*, 1223–1234. 10.1038/ncb1486.
53. Gavard, J., Patel, V., and Gutkind, J.S. (2008). Angiopoietin-1 prevents VEGF-induced endothelial permeability by sequestering Src through mDia. Dev Cell *14*, 25–36. 10.1016/j.devcel.2007.10.019.
54. Nottebaum, A.F., Cagna, G., Winderlich, M., Gamp, A.C., Linnepe, R., Polaschegg, C., Filippova, K., Lyck, R., Engelhardt, B., Kamenyeva, O., et al. (2008). VE-PTP maintains the endothelial barrier via plakoglobin and becomes dissociated from VE-cadherin by leukocytes and by VEGF. J Exp Med *205*, 2929–2945. 10.1084/jem.20080406.
55. Vockel, M., and Vestweber, D. (2013). How T cells trigger the dissociation of the endothelial receptor phosphatase VE-PTP from VE-cadherin. Blood *122*, 2512–2522. 10.1182/blood-2013-04-499228.
56. Nawroth, R., Poell, G., Ranft, A., Kloep, S., Samulowitz, U., Fachinger, G., Golding, M., Shima, D.T., Deutsch, U., and Vestweber, D. (2002). VE-PTP and VE-cadherin ectodomains interact to facilitate regulation of phosphorylation and cell contacts. Embo j *21*, 4885–4895. 10.1093/emboj/cdf497.
57. Giampietro, C., Taddei, A., Corada, M., Sarra-Ferraris, G.M., Alcalay, M., Cavallaro, U., Orsenigo, F., Lampugnani, M.G., and Dejana, E. (2012). Overlapping and divergent signaling pathways of N-cadherin and VE-cadherin in endothelial cells. Blood *119*, 2159–2170. 10.1182/blood-2011-09-381012.
58. Sui, X.F., Kiser, T.D., Hyun, S.W., Angelini, D.J., Del Vecchio, R.L., Young, B.A., Hasday, J.D., Romer, L.H., Passaniti, A., Tonks, N.K., and Goldblum, S.E. (2005). Receptor protein tyrosine phosphatase micro regulates the paracellular pathway in human lung microvascular endothelia. Am J Pathol *166*, 1247–1258. 10.1016/s0002-9440(10)62343-7.
59. Ukropec, J.A., Hollinger, M.K., Salva, S.M., and Woolkalis, M.J. (2000). SHP2 association with VE-cadherin complexes in human endothelial cells is regulated by thrombin. J Biol Chem *275*, 5983–5986. 10.1074/jbc.275.8.5983.
60. Puech, P.H., and Bongrand, P. (2021). Mechanotransduction as a major driver of cell behaviour: mechanisms, and relevance to cell organization and future research. Open Biol *11*, 210256. 10.1098/rsob.210256.
61. Changede, R., and Sheetz, M. (2017). Integrin and cadherin clusters: A robust way to organize adhesions for cell mechanics. Bioessays *39*, 1–12. 10.1002/bies.201600123.
62. Szulcek, R., Beckers, C.M., Hodzic, J., de Wit, J., Chen, Z., Grob, T., Musters, R.J., Minshall, R.D., van Hinsbergh, V.W., and van Nieuw Amerongen, G.P. (2013). Localized RhoA GTPase activity regulates dynamics of endothelial monolayer integrity. Cardiovasc Res *99*, 471–482. 10.1093/cvr/cvt075.
63. van Buul, J.D., Geerts, D., and Huveneers, S. (2014). Rho GAPs and GEFs: controling switches in endothelial cell adhesion. Cell Adh Migr *8*, 108–124. 10.4161/cam.27599.
64. Kroon, J., Heemskerk, N., Kalsbeek, M.J.T., de Waard, V., van Rijssel, J., and van Buul, J.D. (2017). Flow-induced endothelial cell alignment requires the RhoGEF Trio as a scaffold protein to polarize active Rac1 distribution. Mol Biol Cell *28*, 1745–1753. 10.1091/mbc.E16-06-0389.
65. Timmerman, I., Heemskerk, N., Kroon, J., Schaefer, A., van Rijssel, J., Hoogenboezem, M., van Unen, J., Goedhart, J., Gadella, T.W., Jr., Yin, T., et al. (2015). A local VE-cadherin and Trio-based signaling complex stabilizes endothelial junctions through Rac1. J Cell Sci *128*, 3514. 10.1242/jcs.179424.
66. van Rijssel, J., Hoogenboezem, M., Wester, L., Hordijk, P.L., and Van Buul, J.D. (2012). The N-terminal DH-PH domain of Trio induces cell spreading and migration by regulating lamellipodia dynamics in a Rac1-dependent fashion. PLoS One *7*, e29912. 10.1371/journal.pone.0029912.
67. Lampugnani, M.G., Zanetti, A., Breviario, F., Balconi, G., Orsenigo, F., Corada, M., Spagnuolo, R., Betson, M., Braga, V., and Dejana, E. (2002). VE-cadherin regulates endothelial actin activating Rac and increasing membrane association of Tiam. Mol Biol Cell *13*, 1175–1189. 10.1091/mbc.01-07-0368.
68. Birukova, A.A., Tian, Y., Dubrovskyi, O., Zebda, N., Sarich, N., Tian, X., Wang, Y., and Birukov, K.G. (2012). VE-cadherin trans-interactions modulate Rac activation and enhancement of lung endothelial barrier by iloprost. J Cell Physiol *227*, 3405–3416. 10.1002/jcp.24041.
69. Ngok, S.P., Geyer, R., Liu, M., Kourtidis, A., Agrawal, S., Wu, C., Seerapu, H.R., Lewis-Tuffin, L.J., Moodie, K.L., Huveldt, D., et al. (2012). VEGF and Angiopoietin-1 exert opposing effects on cell junctions by regulating the Rho GEF Syx. J Cell Biol *199*, 1103–1115. 10.1083/jcb.201207009.
70. Ngok, S.P., Geyer, R., Kourtidis, A., Mitin, N., Feathers, R., Der, C., and Anastasiadis, P.Z. (2013). TEM4 is a junctional Rho GEF required for cell-cell adhesion, monolayer integrity and barrier function. J Cell Sci *126*, 3271–3277. 10.1242/jcs.123869.

71. Wilson, C.W., and Ye, W. (2014). Regulation of vascular endothelial junction stability and remodeling through Rap1-Rasip1 signaling. Cell Adh Migr *8*, 76–83. 10.4161/cam.28115.
72. Chrzanowska-Wodnicka, M. (2017). Rap1 in endothelial biology. Curr Opin Hematol *24*, 248–255. 10.1097/moh.0000000000000332.
73. Sakurai, A., Fukuhara, S., Yamagishi, A., Sako, K., Kamioka, Y., Masuda, M., Nakaoka, Y., and Mochizuki, N. (2006). MAGI-1 is required for Rap1 activation upon cell-cell contact and for enhancement of vascular endothelial cadherin-mediated cell adhesion. Mol Biol Cell *17*, 966–976. 10.1091/mbc.e05-07-0647.
74. Yao, L., Romero, M.J., Toque, H.A., Yang, G., Caldwell, R.B., and Caldwell, R.W. (2010). The role of RhoA/Rho kinase pathway in endothelial dysfunction. J Cardiovasc Dis Res *1*, 165–170. 10.4103/0975-3583.74258.
75. Marcos-Ramiro, B., Garcia-Weber, D., and Millan, J. (2014). TNF-induced endothelial barrier disruption: beyond actin and Rho. Thromb Haemost *112*, 1088–1102. 10.1160/TH14-04-0299.
76. Huveneers, S., Oldenburg, J., Spanjaard, E., van der Krogt, G., Grigoriev, I., Akhmanova, A., Rehmann, H., and de Rooij, J. (2012). Vinculin associates with endothelial VE-cadherin junctions to control force-dependent remodeling. J Cell Biol *196*, 641–652. 10.1083/jcb.201108120.
77. Yao, M., Qiu, W., Liu, R., Efremov, A.K., Cong, P., Seddiki, R., Payre, M., Lim, C.T., Ladoux, B., Mège, R.-M., and Yan, J. (2014). Force-dependent conformational switch of α-catenin controls vinculin binding. Nature Communications *5*, 4525. 10.1038/ncomms5525.
78. Kotini, M.P., van der Stoel, M.M., Yin, J., Han, M.K., Kirchmaier, B., de Rooij, J., Affolter, M., Huveneers, S., and Belting, H.G. (2022). Vinculin controls endothelial cell junction dynamics during vascular lumen formation. Cell Rep *39*, 110658. 10.1016/j.celrep.2022.110658.
79. Chuntharpursat-Bon, E., Povstyan, O.V., Ludlow, M.J., Carrier, D.J., Debant, M., Shi, J., Gaunt, H.J., Bauer, C.C., Curd, A., Simon Futers, T., et al. (2023). PIEZO1 and PECAM1 interact at cell-cell junctions and partner in endothelial force sensing. Commun Biol *6*, 358. 10.1038/s42003-023-04706-4.
80. Ranade, S.S., Qiu, Z., Woo, S.-H., Hur, S.S., Murthy, S.E., Cahalan, S.M., Xu, J., Mathur, J., Bandell, M., Coste, B., et al. (2014). Piezo1, a mechanically activated ion channel, is required for vascular development in mice. Proceedings of the National Academy of Sciences *111*, 10347–10352. doi:10.1073/pnas.1409233111.
81. Friedrich, E.E., Hong, Z., Xiong, S., Zhong, M., Di, A., Rehman, J., Komarova, Y.A., and Malik, A.B. (2019). Endothelial cell Piezo1 mediates pressure-induced lung vascular hyperpermeability via disruption of adherens junctions. Proc Natl Acad Sci U S A *116*, 12980–12985. 10.1073/pnas.1902165116.
82. Zhong, M., Wu, W., Kang, H., Hong, Z., Xiong, S., Gao, X., Rehman, J., Komarova, Y.A., and Malik, A.B. (2020). Alveolar Stretch Activation of Endothelial Piezo1 Protects Adherens Junctions and Lung Vascular Barrier. Am J Respir Cell Mol Biol *62*, 168–177. 10.1165/rcmb.2019-0024OC.
83. Juettner, V.V., Kruse, K., Dan, A., Vu, V.H., Khan, Y., Le, J., Leckband, D., Komarova, Y., and Malik, A.B. (2019). VE-PTP stabilizes VE-cadherin junctions and the endothelial barrier via a phosphatase-independent mechanism. Journal of Cell Biology *218*, 1725–1742. 10.1083/jcb.201807210.
84. Dorland, Y.L., Malinova, T.S., van Stalborch, A.M., Grieve, A.G., van Geemen, D., Jansen, N.S., de Kreuk, B.J., Nawaz, K., Kole, J., Geerts, D., et al. (2016). The F-BAR protein pacsin2 inhibits asymmetric VE-cadherin internalization from tensile adherens junctions. Nat Commun *7*, 12210. 10.1038/ncomms12210.
85. Tan, J.M.E., van der Stoel, M.M., van den Berg, M., van Loon, N.M., Moeton, M., Scholl, E., van der Wel, N.N., Kovacevic, I., Hordijk, P.L., Loregger, A., et al. (2020). The MARCH6-SQLE Axis Controls Endothelial Cholesterol Homeostasis and Angiogenic Sprouting. Cell Rep *32*, 107944. 10.1016/j.celrep.2020.107944.



Chapter 2

VE-cadherin interaction proteomics identifies ARVCF as stabilizer of endothelial adherens junctions

iScience, (2026)

VE-cadherin interaction proteomics identifies ARVCF as stabilizer of endothelial adherens junctions

Rianne M. Schoon[1], Tsveta S. van Krimpen-Malinova[1], Iris de Heer[1], Arie J. Hoogendijk[2], Floris P.J. van Alphen[2], Annett de Haan[1], Anne-Marieke D. van Stalborch[1], Simon Tol[2], Jaap D. van Buul[1,3], Maartje van den Biggelaar[2] & Stephan Huveneers[1*]

[1] Amsterdam UMC, University of Amsterdam, Department of Medical Biochemistry, Amsterdam Cardiovascular Sciences, 1105 AZ, Amsterdam, The Netherlands.

[2] Department of Molecular Hematology, Joint-AMC-Sanquin Landsteiner Laboratory, 1066 CX, Amsterdam, The Netherlands.

[3] Swammerdam Institute of Life Sciences, University of Amsterdam, 1098 XH, Amsterdam, The Netherlands.

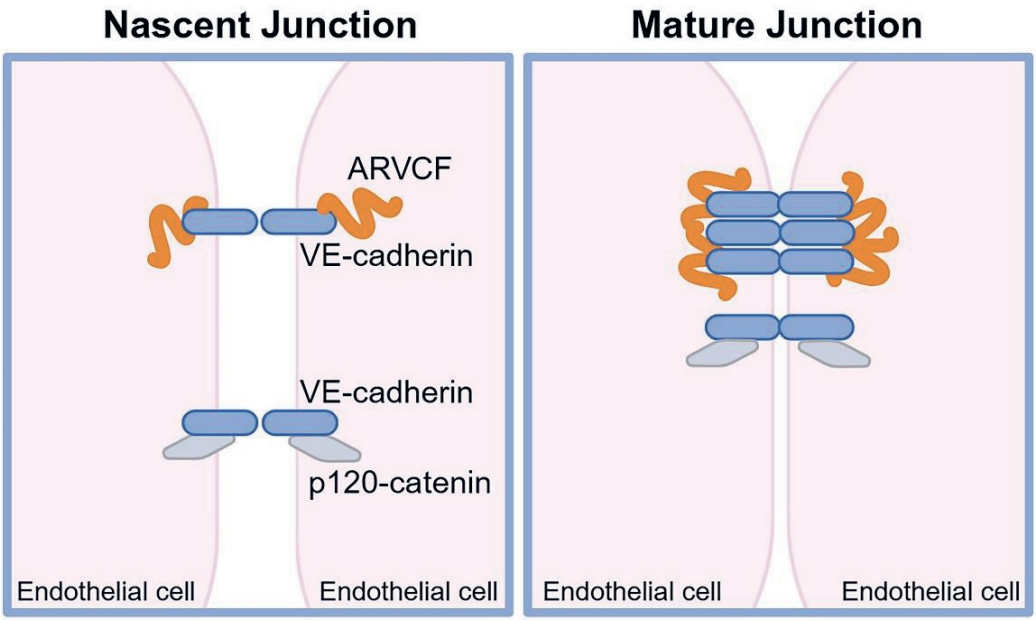
This manuscript has been published in iScience.

*Lead contact:

Stephan Huveneers, PhD; Amsterdam UMC, University of Amsterdam, Department of Medical Biochemistry, Meibergdreef 9, 1105 AZ Amsterdam, the Netherlands. E-mail: s.huveneers@amsterdamumc.nl

SUMMARY

Blood vessel integrity is maintained by vascular endothelial (VE)-cadherin-based adherens junctions, which form structural links between neighboring endothelial cells. In this study, we used mass spectrometry to identify the key proteins that interact with VE-cadherin. The proteomics identified a core group of proteins that bind to VE-cadherin even when its intracellular domain is not tyrosine-phosphorylated. The core VE-cadherin interactome includes known catenin proteins as well as ARVCF, ARHGAP23, KEAP1 and NGLY1. Co-immunoprecipitation and co-localization experiments verified that the VE-cadherin-binding protein ARVCF is a component of endothelial adherens junctions. During junction maturation, ARVCF selectively binds to a pool of VE-cadherin that is unbound from p120-catenin, through a mechanism involving its C-terminal intrinsically disordered regions. Depletion of ARVCF results in instable junctions, loss of endothelial barrier function and impaired collective cell migration. Together, this study demonstrates that ARVCF is an important stabilizer of VE-cadherin junctions to safeguard endothelial integrity.



Graphical abstract

Keywords

VE-cadherin, adherens junctions, barrier function, mass spectrometry, cell migration.

Introduction

The luminal surface of arteries and veins is lined with a monolayer of vascular endothelial cells (ECs) that selectively allows for the exchange of cells and solutes between blood and tissue [1,2]. This selective endothelial barrier is maintained through adherens junctions (AJ) formed through homotypic interactions of the transmembrane protein Vascular Endothelial-cadherin (VE-cadherin) [3-5]. The intracellular domain of VE-cadherin anchors to the actin cytoskeleton, which provides both structural support and allows for mechano-adaptive regulation [6]. When VE-cadherin-based junctions are remodeled, for instance by inflammatory cytokines, angiogenic growth factors, or chronic age-related alterations within the vessel wall, the endothelial barrier weakens, leading to (hyper)permeability, inflammation, and progression of cardiovascular diseases [7-11]. The importance of a resilient endothelial barrier for vascular health is well-established, however the molecular mechanisms that safeguard the endothelial junctions are still incompletely understood.

The stability of endothelial AJs is intricately regulated by proteins that interact with VE-cadherin's cytoplasmic domain. Classically, the AJ complex itself features direct and conserved VE-cadherin-binding proteins p120- and β-catenin, the latter connecting via α-catenin to the actin cytoskeleton [6,12-14]. In addition, other interacting proteins are known to play a role in endothelial barrier modulation [15]. For example, tension across the VE-cadherin complex induces conformational change in α-catenin, exposing a binding site for vinculin, whose presence stabilizes remodeling cell-cell contacts and fortifies attachment to the cytoskeleton network [16,17]. Such force-induced junctional interactions are key for endothelial cell-to-cell communication and coordination across the tissue [18,19]. Finally, phosphorylation and ubiquitination events at the cytoplasmic domain of VE-cadherin modulate its endocytosis, interaction partners, and association with the actin cytoskeleton, which are all important for junction remodeling and barrier maintenance [20-25].

VE-cadherin's cytoplasmic domain contains three tyrosine (Y) residues at positions Y658, Y685, and Y731 that play a role in remodeling of the endothelial barrier [26]. VE-cadherin is phosphorylated at Y658 and Y685 particularly in the venous side of the circulation [8,27]. Phosphorylation of VE-cadherin at Y685 is further promoted by inflammatory cytokines, resulting in weaker AJs and vascular permeability [8,28]. On the other hand, Y731 is constitutively phosphorylated in homeostatic endothelium, and leukocyte-endothelial interactions induce dephosphorylation of pY731, which is an essential event for leukocyte transendothelial migration [7]. VE-cadherin-based AJs are thus tightly regulated through interacting proteins and post-translational modifications, which ensures both barrier function and selective permeability.

Here, we aim to elucidate whether the VE-cadherin complex is regulated through additional protein interactions. To study this, we employed a proteomics approach using mass spectrometry to determine the proteins that bind to VE-cadherin in comparison to VE-cadherin variants in which tyrosines were substituted for phenylalanines. Our results reveal a key set of previously unidentified proteins binding to VE-cadherin. One of the identified core VE-cadherin complex proteins is armadillo repeat deleted in velo-cardio-facial syndrome (ARVCF), which strongly bound to all VE-cadherin variants. We demonstrate that ARVCF is crucial for endothelial barrier integrity of maturing monolayers, and VE-cadherin-based adhesion stability through a unique mechanism that complements the function of other catenin-family proteins in the core AJ complex.

Results

Proteomics identifies VE-cadherin-binding proteins.

To investigate protein interactions with VE-cadherin we performed proteomic analysis on pull-downs of C-terminally GFP-tagged human VE-cadherin in human umbilical vein endothelial cells (HUVECs; hereafter referred to as EC). Mammalian VE-cadherin contains three tyrosine (Y) residues on the intracellular domain (**Figure 1a**), which are relevant for AJ stability and vascular integrity [8,27,29]. We generated non-phosphorylatable VE-cadherin variants by substituting the cytoplasmic tyrosine (Y) residues 658, 685, and 731 by phenylalanine (F). The VE-cadherin-GFP variants were lentivirally expressed in ECs, which in turn were cultured to confluent monolayers. Next, we performed immunoprecipitations using magnetic GFP-trap beads. The obtained VE-cadherin pull-down samples were validated by Western blotting by probing for the known interactor β-catenin [30], which confirmed successful specific co-immunoprecipitations (**Figure S1a**). Next, we performed label-free mass-spectrometry on the GFP-pull-downs compared to blocked beads, showing equal levels of VE-cadherin detection of all variants (**Figure 1b**). The proteomic analysis, based on 3 independent IPs, with each IP derived from a separate transduction, identified 37 proteins to bind to VE-cadherin (**Figure 1c, Figure S1b**). The mass spectrometry-based identification of interaction partners of VE-cadherin and its non-phosphorylatable variants, reveals a core VE-cadherin interactome, consisting of nine proteins, that is independent of Y phosphorylation of the cytoplasmic domain. The core VE-cadherin interactome includes previously reported interactors p120-catenin (*CTNND1*), β-catenin (*CTNNB1*), α-catenin (*CTNNA1*), connexin-43 (*GJA1*) and plakophillin-4 (*PKP4*), and the identified ARVCF, ARHGAP23, KEAP1, and NGLY1 proteins. We detected 28 additional proteins, which displayed enriched binding to one or more of the VE-cadherin variants (**Figure 1c**). STRING analysis using predicted protein interactions indicated that ARVCF is closely linked to the functions of p120-catenin, α-catenin, and β-catenin (**Figure 1d**). Because ARVCF emerged as a previously unreported, but strong binding partner of VE-cadherin, we decided to further investigate their interaction and function in endothelial cells.

Figure 1.

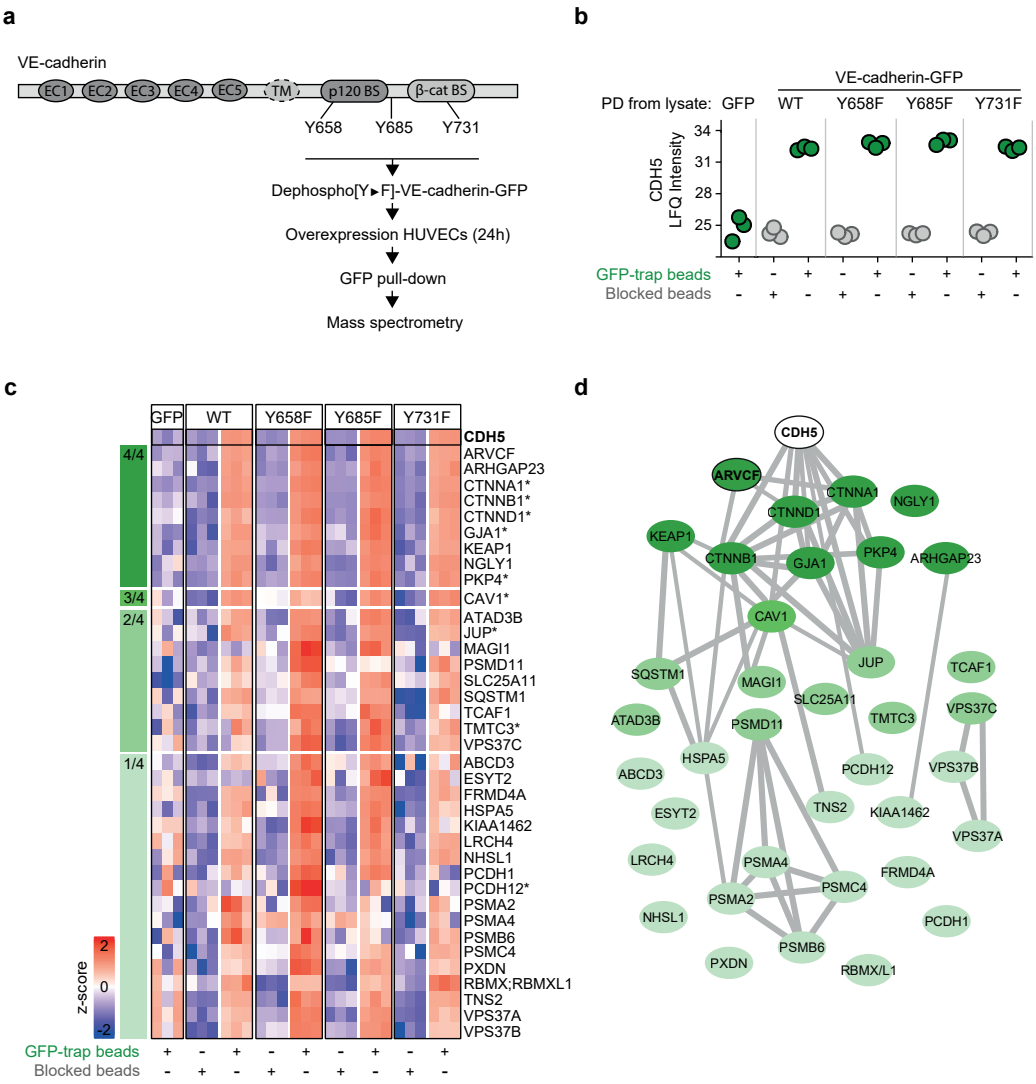


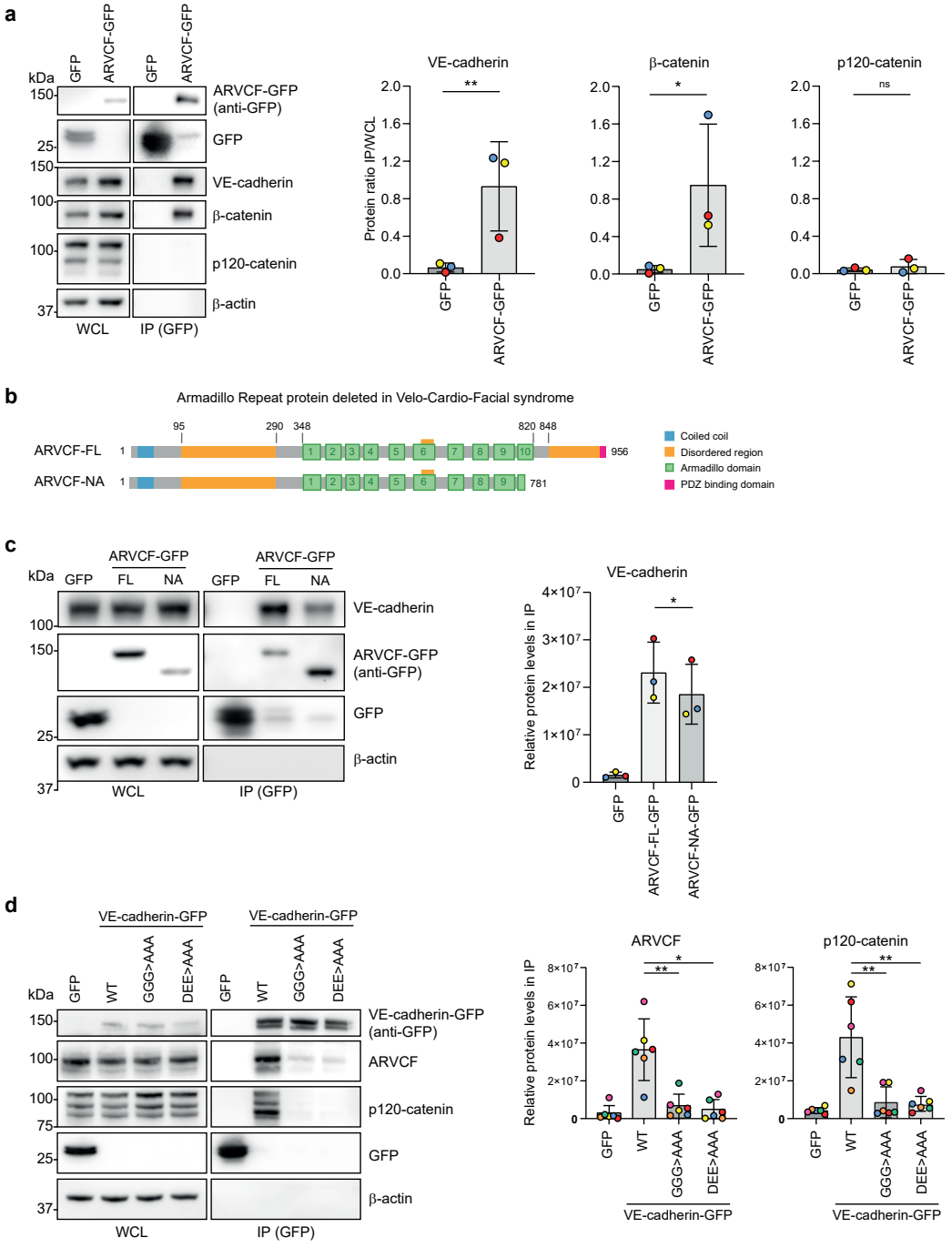
Figure 1. Identification of VE-cadherin binding proteins. a) VE-cadherin contains five extracellular cadherin (EC) domains, a transmembrane (TM) region, and intracellular binding sites (BS) for p120-catenin and β-catenin. Workflow is indicated from generating and overexpressing VE-cadherin non-phosphorylatable [Y►F] variants in human umbilical vein endothelial cells (HUVECs) to mass-spectrometry analysis. **b)** Label-free quantification (LFQ) of VE-cadherin protein abundance detected by mass spectrometry of GFP pull-down (PD) samples versus blocked beads controls. The y-axis indicates log2-transformed LFQ intensities; each dot represents a biological replicate. **c)** Heat map of significantly enriched VE-cadherin binding proteins stratified by their interaction with wild-type and VE-cadherin Y►F variants. * indicates previously reported VE-cadherin interactors. **d)** STRING-based protein network analysis of detected VE-cadherin binding proteins; lines indicating interaction scores >0.4. See also Figure S1.

Mechanism of the VE-cadherin-ARVCF interaction.

To assess the interaction between VE-cadherin and ARVCF, we first generated a lentiviral construct expressing N-terminal GFP-tagged human ARVCF (canonical 'long' isoform 1, O00192-1, 962 amino acids). Immunoprecipitations of GFP-ARVCF from ECs resulted in robust levels of co-precipitated VE-cadherin, as well as the known classical cadherin-binding protein β-catenin, confirming the interactions that were detected by mass-spectrometry (**Figure 2a**). Strikingly, ARVCF's closest relative protein: p120-catenin [31], did not co-precipitate in GFP-ARVCF pull-downs (**Figure 2a**). The ARVCF protein contains an N-terminal coiled-coil domain, followed by a disordered region, central armadillo repeats, and a C-terminal disordered region ending in a PDZ-binding motif (**Figure 2b**). To investigate the molecular mechanism for binding to VE-cadherin, we compared C-terminally GFP-tagged full length ARVCF (E9PDC3 isoform, 956 amino acids) with a truncated ARVCF variant lacking its C-terminal disorded region and PDZ-binding domain in immunoprecipitation assays. VE-cadherin co-immunoprecipitation from ECs was reduced in the absence of the ARVCF C-terminal domain (**Figure 2c**), indicating its importance for optimal binding to VE-cadherin. We next tested whether ARVCF interacts through the p120-catenin-binding domain in VE-cadherin by performing co-immunoprecipitations of ectopically expressed GFP-tagged wild-type VE-cadherin, versus VE-cadherin$^{DEE>AAA}$ or VE-cadherin$^{GGG>AAA}$ variants, which lack a functional juxtamembrane domain [32,33]. These experiments revealed that the VE-cadherin juxtamembrane domain is essential for ARVCF binding (**Figure 2d**). Together, these results indicate that ARVCF binds to the same domain in VE-cadherin as p120-catenin does, but it engages with a separate pool of VE-cadherin proteins that is unbound from p120-catenin.

Figure 2. Mechanism of the VE-cadherin-ARVCF interaction. a) Representative Western blot analysis probed for GFP, VE-cadherin, β-catenin, p120-catenin, and β-actin, on whole-cell lysates (WCL) and GFP immunoprecipitation (IP) samples derived from HUVECs expressing GFP or GFP-ARVCF. Graphs show the ratio between IP and WCL of quantified relative protein levels for VE-cadherin, β-catenin and p120-catenin corrected for total protein loading using β-actin signal from three independent experiments. **b)** Schematic overview of human ARVCF consensus protein, containing an N-terminal coiled-coil domain, a disordered region, 10 central armadillo repeats, and a C-terminal disordered region ending in a PDZ-binding motif. FL: full-length protein; NA: truncated protein containing only the N-terminal disordered region and the first 9 armadillo repeats. **c)** Representative Western blot analysis probed for GFP, VE-cadherin, and β-actin, on WCL and IP samples derived from HUVECs expressing GFP, ARVCF-FL-GFP, or ARVCF-NA-GFP. Graph shows quantified VE-cadherin protein levels in GFP IPs corrected for total protein loading using WCL signal from three independent experiments. **d)** Representative Western blot analysis probed for GFP, ARVCF, p120-catenin, and β-actin, on WCL and IP samples derived from HUVECs expressing GFP, VE-cadherin-GFP wild-type (WT), or its juxtamembrane domain mutants GGG>AAA or DEE>AAA. Graphs compare quantified ARVCF and p120-catenin protein levels in GFP IPs corrected for total protein loading using WCL signal from six independent experiments. Bar graphs show mean ±SD and values per independent experiment. Student's paired t-test (c) or ratio paired t-test (a, d), *p<0.05, **p<0.01, ns: non-significant. See also Figures S4 and S5.

Figure 2.

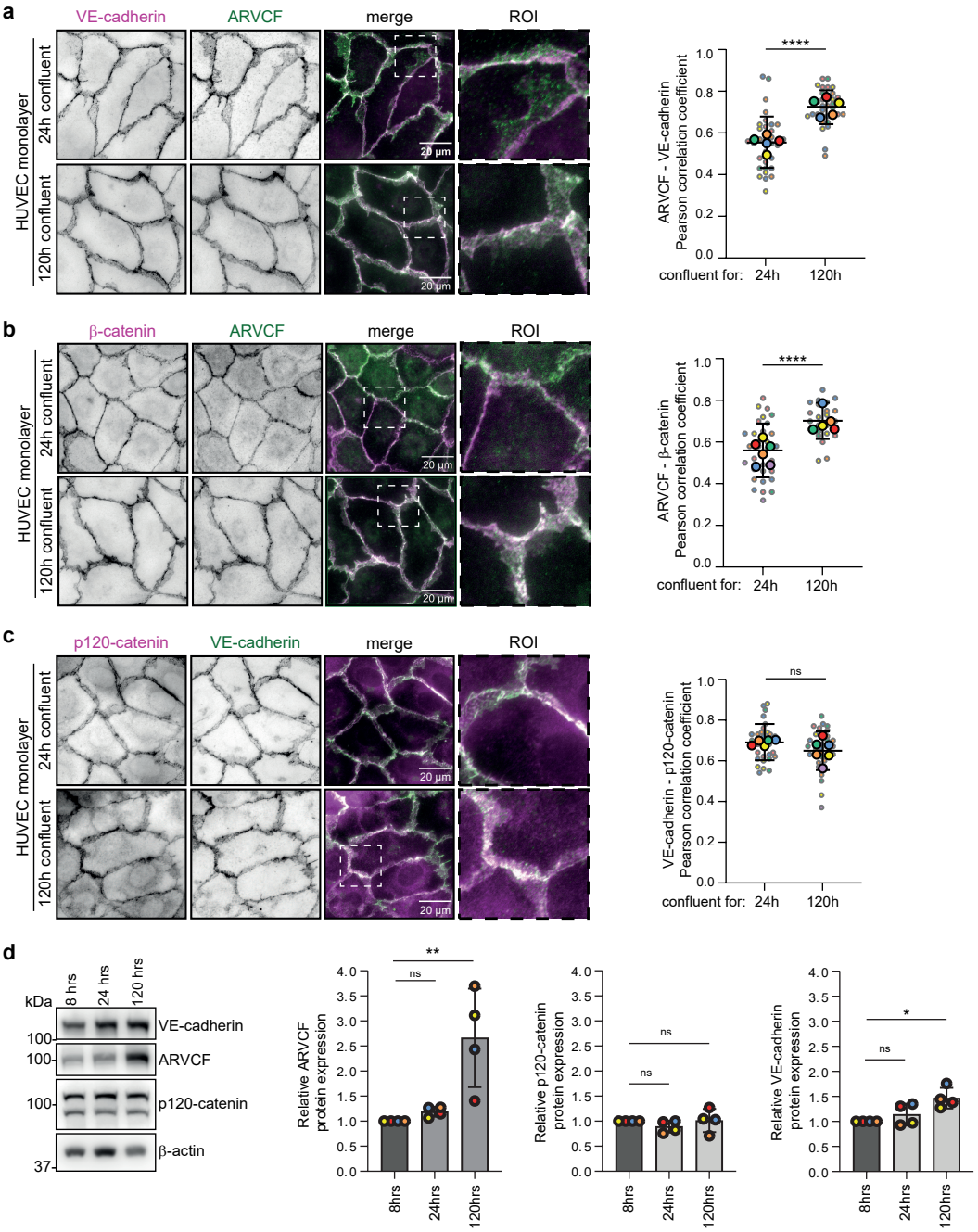

a
kDa
GFP
ARVCF-GFP
GFP
ARVCF-GFP
150
ARVCF-GFP (anti-GFP)
25
GFP
150
VE-cadherin
100
β-catenin
100
p120-catenin
37
β-actin
WCL
IP (GFP)
VE-cadherin
β-catenin
p120-catenin
Protein ratio IP/WCL
2.0
1.6
1.2
0.8
0.4
0.0
**
*
ns
GFP
ARVCF-GFP
b
Armadillo Repeat protein deleted in Velo-Cardio-Facial syndrome
95
290
348
820
848
ARVCF-FL
1
956
ARVCF-NA
781
1
2
3
4
5
6
7
8
9
10
Coiled coil
Disordered region
Armadillo domain
PDZ binding domain
c
kDa
GFP
FL
NA
ARVCF-GFP
100
VE-cadherin
150
ARVCF-GFP (anti-GFP)
25
GFP
37
β-actin
WCL
IP (GFP)
VE-cadherin
Relative protein levels in IP
4×10⁷
3×10⁷
2×10⁷
1×10⁷
0
*
GFP
ARVCF-FL-GFP
ARVCF-NA-GFP
d
kDa
GFP
WT
GGG>AAA
DEE>AAA
VE-cadherin-GFP
150
VE-cadherin-GFP (anti-GFP)
100
ARVCF
100
p120-catenin
75
25
GFP
37
β-actin
WCL
IP (GFP)
ARVCF
p120-catenin
Relative protein levels in IP
8×10⁷
6×10⁷
4×10⁷
2×10⁷
0
**
*
GFP
WT
GGG>AAA
DEE>AAA
VE-cadherin-GFP

ARVCF localizes at VE-cadherin-based adherens junctions

ARVCF is a member of the catenin protein family, structurally related to α-catenin, β-catenin, and most closely to p120-catenin [31,34]. ARVCF has been reported to regulate AJs and tight junctions in epithelial cells [35-37]. To gain insight into where ARVCF and VE-cadherin interact in ECs, we performed immunofluorescence to visualize endogenous ARVCF in endothelial monolayers. ARVCF was pronouncedly localized at cell-cell junctions in both venous and arterial ECs (**Figure 3a, Figure S2a**). The localization of ARVCF and VE-cadherin differed slightly, resulting in junctional regions that were enriched for ARVCF (**Figure 3a**, see region of interest (ROI)). Notably, the level of co-localization between ARVCF and VE-cadherin increased substantially in mature junctions of 120 hours confluent EC monolayers (**Figure 3a**). Similar results were obtained in immunofluorescent stainings of ARVCF with α-catenin or β-catenin **(Figure 3b, Figure S2b)**. The colocalization between ARVCF and the AJ-independent junction protein PECAM1 was unaffected by monolayer maturation (**Figure S2c**), suggesting a specific role for ARVCF at mature VE-cadherin-based AJs. Strikingly, and in contrast to ARVCF, the level of co-localization between VE-cadherin and p120-catenin did not change upon junction maturation in 120 hours confluent monolayers (**Figure 3c**). At 24 hours post-plating, subconfluent endothelial cultures exhibited reduced ARVCF and VE-cadherin colocalization compared with confluent cultures (**Figure S2d**). Western blot analysis of EC monolayers plated for 8, 24, and 120 hours showed that total ARVCF protein levels increased over time in confluency, whereas p120-catenin levels remained unchanged (**Figure 3d**). We next examined VE-cadherin and ARVCF colocalization during junction remodeling in thrombin-treated endothelial monolayers and found that ARVCF remained recruited to VE-cadherin-based junctions, with a slight, non-significant reduction (**Figure S2e**).

Figure 3. ARVCF localizes at VE-cadherin-based endothelial adherens junctions. a) Representative widefield images of HUVECs that were fixed after 24 or 120 hours at full confluence and stained for endogenous VE-cadherin (magenta) and ARVCF (green). Graphs showing Pearson's correlation coefficients of pixel intensity values between ARVCF and VE-cadherin. Data from n=5 independent experiments, unpaired Welch's t-test. Graphs show values per image (small dots) and means from independent experiments (large dots per color) ±SD. **b)** Representative widefield images of HUVECs that were fixed after 24 or 120 hours at full confluence and stained for endogenous β-catenin (magenta) and ARVCF (green). Graphs showing Pearson's correlation coefficients of pixel intensity values between ARVCF and β-catenin. Data from n≥5 independent experiments, unpaired Welch's t-test. Graphs show values per image (small dots) and means from independent experiments (large dots per color) ±SD. **c)** Representative widefield images of HUVECs that were fixed after 24 or 120 hours at full confluence and stained for endogenous p120-catenin (magenta) and ARVCF (green). Graphs showing Pearson's correlation coefficients of pixel intensity values between ARVCF and p120-catenin. Data from n≥5 independent experiments; unpaired Welch's t-test. Graphs show values per image (small dots) and means from independent experiments (large dots per color) ±SD. **d)** Representative Western blot analysis of lysates derived from HUVECs after 8, 24 or 120 hours at full confluence, probed for ARVCF, VE-cadherin, p120-catenin and β-actin. Graph shows protein expression levels. Signal corrected for background, β-actin expression levels, and normalized to

Figure 3.



expression levels in the 8 hours confluent condition. Data from n=4 independent experiments; ANOVA with Dunnett's multiple comparison test. Bar graphs show mean ±SD and values per independent experiment. *p<0.05, **p<0.01, ns: non-significant. Scale bars are 20 mm. See also Figure S3 and S5.

To investigate how ARVCF is recruited to junctions, we overexpressed GFP-ARVCF in ECs and subsequently inhibited the homotypic binding between VE-cadherin extracellular domains using clone 75 function-blocking antibody [16] . The junctional localization of ARVCF was readily perturbed upon clone 75 treatment, showing that junctional ARVCF recruitment depends on VE-cadherin adhesion (**Figure 4a-b**, **Video S1**). Toghether, these experiments indicate that ARVCF-associated VE-cadherin-based adherens junctions are enhanced during maturation.

Figure 4.

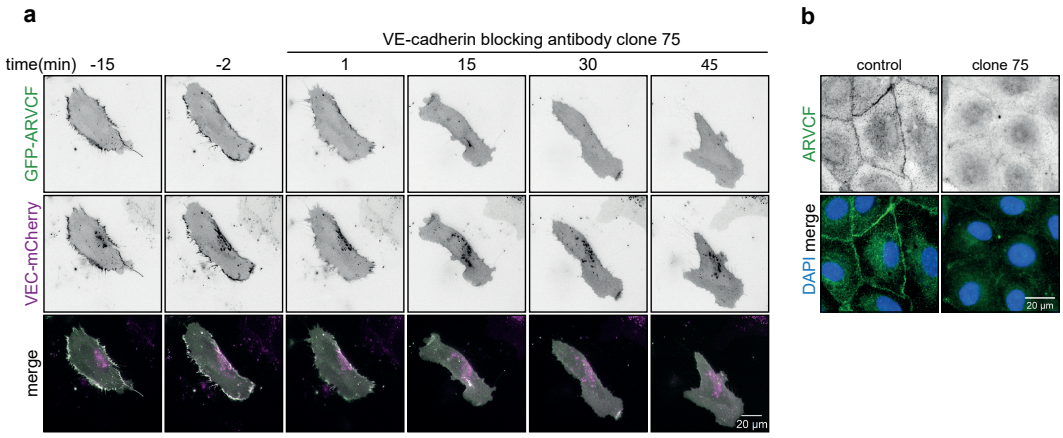


Figure 4. Junctional ARVCF localization depends on VE-cadherin. a) Stills from representative live imaging of HUVEC expressing both GFP-ARVCF (green) and VE-cadherin-mCherry (magenta) within an endothelial monolayer. VE-cadherin blocking antibody clone 75 (12.5 µg/mL) was added at t=0 and cells were subsequently recorded for 1 hour. **b)** Representative widefield images of fixed HUVEC monolayers treated with 12.5 µg/mL VE-cadherin blocking antibidy clone 75 for 1 hour and immunostained for VE-cadherin and DAPI. Scale bars are 20 mm.

Depletion of ARVCF perturbs endothelial AJs and barrier function

To assess the importance of ARVCF in endothelial cell-cell junctions, we silenced *ARVCF* expression using two independent lentiviral short hairpin RNAs (shRNAs), both of which induced efficient knockdown levels (**Figure 5a-b**). Flow cytometry analysis showed that VE-cadherin surface expression was maintained in ARVCF knockdown cells, with levels comparable to shControl cells (**Figure S3a**). Immunofluorescence imaging confirmed that ARVCF knockdown cells still formed VE-cadherin-based AJs with an overall fluorescence intensity that was comparable to shControl (**Figure S3b**). Interestingly, the junction organization was altered in shARVCF ECs, with disrupted adhesions at cell-cell contact interfaces, resulting in non-continuous VE-cadherin distribution between ECs (**Figure S3b**). To understand how ARVCF controls junctions, we next investigated the dynamics of VE-cadherin by lentiviral overexpression of VE-cadherin-GFP in shControl and shARVCF ECs. Subsequent live cell imaging experiments showed that the junctional interface between ARVCF-depleted cells was highly unstable, going through repeated cycles of junction formation and breakdown without junctional stabilization. This led to the formation of intercellular gaps along junctions over time (**Figure 5c, Video S2**). Live imaging of GFP-ARVCF in ECs further showed that ARVCF was recruited to the junctions in a punctate pattern during nascent junction formation (**Figure 5d**, top row; **Video S3**). After initial cell-cell contact formation, and when junctions were stabilized through cell protrusions, ARVCF was redistributed in a continuous, uninterrupted pattern between adjoining cells (**Figure 5d**, lower row; **Video S3**). Hence, the majority of ARVCF is recruited during cell-cell junction maturation, fitting with its role in junctional stabilization. To test whether ARVCF is necessary for stable cell-cell contacts, we assessed the integrity of the endothelial junctions by culturing the ECs on biotin-coated gelatin substrates. Once confluent monolayers were established, fluorescent streptavidin was added to the apical side of the monolayers for 10 minutes to determine the level of junction leakiness. These experiments indicate that the depletion of ARVCF induces a considerable increase in intercellular gaps and leads to monolayer leakiness (**Figure 5e**). To investigate the importance of ARVCF for endothelial barrier function, we next used electrical cell-substrate impedance sensing (ECIS) measurements at 4000 Hz across shControl and shARVCF endothelial cultures. These experiments showed that shARVCF cells had a significantly reduced capacity to form stable endothelial barriers, resulting in impaired endothelial barrier function over time (**Figure 5f**). We conclude that ARVCF is necessary for endothelial junction stabilization and monolayer barrier formation.

Figure 5.

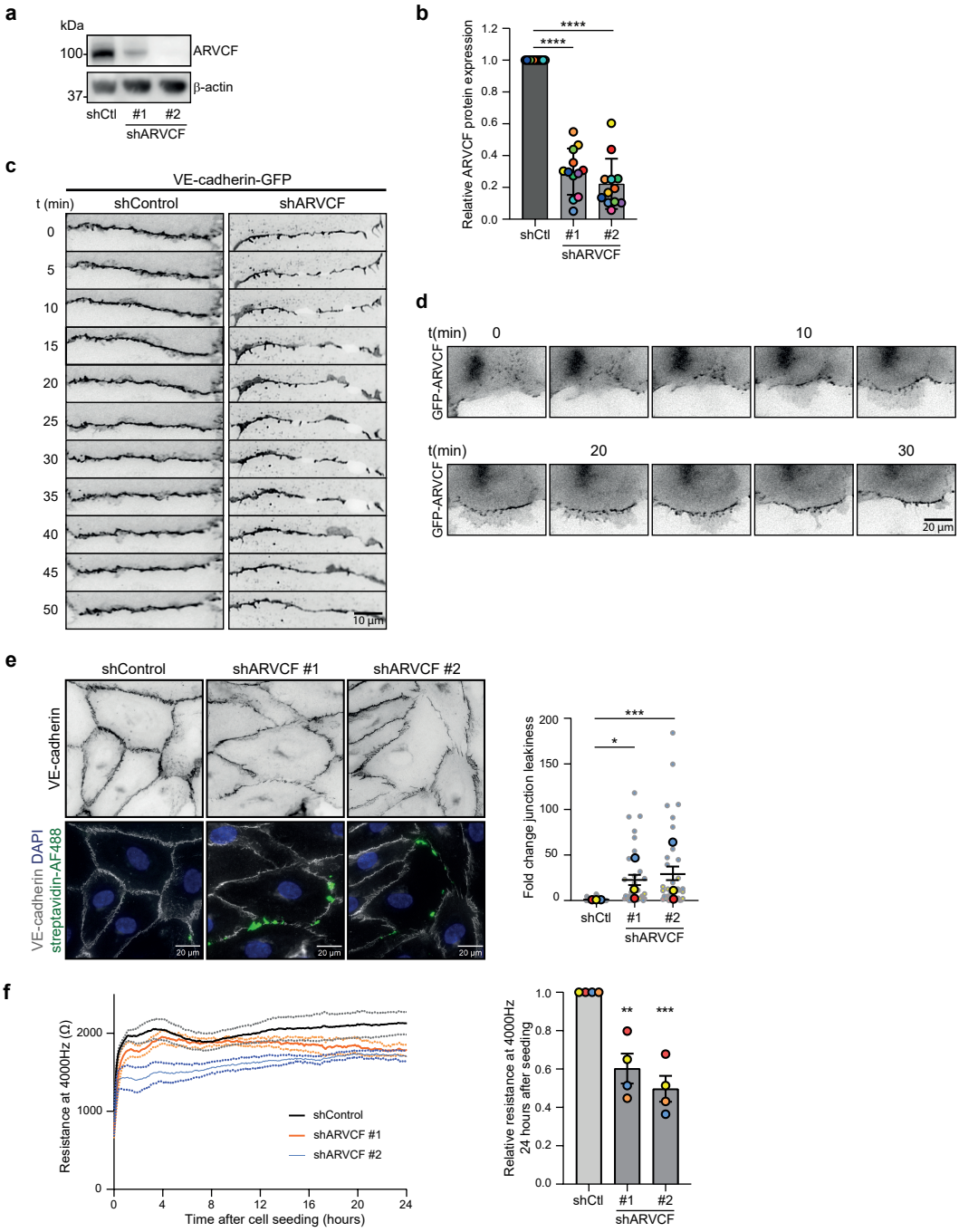

a
kDa
100
ARVCF
37
β-actin
shCtl
#1
#2
shARVCF
b
Relative ARVCF protein expression
1.2
1.0
0.8
0.6
0.4
0.2
0.0
****
****
shCtl
#1
#2
shARVCF
c
VE-cadherin-GFP
t (min)
shControl
shARVCF
0
5
10
15
20
25
30
35
40
45
50
10 µm
d
t(min)
0
10
GFP-ARVCF
t(min)
20
30
GFP-ARVCF
20 µm
e
shControl
shARVCF #1
shARVCF #2
VE-cadherin
VE-cadherin DAPI
streptavidin-AF488
20 µm
20 µm
20 µm
Fold change junction leakiness
200
150
100
50
0
***
*
shCtl
#1
#2
shARVCF
f
Resistance at 4000Hz (Ω)
2000
1000
0
0
4
8
12
16
20
24
Time after cell seeding (hours)
shControl
shARVCF #1
shARVCF #2
Relative resistance at 4000Hz 24 hours after seeding
1.0
0.8
0.6
0.4
0.2
0.0
**
***
shCtl
#1
#2
shARVCF

Figure 5. Depletion of ARVCF perturbs endothelial AJs and barrier function. a) Representative Western blot analysis of lysates derived from HUVECs transduced with control or ARVCF shRNAs, probed for ARVCF and β-actin. **b)** Graph shows the ARVCF protein expression levels. Signal corrected for background, β-actin expression levels, and normalized to expression levels in control cells. Data from n=12 independent experiments, ANOVA with Dunnett's multiple comparison test. Bar graphs show mean ±SD and values per independent experiment. **c)** Representative stills from time-lapse widefield imaging every 5 minutes for one hour of live HUVECs transduced with shControl or shARVCF and VE-cadherin-GFP. **d)** Representative stills from time-lapse imaging every 10 minutes of live HUVECs transduced with GFP-ARVCF. **e)** Representative images of fixed shControl and shARVCF HUVECs grown on biotin-gelatin and stained for endogenous VE-cadherin (grey), nucleus (blue), and streptavidin-AlexaFluor488 (green). Graph showing fold change in junction leakiness between shControl and shARVCF HUVECs. Data from n=3 independent experiments ANOVA with Dunnett's multiple comparison test. Graphs show values per image (small dots) and means from independent experiments (large dots per color) ±SEM. **f)** Line graph showing the average resistance (±SEM, dotted lines) measured with ECIS at 4000 Hz of shControl and shARVCF HUVECs monolayers over time. Data from n=4 independent experiments. Bar graph showing the relative, compared to shControl cells, resistance of shARVCF monolayers at 4000 Hz 24 hours after cell seeding. Data from n=4 independent experiments, ANOVA with Dunnett's multiple comparison test. Bar graphs show mean ±SEM and values per independent experiments. *p<0.05, **p<0.01, ***p<0.001, ****p<0.0001. Scale bars are 10 or 20 mm. See also Figure S4 and S5.

Junctional reinforcement restores endothelial integrity in the absence of ARVCF

Previous studies on other tissues showed that ARVCF controls intracellular force production by linking cell-cell adhesions [38,39]. As such, ARVCF has been shown to regulate tension on junctions during xenopus embryonal axis elongation [38]. To investigate whether the leaky junctions between ARVCF-depleted ECs were caused by a lack of junctional reinforcement, shControl and shARVCF ECs were treated with 8-(4-chlorophenylthio)-2'-O-methyladenosine 3',5'-cyclic monophosphate (also known as 007-AM), a selective EPAC1 agonist that tightens the endothelial barrier through Rap1-mediated junctional reinforcement [40]. After 10 minutes of 1 µM 007-AM treatment, endothelial cells adopted hexagonal organizations within monolayers in all conditions (**Figure 6a**), which is indicative of an optimal distribution of radial forces and junctional tension in support of junction stabilization [41-43]. Intriguingly, 007-AM fully restored the intercellular gaps between shARVCF ECs, thereby reducing junction leakiness (**Figure 6a-b**). These results point to a role for ARVCF in junctional reinforcement for endothelial barrier function.

Figure 6.

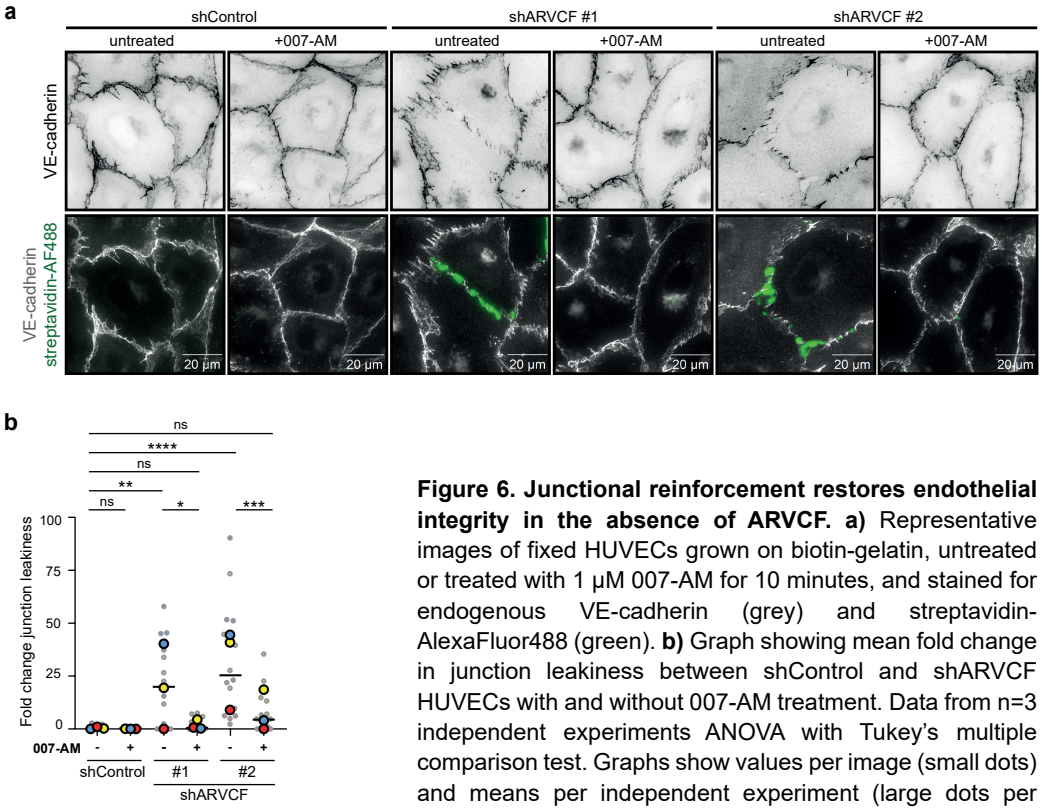


Figure 6. Junctional reinforcement restores endothelial integrity in the absence of ARVCF. a) Representative images of fixed HUVECs grown on biotin-gelatin, untreated or treated with 1 µM 007-AM for 10 minutes, and stained for endogenous VE-cadherin (grey) and streptavidin-AlexaFluor488 (green). **b)** Graph showing mean fold change in junction leakiness between shControl and shARVCF HUVECs with and without 007-AM treatment. Data from n=3 independent experiments ANOVA with Tukey's multiple comparison test. Graphs show values per image (small dots) and means per independent experiment (large dots per color). *p<0.05, **p<0.01, ***p<0.001, ****p<0.0001, ns: non-significant. Scale bars are 20 mm.

ARVCF is needed for collective cell migration

Endothelial junctions integrate mechanical cues derived from the pushing and pulling between cells to coordinate collective cell migration [44,45]. To assess the importance of ARVCF for endothelial collective cell migration, we performed scratch wound assays in shControl and shARVCF monolayers. The depletion of ARVCF strongly inhibited migration during wound healing (**Figure 7a**). The defect in collective cell migration was related to an intrinsic lack of coordinated directionality between migrating shARVCF cells (**Figure 7a**). Moreover, intercellular gaps appeared between migrating leader and follower shARVCF cells (**Figure 7b**). These results show that ARVCF is important for junction remodeling during collective cell migration.

Figure 7.

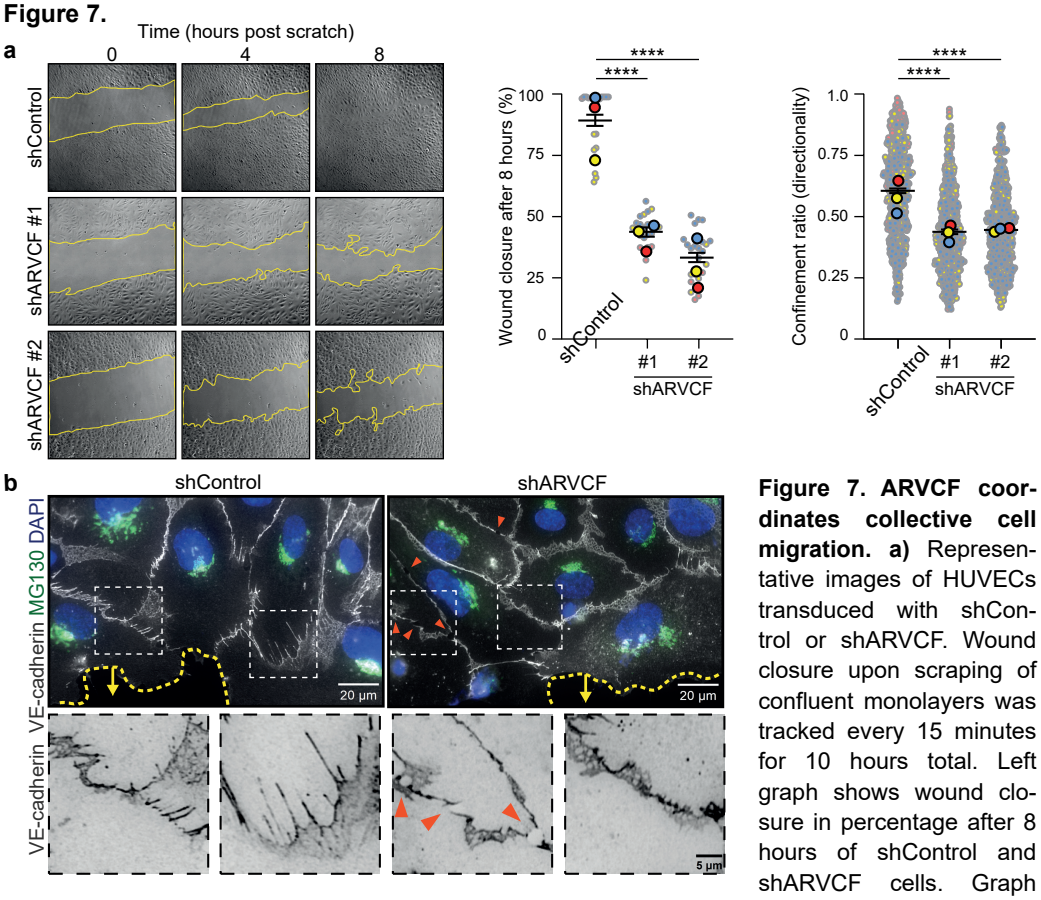


Figure 7. ARVCF coordinates collective cell migration. a) Representative images of HUVECs transduced with shControl or shARVCF. Wound closure upon scraping of confluent monolayers was tracked every 15 minutes for 10 hours total. Left graph shows wound closure in percentage after 8 hours of shControl and shARVCF cells. Graph shows values per scratch wound (small dots) and means from independent experiments (large dots per color) ±SEM. Right graph shows confinement ratio over 8 hours of wound closure of shControl and shARVCF cells. Graph shows values per cell (small dots) and means from independent experiments (large dots per color) ±SEM. Data from n=3 independent experiments, ANOVA with Dunnett's multiple comparison test. ****p<0.0001. **b)** Representative images of HUVECs transduced with shControl or shARVCF stained for endogenous VE-cadherin (grey), Golgi (green) and nucleus (blue). Orange arrowheads indicate AJ disruptions. Scale bars are 5 or 20 mm.

Discussion

VE-cadherin is central to the build-up of endothelial AJs, yet the molecular diversity of its composition and its regulation remain incompletely understood. In this study, we used a proteomics approach through which four core VE-cadherin interactors were identified: ARVCF, ARHGAP23, KEAP1, and NGLY1. Co-immunoprecipitation and co-localization experiments verified that ARVCF is an important component of endothelial AJs. Further functional experiments showed that ARVCF plays a significant role in the maturation of VE-cadherin-based AJs: ARVCF associates with a selective pool of VE-cadherin molecules that are unbound to p120-catenin through a mechanism involving the intrinsically disordered regions of ARVCF. The direct association of ARVCF to VE-cadherin is important for junction stabilization. The existence of two types of VE-cadherin pools, one bound to p120-catenin and one bound to ARVCF, and the notion that ARVCF binds to E-cadherin in epithelial cells [46], indicates that the contribution of ARVCF to junction strengthening is conserved for classical cadherins. Together, our results present ARVCF at an essential position in the AJ complex where it regulates junction maturation to safeguard endothelial barrier integrity.

The core VE-cadherin-interactome contains several catenins, all members of the armadillo-domain protein family to which ARVCF also belongs. Within this family, ARVCF shares the greatest structural similarities with p120-catenin [31], a well-characterized cadherin interactor in a multitude of cell types [47,48]. ARVCF has been reported to bind to E-cadherin via the same domain as through which p120-catenin binds [49,50]. Our study shows enhanced interaction between ARVCF and VE-cadherin at junctions as endothelial monolayers mature, while the association between VE-cadherin and p120-catenin remains stable during this process. Furthermore, we found that ARVCF binds mutually exclusively to unique pools of VE-cadherin that are unbound to p120-catenin, supporting the idea of distinct or sequential roles for these proteins. This is consistent with earlier work in epithelial cells where ARVCF competes with p120-catenin for binding to E-cadherin through their central armadillo repeats [46,49,50]. We find that the C-terminal intrinsically disordered regions (IDR) of ARVCF support binding to VE-cadherin. Such regions lack a stable, well-defined, three-dimensional structure and are known for their scaffolding potential [51,52]. Intriguingly, ARVCF-IDRs are sequentially distinct from the protein domain in p120-catenin [53], pointing to a specialized function of ARVCF at AJs.

The increased junctional association of ARVCF during junction maturation indicates that ARVCF contributes to assembly or stabilization of cadherin-based complexes. The formation of tightly packed cadherin clusters confers strong adhesion between cells [54]. We find that the genetic depletion of *ARVCF* results in gaps in endothelial monolayers. This result can be explained by a potential loss of cadherin clustering or disruption of avidity [55,56]. These observations support a model where ARVCF maintains strong cell-cell adhesions by facilitating cadherin clustering.

An alternative mechanism of how ARVCF supports junction maturation may involve the ARVCF IDRs in coupling of distinct adhesion systems. In epithelial cells, ARVCF has been reported to interact with both E-cadherin and the tight junction proteins ZO-1 and ZO-2 [37]. Notably, ARVCF appears at early contact sites where the formation of both junction types begins, suggesting it may participate in coordinating the spatial or temporal assembly of AJs and tight junctions. In endothelium, tight junction organization follows AJ formation [4,57,58]. The presence of ARVCF at sites of early adhesion, and its known interactions with both junction types, raises the possibility that it contributes to junctional crosstalk during cell-cell contact maturation. Additionally, the conformational flexibility of ARVCF terminal IDRs may facilitate homotypic interactions, potentially creating a feedback loop that promotes its junctional enrichment. A similar function has been described for the N-terminal disordered region of the β-catenin-related protein WRM-1 in *C. elegans* which is required for self-association [59]. Such IDR-features point to a role for ARVCF as a tunable factor in junctional stabilization.

Given that ARVCF appears to function primarily during the maturation of endothelial junctions, we do not assume that its junctional interaction is directly controlled by permeability-inducing factors. The mass spectrometry analysis demonstrates that ARVCF can bind to VE-cadherin in the absence of phosphorylation; however, we do not exclude the possibility that this interaction is maintained under phosphorylated conditions. Notably, under standard culture conditions, phosphorylation at Y731 is already high, yet ARVCF binding remains strong. In addition, ARVCF still colocalizes with VE-cadherin in thrombin-treated endothelial cells, a condition in which VE-cadherin Y685 phosphorylation levels are elevated [23].

Endothelial migration and junction remodeling are inherently force-regulated [16,60-62]. The importance of ARVCF for these processes suggests that it contributes to junctional mechanotransduction. In the mouse lens, ARVCF is required for maintaining normal biomechanical properties; its absence leads to lens stiffening and ultimately cataract formation [36]. Interestingly, *Arvcf* depletion resulted in reduced membrane localization of N-cadherin, β-catenin, and α-catenin in the lens epithelia, an effect we did not observe in endothelial cells. These cell types differ in relative expression levels of junctional proteins: ARVCF is markedly more abundant than p120-catenin in lens tissue, in contrast to other connecting tissues, including endothelium, where p120-catenin typically predominates. p120-catenin is necessary to retain (V)E-cadherin at the membrane [49,63]. In endothelial cells, the pool of p120-catenin-bound VE-cadherin suffices to maintain surface levels in the absence of ARVCF. By contrast, in xenopus, surface levels of C-cadherin were reduced after depleting both ARVCF and p120-catenin [64], indicating partial functional compensation between the two. ARVCF and p120-catenin likely act as context-dependent regulators of VE-cadherin-mediated adhesion, with their relative abundance

and recruitment contributing to junctional resilience in various mechanical environments within the vasculature. In summary, our study points to a reinforcing role for ARVCF in endothelial junction maturation and stability.

Resource availability

Lead contact: Stephan Huveneers, PhD; Amsterdam UMC, University of Amsterdam, Department of Medical Biochemistry, Meibergdreef 9, 1105 AZ Amsterdam, the Netherlands. E-mail: s.huveneers@amsterdamumc.nl.

Material availability: Materials generated and used in this study are available upon request to the lead contact.

Data and code availability: Mass spectrometry proteomics data are available via ProteomeXchange with identifier PXD068012.

Limitations of the study

A limitation of this study is that overexpression of fluorescently tagged proteins may not fully recapitulate the dynamics or biochemical properties of their endogenous counterparts. In addition, lentiviral-mediated knockdown approaches may not result in complete depletion of target proteins, which could lead to an underestimation of ARVCF function in endothelial cells. Finally, the imaging approaches used here are limited in spatial resolution, the application of super-resolution microscopy in future studies may provide deeper insight into the mechanisms underlying ARVCF recruitment to endothelial cell-cell junctions.

Acknowledgements

This work is financially supported by the Netherlands Organization of Scientific Research (ZonMw VIDI grant 016.156.327, ZonMw Vici grant 09150182310041) and a grant from the Rembrandt Institute for Cardiovascular Sciences. Graphical abstract was created with Biorender.com.

Author contributions

Conceptualization: R.S., T.v.K-M., S.H.; Data curation: A.H.; Formal analysis: R.S., I.d.H., A.H.; M.v.d.B. Funding acquisition: S.H. Investigation: R.S., T.v.K-M., I.d.H., A.H., F.v.A., A.d.H., A-M.v.S., S.T., S.H. Methodology: R.S.; Supervision: J.v.B., M.v.d.B., S.H. Validation: R.S., I.d.H.; Visualization: R.S., T.v.K-M., S.H.; Writing - original draft: R.S., T.v.K-M., S.H.; Writing - review & editing: R.S., J.v.B., M.v.d.B, S.H.

Declaration of interests

The authors declare no competing interests.

STAR METHODS

EXPERIMENTAL MODEL AND STUDY PARTICIPANT DETAILS

Cell culture: All cells were maintained in standard humidified incubators set to 37°C with 5% CO_2. Pooled human umbilical vein endothelial cells (HUVECs; mix of female and male donors, P1052, #C2519A, Lonza) and human arterial endothelial cells (HAECs; male donor, #CC2535, Lonza) were cultured until at most passage 8 in endothelial growth medium supplemented with endothelial growth factor-FCS mix (EGM2; #C-22211 + #C-39216, Promocell), 100 U/mL penicillin, and 100 µg/mL streptomycin (#15140122, Gibco) on fibronectin (FN) coated surfaces. Endothelial cells tested negative for mycoplasma and were authenticated by immunostaining for VE-cadherin. Lenti-X HEK293T cells (#632180, Takara) were cultured in DMEM (#11320033, Gibco) + 10% FCS (#10270106, Gibco).

Lentiviral transduction: Lenti-X HEK293T cells were used to produce lentivirus by transfecting gene plasmids together with third generation packaging plasmids [65] and using Trans-IT-LT1 (MIR 2300, Mirus) as described previously [66]. HUVECs were transduced at 60% confluence by overnight incubation with the lentiviral particles and subsequently selected overnight with 250 ng/mL puromycin (#P8833, Sigma). Selected HUVECs were analyzed at least 72h after transduction to ensure knockdown efficiency.

METHOD DETAILS

Plasmids and cloning: The pLV-hVE-cadherin-GFP and pLV-hp120-catenin-mCherry constructs were described before [16,67]. The three VE-cadherin[Y>F] mutations were generated through site directed mutagenesis in a pEGFP-hVE-cadherin-GFP. The [Y658F] mutation was generated using primers 5'-TACATCTACGTATTAGTCATCGCTA-3' and 5'-CCTCTACAAATGTGGTATGGCT-GATTATGATC-3'. The [Y685F] mutation was generated using primers 5'-TACATCTACGTATTAGTCATCGCTA-3' and 5'-CCTCTACAAATGTGGTATGGCTGATTATGATC-3'. The [Y731F] mutation was generated using primers 5'-TACATCTACGTATTAGTCATCGCTA-3' and 5'-CCTCTACAAATGTGGTATGGCTGATTATGATC-3'. Resulting plasmids were digested with restriction enzymes SnaBI and XbaI and inserts were ligated into a pLV-CMV-MCS-IRES-puro-SIN vector using enzymes SnaBI and NheI. A GFP-human ARVCF (long isoform 1, 962 amino acids (UniProt O00192-1)) cDNA within pLV plasmid was obtained from VectorBuilder (VB230406-1221, VectorBuilder). pEGFP-hARVCF plasmids (based on long isoform 1, 956 amino acids (UniProt E9PDC3)) were a kind gift from Dr. Ilse Hofmann [68] ([FL] = full length; [NA] = N-terminus + armadillo regions). For protein knock-down we used shRNA plasmids targeting human genes (TSC2 MISSION® library, Sigma) or control shRNA (SHC002; Sigma-Aldrich). To deplete ARVCF we used shRNA TRCN0000123310 as shARVCF#1; and TRCN0000123313 as shARVCF#2.

Co-immunoprecipitation: Co-IP on untransduced HUVECs, HUVECs expressing GFP alone or GFP-tagged proteins was performed with magnetic GFP-trap agarose beads (#gtma-20, Chromotek). Cells were washed 2 times with cold PBS supplemented with 1 mM $CaCl_2$ and 0,5 mM $MgCl_2$ and incubated for 10 minutes with freshly made ice-cold lysis buffer comprised of 10 mM Tris-HCl pH 7.5, 150 mM NaCl, 0.5 mM ethylenediaminetetraacetic acid (EDTA) (all reagents Sigma Aldrich), protease and phosphatase inhibitors (#A32955, Thermo Fisher; #4906845001, Roche), and 0.5% Nonidet P-40 substitute (NP-40, #492018, Sigma Aldrich). Cell lysates were collected in protein LoBind tubes (#0030108116, Eppendorf; used throughout this procedure), and centrifuged at 12,000 g at 4°C for 10 minutes. Supernatants were transferred to clean tubes and incubated at 4°C overnight with GFP nanobeads that were washed and equilibrated 3 times with PBS and 3 times with lysis buffer. The next day, immunoprecipitated beads were washed 3 times with freshly made wash buffer (lysis buffer without NP-40) followed by 2 washes with ice-cold PBS, each time transferring to clean tubes. The resulting samples were then used either for Western Blot analysis or processed for mass spectrometry analysis.

Mass spectrometry sample preparation: For mass spectrometry (MS) analysis, co-immunoprecipitated proteins were reduced on-bead in 1 M urea (#AM9902, Life Technologies), 10 mM dithiothreitol (#R0861, Thermo Scientific) in 100 mM Tris-HCl pH 7.5 (#17926, Life Technologies) for 20 minutes at 20°C and alkylated with 50 mM iodoacetamide (#122271000, Thermo Scientific) for 10 minutes at 20°C. Proteins were detached from the GFP nanobeads by incubation with 250 ng MS-grade trypsin (cat# V5280, Promega) for 2 hours at 20°C. Beads were removed and proteins were further digested for 16 hours at 20°C with 350 ng MS-grade trypsin. Tryptic peptides were desalted and concentrated using Empore-C18 StageTips (3M) and eluted with 0.5% (v/v) acetic acid (#695092, Sigma), 80% (v/v) acetonitrile (#012078, BioSolve). Sample volume was reduced by SpeedVac (Thermo Scientific) and supplemented with 2% acetonitrile, 0.1% trifluoracetic acid (#A12198, Thermo Scientific) to a final volume of 5 µl. 3 µl of each sample was injected for mass spectrometry analysis.

Mass spectrometry processing: Eluted peptides were separated using a reverse-phase C18 column made in-house from a Silica tip emitter (New objective, Woburn, MA, USA) filled with 1.9 µm C18 particles (Dr. Maisch, Ammerbuch-Entringen, Germany) at a flow rate of 300 nL/min with a gradient from 4% to 30% (vol/vol) acetonitrile with 0,5% acetic acid. Separated peptides were sprayed directly into a Orbitrap Fusion mass spectrometer (Thermo Fisher Scientific, Waltham, MA, USA) using a nanoflow source with a spray voltage of 2.15 kV. A Higher-energy Collisional Dissociation was performed for the most intense precursor ions selected from each 3s-duration full scan in the Orbitrap (400 to 1500 m/z, resolution 120,000). An isolation width of 1.6 m/z was used

for the selected ions (charge ≥2). Dynamic exclusion was activated for the MS/MS scan with a repeat count of 1 and an exclusion duration of 30s.

Mass spectrometry analysis: The RAW mass spectrometry files were processed with the MaxQuant computational platform, 1.6.2.10 [69]. Proteins and peptides were identified using the Andromeda search engine by querying the human Uniprot database. Standard settings with the additional options match between runs, Label Free Quantification (LFQ), and unique peptides for quantification were selected. The generated 'proteingroups.txt' table was filtered for potential contaminants, reverse hits and 'only identified by site' using R. LFQ values were transformed in log2 scale and proteins were filtered for three valid values in at least one of the experimental groups. Missing values were imputed by normal distribution (width=0.3, shift=1.8), assuming these proteins were close to the detection limit. Statistically significant different proteins were determined using moderated T-tests using the LIMMA package in R, applying a Benjamini-Hochberg adjusted p-value of 0.05 and a log fold change of 1 as thresholds.

Western blot: Cells lysates in Laemmli reduced sample buffer with 4% β-mercaptoethanol (#444203, Sigma Aldrich) were denatured 10 minutes at 96°C and loaded on 4-12% gradient SDS-page gels (#NW042125BOX, Thermo Fisher Scientific) and run according to the manufacturer's instructions. After wet or semi-dry transfer onto ethanol-activated PVDF membranes and blocking in 3% bovine serum albumin (BSA; #A8806-5G, Sigma Aldrich) or 5% milk in Tris-buffered saline (TBS; Sigma Aldrich) for at least 45 minutes at room temperature (RT), blots were incubated overnight at 4°C in primary antibody in TBS+blocking buffer: rabbit anti-ARVCF (#PA5-64129, Thermo Fisher Scientific or ab172633, Abcam), mouse anti-GFP (#SC-9996, Santa Cruz), rabbit anti-VE-cadherin (#D87F2, Cell Signaling Technology), mouse anti-p120-catenin (#610134, BD Biosciences), rabbit anti-β-catenin (#C2206, Sigma Aldrich), and anti-β-actin (#4967, Cell Signaling Technology); washed 3 times for 5 minutes in TBS; incubated 1 hour at RT in secondary antibody in TBS+blocking buffer: anti-rabbit-HRP (#170-6515, Bio-Rad) or anti-mouse-HRP (#172-1011, Bio-Rad); washed another 3 times 5 minutes in TBS; and finally imaged using enhanced chemiluminescence detection (#34580, Thermo Fisher Scientific) on an Amersham ImageQuant 800 GxP machine (29653452, Cytiva) or by X-ray films. Protein band intensity was quantified using the FIJI/ImageJ Gel Analyzer plugin [70,71]. Full scans of the original uncropped Western blots are included as supplemental data (**Figure S4 and S5**).

Immunofluorescence: For antibody stainings, HUVECs or HAECs were seeded at confluence and grown until desired density with medium changes every 24 hours on microscope-compatible surfaces: FN-coated glass coverslips, Labtek 8-chamber imaging slides (177380, Thermo Fisher

Scientific), or ibidi µ-slides VI$^{0.4}$ (#80666, ibidi, Munich, Germany). Cells were fixed in 4% PFA in PBS++ with 1 mM $CaCl_2$ and 0.5 mM $MgCl_2$ for 5 minutes at 37°C. Fixed cells were permeabilized using 0.01% Triton (X100, Sigma Aldrich) in PBS++ for 10 minutes at RT, blocked in 3% BSA in PBS++ at RT for 45 minutes, stained with primary antibody for 1 hour at RT and secondary antibodies for 45 minutes at RT: rabbit anti-ARVCF (#PA5-64129, Thermo Fisher Scientific), rabbit anti-VE-cadherin (#D87F2, Cell Signaling Technology), or mouse anti-VE-cadherin (#610252, BD Biosciences), mouse anti-p120-catenin (610134, BD Biosciences), mouse anti-α-catenin (13-9700, Thermo Fisher Scientific), mouse anti-β-catenin (610153, BD Biosciences), mouse anti-CD31 (monoclonal IgG1κ purified in-house from hybridoma), mouse anti-GM130 (clone 35, cat#610823, BD Biosciences), anti-mouse AlexaFluor (AF) AF488 (A-21200), AF594 (A-21201), AF647 (A-21463), anti-rabbit AF488 (A-21441), AF594 (A-21442), AF647 (A-21443) (all Thermo Fisher Scientific). Coverslips and imaging slides were mounted in Mowiol/DABCO solution or ProLong Diamond Antifade (P36961, Thermo Fisher Scientific) and stored in a dark chamber at 4°C. Cells on coverslips were washed 2 times with PBS, once with Milli-Q, and mounted in anti-fade media. Fluorescence was captured on a Nikon Eclipse TI microscope with SOLA SEII light source, 60x 1.49NA Apo TIRF oil objective, standard NIKON filter cubes, using a Andor Zyla 4.2 plus sCMOS camera. Images were analyzed and prepared for inclusion in this manuscript using FIJI/ImageJ software.

Intensity correlation imaging analysis: Immunofluorescent images were obtained using fluorescent tag or label combinations specifically chosen to minimize overlapping excitation and emission spectra. All conditions were imaged on the same day with the same microscope settings to reduce external variation. For analysis, FIJI/ImageJ software was used to obtain junctional masks through intensity thresholding. Within masks, raw fluorescence intensity measurements per pixel across channels were analyzed using the Coloc2 plugin for FIJI/ImageJ to calculate a Pearson's correlation coefficient using Costes' method [72].

Biotin/streptavidin permeability assay: HUVEC monolayer permeability was analyzed for control or ARVCF-depleted cells that were plated at full confluence on ibidi µ-slides VI$^{0.4}$ (#80666, ibidi, Munich, Germany) coated with biotinylated gelatin (produced as described previously in [73,74]). After a day of confluent culture, medium was supplemented with AF488-conjugated streptavidin in a surplus stoichiometric ratio to the amount of biotin molecules. After 10 minutes of exposure, HUVEC monolayers were washed and immediately fixed and processed for staining with VE-cadherin antibody as described above. Biotin-bound AF488-conjugated streptavidin was analyzed using a Nikon Eclipse TI microscope with SOLA SEII light source, 60x 1.49 NA Apo TIRF oil objective, standard NIKON filter cubes, using a Andor Zyla 4.2 plus sCMOS camera. FIJI/ImageJ was used to

quantify GFP-positive area and intensity using the Thresholding tool, excluding areas without accompanying VE-cadherin signal, and results were corrected for cell confluence and intensity.

Electric cell-substrate impedance sensing: Endothelial barrier function was measured using ECIS as previously described [17]: gold electrodes (8w10E+, #72040, Applied BioPhysics) were treated with 10 mM L-cysteine (Sigma Aldrich) in PBS for 15 minutes at RT and coated with fibronectin for 2 hours at 37°C and impedance was measured in real time for 50 hours at 4000 Hz to assess junction integrity [75-79], starting immediately after seeding of 120,000 HUVECs per chamber, using the ZTheta machine (Applied BioPhysics). During measurement, cells were maintained at 37°C with 5% CO_2. Analysis was done in GraphPad Prism.

Flow cytometry: VE-cadherin surface expression levels were assessed using flow cytometry. Cells were harvested with TriplE (#12563011, Gibco) and resuspended FACS buffer (PBS supplemented with 0.5% BSA and 1 mM EDTA pH 7.4-7.8, all from Sigma Aldrich). For surface receptor staining, $1*10^5$ cells were incubated at 4°C in the dark with antibodies: first for 30 minutes with a surplus of mouse anti-VE-cadherin (#610252, BD Biosciences) and then, after washing, with secondary goat anti-mouse IgG-APC (#31981, Thermo Fisher Scientific). After staining, cells were washed twice with FACS buffer and resuspended in 200 µL FACS buffer for analysis. Flow cytometric acquisition was performed on a CytoFLEX flow cytometer (Beckman Coulter), and data were analyzed using FlowJo software. Isotype and single-stain controls were included for each condition.

Scratch wound healing: A scratch wound was introduced on confluent HUVEC monolayers grown on microscope-compatible surfaces by scraping a p200 pipette tip in a straight line across the bottom of the plate. After rinsing with EGM2, the wounded monolayers were either used for immunofluorescence or live-cell imaging. For IF imaging, monolayers were fixed 5 hours after wound induction in 4% PFA in PBS++ and processed for staining as described above. For live cell imaging, cells were placed in a humidified 37°C incubated chamber (Okolab) with 5% CO_2 on an inverted NIKON Eclipse TI microscope and phase-contrast images were captured every 15 minutes for 10 hours using a 10x CFI Achromat DL 0.25 NA dry objective and Andor Zyla sCMOS camera. Images were analyzed and prepared for inclusion in this manuscript using ImageJ/FIJI software; scratch wound migration was analyzed using the TrackMate plugin [80,81].

QUANTIFICATION AND STATISTICAL ANALYSIS

Data analysis and statistics: FIJI/ImageJ was used for image analysis using the plugins mentioned above, and for image preparation for inclusion in this manuscript. Data was analyzed for statistical significance using GraphPad PRISM software. For ECIS experiments, technical duplicates were

averaged per biological replicate. Western blots were corrected for background, for total protein loading, and related to control band intensity within a biological replicate condition. Statistical comparison between two groups was made using Student's t-test after Shapiro-Wilk normality test or Welch's t test. Comparison between multiple groups was made using one-way ANOVA in combination with a D'Agostino-Pearson test for normality and the corresponding Tukey's/Dunnett's multiple comparisons and post-hoc tests. p-values are indicated in figure legends and denoted within the graph as *p<0.05, **p<0.01, ***p<0.001, ****p<0.0001.

Supplemental Information

Document S1. Supplemental Figures S1-S5.

Video S1. Junctional ARVCF recruitment depends on VE-cadherin adhesion. Related to Figure 4. Representative widefield movie of HUVECs overexpressing GFP-ARVCF and VE-cadherin-mCherry treated with 12.5 µg/ml VE-cadherin blocking antibody clone 75. Timescale 30s per frame.

Video S2. Depletion of ARVCF perturbs endothelial AJs. Related to Figure 5. Representative widefield movies of shControl and shARVCF transduced HUVECs overexpressing VE-cadherin-GFP. Timescale 30s per frame.

Video S3. ARVCF recruitment during AJ maturation. Related to Figure 5 Representative widefield movies of HUVECs overexpressing GFP-ARVCF. Timescale 30s per frame.

References

1. Bazzoni, G., and Dejana, E. (2004). Endothelial Cell-to-Cell Junctions: Molecular Organization and Role in Vascular Homeostasis. Physiological Reviews *84*, 869–901. 10.1152/physrev.00035.2003.
2. Hartsock, A., and Nelson, W.J. (2008). Adherens and tight junctions: structure, function and connections to the actin cytoskeleton. Biochim Biophys Acta *1778*, 660–669. 10.1016/j.bbamem.2007.07.012.
3. Dejana, E. (2004). Endothelial cell-cell junctions: happy together. Nat Rev Mol Cell Biol *5*, 261–270. 10.1038/nrm1357.
4. Dejana, E., Tournier-Lasserve, E., and Weinstein, B.M. (2009). The control of vascular integrity by endothelial cell junctions: molecular basis and pathological implications. Dev Cell *16*, 209–221. 10.1016/j.devcel.2009.01.004.
5. Vincent, P.A., Xiao, K., Buckley, K.M., and Kowalczyk, A.P. (2004). VE-cadherin: adhesion at arm's length. American Journal of Physiology-Cell Physiology *286*, C987–C997. 10.1152/ajpcell.00522.2003.
6. Angulo-Urarte, A., van der Wal, T., and Huveneers, S. (2020). Cell-cell junctions as sensors and transducers of mechanical forces. Biochim Biophys Acta Biomembr *1862*, 183316. 10.1016/j.bbamem.2020.183316.
7. Arif, N., Zinnhardt, M., Nyamay'Antu, A., Teber, D., Bruckner, R., Schaefer, K., Li, Y.T., Trappmann, B., Grashoff, C., and Vestweber, D. (2021). PECAM-1 supports leukocyte diapedesis by tension-dependent dephosphorylation of VE-cadherin. EMBO J *40*, e106113. 10.15252/embj.2020106113.
8. Wessel, F., Winderlich, M., Holm, M., Frye, M., Rivera-Galdos, R., Vockel, M., Linnepe, R., Ipe, U., Stadtmann, A., Zarbock, A., et al. (2014). Leukocyte extravasation and vascular permeability are each controlled in vivo by different tyrosine residues of VE-cadherin. Nat Immunol *15*, 223–230. 10.1038/ni.2824.
9. Wilkens, M., Holtermann, L., Stahl, A.K., Stegmeyer, R.I., Nottebaum, A.F., and Vestweber, D. (2024). Ubiquitination of VE-cadherin regulates inflammation-induced vascular permeability in vivo. EMBO Rep *25*, 4013–4032. 10.1038/s44319-024-00221-7.
10. Hakanpaa, L., Kiss, E.A., Jacquemet, G., Miinalainen, I., Lerche, M., Guzmán, C., Mervaala, E., Eklund, L., Ivaska, J., and Saharinen, P. (2018). Targeting β1-integrin inhibits vascular leakage in endotoxemia. Proceedings of the National Academy of Sciences *115*, E6467–E6476. doi:10.1073/pnas.1722317115.
11. Claesson-Welsh, L., Dejana, E., and McDonald, D.M. (2021). Permeability of the Endothelial Barrier: Identifying and Reconciling Controversies. Trends Mol Med *27*, 314–331. 10.1016/j.molmed.2020.11.006.
12. Garrett, J.P., Lowery, A.M., Adam, A.P., Kowalczyk, A.P., and Vincent, P.A. (2017). Regulation of endothelial barrier function by p120-catenin·VE-cadherin interaction. Mol Biol Cell *28*, 85–97. 10.1091/mbc.E16-08-0616.
13. Kim, Y.M., Krantz, S., Jambusaria, A., Toth, P.T., Moon, H.G., Gunarathna, I., Park, G.Y., and Rehman, J. (2021). Mitofusin-2 stabilizes adherens junctions and suppresses endothelial inflammation via modulation of beta-catenin signaling. Nat Commun *12*, 2736. 10.1038/s41467-021-23047-6.
14. Schulte, D., Kuppers, V., Dartsch, N., Broermann, A., Li, H., Zarbock, A., Kamenyeva, O., Kiefer, F., Khandoga, A., Massberg, S., and Vestweber, D. (2011). Stabilizing the VE-cadherin-catenin complex blocks leukocyte extravasation and vascular permeability. EMBO J *30*, 4157–4170. 10.1038/emboj.2011.304.
15. Lampugnani, M.G., Dejana, E., and Giampietro, C. (2018). Vascular Endothelial (VE)-Cadherin, Endothelial Adherens Junctions, and Vascular Disease. Cold Spring Harb Perspect Biol *10*. 10.1101/cshperspect.a029322.
16. Huveneers, S., Oldenburg, J., Spanjaard, E., van der Krogt, G., Grigoriev, I., Akhmanova, A., Rehmann, H., and de Rooij, J. (2012). Vinculin associates with endothelial VE-cadherin junctions to control force-dependent remodeling. J Cell Biol *196*, 641–652. 10.1083/jcb.201108120.
17. van der Stoel, M.M., Kotini, M.P., Schoon, R.M., Affolter, M., Belting, H.G., and Huveneers, S. (2023). Vinculin strengthens the endothelial barrier during vascular development. Vasc Biol *5*. 10.1530/VB-22-0012.
18. Barry, A.K., Wang, N., and Leckband, D.E. (2015). Local VE-cadherin mechanotransduction triggers long-ranged remodeling of endothelial monolayers. J Cell Sci *128*, 1341–1351. 10.1242/jcs.159954.
19. Andresen Eguiluz, R.C., Kaylan, K.B., Underhill, G.H., and Leckband, D.E. (2017). Substrate stiffness and VE-cadherin mechano-transduction coordinate to regulate endothelial monolayer integrity. Biomaterials *140*, 45–57. 10.1016/j.biomaterials.2017.06.010.
20. Conway, D.E., Breckenridge, M.T., Hinde, E., Gratton, E., Chen, C.S., and Schwartz, M.A. (2013). Fluid shear stress on endothelial cells modulates mechanical tension across VE-cadherin and PECAM-1. Curr Biol *23*, 1024–1030. 10.1016/j.cub.2013.04.049.
21. Seebach, J., Klusmeier, N., and Schnittler, H. (2021). Autoregulatory “Multitasking” at Endothelial Cell Junctions by Junction-Associated Intermittent Lamellipodia Controls Barrier Properties. Frontiers in Physiology *Volume 11 - 2020*. 10.3389/fphys.2020.586921.
22. Arribas, V., Onetti, Y., Ramiro-Pareta, M., Villacampa, P., Beck, H., Alberola, M., Esteve-Codina, A., Merkel, A., Sperandio, M., Martínez-Estrada, O.M., et al. (2024). Endothelial TDP-43 controls sprouting angiogenesis and vascular barrier integrity, and its deletion triggers neuroinflammation. JCI Insight *9*. 10.1172/jci.insight.177819.
23. Holtermann, L., Rivera-Galdos, R., Nottebaum, A.F., Wessel, F., Ipe, U., and Vestweber, D. (2025). Distinct VE-cadherin serine and tyrosine phosphorylation sites and their role for inflammation-induced vascular permeability in vivo. Cell Mol Life Sci *82*, 223. 10.1007/s00018-025-05753-2.
24. Seo, T., Lowery, A.M., Xu, H., Giang, W., Troyanovsky, S.M., Vincent, P.A., and Kowalczyk, A.P. (2024). MARCH family E3 ubiquitin ligases selectively target and degrade cadherin family proteins. PLoS One *19*, e0290485. 10.1371/journal.pone.0290485.

25. Tiruppathi, C., Wang, D.M., Ansari, M.O., Bano, S., Tsukasaki, Y., Mukhopadhyay, A., Joshi, J.C., Loch, C., Niessen, H.W.M., and Malik, A.B. (2023). Ubiquitin ligase CHFR mediated degradation of VE-cadherin through ubiquitylation disrupts endothelial adherens junctions. Nat Commun *14*, 6582. 10.1038/s41467-023-42225-2.
26. Jin, Y., Ding, Y., Richards, M., Kaakinen, M., Giese, W., Baumann, E., Szymborska, A., Rosa, A., Nordling, S., Schimmel, L., et al. (2022). Tyrosine-protein kinase Yes controls endothelial junctional plasticity and barrier integrity by regulating VE-cadherin phosphorylation and endocytosis. Nat Cardiovasc Res *1*, 1156–1173. 10.1038/s44161-022-00172-z.
27. Orsenigo, F., Giampietro, C., Ferrari, A., Corada, M., Galaup, A., Sigismund, S., Ristagno, G., Maddaluno, L., Koh, G.Y., Franco, D., et al. (2012). Phosphorylation of VE-cadherin is modulated by haemodynamic forces and contributes to the regulation of vascular permeability in vivo. Nat Commun *3*, 1208. 10.1038/ncomms2199.
28. Stegmeyer, R.I., Holstein, K., Spring, K., Timmerman, I., Xia, M., Stasch, M., Moller, T., Nottebaum, A.F., and Vestweber, D. (2024). Csk controls leukocyte extravasation via local regulation of Src family kinases and cortactin signaling. Front Immunol *15*, 1480152. 10.3389/fimmu.2024.1480152.
29. Potter, M.D., Barbero, S., and Cheresh, D.A. (2005). Tyrosine phosphorylation of VE-cadherin prevents binding of p120- and beta-catenin and maintains the cellular mesenchymal state. J Biol Chem *280*, 31906–31912. 10.1074/jbc.M505568200.
30. Guo, M., Breslin, J.W., Wu, M.H., Gottardi, C.J., and Yuan, S.Y. (2008). VE-cadherin and beta-catenin binding dynamics during histamine-induced endothelial hyperpermeability. Am J Physiol Cell Physiol *294*, C977–984. 10.1152/ajpcell.90607.2007.
31. Carnahan, R.H., Rokas, A., Gaucher, E.A., and Reynolds, A.B. (2010). The molecular evolution of the p120-catenin subfamily and its functional associations. PLoS One *5*, e15747. 10.1371/journal.pone.0015747.
32. Grimsley-Myers, C.M., Isaacson, R.H., Cadwell, C.M., Campos, J., Hernandes, M.S., Myers, K.R., Seo, T., Giang, W., Griendling, K.K., and Kowalczyk, A.P. (2020). VE-cadherin endocytosis controls vascular integrity and patterning during development. J Cell Biol *219*. 10.1083/jcb.201909081.
33. Ishiyama, N., Lee, S.H., Liu, S., Li, G.Y., Smith, M.J., Reichardt, L.F., and Ikura, M. (2010). Dynamic and static interactions between p120 catenin and E-cadherin regulate the stability of cell-cell adhesion. Cell *141*, 117–128. 10.1016/j.cell.2010.01.017.
34. Sirotkin, H., O'Donnell, H., DasGupta, R., Halford, S., St Jore, B., Puech, A., Parimoo, S., Morrow, B., Skoultchi, A., Weissman, S.M., et al. (1997). Identification of a new human catenin gene family member (ARVCF) from the region deleted in velo-cardio-facial syndrome. Genomics *41*, 75–83. 10.1006/geno.1997.4627.
35. Kaufmann, U., Zuppinger, C., Waibler, Z., Rudiger, M., Urbich, C., Martin, B., Jockusch, B.M., Eppenberger, H., and Starzinski-Powitz, A. (2000). The armadillo repeat region targets ARVCF to cadherin-based cellular junctions. J Cell Sci *113 (Pt 22)*, 4121–4135. 10.1242/jcs.113.22.4121.
36. Martin, J.B., Herman, K., Houssin, N.S., Rich, W., Reilly, M.A., and Plageman, T.F., Jr. (2022). Arvcf Dependent Adherens Junction Stability is Required to Prevent Age-Related Cortical Cataracts. Front Cell Dev Biol *10*, 840129. 10.3389/fcell.2022.840129.
37. Kausalya, P.J., Phua, D.C., and Hunziker, W. (2004). Association of ARVCF with zonula occludens (ZO)-1 and ZO-2: binding to PDZ-domain proteins and cell-cell adhesion regulate plasma membrane and nuclear localization of ARVCF. Mol Biol Cell *15*, 5503–5515. 10.1091/mbc.e04-04-0350.
38. Huebner, R.J., Weng, S., Lee, C., Sarikaya, S., Papoulas, O., Cox, R.M., Marcotte, E.M., and Wallingford, J.B. (2022). ARVCF catenin controls force production during vertebrate convergent extension. Dev Cell *57*, 1119–1131 e1115. 10.1016/j.devcel.2022.04.001.
39. Weng, S., Huebner, R.J., and Wallingford, J.B. (2022). Convergent extension requires adhesion-dependent biomechanical integration of cell crawling and junction contraction. Cell Rep *39*, 110666. 10.1016/j.celrep.2022.110666.
40. Pannekoek, W.J., Vliem, M.J., and Bos, J.L. (2020). Multiple Rap1 effectors control Epac1-mediated tightening of endothelial junctions. Small GTPases *11*, 346–353. 10.1080/21541248.2018.1431512.
41. Cavey, M., and Lecuit, T. (2009). Molecular bases of cell-cell junctions stability and dynamics. Cold Spring Harb Perspect Biol *1*, a002998. 10.1101/cshperspect.a002998.
42. Hultin, S., Subramani, A., Hildebrand, S., Zheng, Y., Majumdar, A., and Holmgren, L. (2017). AmotL2 integrates polarity and junctional cues to modulate cell shape. Scientific Reports *7*, 7548. 10.1038/s41598-017-07968-1.
43. Sun, X., Decker, J., Sanchez-Luege, N., and Rebay, I. (2024). Inter-plane feedback coordinates cell morphogenesis and maintains 3D tissue organization in the Drosophila pupal retina. Development *151*. 10.1242/dev.201757.
44. Malinova, T.S., Angulo-Urarte, A., Nuchel, J., Tauber, M., van der Stoel, M.M., Janssen, V., de Haan, A., Groenen, A.G., Tebbens, M., Graupera, M., et al. (2021). A junctional PACSIN2/EHD4/MICAL-L1 complex coordinates VE-cadherin trafficking for endothelial migration and angiogenesis. Nat Commun *12*, 2610. 10.1038/s41467-021-22873-y.
45. Hayer, A., Shao, L., Chung, M., Joubert, L.M., Yang, H.W., Tsai, F.C., Bisaria, A., Betzig, E., and Meyer, T. (2016). Engulfed cadherin fingers are polarized junctional structures between collectively migrating endothelial cells. Nat Cell Biol *18*, 1311–1323. 10.1038/ncb3438.
46. Mariner, D.J., Wang, J., and Reynolds, A.B. (2000). ARVCF localizes to the nucleus and adherens junction and is mutually exclusive with p120(ctn) in E-cadherin complexes. J Cell Sci *113 (Pt 8)*, 1481–1490. 10.1242/jcs.113.8.1481.

47. Xiao, K., Allison, D.F., Buckley, K.M., Kottke, M.D., Vincent, P.A., Faundez, V., and Kowalczyk, A.P. (2003). Cellular levels of p120 catenin function as a set point for cadherin expression levels in microvascular endothelial cells. J Cell Biol *163*, 535–545. 10.1083/jcb.200306001.
48. Kourtidis, A., Ngok, S.P., and Anastasiadis, P.Z. (2013). p120 catenin: an essential regulator of cadherin stability, adhesion-induced signaling, and cancer progression. Prog Mol Biol Transl Sci *116*, 409–432. 10.1016/B978-0-12-394311-8.00018-2.
49. Chiasson, C.M., Wittich, K.B., Vincent, P.A., Faundez, V., and Kowalczyk, A.P. (2009). p120-catenin inhibits VE-cadherin internalization through a Rho-independent mechanism. Mol Biol Cell *20*, 1970–1980. 10.1091/mbc.e08-07-0735.
50. Xiao, K., Garner, J., Buckley, K.M., Vincent, P.A., Chiasson, C.M., Dejana, E., Faundez, V., and Kowalczyk, A.P. (2005). p120-Catenin regulates clathrin-dependent endocytosis of VE-cadherin. Mol Biol Cell *16*, 5141–5151. 10.1091/mbc.e05-05-0440.
51. Struhl, K. (2024). Intrinsically disordered regions (IDRs): A vague and confusing concept for protein function. Mol Cell *84*, 1186–1187. 10.1016/j.molcel.2024.02.023.
52. Chakrabarti, P., and Chakravarty, D. (2022). Intrinsically disordered proteins/regions and insight into their biomolecular interactions. Biophys Chem *283*, 106769. 10.1016/j.bpc.2022.106769.
53. Keirsebilck, A., Bonné, S., Staes, K., van Hengel, J., Nollet, F., Reynolds, A., and van Roy, F. (1998). Molecular cloning of the human p120ctn catenin gene (CTNND1): expression of multiple alternatively spliced isoforms. Genomics *50*, 129–146. 10.1006/geno.1998.5325.
54. Chen, C.S., Hong, S., Indra, I., Sergeeva, A.P., Troyanovsky, R.B., Shapiro, L., Honig, B., and Troyanovsky, S.M. (2015). α-Catenin-mediated cadherin clustering couples cadherin and actin dynamics. J Cell Biol *210*, 647–661. 10.1083/jcb.201412064.
55. Troyanovsky, S.M. (2023). Adherens junction: the ensemble of specialized cadherin clusters. Trends Cell Biol *33*, 374–387. 10.1016/j.tcb.2022.08.007.
56. Changede, R., and Sheetz, M. (2017). Integrin and cadherin clusters: A robust way to organize adhesions for cell mechanics. Bioessays *39*, 1–12. 10.1002/bies.201600123.
57. Cong, X., and Kong, W. (2020). Endothelial tight junctions and their regulatory signaling pathways in vascular homeostasis and disease. Cell Signal *66*, 109485. 10.1016/j.cellsig.2019.109485.
58. Dejana, E., and Giampietro, C. (2012). Vascular endothelial-cadherin and vascular stability. Curr Opin Hematol *19*, 218–223. 10.1097/MOH.0b013e3283523e1c.
59. Yang, X.D., Karhadkar, T.R., Medina, J., Robertson, S.M., and Lin, R. (2015). β-Catenin-related protein WRM-1 is a multifunctional regulatory subunit of the LIT-1 MAPK complex. Proc Natl Acad Sci U S A *112*, E137–146. 10.1073/pnas.1416339112.
60. Miroshnikova, Y.A., Manet, S., Li, X., Wickstrom, S.A., Faurobert, E., and Albiges-Rizo, C. (2021). Calcium signaling mediates a biphasic mechanoadaptive response of endothelial cells to cyclic mechanical stretch. Mol Biol Cell *32*, 1724–1736. 10.1091/mbc.E21-03-0106.
61. Priest, A.V., Shafraz, O., and Sivasankar, S. (2017). Biophysical basis of cadherin mediated cell-cell adhesion. Exp Cell Res *358*, 10–13. 10.1016/j.yexcr.2017.03.015.
62. McEvoy, E., Sneh, T., Moeendarbary, E., Javanmardi, Y., Efimova, N., Yang, C., Marino-Bravante, G.E., Chen, X., Escribano, J., Spill, F., et al. (2022). Feedback between mechanosensitive signaling and active forces governs endothelial junction integrity. Nat Commun *13*, 7089. 10.1038/s41467-022-34701-y.
63. Jin, X., Lin, T., Wang, Y., Li, X., and Yang, Y. (2024). Functions of p120-catenin in physiology and diseases. Frontiers in Molecular Biosciences *Volume 11 - 2024*. 10.3389/fmolb.2024.1486576.
64. Fang, X., Ji, H., Kim, S.W., Park, J.I., Vaught, T.G., Anastasiadis, P.Z., Ciesiolka, M., and McCrea, P.D. (2004). Vertebrate development requires ARVCF and p120 catenins and their interplay with RhoA and Rac. J Cell Biol *165*, 87–98. 10.1083/jcb.200307109.
65. Dull, T., Zufferey, R., Kelly, M., Mandel, R.J., Nguyen, M., Trono, D., and Naldini, L. (1998). A third-generation lentivirus vector with a conditional packaging system. J Virol *72*, 8463–8471. 10.1128/jvi.72.11.8463-8471.1998.
66. van der Stoel, M., Schimmel, L., Nawaz, K., van Stalborch, A.M., de Haan, A., Klaus-Bergmann, A., Valent, E.T., Koenis, D.S., van Nieuw Amerongen, G.P., de Vries, C.J., et al. (2020). DLC1 is a direct target of activated YAP/TAZ that drives collective migration and sprouting angiogenesis. J Cell Sci *133*. 10.1242/jcs.239947.
67. Dorland, Y.L., Malinova, T.S., van Stalborch, A.M., Grieve, A.G., van Geemen, D., Jansen, N.S., de Kreuk, B.J., Nawaz, K., Kole, J., Geerts, D., et al. (2016). The F-BAR protein pacsin2 inhibits asymmetric VE-cadherin internalization from tensile adherens junctions. Nat Commun *7*, 12210. 10.1038/ncomms12210.
68. Rappe, U., Schlechter, T., Aschoff, M., Hotz-Wagenblatt, A., and Hofmann, I. (2014). Nuclear ARVCF protein binds splicing factors and contributes to the regulation of alternative splicing. J Biol Chem *289*, 12421–12434. 10.1074/jbc.M113.530717.
69. Tyanova, S., Temu, T., and Cox, J. (2016). The MaxQuant computational platform for mass spectrometry-based shotgun proteomics. Nat Protoc *11*, 2301–2319. 10.1038/nprot.2016.136.
70. Schneider, C.A., Rasband, W.S., and Eliceiri, K.W. (2012). NIH Image to ImageJ: 25 years of image analysis. Nature Methods *9*, 671–675. 10.1038/nmeth.2089.
71. Schindelin, J., Arganda-Carreras, I., Frise, E., Kaynig, V., Longair, M., Pietzsch, T., Preibisch, S., Rueden, C., Saalfeld, S., Schmid, B., et al. (2012). Fiji: an open-source platform for biological-image analysis. Nat Methods *9*, 676–682. 10.1038/nmeth.2019.

72. Costes, S.V., Daelemans, D., Cho, E.H., Dobbin, Z., Pavlakis, G., and Lockett, S. (2004). Automatic and quantitative measurement of protein-protein colocalization in live cells. Biophys J *86*, 3993–4003. 10.1529/biophysj.103.038422.
73. Dubrovskyi, O., Birukova, A.A., and Birukov, K.G. (2013). Measurement of local permeability at subcellular level in cell models of agonist- and ventilator-induced lung injury. Lab Invest *93*, 254–263. 10.1038/labinvest.2012.159.
74. Shirakura, K., Baluk, P., Nottebaum, A.F., Ipe, U., Peters, K.G., McDonald, D.M., and Vestweber, D. (2023). Shear stress control of vascular leaks and atheromas through Tie2 activation by VE-PTP sequestration. EMBO Mol Med *15*, e16128. 10.15252/emmm.202216128.
75. Luong, J.H.T., Xiao, C., Lachance, B., Leabu, Š.M., Li, X., Uniyal, S., and Chan, B.M.C. (2004). Extended applications of electric cell-substrate impedance sensing for assessment of the structure–function of α2β1 integrin. Analytica Chimica Acta *501*, 61–69. 10.1016/j.aca.2003.09.016.
76. Robilliard, L.D., Kho, D.T., Johnson, R.H., Anchan, A., O'Carroll, S.J., and Graham, E.S. (2018). The Importance of Multifrequency Impedance Sensing of Endothelial Barrier Formation Using ECIS Technology for the Generation of a Strong and Durable Paracellular Barrier. Biosensors (Basel) *8*. 10.3390/bios8030064.
77. Tiruppathi, C., Malik, A.B., Del Vecchio, P.J., Keese, C.R., and Giaever, I. (1992). Electrical method for detection of endothelial cell shape change in real time: assessment of endothelial barrier function. Proc Natl Acad Sci U S A *89*, 7919–7923. 10.1073/pnas.89.17.7919.
78. Zhang, Z., Huang, X., Liu, K., Lan, T., Wang, Z., and Zhu, Z. (2021). Recent Advances in Electrical Impedance Sensing Technology for Single-Cell Analysis. Biosensors (Basel) *11*. 10.3390/bios11110470.
79. Benson, K., Cramer, S., and Galla, H.J. (2013). Impedance-based cell monitoring: barrier properties and beyond. Fluids Barriers CNS *10*, 5. 10.1186/2045-8118-10-5.
80. Ershov, D., Phan, M.S., Pylvänäinen, J.W., Rigaud, S.U., Le Blanc, L., Charles-Orszag, A., Conway, J.R.W., Laine, R.F., Roy, N.H., Bonazzi, D., et al. (2022). TrackMate 7: integrating state-of-the-art segmentation algorithms into tracking pipelines. Nat Methods *19*, 829–832. 10.1038/s41592-022-01507-1.
81. Tinevez, J.Y., Perry, N., Schindelin, J., Hoopes, G.M., Reynolds, G.D., Laplantine, E., Bednarek, S.Y., Shorte, S.L., and Eliceiri, K.W. (2017). TrackMate: An open and extensible platform for single-particle tracking. Methods *115*, 80–90. 10.1016/j.ymeth.2016.09.016.

Figure S1.

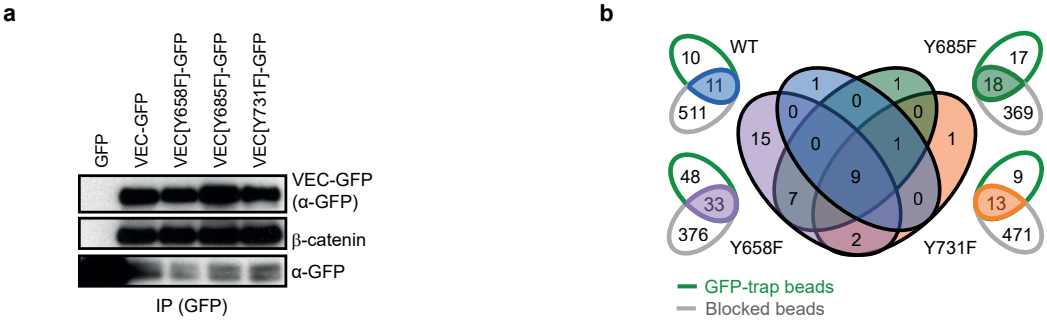


Figure 1. Identification of VE-cadherin binding proteins. a) Representative Western blot of lysates used for co-immunoprecipitation and mass-spectrometry analysis, probed for β-catenin and GFP. **b)** Venn diagram illustrating the amount of higher abundant proteins (Benjamini-Hochberg-adjusted p-value <0.05 & LOG2 FC>1 versus GFP beads and blocked beads) per VE-cadherin variant and the overlap in binding proteins between the different non-phosphorylatable [Y►F] VE-cadherin-GFP variants. Visualized using the online tool available at http://bioinformatics.psb.ugent.be/webtools/venn. Related to Figure 1.

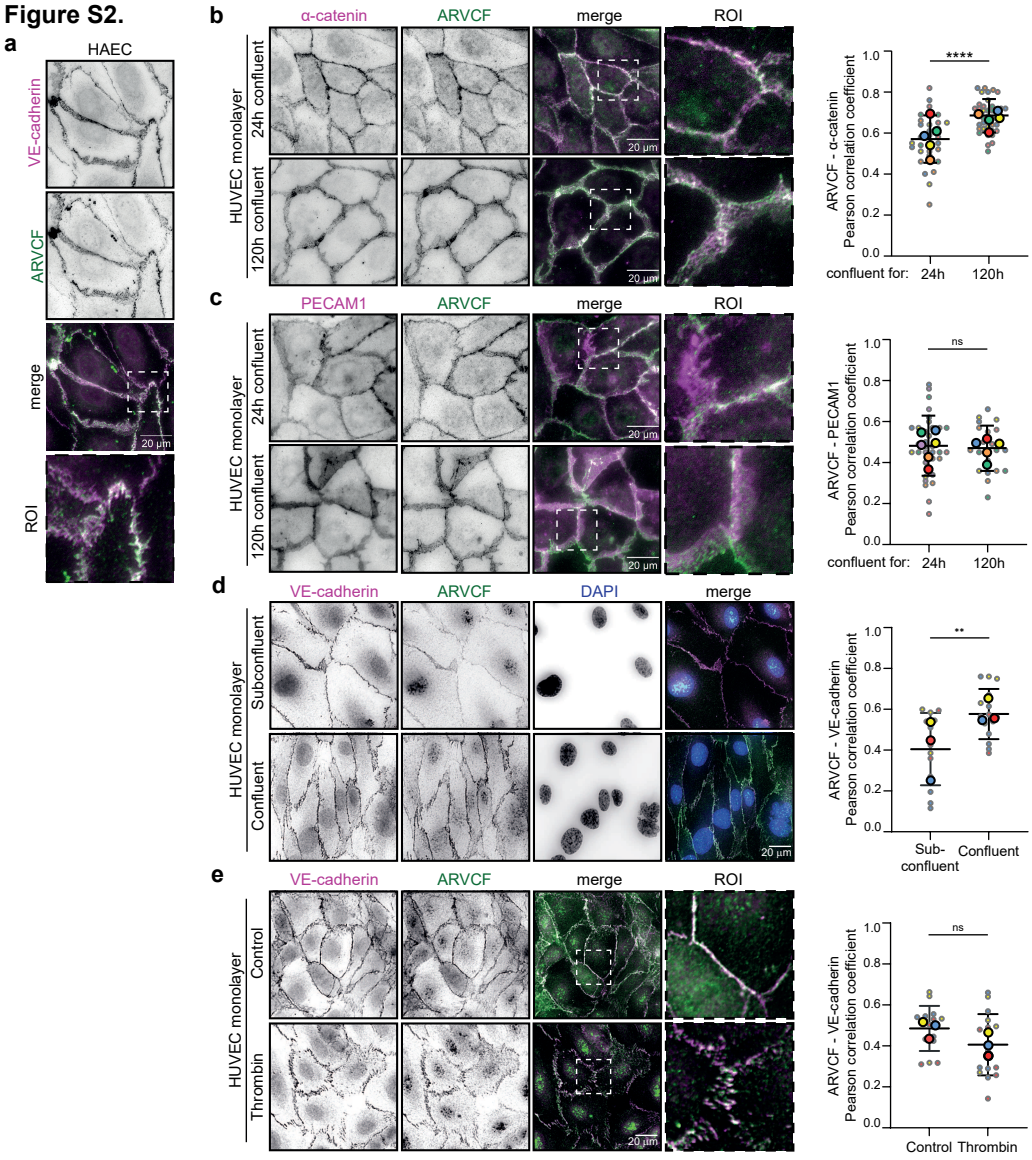
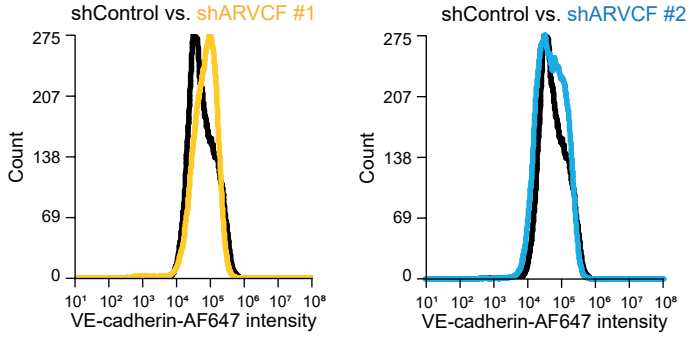


Figure S2. ARVCF localizes at VE-cadherin-based endothelial adherens junctions. a) Representative images of human arterial endothelial cells (HAECs) that were stained for endogenous ARVCF (green) and VE-cadherin (magenta). **b-c)** Representative images of human umbilical vein ECs (HUVECs) that were fixed after 24 or 120 hours at full confluence and stained for endogenous ARVCF (green) and α-catenin (b) or PECAM1 (c) in magenta. Graphs showing Pearson's correlation coefficients of pixel intensity values between ARVCF and α-catenin or PECAM1. **d)** Representative images of HUVECS at subconfluent and confluent densities 24 hours after plating, stained for endogenous ARVCF (green), VE-cadherin (magenta) and DAPI (blue). Graphs showing Pearson's correlation coefficients of pixel intensity values between ARVCF and VE-cadherin. **e)** Representative images of HUVECs fixed after control or thrombin treatment (1U/mL; 10 minutes) and stained for endogenous ARVCF (green) and VE-cadherin (magenta). Graphs showing Pearson's correlation coefficients of pixel intensity values between ARVCF and VE-cadherin. Graphs show values per image (small dots) and means per independent experiment (large dots per color) ±SD. Welch's unpaired t-test, **p<0.01, ns: non-significant. Related to Figure 3.

Figure S3.

a



b

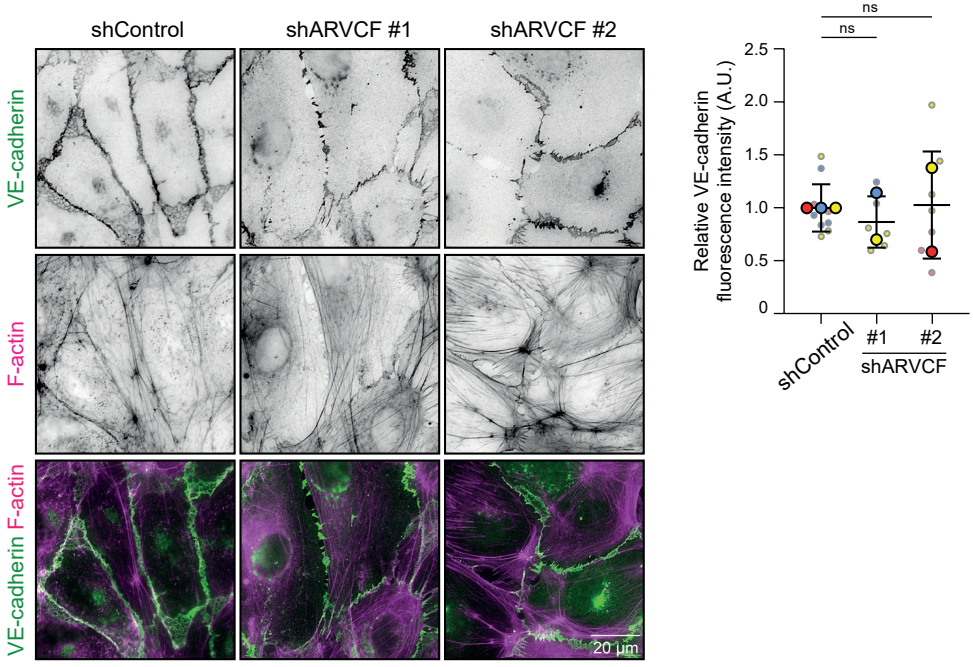


Figure S3. Characterization of shARVCF HUVECs. a) Representative graphs from fluorescence activated cell sorting analysis of VE-cadherin surface expression on HUVECs transduced with shControl or shARVCF. **b)** Representative images of HUVECs transduced with shControl or shARVCF stained for endogenous VE-cadherin (green) and F-actin (magenta). Graph showing VE-cadherin fluorescence intensity of shControl and shARVCF cells relative to control. Values per image (small dots) and means per independent experiment (large dots per color) ±SD. Data from n=3 independent experiments, ANOVA with Dunnett's multiple xomparison test. ns: non-significant. Related to Figure 5.

Figure S4.

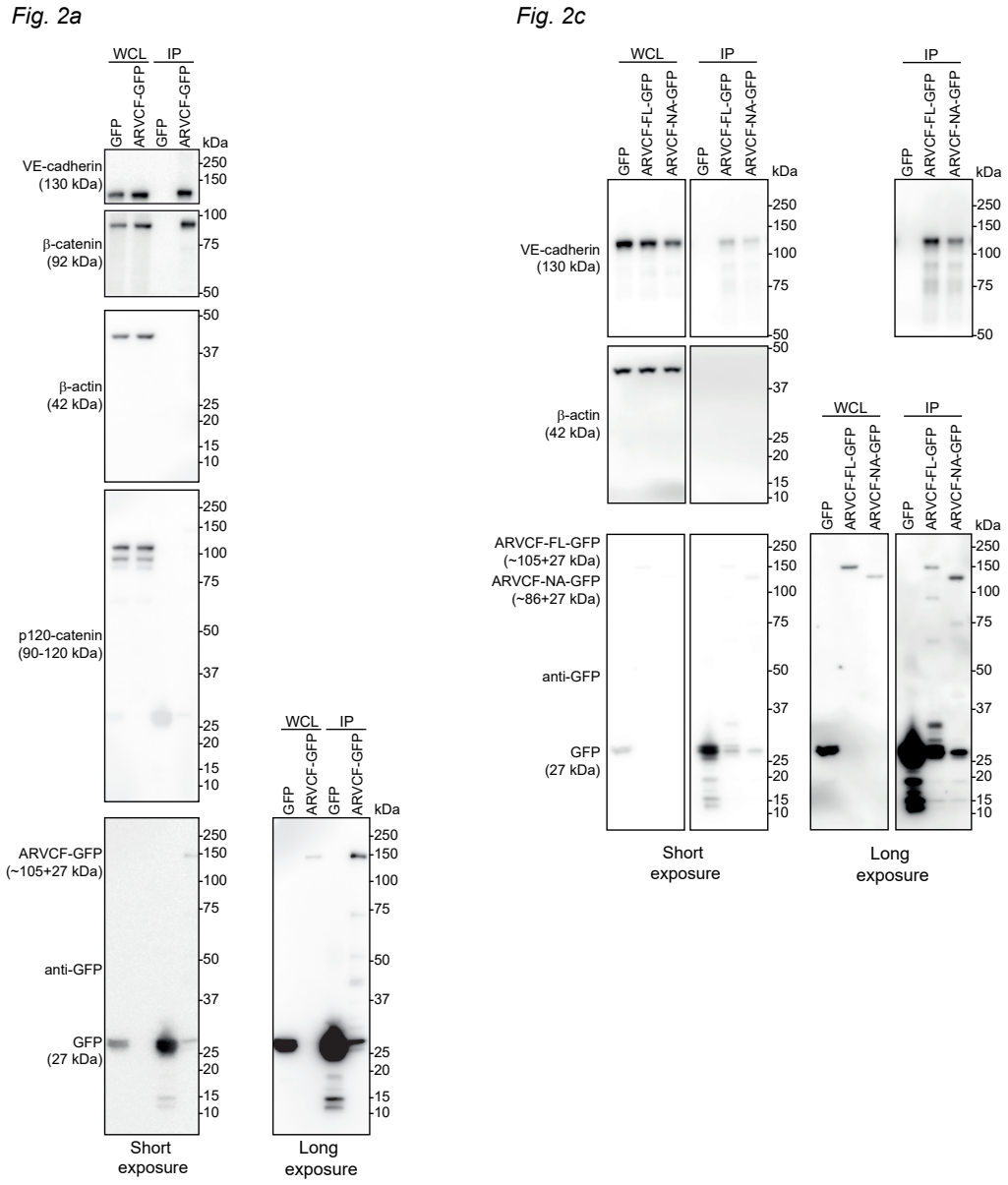


Figure S4. Full scans of the original uncropped Western blots Part 1. Related to Figure 2.

Figure S5.

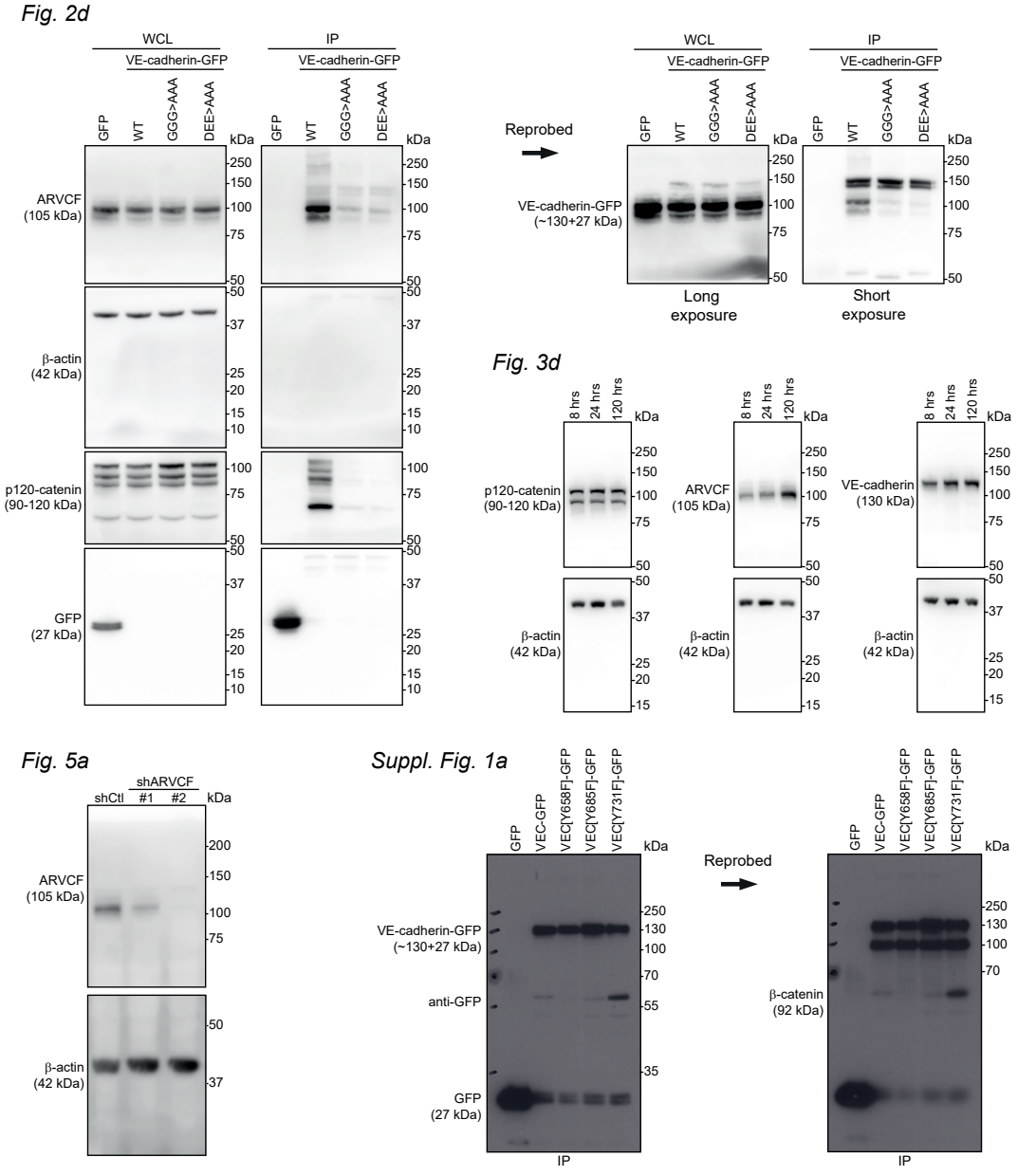


Figure S5. Full scans of the original uncropped Western blots Part 2. Related to Figure 2, 3, 5, S1.



Chapter 3

Characterization of the role of identified VE-cadherin interactors

Characterization of the role of identified VE-cadherin interactors

Rianne Schoon[1], Iris de Heer[1], Stephan Huveneers[1]

[1] Amsterdam UMC, University of Amsterdam, Department of Medical Biochemistry, Amsterdam Cardiovascular Sciences, 1105 AZ, Amsterdam, The Netherlands.

Abstract

The endothelial cells lining the vessel wall maintain a selective barrier between blood and tissue. Structural connections between endothelial cells are formed by VE-cadherin-based adherens junctions (AJs), which are linked to the actin cytoskeleton via a multiprotein complex including α-, ß- and p120-catenin. It is likely that potential additional molecular interactions can control VE-cadherin's function. Therefore, we previously used mass-spectrometry following VE-cadherin co-immunoprecipitations to investigate the composition of the VE-cadherin interactome. This identified a set of VE-cadherin-binding proteins that interact independently of phosphorylation events at VE-cadherin's cytoplasmic domain. Here, we investigated the potential roles of three of the identified interactors being: ARHGAP23, KEAP1 and PKP4. Immunofluorescence stainings reveal that ARHGAP23 and PKP4 colocalize with VE-cadherin at endothelial junctions, whereas KEAP1 is distributed throughout endothelial cells. Functional assays demonstrate that knockdown of each identified VE-cadherin-interacting protein reduces endothelial barrier function to different extents, as measured by ECIS, indicating their role in maintaining barrier integrity. Together, these data position ARHGAP23, KEAP1, and PKP4 as novel regulators of VE-cadherin with potential roles in Rho GTPase signaling, redox regulation, and junctional scaffolding. While the mechanistic basis of their association and function remains to be determined, these findings highlight new candidate regulators of endothelial barrier function and provide a foundation for future investigation.

Introduction

The vascular endothelium maintains barrier function through forming cell-to-cell contacts built around the VE-cadherin adhesion receptor. Cell-cell contacts are dynamically regulated through force-dependent integration of cytoskeletal anchoring and inputs from cellular signaling [1-3]. The importance of a tightly modulated and resilient endothelium is crucial for healthy tissue properties such as the transport between blood and tissue, angiogenesis, and immunity. Vice versa, dysregulation of VE-cadherin-based adherens junctions (AJs) lead to endothelial permeability, hyperinflammation and contribute to cardiovascular disease [4-7]. The balance between endothelial barrier stability and plasticity is achieved through the association of VE-cadherin with a diverse network of intracellular proteins, as well as regulation by post-translational modifications including phosphorylation and ubiquitination [8-15]. Importantly, tyrosines Y658, Y685, and Y731 in the cytoplasmic domain of VE-cadherin are well-established phosphorylation sites that, when (de)phosphorylated in response to various stimuli, regulate appropriate endothelial barrier remodeling [4,11,12,16].

As discussed in **Chapter 2** of the thesis, we have previously performed mass-spectrometry analysis of VE-cadherin co-immunoprecipitates which revealed a set of 37 interaction partners. Of these, we delineated a core group of proteins that bind not only to wild-type VE-cadherin but also to its variants in which tyrosines Y658, Y685, and Y731 were mutated to phenylalanines. The consistent association of these proteins with VE-cadherin in the absence of its phosphorylation suggests the existence of robust phosphorylation-independent interactions that may be preserved across diverse endothelial microenvironmental conditions, including vascular bed type, hemodynamic blood flow, or inflammatory state. In the current chapter we investigated the roles of three identified core VE-cadherin-binding proteins being: ARHGAP23, KEAP1, and Plakophilin-4 (PKP4).

ARHGAP23 belongs to the family of Rho GTPase-activating (RhoGAP) proteins, which inactivate Rho GTPases by accelerating GTP hydrolysis [17]. These molecular switches are central to the regulation of actin cytoskeletal dynamics and actomyosin contractility; with RhoA promoting stress fibers, Rac1 driving lamellipodia, and Cdc42 controlling filopodia [18-23]. ARHGAP23 has been shown to interact with the planar cell polarity protein Prickle1 at the lateral cell cortex to locally inhibit RhoA [24]. While ARHGAP23 itself has not been studied extensively in endothelial cells, its domain structure includes PH and PDZ-binding motifs, which are also present in related GTPase regulating proteins that control endothelial barrier function [25]. The interaction of ARHGAP23 with VE-cadherin may thus represent a link between cell-cell adhesion and the spatial regulation of Rho GTPase signaling.

KEAP1 (Kelch-like ECH-associated protein 1) is known as a cytosolic adaptor that targets the transcription factor NRF2 for ubiquitination and degradation as a function of oxidative stress, thereby suppressing antioxidant gene expression under basal conditions [26-30]. In endothelial cells, KEAP1-NRF2 signaling has been implicated in regulating redox homeostasis, nitric oxide production, and vascular aging [28,29]. Its identification as a VE-cadherin interactor is unexpected, particularly since KEAP1 localization in human arterial endothelial cells shows no junctional enrichment but rather a diffuse cytosolic localization [28], as is the case in epithelial cells [31]. Hence, although KEAP1 is therefore not traditionally linked to cell-cell adhesion, its co-immunoprecipitation with VE-cadherin suggests a possible, previously unrecognized interface between redox signaling and endothelial junction regulation. Such a link may be relevant in inflammatory or oxidative stress microenvironments where endothelial barrier function is challenged.

Plakophilin-4 (PKP4), also known as p0071, is an armadillo-repeat protein originally described as a member of desmosomes, but later also found to associate with classical cadherins at adherens junctions [24,32]. PKP4 has been implicated in cadherin clustering, regulation of small GTPases such as RhoA to increase tissue tension through junctional actin remodeling [24], and intracellular trafficking of junctional proteins [33,34]. A direct interaction of PKP4 with VE-cadherin has been mapped through the armadillo-repeat domain, and its binding is competitive with p120-catenin. Notably, PKP4 overexpression can displace p120-catenin from junctions [35]. Although most mechanistic insights are derived from experiments with epithelial cells, PKP4 may regulate endothelial actin cytoskeletal dynamics and contribute to the organization at VE-cadherin-based junctions.

Here, we present exploratory functional validations of the roles of ARHGAP23, KEAP1, and PKP4 as VE-cadherin binding partners.

Results

KEAP1 and PKP4 co-immunoprecipitate with VE-cadherin

To further investigate findings from our previous mass-spectrometry defining the VE-cadherin interactome **(Chapter 2)**, we performed GFP-trap pull-downs of GFP-tagged VE-cadherin (wild-type (WT) and phosphorylation deficient variants (Y658F, Y685F, Y731F) expressed in confluent endothelial cell (EC) monolayers. Western blotting of these pull-downs showed strong co-immunoprecipitation of PKP4 and KEAP1 with VE-cadherin across all variants **(Figure 1a)**. In contrast, ARHGAP23, despite its earlier robust detection by mass-spectrometry, was not detected in those experiments **(Figure 1a)**, suggesting either low abundance of the interaction, weak binding, or epitope masking under the lysis conditions employed.

To further explore protein localization relative to VE-cadherin, we next immunostained confluent EC monolayers for endogenous ARHGAP23, PKP4, and KEAP1. These experiments show that both ARHGAP23 and PKP4 are enriched at cell-cell junctions and clearly colocalize with junctional VE-cadherin **(Figure 1b, c)**. Quantification by pixel-intensity correlation analysis demonstrated a significant increase in ARHGAP23- and PKP4-VE-cadherin colocalization in mature endothelial monolayers at 120 hours of confluence compared to 24 hours **(Figure 1b, c)**. These results suggest a progressive recruitment of these proteins during junction maturation. By contrast, KEAP1 was localized in the cytosol as well as in the nucleus of confluent ECs **(Figure 1d)**. However, no signal was detected along VE-cadherin-based junctions in venous **(Figure 1d)** nor arterial ECs **(Figure S1a)**. The discrepancy between robust biochemical interaction between VE-cadherin and KEAP1, and the absence of its junctional localization, indicates that KEAP1 may interact with VE-cadherin elsewhere in the cells. Intriguingly, KEAP1 nuclear distribution was heterogeneous across ECs: some cells showed cytosolic predominance, whereas others exhibited nuclear enrichment **(Figure 1d, S1A)**. Quantification of young versus mature monolayers revealed a modest shift toward nuclear KEAP1 in older cultures **(Figure 1d)**, potentially reflecting altered redox signaling or Nrf2 pathway engagement during monolayer maturation.

Together, these experiments validated the biochemical association of PKP4 and KEAP1 with VE-cadherin. Moreover, ARHGAP23 and PKP4 accumulate at endothelial AJs in a maturation-dependent manner, whereas KEAP1 remains cytosolic and nuclear, implying mechanistically diverse modes and/or functions of these VE-cadherin interactors.

Figure 1.

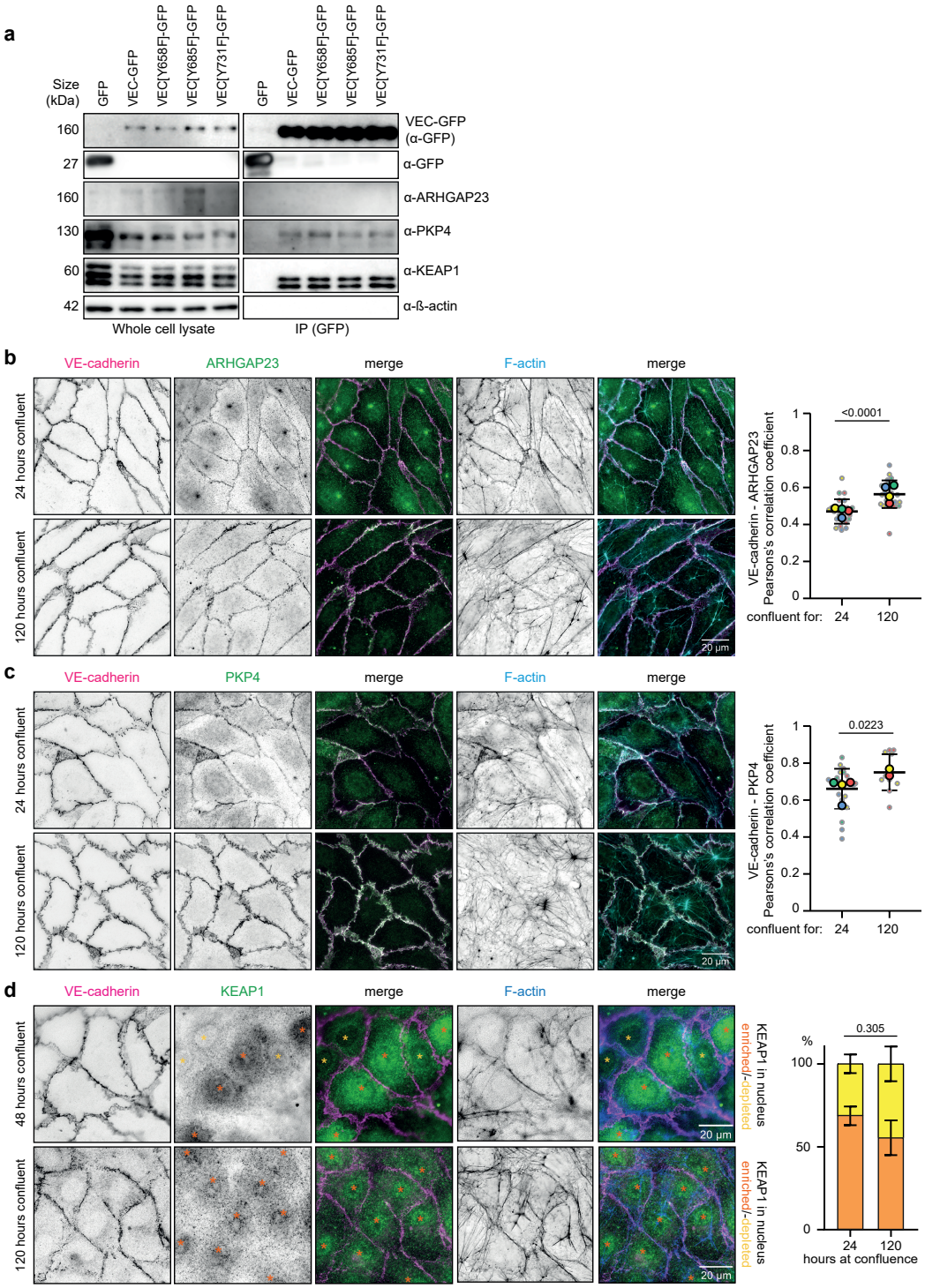

a
Size (kDa)
GFP
VEC-GFP
VEC[Y658F]-GFP
VEC[Y685F]-GFP
VEC[Y731F]-GFP
160
27
160
130
60
42
VEC-GFP (α-GFP)
α-GFP
α-ARHGAP23
α-PKP4
α-KEAP1
α-ß-actin
Whole cell lysate
IP (GFP)
b
VE-cadherin
ARHGAP23
merge
F-actin
24 hours confluent
120 hours confluent
20 µm
VE-cadherin - ARHGAP23 Pearsons's correlation coefficient
<0.0001
confluent for: 24 120
c
VE-cadherin
PKP4
VE-cadherin - PKP4 Pearsons's correlation coefficient
0.0223
d
VE-cadherin
KEAP1
48 hours confluent
KEAP1 in nucleus enriched/-depleted
0.305
%
hours at confluence

Figure 1. VE-cadherin co-immunoprecipitations and junctional localization experiments. a) Representative Western blot analysis probed for GFP, ARHGAP23, PKP4, KEAP1, and β-actin, on whole-cell lysates and GFP immunoprecipitation (IP) samples derived from human umbilical vein endothelial cells (HUVEC) expressing GFP, VE-cadherin-GFP and indicated VE-cadherin non-phosphorylatable [Y►F] variants. **b, c)** Representative widefield images of HUVECs that were fixed after 24 or 120 hours at full confluence and stained for endogenous VE-cadherin (magenta) and in green ARHGAP23 (b) or PKP4 (c). Graphs show Pearson's correlation coefficients of pixel intensity values between VE-cadherin and ARHGAP23 or PKP4. Graphs show values per image (small dots) and means per independent experiments (large dots per color) ±SD. Data from n≥2 independent experiments, Student's paired t-test, p-values indicated. **d)** Representative widefield images of HUVECs that were fixed after 24 or 120 hours at full confluence and stained for endogenous VE-cadherin (magenta) and KEAP1 (green). KEAP1 localization is denoted with * in the color orange in case of nuclear enrichment and yellow for nuclear depletion relative to the immediately surrounding cytosol. Graph shows the percentage of cell nuclei that are KEAP1-enriched (orange) versus -depleted (yellow) as mean ±SD per monolayer age condition. Data from n=2 independent experiments, Student's paired t-test, p-value indicated.

shRNA-mediated knock-down of ARHGAP23, PKP4, and KEAP1

To examine the function of ARHGAP23, PKP4, and KEAP1 in ECs, we silenced their expression using two independent lentiviral short hairpin RNAs (shRNAs) targeting each gene **(Figure 2a-c)**. Next, we examined monolayer organization and AJ organization by immunofluorescence. ARHGAP23- and KEAP1-deficient ECs were able to form confluent monolayers similar to shControl cells **(Figure 2d, e)**. The knock-down of ARHGAP23 or KEAP1 did not perturb the formation of VE-cadherin-based junctions. Furthermore, we did not observe prominent changes in the organization of the actin cytoskeleton in shARHGAP23 ECs **(Figure 2d)**. Although we achieved efficient knock-down levels of PKP4 **(Figure 2b)**, we were unable to image PKP4-deficient cells by immunofluorescence. shPKP4 ECs plated on glass failed to remain adherent through fixation and washing steps; even on tissue-culture plastic and in combination with different types of extracellular matrix coatings (fibronectin, laminin, poly-L-lysine, ibiTreat) the staining protocol resulted in detachment. This technical limitation unfortunately prevented an assessment of junction organization in PKP4 knock-down monolayers. Together, these results show that we have a robust knock-down of ARHGAP23, PKP4, and KEAP1, and that ARHGAP23- and KEAP1-deficient ECs still formed AJs.

Figure 2.

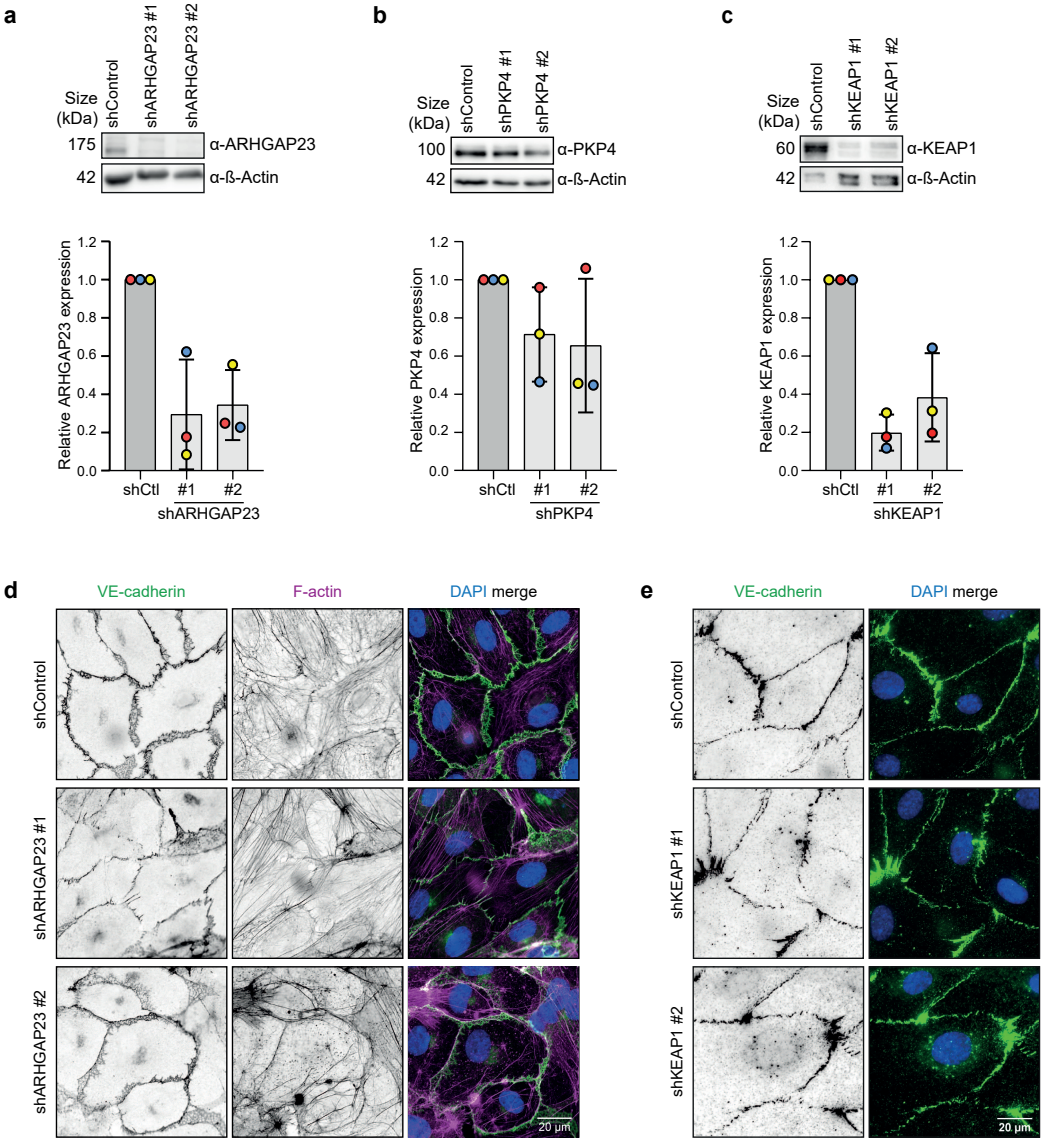


Figure 2. shRNA-induced knock-down of ARHGAP23, PKP4, and KEAP1. a-c) Representative Western blot analysis of lysates derived from HUVECs transduced with control or indicated shRNAs probed for ARHGAP23 (a), PKP4 (b), KEAP1 (c), and β-actin (all). Graphs show relative protein levels ±SD. Signal corrected for background, ß-actin expression levels, and expression levels in control cells. Data from n=3 independent experiments, Student's paired t-test. **d)** Representative images of fixed HUVECs transduced with shControl or shARHGAP23 stained for endogenous VE-cadherin (green), F-actin (magenta), and nucleus (blue). **d)** Representative images of fixed shControl and shKEAP1 HUVECs stained for endogenous VE-cadherin (green) and nucleus (blue).

Depletion of VE-cadherin interactors perturbs endothelial barrier function

Next, we investigated whether depletion of ARHGAP23, PKP4, and KEAP1 affects endothelial barrier function. Electrical cell-substrate impedance sensing (ECIS) was used to monitor transendothelial resistance at 4000 Hz over 48 hours after cell seeding on electrodes. All generated cell types, including shPKP4 ECs, adhered well in the ECIS culture wells. ARHGAP23 knock-down consistently reduced resistance levels relative to shControl monolayers throughout the recording **(Figure 3a, left)**. Quantification showed significantly decreased normalized and absolute resistance of shARHGAP24 monolayers at both 24 and 48 hours after cell seeding **(Figure 3a,** middle and right**; Figure S2a)**. The depletion of PKP4 resulted in a trend towards reduced resistance, but was only significant for shRNA#2 after 48 hours **(Figure 3b, Figure S2b)**. KEAP1 knock-downs yielded the most pronounced effect: around 15 hours after seeding the shKEAP1 monolayers were unable to maintain endothelial barrier function, with significant reductions of relative and absolute resistance at both 24 and 48 hours **(Figure 3c, Figure S2c)**. Phase-contrast microscopy of the cells after completion of the ECIS experiment showed that the monolayers were confluent in all conditions (data not shown). Together, these results show that depletion of KEAP1 or ARHGAP23 weakens endothelial barrier function under basal conditions.

VE-cadherin complex characterization in ARHGAP23, PKP4, or KEAP1 knock-down ECs

To determine whether the observed altered barrier properties might stem from changes in VE-cadherin protein abundance, we immunoblotted lysates from shControl and knock-down ECs for VE-cadherin and β-actin **(Figure 4a, b)**. These experiments did not demonstrate differences in VE-cadherin levels in ARHGAP23- or PKP4-deficient cells compared to controls **(Figure 4a)**. Only in shKEAP1#2 knock-down ECs a slight reduction of VE-cadherin was observed **(Figure 4b)**. The experiments need to be repeated to confirm these findings.

Because KEAP1 displayed a cytosolic and nuclear distribution consistent with its role in redox signaling (**Figure 1d)**, we next investigated whether oxidative stress influences its association with VE-cadherin. ECs expressing VE-cadherin-GFP were stimulated with hydrogen peroxide (500µM extracellular concentration, corresponding to ~5µM intracellular [36]) for 5 and 20 minutes, after which VE-cadherin pull-downs were performed **(Figure 4c)**. These timepoints were chosen to reflect the rapid redox regulation of KEAP1 in which cysteine oxidation promotes NRF2 release [37], which can then translocate to the nucleus for transcriptional activity [31]. KEAP1 co-immunoprecipitation was preserved following hydrogen peroxide treatment **(Figure 4c,** rightmost lanes**)**. Robust β-catenin co-precipitation in all conditions confirmed pulldown efficiency and indicated that the treatment did not compromise VE-cadherin complex integrity. These results suggest that KEAP1 binding with VE-cadherin is not regulated by acute oxidative stress. Unlike its redox-dependent dissociation from NRF2, KEAP1-VE-cadherin binding remains stable, pointing to a distinct mode of interaction.

Figure 3.

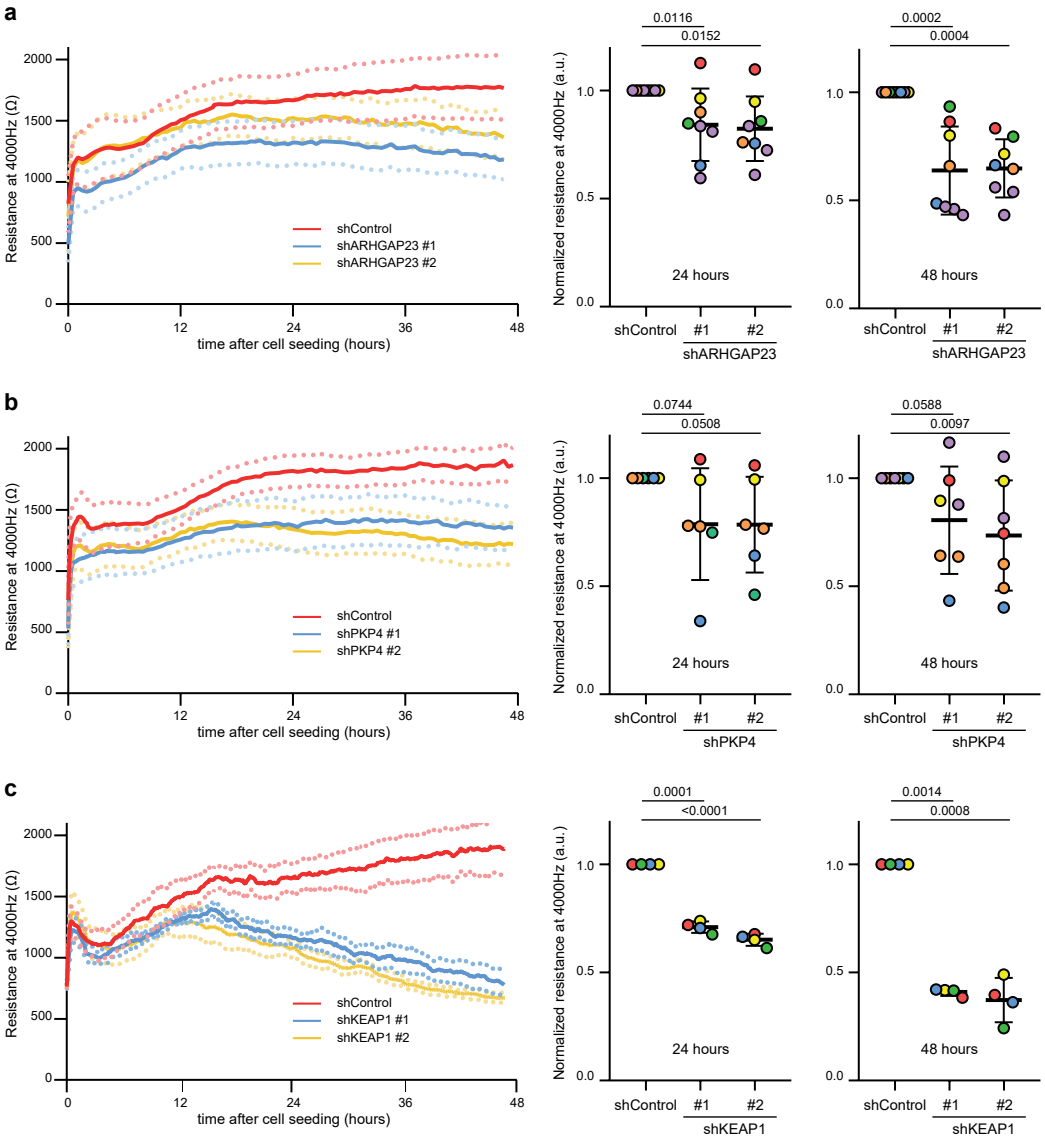


Figure 3. Depletion of ARHGAP23, PKP4, and KEAP1 and assessment of endothelial barrier function. a-c) Line graph showing the average resistance (±SEM, dotted lines) measured with ECIS at 4000Hz of shControl and indicated knock-down HUVEC monolayers over time for a) shARHGAP23, b) shPKP4, c) shKEAP1. Data from n≥4 independent experiments. Graphs show the normalized relative, compared to shControl cells, resistance at 4000Hz of knock-down monolayers 24 hours after cell seeding (middle panels), or after 48 hours (left panels). Data from n=4 independent experiments, means ±SD, ANOVA with Dunnett's multiple comparison test, p-values indicated.

Figure 4.

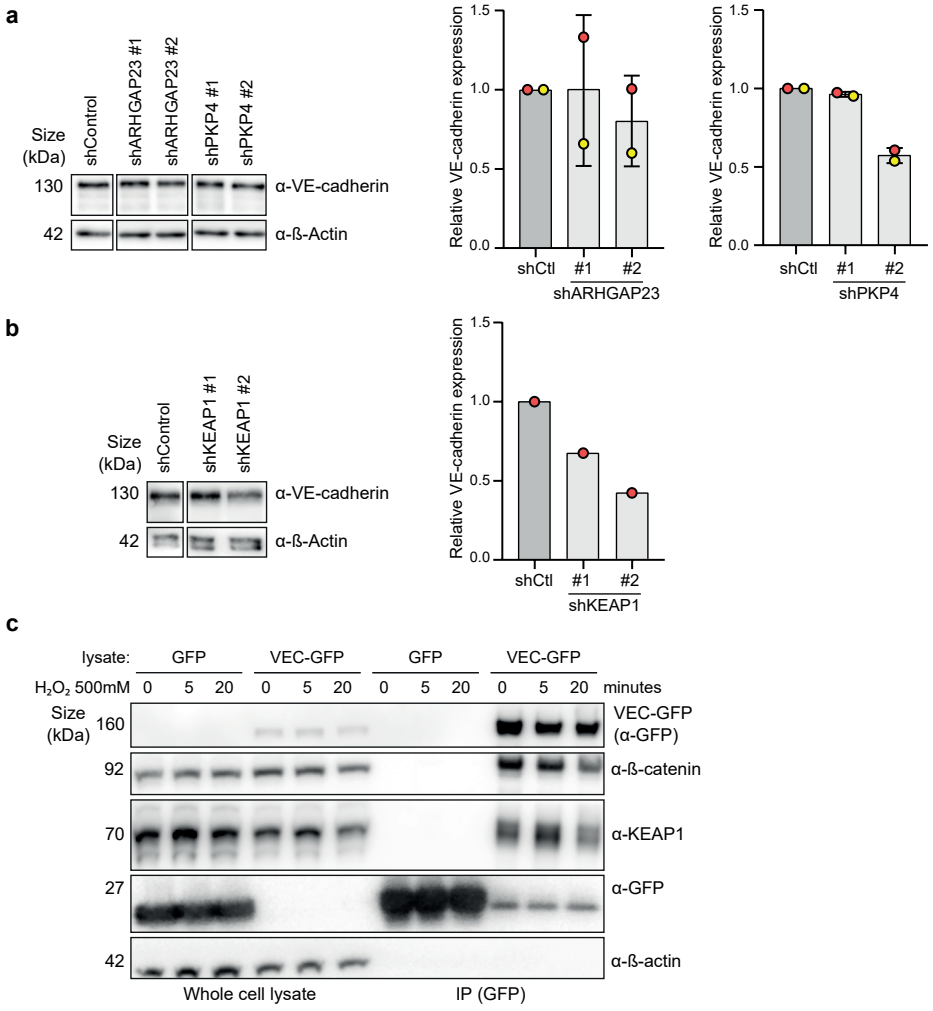


Figure 4. Characterization of VE-cadherin protein complex in ARHGAP23, PKP4, or KEAP1 knock-down ECs. a) Representative Western blot analysis of lysates derived from HUVECs transduced with shControl or shRNAs against ARHGAP23 or PKP4, probed for VE-cadherin and β-actin. Graphs show relative VE-cadherin protein expression levels ±SD upon shRNA knock-down of ARHGAP23 (middle panels) or PKP4 (right panels). Signal corrected for background, ß-actin expression levels, and expression levels in shControl cells. Data from n=2 independent experiments. **b)** Representative Western blot analysis of lysates derived from HUVECs transduced with shControl or shRNAs against KEAP1, probed for VE-cadherin and β-actin. Graph shows relative VE-cadherin protein expression levels ±SD upon shRNA knock-down of KEAP1. Signal corrected for background, ß-actin expression levels, and expression levels in shControl cells. Data from n=1 independent experiment. **c)** Representative Western blot analysis probed for GFP, β-catenin, KEAP1, and β-actin, on whole cell lysate and co-immunoprecipitated samples (IP) derived from HUVECs expressing GFP or VE-cadherin GFP. Treatment time with 500µM hydrogen peroxide (H_2O_2) indicated in minutes for every condition lane.

Discussion

In the present study, we focused on three of the core VE-cadherin-binding proteins identified in **Chapter 2.** Our preliminary data on the assessment of the importance of KEAP1, ARHGAP23, and PKP4 shows that they may serve distinct roles. PKP4 and KEAP1 co-immunoprecipitated with VE-cadherin and its non-phosphorylatable Y-to-F mutated variants, indicating a strong biochemical association that does not require VE-cadherin phosphorylation. For ARHGAP23 and PKP4 we could show that they are recruited to endothelial junctions and showed increasing colocalization with VE-cadherin as the monolayers and junctions mature. KEAP1 localization was restricted to the cytosol and nucleus without detectable junctional enrichment. Functional assays further demonstrated that in particular the depletion ARHGAP23 or KEAP1 led to impaired endothelial barrier function. These findings provide exploratory but meaningful first insights into how non-canonical VE-cadherin interactors may regulate the endothelial barrier.

ARHGAP23 is a RhoGAP that inactivates small GTPases like RhoA by stimulating GTP hydrolysis. GAPs fine-tune the amplitude and spatial extent of GTPase signaling, thereby curbing excessive contractility or spreading signals [38]. In various cell types, the spatiotemporal regulation by GAPs is important for junction integrity and to maintain a tissue barrier [39]. In our experiments, ARHGAP23 strongly co-localized with VE-cadherin at the cell-cell junctions. Actomyosin-generated tension across VE-cadherin is needed for proper endothelial barrier establishment [40]. Since ARHGAP23 depletion weakens barrier resistance, our findings may point to a role for ARHGAP23 in limiting local Rho GTPase-driven actomyosin contractility in the vicinity of VE-cadherin. To test this, future experiments could measure local RhoA activity in ARHGAP23-deficient versus control endothelial cells, for example by using Rho biosensors (see [41-43]). It would be interesting to include physiological stimulations of actin contractility and junction remodeling, for example through addition of thrombin or the application of shear stress through flow. Additionally, further investigations into the interdependence of ARHGAP23 with related endothelial junctional adaptors, such as its known-binding protein PKP4 [24] and p120-catenin, which also controls RhoGTPase signaling at AJs [44], may help to unravel the mechanism by which ARHGAP23 regulates endothelial junctions.

PKP4 is structurally closely related to p120-catenin and ARVCF, both armadillo-repeat domain proteins [45]. It has been shown before that PKP4 directly binds VE-cadherin through its armadillo domains [35,46]. In epithelial contexts, PKP4 localizes to junctions and competes with p120-catenin for cadherin tail binding. PKP4 overexpression can displace p120-catenin from junctions, thereby influencing cadherin turnover and stability [47]. PKP4 also regulates spatial RhoA signaling by scaffolding ARHGEF2 and RhoA effectors at AJs to promote cortical actin ring formation and junction maturation [24]. Additionally, and perhaps unsurprisingly considering this convergence in function,

PKP4 associates with ARHGAP23 and was shown to limit the suppressive activity of ARHGAP23 on RhoA [24]. It is plausible that in endothelial cells PKP4 serves a similar junctional scaffolding role in recruiting local GEFs or effectors to organize the junctional actin cytoskeleton. As a next experimental step, live-cell imaging of actin dynamics and local RhoA biosensors in PKP4-depleted endothelial cells could assess whether junctional RhoA activity is dampened or spatially mislocalized when barrier function is compromised. However, first the technical limitations that prevent culturing the PKP4 knock-downs cells in imaging substrates need to be solved.

KEAP1 is classically understood as the cytosolic adaptor that holds NRF2 in check via ubiquitin-mediated degradation. Under oxidative (or electrophilic) stress, three cysteine residues in KEAP1 become oxidized, leading to a conformational change that releases NRF2, which in turn can translocate to the nucleus to drive expression of antioxidant genes [48]. In endothelial cells, NRF2 has been implicated in vascular protection, resisting oxidative injury, and preserving barrier function [49] as well as in mechanosensing [50]. The notion that KEAP1 co-immunoprecipitated with VE-cadherin but is not localized at junctions, indicates that they may interact elsewhere in the cell. The VE-cadherin pulldown experiments with hydrogen peroxide-treated ECs did not show acute loss of KEAP1 binding under oxidative stress, indicating that their interaction is not controlled through short-term redox shifts. This suggests that the VE-cadherin-KEAP1 association may be regulated beyond KEAP1's cysteine oxidation. Future studies should investigate whether KEAP1 binding to VE-cadherin modulates ROS signaling in junctional vs. non-junctional compartments: live-cell FRET or FLIM-based interaction sensors might resolve where KEAP1-VE-cadherin binding occurs. We think that certain stimuli, such as changes in flow or inflammation, might result in KEAP1 recruitment to AJs.

The different localization patterns of identified VE-cadherin interactors highlights that VE-cadherin interacts with distinct subcellular compartments, even beyond the AJ. In addition to being a stable adhesion structure, the VE-cadherin complex's signaling platform may include modules for regulating RhoGTPase activities and redox sensing. This modular view aligns with emerging models in junction biology where adhesion complexes integrate physical, signaling, and metabolic cues in parallel.

Altogether, these findings strengthen the notion that VE-cadherin does not simply rely on its classical catenins and cytoskeletal anchors but engages with additional molecular regulators. The modest changes in barrier function observed upon knock-down suggest that the proteins studied here act as modulators or buffers rather than primary structural anchors, not ruling out their role under conditions of vascular stress or inflammation. By mapping how VE-cadherin coordinates adhesion, signaling, and homeostasis via diverse partners, these results lay the foundation for more mechanistic, context-dependent studies that could reveal new switches for controlling endothelial barrier integrity.

Materials & Methods

Cell culture and lentiviral transduction

All cells were maintained in standard humidified incubators set to 37°C with 5% CO_2. Pooled human umbilical vein endothelial cells (HUVECs; P1052, #C2519A, Lonza) and pooled human arterial endothelial cells (HAECs; #CC2535, Lonza) were cultured until at most passage 8 in endothelial growth medium supplemented with endothelial growth factor-FCS mix (EGM2; #C-22211 + #C-39216, Promocell), 100 U/mL penicillin, and 100 µg/mL streptomycin (#151 40122, Gibco on fibronectin (FN; CLB) coated surfaces. Lenti-X HEK293T cells (#632180, Takara) were cultured in DMEM (#11320033, Gibco) + 10% FCS (#10270106, Gibco) and used to produce lentivirus by transfecting gene plasmids together with third generation packaging plasmids [51] and using Trans-IT-LT1 (MIR 2300, Mirus) as described previously [52]. HUVECs were transduced at 60% confluence by overnight incubation with the lentiviral particles and subsequently selected overnight with 250 ng/mL puromycin (P8833, Sigma). Selected HUVECs were analyzed at least 72h after transduction to ensure knockdown efficiency or ectopic protein expression.

Plasmids and cloning

The pLV-hVE-cadherin-GFP construct was described before [53]. For protein knock-down we used shRNA plasmids targeting human genes (TSC2 MISSION® library, Sigma) or control shRNA-scramble (pLKO.1-scrambled (136035, Addgene)). To deplete ARHGAP23 we used shRNA TRCN0000048468 (shARHGAP23#1) and TRCN0000048469 (shARHGAP23#2); to deplete PKP4 we used TRCN0000123179 (shPKP4#1) and TRCN0000123181 (shPKP4#2); and to deplete KEAP1 we used shRNA TRCN0000155340 (shKEAP#1) and TRCN0000154656 (shKEAP1#2).

Co-immunoprecipitation

Co-IP on HUVECs expressing GFP alone or GFP-tagged proteins was performed with magnetic GFP-trap agarose beads (gtma-20, Chromotek). Cells were washed 2 times with cold PBS supplemented with 1mM CaCl and 0,5mM MgCl and incubated for 10 minutes with freshly made ice-cold lysis buffer comprised of 10 mM TrisHCl pH 7.5, 150 mM NaCl, 0.5mM EDTA (all Sigma-Aldrich), protease- and phosphatase inhibitors (#A32955, Thermo Fisher; #4906845001, Roche), and 0.5% NP40 (#492018, Sigma-Aldrich). Cell lysates were collected in protein LoBind tubes (#0030108116, Eppendorf; used throughout this procedure), sonicated thoroughly, and centrifuged at 12000g at 4°C for 10 minutes. Supernatants were transferred to clean tubes and incubated at 4°C overnight with anti-GFP nanobeads that were washed and equilibrated 3 times with PBS and 3 times with lysis buffer. The next day, immunoprecipitated beads were washed 3 times with freshly made wash buffer (=lysis buffer without NP40) followed by 2 washes with ice-cold PBS, each time transferring to clean tubes. The resulting samples were then used for Western Blot analysis.

Western blot

Cell lysates in Laemmli reduced sample buffer with 4% ß-mercaptoethanol (#444203, Sigma Aldrich) were denatured 10 minutes at 96°C and loaded on 4-12% gradient SDS-page gels (#NW042125BOX, Thermo Fisher Scientific) and run according to the manufacturer's instructions. After wet or semi-dry transfer onto ethanol-activated PVDF membranes and blocking in 3% bovine serum albumin (BSA; #A8806-5G, Sigma Aldrich) in Tris-buffered saline (TBS; Sigma Aldrich) for 45 minutes at room temperature (RT), blots were incubated overnight at 4°C in primary antibody in TBS+3%BSA: rabbit anti-ARHGAP23 (#HPA019818, Sigma Aldrich), rabbit/mouse anti-PKP4 (ab222194, abcam/#85-104, Origene), rabbit anti-KEAP1 (10503-2-AP, Proteintech), mouse anti-GFP (#SC-9996, Santa Cruz), rabbit/mouse anti-VE-cadherin (#D87F2, Cell Signaling Technology/#610252, BD Biosciences), rabbit anti-ß-catenin (#C2206, Sigma Aldrich), and rabbit anti-ß-actin (#4967, Cell Signaling Technology); washed 3 times for 5 minutes in TBS; incubated 1 hour at RT in secondary antibody in TBS+3%BSA: anti-rabbit-HRP (#170-6515, Bio-Rad) or anti-mouse-HRP (#172-1011, Bio-Rad); washed another 3 times 5 minutes in TBS; and finally imaged using enhanced chemiluminescence detection (#34580, Thermo Fisher Scientific) on an Amersham ImageQuant 800 GxP machine (#29653452, Cytiva). Protein band intensity was quantified using the FIJI/ImageJ Gel Analyzer plugin [54,55].

Immunofluorescence

For antibody stainings, HUVECs or HAECs were seeded at confluence and grown until desired density with medium changes every 24 hours on microscope-compatible surfaces: FN-coated glass coverslips, Labtek 8-chamber imaging slides (#177380, Thermo Fisher Scientific), or ibidi µ-slides $VI^{0.4}$ (#80666, ibidi, Munich, Germany). Cells were fixed in 4% PFA in PBS++ with 1µg/mL $CaCl_2$ and 0.5 µg/mL $MgCl_2$ for 5 minutes at 37°C. Fixed cells were permeabilized using 0.01% Triton (X100, Sigma Aldrich) in PBS++ for 10 minutes at RT, blocked in 3%BSA in PBS++ at RT for 45 minutes, stained with primary antibody for 1 hour at RT and secondary antibodies for 45 minutes at RT: rabbit anti-ARHGAP23 (HPA019818, Sigma Aldrich), rabbit/mouse anti-PKP4 (ab222194, abcam/#85-104, Origene), rabbit anti-KEAP1 (#10503-2-AP, Proteintech), rabbit anti-VE-cadherin (#D87F2, Cell Signaling Technology), or mouse anti-VE-cadherin (#610252, BD Biosciences), DAPI-AF405 (#62248, Thermo Fisher Scientific), anti-mouse AlexaFluor (AF) AF488 (A-21200), AF647 (A-21463), anti-rabbit AF488 (A-21441), AF647 (A-21443) (all Thermo Fisher Scientific). Coverslips and imaging slides were washed two times with PBS, once with Milli-Q, and mounted in antifade media: Mowiol/DABCO solution or ProLong Diamond Antifade (#P36961, Thermo Fisher Scientific) and stored in a dark chamber at 4°C. Fluorescence was captured on a Nikon Eclipse TI microscope with SOLA SEII light source, 60x 1.49NA Apo TIRF oil objective, standard NIKON filter cubes, using a Andor Zyla 4.2 plus sCMOS camera.

Intensity correlation imaging analysis

Immunofluorescent images were obtained using tag combinations specifically chosen to minimize overlapping excitation and emission spectra. All conditions were imaged on the same day with the same microscope settings to reduce external variation. For analysis, FIJI/ImageJ software was used to obtain junctional masks through intensity thresholding. Within masks, raw fluorescence intensity measurements per pixel across channels were analyzed using the Coloc2 plugin for FIJI/ImageJ to calculate a Pearson's correlation coefficient using Costes' method [56].

Electric cell-substrate impedance sensing (ECIS)

Endothelial barrier function was measured using ECIS as previously described [57]. In short, gold electrodes (8w10E+, #72040, Applied BioPhysics) were treated with 10mM L-cysteine (Sigma Aldrich) in saline for 15 minutes at RT and coated with fibronectin for 2 hours at 37°C. Impedance was measured in real time for 50 hours at 4000Hz to assess adherens junction integrity [58-62], starting immediately after seeding of 120000 HUVECs per chamber, using the ZTheta machine (Applied BioPhysics). During measurement, cells were maintained at 37°C with 5% CO2. Analysis was done in GraphPad Prism.

Data analysis and statistics

FIJI/ImageJ was used for image analysis using the plugins mentioned above, and for image preparation for inclusion in this manuscript. All data was analyzed for statistical significance using GraphPad PRISM software. For ECIS data, data points were corrected for background signal of medium-only conditions and technical duplicates were averaged per biological replicate. Western blots were corrected for background, for total protein loading, and related to control band intensity within a biological replicate condition. Comparison between two groups was made using Student's t-test after Shapiro-Wilk normality test. All graphs show mean and standard deviation; p-values are indicated.

References

1. Dejana, E., and Giampietro, C. (2012). Vascular endothelial-cadherin and vascular stability. Curr Opin Hematol *19*, 218–223. 10.1097/MOH.0b013e3283523e1c.
2. Hartsock, A., and Nelson, W.J. (2008). Adherens and tight junctions: structure, function and connections to the actin cytoskeleton. Biochim Biophys Acta *1778*, 660–669. 10.1016/j.bbamem.2007.07.012.
3. Angulo-Urarte, A., van der Wal, T., and Huveneers, S. (2020). Cell-cell junctions as sensors and transducers of mechanical forces. Biochim Biophys Acta Biomembr *1862*, 183316. 10.1016/j.bbamem.2020.183316.
4. Wessel, F., Winderlich, M., Holm, M., Frye, M., Rivera-Galdos, R., Vockel, M., Linnepe, R., Ipe, U., Stadtmann, A., Zarbock, A., et al. (2014). Leukocyte extravasation and vascular permeability are each controlled in vivo by different tyrosine residues of VE-cadherin. Nat Immunol *15*, 223–230. 10.1038/ni.2824.
5. Hakanpaa, L., Kiss, E.A., Jacquemet, G., Miinalainen, I., Lerche, M., Guzmán, C., Mervaala, E., Eklund, L., Ivaska, J., and Saharinen, P. (2018). Targeting β1-integrin inhibits vascular leakage in endotoxemia. Proceedings of the National Academy of Sciences *115*, E6467–E6476. doi:10.1073/pnas.1722317115.
6. Claesson-Welsh, L., Dejana, E., and McDonald, D.M. (2021). Permeability of the Endothelial Barrier: Identifying and Reconciling Controversies. Trends Mol Med *27*, 314–331. 10.1016/j.molmed.2020.11.006.
7. Arif, N., Zinnhardt, M., Nyamay'Antu, A., Teber, D., Bruckner, R., Schaefer, K., Li, Y.T., Trappmann, B., Grashoff, C., and Vestweber, D. (2021). PECAM-1 supports leukocyte diapedesis by tension-dependent dephosphorylation of VE-cadherin. EMBO J *40*, e106113. 10.15252/embj.2020106113.
8. Lampugnani, M.G., Dejana, E., and Giampietro, C. (2018). Vascular Endothelial (VE)-Cadherin, Endothelial Adherens Junctions, and Vascular Disease. Cold Spring Harb Perspect Biol *10*. 10.1101/cshperspect.a029322.
9. Shih, Y.T., Wei, S.Y., Chen, J.H., Wang, W.L., Wu, H.Y., Wang, M.C., Lin, C.Y., Lee, P.L., Lin, C.Y., Chiang, H.C., et al. (2023). Vinculin phosphorylation impairs vascular endothelial junctions promoting atherosclerosis. Eur Heart J *44*, 304–318. 10.1093/eurheartj/ehac647.
10. Vestweber, D. (2021). Vascular Endothelial Protein Tyrosine Phosphatase Regulates Endothelial Function. Physiology (Bethesda) *36*, 84–93. 10.1152/physiol.00026.2020.
11. Jin, Y., Ding, Y., Richards, M., Kaakinen, M., Giese, W., Baumann, E., Szymborska, A., Rosa, A., Nordling, S., Schimmel, L., et al. (2022). Tyrosine-protein kinase Yes controls endothelial junctional plasticity and barrier integrity by regulating VE-cadherin phosphorylation and endocytosis. Nat Cardiovasc Res *1*, 1156–1173. 10.1038/s44161-022-00172-z.
12. Holtermann, L., Rivera-Galdos, R., Nottebaum, A.F., Wessel, F., Ipe, U., and Vestweber, D. (2025). Distinct VE-cadherin serine and tyrosine phosphorylation sites and their role for inflammation-induced vascular permeability in vivo. Cell Mol Life Sci *82*, 223. 10.1007/s00018-025-05753-2.
13. Wilkens, M., Holtermann, L., Stahl, A.K., Stegmeyer, R.I., Nottebaum, A.F., and Vestweber, D. (2024). Ubiquitination of VE-cadherin regulates inflammation-induced vascular permeability in vivo. EMBO Rep *25*, 4013–4032. 10.1038/s44319-024-00221-7.
14. Tiruppathi, C., Wang, D.M., Ansari, M.O., Bano, S., Tsukasaki, Y., Mukhopadhyay, A., Joshi, J.C., Loch, C., Niessen, H.W.M., and Malik, A.B. (2023). Ubiquitin ligase CHFR mediated degradation of VE-cadherin through ubiquitylation disrupts endothelial adherens junctions. Nat Commun *14*, 6582. 10.1038/s41467-023-42225-2.
15. Seo, T., Lowery, A.M., Xu, H., Giang, W., Troyanovsky, S.M., Vincent, P.A., and Kowalczyk, A.P. (2024). MARCH family E3 ubiquitin ligases selectively target and degrade cadherin family proteins. PLoS One *19*, e0290485. 10.1371/journal.pone.0290485.
16. Orsenigo, F., Giampietro, C., Ferrari, A., Corada, M., Galaup, A., Sigismund, S., Ristagno, G., Maddaluno, L., Koh, G.Y., Franco, D., et al. (2012). Phosphorylation of VE-cadherin is modulated by haemodynamic forces and contributes to the regulation of vascular permeability in vivo. Nat Commun *3*, 1208. 10.1038/ncomms2199.
17. Katoh, M., and Katoh, M. (2004). Identification and characterization of human ARHGAP23 gene in silico. Int J Oncol *25*, 535–540.
18. Soares, G.M., Zangerolamo, L., Costa-Junior, J.M., Vettorazzi, J.F., Carneiro, E.M., Saad, S.T., Boschero, A.C., and Barbosa-Sampaio, H.C. (2019). Whole-Body ARHGAP21-Deficiency Improves Energetic Homeostasis in Lean and Obese Mice. Front Endocrinol (Lausanne) *10*, 338. 10.3389/fendo.2019.00338.
19. Chiasson, C.M., Wittich, K.B., Vincent, P.A., Faundez, V., and Kowalczyk, A.P. (2009). p120-catenin inhibits VE-cadherin internalization through a Rho-independent mechanism. Mol Biol Cell *20*, 1970–1980. 10.1091/mbc.e08-07-0735.
20. Dubois, T., Paleotti, O., Mironov, A.A., Fraisier, V., Stradal, T.E., De Matteis, M.A., Franco, M., and Chavrier, P. (2005). Golgi-localized GAP for Cdc42 functions downstream of ARF1 to control Arp2/3 complex and F-actin dynamics. Nat Cell Biol *7*, 353–364. 10.1038/ncb1244.
21. Hooglugt, A., van der Stoel, M.M., Shapeti, A., Neep, B.F., de Haan, A., van Oosterwyck, H., Boon, R.A., and Huveneers, S. (2024). DLC1 promotes mechanotransductive feedback for YAP via RhoGAP-mediated focal adhesion turnover. J Cell Sci *137*. 10.1242/jcs.261687.
22. Amado-Azevedo, J., Reinhard, N.R., van Bezu, J., de Menezes, R.X., van Beusechem, V.W., van Nieuw Amerongen, G.P., van Hinsbergh, V.W.M., and Hordijk, P.L. (2017). A CDC42-centered signaling unit is a dominant positive regulator of endothelial integrity. Sci Rep *7*, 10132. 10.1038/s41598-017-10392-0.
23. Barcellos, K.S., Bigarella, C.L., Wagner, M.V., Vieira, K.P., Lazarini, M., Langford, P.R., Machado-Neto, J.A., Call, S.G., Staley, D.M., Chung, J.Y., et al. (2013). ARHGAP21 protein, a new partner of alpha-tubulin involved in cell-cell adhesion formation and essential for epithelial-mesenchymal transition. J Biol Chem *288*, 2179–2189. 10.1074/jbc.M112.432716.

24. Müller, L., Keil, R., Glaß, M., and Hatzfeld, M. (2024). Plakophilin 4 controls the spatio-temporal activity of RhoA at adherens junctions to promote cortical actin ring formation and tissue tension. Cell Mol Life Sci *81*, 291. 10.1007/s00018-024-05329-6.
25. Pannekoek, W.J., van Dijk, J.J., Chan, O.Y., Huveneers, S., Linnemann, J.R., Spanjaard, E., Brouwer, P.M., van der Meer, A.J., Zwartkruis, F.J., Rehmann, H., et al. (2011). Epac1 and PDZ-GEF cooperate in Rap1 mediated endothelial junction control. Cell Signal *23*, 2056–2064. 10.1016/j.cellsig.2011.07.022.
26. Guo, Z., and Mo, Z. (2020). Keap1-Nrf2 signaling pathway in angiogenesis and vascular diseases. J Tissue Eng Regen Med *14*, 869–883. 10.1002/term.3053.
27. Knatko, E.V., Tatham, M.H., Zhang, Y., Castro, C., Higgins, M., Dayalan Naidu, S., Leonardi, C., de la Vega, L., Honda, T., Griffin, J.L., et al. (2020). Downregulation of Keap1 Confers Features of a Fasted Metabolic State. iScience *23*, 101638. 10.1016/j.isci.2020.101638.
28. Kopacz, A., Kloska, D., Targosz-Korecka, M., Zapotoczny, B., Cysewski, D., Personnic, N., Werner, E., Hajduk, K., Jozkowicz, A., and Grochot-Przeczek, A. (2020). Keap1 governs ageing-induced protein aggregation in endothelial cells. Redox Biol *34*, 101572. 10.1016/j.redox.2020.101572.
29. Kopacz, A., Kloska, D., Proniewski, B., Cysewski, D., Personnic, N., Piechota-Polanczyk, A., Kaczara, P., Zakrzewska, A., Forman, H.J., Dulak, J., et al. (2020). Keap1 controls protein S-nitrosation and apoptosis-senescence switch in endothelial cells. Redox Biol *28*, 101304. 10.1016/j.redox.2019.101304.
30. Kopacz, A., Kloska, D., Forman, H.J., Jozkowicz, A., and Grochot-Przeczek, A. (2020). Beyond repression of Nrf2: An update on Keap1. Free Radic Biol Med *157*, 63–74. 10.1016/j.freeradbiomed.2020.03.023.
31. Li, C., Cheng, L., Wu, H., He, P., Zhang, Y., Yang, Y., Chen, J., and Chen, M. (2018). Activation of the KEAP1-NRF2-ARE signaling pathway reduces oxidative stress in Hep2 cells. Mol Med Rep *18*, 2541–2550. 10.3892/mmr.2018.9288.
32. Müller, L., and Hatzfeld, M. (2025). Emerging functions of Plakophilin 4 in the control of cell contact dynamics. Cell Commun Signal *23*, 109. 10.1186/s12964-025-02106-1.
33. Keil, R., Wolf, A., Hüttelmaier, S., and Hatzfeld, M. (2007). Beyond regulation of cell adhesion: local control of RhoA at the cleavage furrow by the p0071 catenin. Cell Cycle *6*, 122–127. 10.4161/cc.6.2.3741.
34. Keil, R., and Hatzfeld, M. (2014). The armadillo protein p0071 is involved in Rab11-dependent recycling. J Cell Sci *127*, 60–71. 10.1242/jcs.132266.
35. Calkins, C.C., Hoepner, B.L., Law, C.M., Novak, M.R., Setzer, S.V., Hatzfeld, M., and Kowalczyk, A.P. (2003). The Armadillo family protein p0071 is a VE-cadherin- and desmoplakin-binding protein. J Biol Chem *278*, 1774–1783. 10.1074/jbc.M205693200.
36. Sies, H. (2017). Hydrogen peroxide as a central redox signaling molecule in physiological oxidative stress: Oxidative eustress. Redox Biol *11*, 613–619. 10.1016/j.redox.2016.12.035.
37. Kaspar, J.W., Niture, S.K., and Jaiswal, A.K. (2009). Nrf2:INrf2 (Keap1) signaling in oxidative stress. Free Radic Biol Med *47*, 1304–1309. 10.1016/j.freeradbiomed.2009.07.035.
38. van Buul, J.D., Geerts, D., and Huveneers, S. (2014). Rho GAPs and GEFs: controling switches in endothelial cell adhesion. Cell Adh Migr *8*, 108–124. 10.4161/cam.27599.
39. Dahmene, M., Quirion, L., and Laurin, M. (2020). High Throughput strategies Aimed at Closing the GAP in Our Knowledge of Rho GTPase Signaling. Cells *9*, 1430.
40. Daneshjou, N., Sieracki, N., van Nieuw Amerongen, G.P., Conway, D.E., Schwartz, M.A., Komarova, Y.A., and Malik, A.B. (2015). Rac1 functions as a reversible tension modulator to stabilize VE-cadherin trans-interaction. Journal of Cell Biology *209*, 181–181. 10.1083/jcb.20140910803202015c.
41. Szulcek, R., Beckers, C.M., Hodzic, J., de Wit, J., Chen, Z., Grob, T., Musters, R.J., Minshall, R.D., van Hinsbergh, V.W., and van Nieuw Amerongen, G.P. (2013). Localized RhoA GTPase activity regulates dynamics of endothelial monolayer integrity. Cardiovasc Res *99*, 471–482. 10.1093/cvr/cvt075.
42. Zhang, X.E., Adderley, S.P., and Breslin, J.W. (2016). Activation of RhoA, but Not Rac1, Mediates Early Stages of S1P-Induced Endothelial Barrier Enhancement. PLOS ONE *11*, e0155490. 10.1371/journal.pone.0155490.
43. Reinhard, N.R., van Helden, S.F., Anthony, E.C., Yin, T., Wu, Y.I., Goedhart, J., Gadella, T.W., and Hordijk, P.L. (2016). Spatiotemporal analysis of RhoA/B/C activation in primary human endothelial cells. Sci Rep *6*, 25502. 10.1038/srep25502.
44. Smith, A.L., Dohn, M.R., Brown, M.V., and Reynolds, A.B. (2012). Association of Rho-associated protein kinase 1 with E-cadherin complexes is mediated by p120-catenin. Molecular Biology of the Cell *23*, 99–110. 10.1091/mbc.e11-06-0497.
45. Carnahan, R.H., Rokas, A., Gaucher, E.A., and Reynolds, A.B. (2010). The molecular evolution of the p120-catenin subfamily and its functional associations. PLoS One *5*, e15747. 10.1371/journal.pone.0015747.
46. Hatzfeld, M., Green, K.J., and Sauter, H. (2003). Targeting of p0071 to desmosomes and adherens junctions is mediated by different protein domains. J Cell Sci *116*, 1219–1233. 10.1242/jcs.00275.
47. Kourtidis, A., Ngok, S.P., and Anastasiadis, P.Z. (2013). p120 catenin: an essential regulator of cadherin stability, adhesion-induced signaling, and cancer progression. Prog Mol Biol Transl Sci *116*, 409–432. 10.1016/B978-0-12-394311-8.00018-2.
48. Suzuki, T., Takahashi, J., and Yamamoto, M. (2023). Molecular Basis of the KEAP1-NRF2 Signaling Pathway. Mol Cells *46*, 133–141. 10.14348/molcells.2023.0028.
49. Chen, B., Lu, Y., Chen, Y., and Cheng, J. (2015). The role of Nrf2 in oxidative stress-induced endothelial injuries. J Endocrinol *225*, R83–99. 10.1530/joe-14-0662.
50. McSweeney, S.R., Warabi, E., and Siow, R.C.M. (2016). Nrf2 as an Endothelial Mechanosensitive Transcription Factor. Hypertension *67*, 20–29. 10.1161/HYPERTENSIONAHA.115.06146.

51. Dull, T., Zufferey, R., Kelly, M., Mandel, R.J., Nguyen, M., Trono, D., and Naldini, L. (1998). A third-generation lentivirus vector with a conditional packaging system. J Virol *72*, 8463–8471. 10.1128/jvi.72.11.8463-8471.1998.
52. van der Stoel, M., Schimmel, L., Nawaz, K., van Stalborch, A.M., de Haan, A., Klaus-Bergmann, A., Valent, E.T., Koenis, D.S., van Nieuw Amerongen, G.P., de Vries, C.J., et al. (2020). DLC1 is a direct target of activated YAP/TAZ that drives collective migration and sprouting angiogenesis. J Cell Sci *133*. 10.1242/jcs.239947.
53. Huveneers, S., Oldenburg, J., Spanjaard, E., van der Krogt, G., Grigoriev, I., Akhmanova, A., Rehmann, H., and de Rooij, J. (2012). Vinculin associates with endothelial VE-cadherin junctions to control force-dependent remodeling. J Cell Biol *196*, 641–652. 10.1083/jcb.201108120.
54. Schneider, C.A., Rasband, W.S., and Eliceiri, K.W. (2012). NIH Image to ImageJ: 25 years of image analysis. Nature Methods *9*, 671–675. 10.1038/nmeth.2089.
55. Schindelin, J., Arganda-Carreras, I., Frise, E., Kaynig, V., Longair, M., Pietzsch, T., Preibisch, S., Rueden, C., Saalfeld, S., Schmid, B., et al. (2012). Fiji: an open-source platform for biological-image analysis. Nat Methods *9*, 676–682. 10.1038/nmeth.2019.
56. Costes, S.V., Daelemans, D., Cho, E.H., Dobbin, Z., Pavlakis, G., and Lockett, S. (2004). Automatic and quantitative measurement of protein-protein colocalization in live cells. Biophys J *86*, 3993–4003. 10.1529/biophysj.103.038422.
57. van der Stoel, M.M., Kotini, M.P., Schoon, R.M., Affolter, M., Belting, H.G., and Huveneers, S. (2023). Vinculin strengthens the endothelial barrier during vascular development. Vasc Biol *5*. 10.1530/VB-22-0012.
58. Luong, J.H.T., Xiao, C., Lachance, B., Leabu, Š.M., Li, X., Uniyal, S., and Chan, B.M.C. (2004). Extended applications of electric cell-substrate impedance sensing for assessment of the structure–function of α2β1 integrin. Analytica Chimica Acta *501*, 61–69. 10.1016/j.aca.2003.09.016.
59. Robilliard, L.D., Kho, D.T., Johnson, R.H., Anchan, A., O'Carroll, S.J., and Graham, E.S. (2018). The Importance of Multifrequency Impedance Sensing of Endothelial Barrier Formation Using ECIS Technology for the Generation of a Strong and Durable Paracellular Barrier. Biosensors (Basel) *8*. 10.3390/bios8030064.
60. Tiruppathi, C., Malik, A.B., Del Vecchio, P.J., Keese, C.R., and Giaever, I. (1992). Electrical method for detection of endothelial cell shape change in real time: assessment of endothelial barrier function. Proc Natl Acad Sci U S A *89*, 7919–7923. 10.1073/pnas.89.17.7919.
61. Zhang, Z., Huang, X., Liu, K., Lan, T., Wang, Z., and Zhu, Z. (2021). Recent Advances in Electrical Impedance Sensing Technology for Single-Cell Analysis. Biosensors (Basel) *11*. 10.3390/bios11110470.
62. Benson, K., Cramer, S., and Galla, H.J. (2013). Impedance-based cell monitoring: barrier properties and beyond. Fluids Barriers CNS *10*, 5. 10.1186/2045-8118-10-5.

Figure S1.

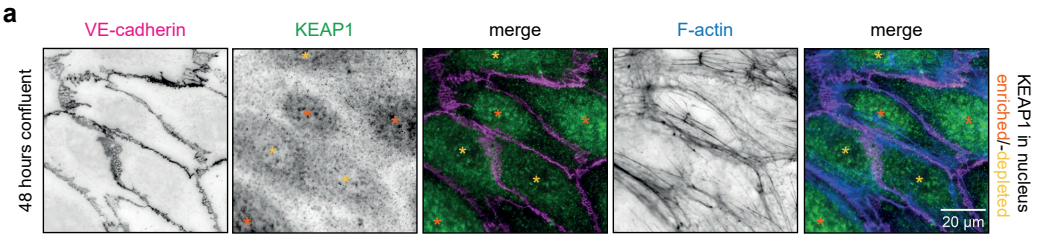


Figure S1. KEAP1 does not localize at adherens junctions of human arterial endothelial cells. **a)** Representative widefield images of human arterial endothelial cells (HAECs) that were fixed after 48 hours at full confluence and stained for endogenous VE-cadherin (magenta) and KEAP1 (green). KEAP1 localization is denoted with * in the color orange in case of nuclear enrichment and yellow for nuclear depletion relative to the immediately surrounding cytosol.

Figure S2.

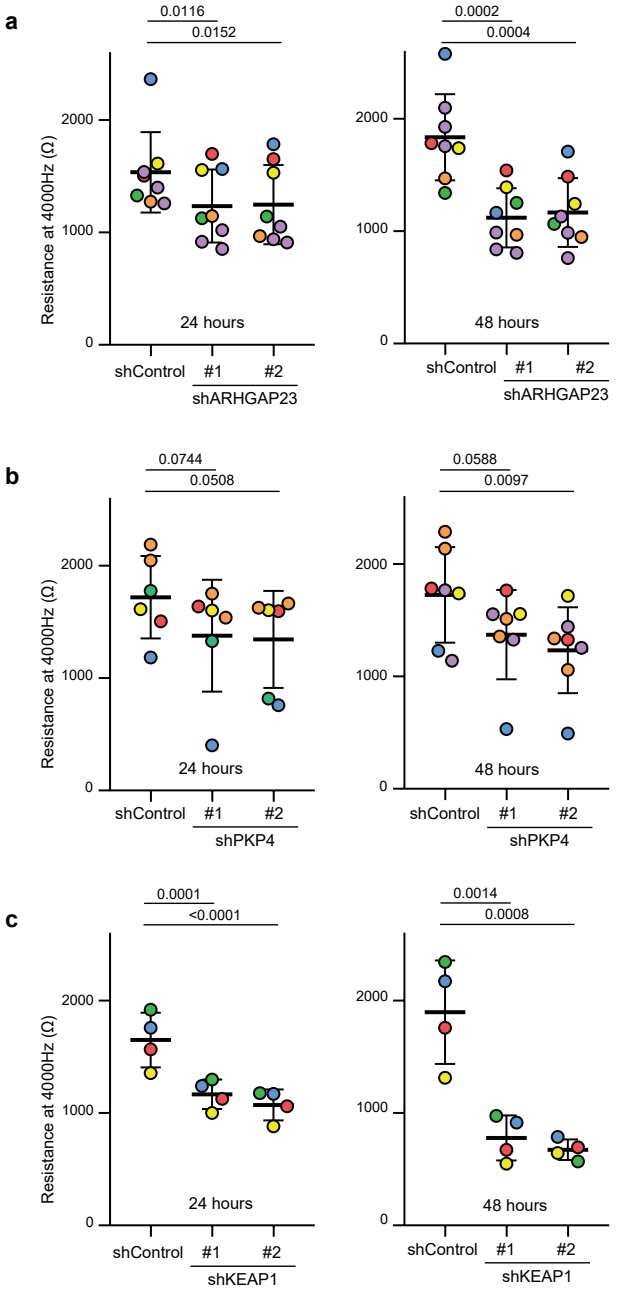


Figure S2. Absolute values ECIS experiments. a-c) Graphs show the absolute raw resistance values at 4000Hz of knock-down monolayers 24 hours after cell seeding (left panels), or after 48 hours (right panels). Data from n≥4 independent experiments, means ±SD, ANOVA with Dunnett's multiple comparison test, p-values indicated.

Figure S3.

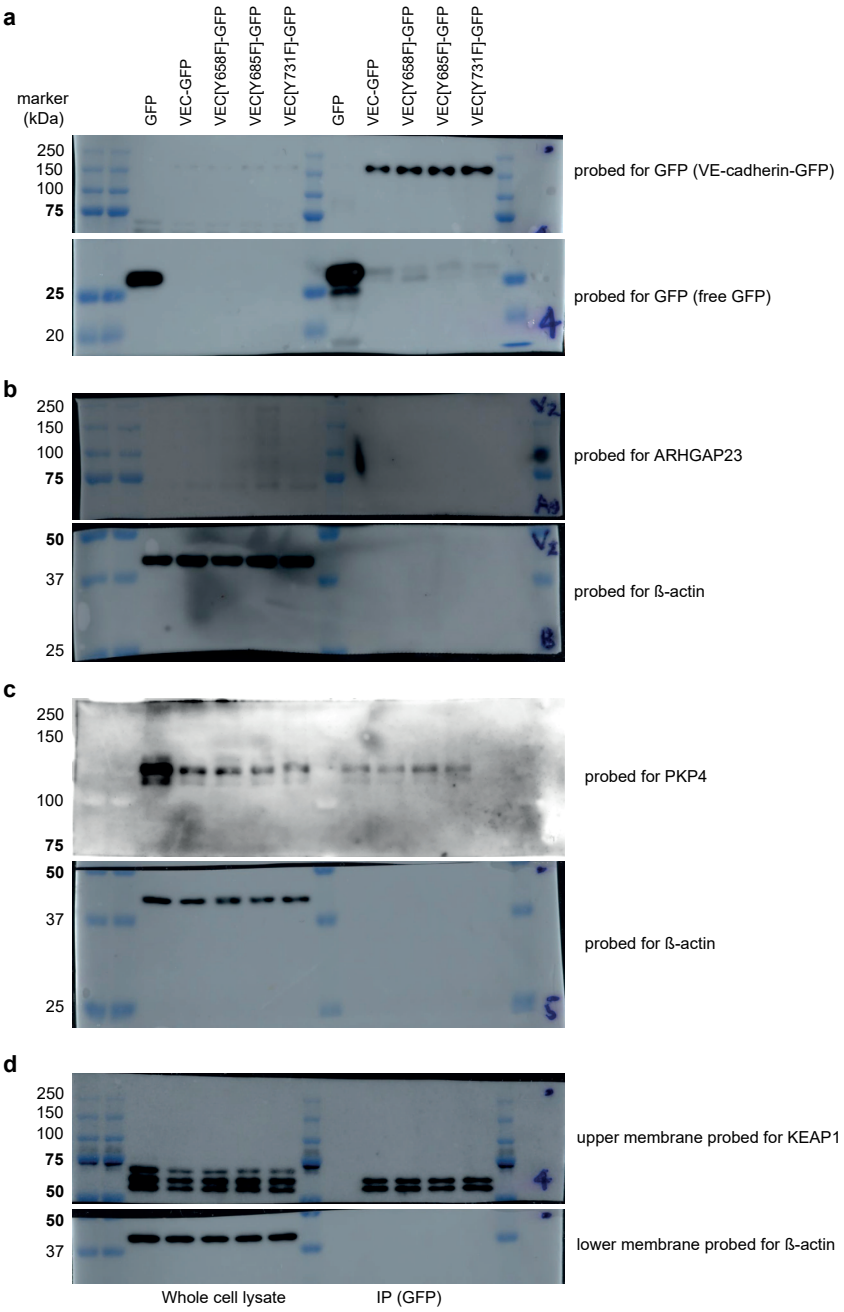


Figure S3. Whole western blot overlay images for Figure 1a. a) Membranes probed for GFP. **b)** Upper membrane probed for ARHGAP23; corresponding lower membrane probed for ß-actin. **c)** Upper membrane probed for PKP4 with corresponding lower membrane probed for ß-actin. **d)** Upper membrane probed for KEAP1; corresponding lower membrane probed for ß-actin.



Chapter 4

VE-cadherin RGD motifs are dispensable for cell-cell junctions, endothelial barrier function and monocyte extravasation

Tissue Barriers, (2024)

TISSUE BARRIERS
https://doi.org/10.1080/21688370.2025.2478349

Taylor & Francis
Taylor & Francis Group

RESEARCH ARTICLE

OPEN ACCESS Check for updates

VE-cadherin RGD motifs are dispensable for cell–cell junctions, endothelial barrier function and monocyte extravasation

Rianne M. Schoon[a*], Werner J. van der Meer[a*], Anne-Marieke D. van Stalborch[a], Jaap D. van Buul[a,b#], and Stephan Huveneers[a#]

[a]Amsterdam UMC, University of Amsterdam, Amsterdam, The Netherlands; [b]Swammerdam Institute of Life Sciences, University of Amsterdam, Amsterdam, The Netherlands

ABSTRACT

VE-cadherin is a key transmembrane protein involved in endothelial cell–cell junctions, playing a crucial role in maintaining vascular integrity and regulating selective leukocyte extravasation into inflamed tissue. The extracellular domain of human VE-cadherin contains two arginine-glycine-aspartate (RGD) motifs, which are known integrin-binding sites within extracellular matrix proteins, particularly for integrins of the β1, β3, and β5 families. In this study, we examined the functional relevance of these RGD motifs by generating VE-cadherin variants in which the RGD sequences were mutated to nonfunctional RGE. Immunofluorescence analysis showed that the VE-cadherin [D238E], VE-cadherin [D301E], and double-mutant VE-cadherin [D238/301E] variants formed stable endothelial cell–cell junctions that were comparable to junctions based on wild-type VE-cadherin. Additionally, electric cell-substrate impedance sensing (ECIS) confirmed that endothelial cells expressing each VE-cadherin RGD>RGE variant maintained efficient barrier function capacity. Moreover, monocyte transmigration assays demonstrated that the RGD>RGE mutations did not affect monocyte-endothelial interactions during transmigration. In summary, our findings indicate that the VE-cadherin RGD motifs are not essential for endothelial junction formation or monocyte transmigration.

ARTICLE HISTORY
Received 8 November 2024
Revised 21 February 2025
Accepted 24 February 2025

KEYWORDS
Adherens junctions; barrier integrity; integrins; leukocyte extravasation; RGD motif; VE-cadherin

Introduction

The luminal surface of arteries and veins is lined with endothelium, a single layer of cells that maintains a strong yet selectively permeable barrier between the blood and the surrounding tissue. In homeostasis, the endothelium prevents leakage of plasma and other blood components by forming interconnected cell–cell junctions.[1,2] A key component of these structures is the adherens junction, which is formed by the transmembrane receptor vascular endothelial (VE)-cadherin, a mediator of homotypic adhesion between adjacent cells.[3] During inflammation, the endothelial cells capture circulating leukocytes and direct them to exit the bloodstream to reach the affected tissue.[4–6] The transmigration process is controlled by a sequence of receptor–ligand interactions between the leukocytes and endothelium, including heterotypic adhesions mediated through selectins, ICAM-1, VCAM-1 and integrin receptors.[7–9]

VE-cadherin plays a crucial role in inflammation by regulating the integrity of endothelial cell–cell junctions and the paracellular extravasation of leukocytes.[6] The regulation of VE-cadherin-based junctions during transmigration involves various signal transduction-induced phosphorylation and ubiquitination events at the cytoplasmic domain of VE-cadherin, which modulates its endocytosis and the interaction of the junctional complex with the actin cytoskeleton.[10–12] VE-cadherin-based junctions are transiently displaced during leukocyte transmigration.[13–15] In addition, the interaction of the VE-cadherin complex with the actin cytoskeleton is key for junction remodeling during leukocyte extravasation and endothelial barrier recovery afterward.[16,17]

CONTACT Stephan Huveneers s.huveneers@amsterdamumc.nl Amsterdam UMC, University of Amsterdam, Department of Medical Biochemistry, Meibergdreef 9, 1105 AZ Amsterdam, The Netherlands

*shared first authors.
#shared last authors.

Supplemental data for this article can be accessed online at https://doi.org/10.1080/21688370.2025.2478349.

© 2025 The Author(s). Published with license by Taylor & Francis Group, LLC.
This is an Open Access article distributed under the terms of the Creative Commons Attribution License (http://creativecommons.org/licenses/by/4.0/), which permits unrestricted use, distribution, and reproduction in any medium, provided the original work is properly cited. The terms on which this article has been published allow the posting of the Accepted Manuscript in a repository by the author(s) or with their consent.

The extracellular domain of VE-cadherin mediates the homotypic binding between adjacent cells. Intriguingly, the human VE-cadherin protein contains two arginine-glycine-aspartate (RGD) motifs that are evolutionary conserved among primates: one in the second and one in the third extracellular calcium-dependent cadherin-like binding domain.[18,19] RGD motifs, often present in extracellular matrix proteins, are well-known potential integrin-binding sites particularly for the β1, β3, and β5 families.[20–22] A variety of these RGD-binding integrins are expressed on the surface of endothelial cells, as well as on monocytes.[23] Leukocytes express integrin α4β1 (VLA-4), which in addition to its function as a receptor for the inflammatory adhesion protein VCAM-1, can bind to RGD-containing ligands.[24,25] Furthermore, endothelial cells express various β1 integrins, which are required for the proper organization of VE-cadherin-based junctions in the developing vasculature,[26] highlighting that there is close crosstalk between these adhesion receptors. Although, at present there is no direct evidence for a molecular interaction between VE-cadherin and integrin proteins, the aforementioned observations suggest that the RGD motifs of VE-cadherin may serve as ligands for integrins on endothelial and/or leukocytes.

Here, we investigated the potential functional relevance of the RGD motifs in VE-cadherin. Endothelial cells in which endogenous VE-cadherin was replaced with variants in which the RGD motifs were mutated to nonfunctional RGE sequences, still formed normal adherens junctions and maintained endothelial barrier function. Furthermore, we show that the RGD motifs of VE-cadherin are not needed for interactions between monocytes and endothelial cells during transmigration. Together, this work provides evidence that VE-cadherin's RGD motifs are not of major importance to junction-dependent endothelial functions.

Materials and methods

Cells

Cord blood outgrowth endothelial cells (BOECs[27,28]), isolated according to protocol,[29] were cultured at 37°C with 5% CO_2 in endothelial growth medium (#c -22,211, Promocell) supplemented endothelial growth factor mix (#C-39216, Promocell), 15% heat-inactivated fetal calf serum (#1156036, Gibco), 100 U/mL penicillin (#11548876, Gibco), and 100 µg/mL streptomycin (#15140122, Gibco). Cells were cultured on fibronectin (FN; source Sanquin) coated surfaces. To obtain knockdown lines, cells were lentivirally transduced with pLKO.1-shRNA targeting the VE-cadherin 3'UTR (previously validated in Malinova et al.[30] and were selected with 2.5 ng/mL puromycin (#P8833, Sigma-Aldrich) and compared to shControl (shC002) transduced cells. Next, the knockdown cells were transduced with lentivirus containing GFP-tagged VE-cadherin variants. VE-cadherin-GFP overexpression was selected by fluorescence activated cell sorting (FACS).

DNA plasmids

The VE-cadherin [D238E] mutation was introduced using site directed mutagenesis on a pEGFP-hVE-cadherin-GFP plasmid using 5'-CCTCCGGG GG**GA**<u>**G**</u>TCGGGCACGGCC-3' and 5'-GGCCG TGCCCGA<u>**C**</u>**TC**CCCCCGGAGG-3' primers. The VE-cadherin[D301E] mutation was introduced using 5'-GCATCTTGCGGGGC**GA**<u>**G**</u>TACCAGG ACGCTTTCAC-3' and 5'-GTGAAAGCGTCCTG GTA<u>**C**</u>**TC**GCCCCGCAAGATGC-3' primers. The generated VE-cadherin sequences were next amplified using PCR with primers 5'-TACATCTACGTA TTAGTCATCGCTA-3' and 5'- CCTCTACA AATGTGGTATGGCTGATTATGATC –3' and inserted into a pLV-CMV-Puro lentiviral plasmid using restriction-ligation protocols with enzymes SnaBI, XbaI, NheI, PstI, and XhoI. Resulting pEGFP and pLV constructs were all verified by Sanger sequencing.

Western blotting

Cells were lysed in Laemmli reduced sample buffer with 4% ß-mercaptoethanol, denatured for 10 min at 96°C and loaded on 4%–12% gradient SDS-page gels (NW042125BOX, Thermo Fisher Scientific) and run according to the manufacturer's instructions. After semi-dry transfer onto ethanol-activated PVDF membranes and blocking in 3% bovine serum albumin (BSA; A8806-5 G, Sigma

Aldrich) in Tris-buffered saline (TBS; Sigma Aldrich) for 45 min at room temperature (RT), blots were incubated overnight at 4°C in primary antibody in TBS + 3%BSA: rabbit anti-VE-cadherin (D87F2, Cell Signaling Technology), mouse anti-GFP (SC-9996, Santa Cruz), and anti-ß-actin (#4967, Cell Signaling Technology); washed 3 times for 5 min in TBS; incubated at RT in secondary antibody in TBS + 3%BSA: anti-rabbit-HRP (-170–6515, Biorad) or anti-mouse-HRP (172–1011, Biorad); washed another 3 times for 5 min in TBS; and imaged using enhanced chemiluminescence detection (34580, Thermo Fisher Scientific) on an Amersham ImageQuant 800 GxP machine (29653452, Cytiva). Protein band intensity was quantified using the FIJI/ImageJ Gel Analyser plugin.

Electric cell-substrate impedance sensing (ECIS)

Endothelial barrier function was measured using ECIS as previously described.[31] In short, gold electrodes (8w10E+, #72040, Applied BioPhysics) were treated with 10 mm L-cysteine (Sigma Aldrich) in saline for 15 min at RT and FN-coated for 2 h at 37°C. Impedance measuring at 4,000 hz to assess cell–cell junction integrity and at 16,000 hz to assess cell-extracellular matrix adhesion[32–36] was performed for 50 h, starting immediately after seeding of 120,000 BOECs per chamber, using the ZTheta machine (Applied BioPhysics). Data analysis was performed in GraphPad Prism.

Monocyte isolation

Pan-monocytes were isolated from whole-peripheral blood from healthy voluntary donors that signed an informed consent from the Amsterdam University Medical Center medical ethical committee in accordance with the rules and regulations within the Netherlands, based on the declaration of Helsinki and the guidelines for good clinical practice. Within 1 h after donation, blood was diluted (1:1) in RT phosphate buffered saline (PBS; #M09001/02, Fresenius Kabi) with 1:10 TNC, transferred onto 1.076 g/mL Percoll separation medium at RT, and separated by centrifuging at RT for 20 min at 800 G with start and brake at setting 3. After Percoll separation, the ring fraction was taken, and erythrocytes were lysed in ice-cold buffer (water for injection with 155 mm NH_4Cl, 10 mm $KHCO_3$, 0.1 mm EDTA (all Sigma-Aldrich)) on ice for 25 min. Monocytes were then isolated using the human pan-monocyte isolation kit (#130-096-537, Miltenyi Biotech) according to the manufacturer's protocol and kept at 37°C for the duration of the experiment.

Monocyte transmigration under physiological flow

For flow assays, 45,000 BOECs were seeded per channel of FN-coated ibidi µ-slides $VI^{0.4}$ (#80666, ibidi, Munich, Germany) and grown for 48 h until confluence and stimulated for 4 h with 10 ng/mL recombinant human TNFα (300-01A, Peprotech) in endothelial culture medium. During microscopy at 37°C and 5% CO_2, ibidi slide flow channels were connected to a pump system providing a laminar flow of 0.8 dyne/cm^2 of 37°C HEPES++ buffer (20 mm HEPES, 132 mm NaCl, 6 mm KCl, 1 mm $MgSO_4$, 1.4 mm K_2HPO_4 (pH 7.4), 1 mm $CaCl_2$, 5 mm D-glucose (all Sigma-Aldrich) and 0.4%w/v human serum albumin (Sequence). Cells received laminar flow for 2 min before 1 million monocytes were introduced into the system. After monocyte introduction, transmigration was captured every 5 s during 15 min on two mid-channel positions using an Axiovert 200 M widefield microscope with a TL Halogen lamp at 6.06 V exposing for 32 ms, detected through a 10× DIC NA0.30 Air objective (Zeiss) by an AxioCam ICc3 camera (Zeiss). In addition, immediately after the 15 min, an image overview of the channels was generated by stitching a tile scan of 4 × 6 frames. These images were used to quantify total adhesion and transmigration of monocytes. Tested endothelial monolayers were randomized to exclude variations of leukocyte freshness post-isolation. Analysis was performed as previously described in Grönloh et al.[37]

Immunofluorescence

For immunofluorescence stainings, 90,000 BOECs were grown until 48 h at confluence on FN-coated ibidi µ-slides $VI^{0.4}$ (#80666, ibidi, Munich,

Germany) and fixed in 4% PFA in PBS with 1 µg/mL $CaCl_2$ and 0.5 µg/mL $MgCl_2$ (PBS++) for 5 min at 37°C. Fixed cells were permeabilized using 0.01% Triton (X100, Sigma Aldrich) in PBS++ for 10 min at RT, blocked in 3% BSA in PBS++ at RT for 45 min, stained with primary antibody for 1 h at RT and secondary antibodies for 45 min at RT. Alexa Fluor 488-conjugated VE-cadherin mouse monoclonal antibody was purchased from ABCAM (ab272345; diluted 1:250). Anti-α-catenin mouse monoclonal antibody was purchased from Enzo Life Sciences (ALX-804-101; diluted 1:300). Alexa Fluor 594-conjugated chicken anti-mouse antibody was purchased from Invitrogen (A21201; diluted 1:400). Hoechst 33342 was purchased from Molecular Probes (H-1399; diluted 1:25,000). PromoFluor 415-Phalloidin was purchased from PromoKine (PK-PF415-7-01, diluted 1:200). Fluorescence was captured on a Nikon Eclipse TI microscope with SOLA SEII light source, 60 × 1.49NA Apo TIRF oil objective, standard NIKON filter cubes, using a Andor Zyla 4.2 plus sCMOS camera. Images were enhanced for display using an unsharp mask filter and adjusted for brightness and contrast using FIJI/ImageJ software.

Statistical analysis

GraphPad Prism was used for the statistical analysis of all data. For ECIS data, all data points were corrected for background signal of medium only conditions and technical duplicates were averaged per biological replicate. Western blots were corrected for background, for total protein loading, and related to control band intensity within a biological replicate condition. Comparison between multiple groups was made using one-way ANOVA in combination with Dunnett's post-hoc test for multiple comparisons and a D'Agostino-Pearson test for normality. All graphs show mean and standard deviation and p-values are indicated in the graphs.

Results

Replacing endogenous VE-cadherin with VE-cadherin-[RGD>RGE] variants in endothelial cells

Mammalian VE-cadherin contains two RGD motifs that are located on the extracellular part of the protein within the second and third cadherin domain (Figure 1(a)). RGD motifs, as adhesion ligand, can be rendered inactive by substituting the aspartic acid for glutamic acid (D>E), which retains the motif's negative charge while altering its steric composition[39] (Figure 1(b)). We generated lentiviral plasmids expressing GFP-tagged human wild-type VE-cadherin (WT), its variants in which the individual RGD motifs are converted to nonfunctional RGE sequences (D238E and D301E), and a double mutated variant in which both RGD motifs were converted to RGE (D238/301E). These point mutations would prevent potential integrin interactions with the RGD motifs while keeping the rest of the extracellular VE-cadherin protein structure intact. To assess the function of each VE-cadherin RGD>RGE variant in endothelial cells (ECs), we first knocked down the expression of endogenous VE-cadherin by using lentiviral shRNAs targeting the 3′-untranslated region (3′-UTR) of the CDH5 messenger RNA in cord blood outgrowth endothelial cells (BOECs) (Figure 1(c,d)). VE-cadherin endogenous protein depletion was confirmed by Western blot (Figure 1(c,d)) and resulted in a loss of adherens junctions as verified by immunofluorescent (IF) imaging of VE-cadherin and α-catenin (Figure 1(e)). Next, the VE-cadherin knockdown ECs were rescued by stable expression of lentivirally transduced wild-type (WT) VE-cadherin-GFP, or the RGE variants, and GFP-based fluorescence-activated cell sorting (Figure 1(c,d)). Total VE-cadherin protein levels after rescue were comparable to endogenous levels (Figure 1(c, d); Supplemental Figure S1A, Supplemental Figure S2). IF imaging of the generated endothelial cell lines showed that the VE-cadherin [D238E], VE-cadherin [D301E] and VE-cadherin [D238/301E] protein variants all efficiently restored the formation of adherens junctions, to similar extent as VE-cadherin [WT] (Figure 1(e)). In addition, no obvious differences were detected in junctional localization of the VE-cadherin variants or the actin cytoskeletal organization of the generated cell lines (Supplemental Figure S1B), nor in the localization of the core adherens junction protein α-catenin (Figure 1(e)).

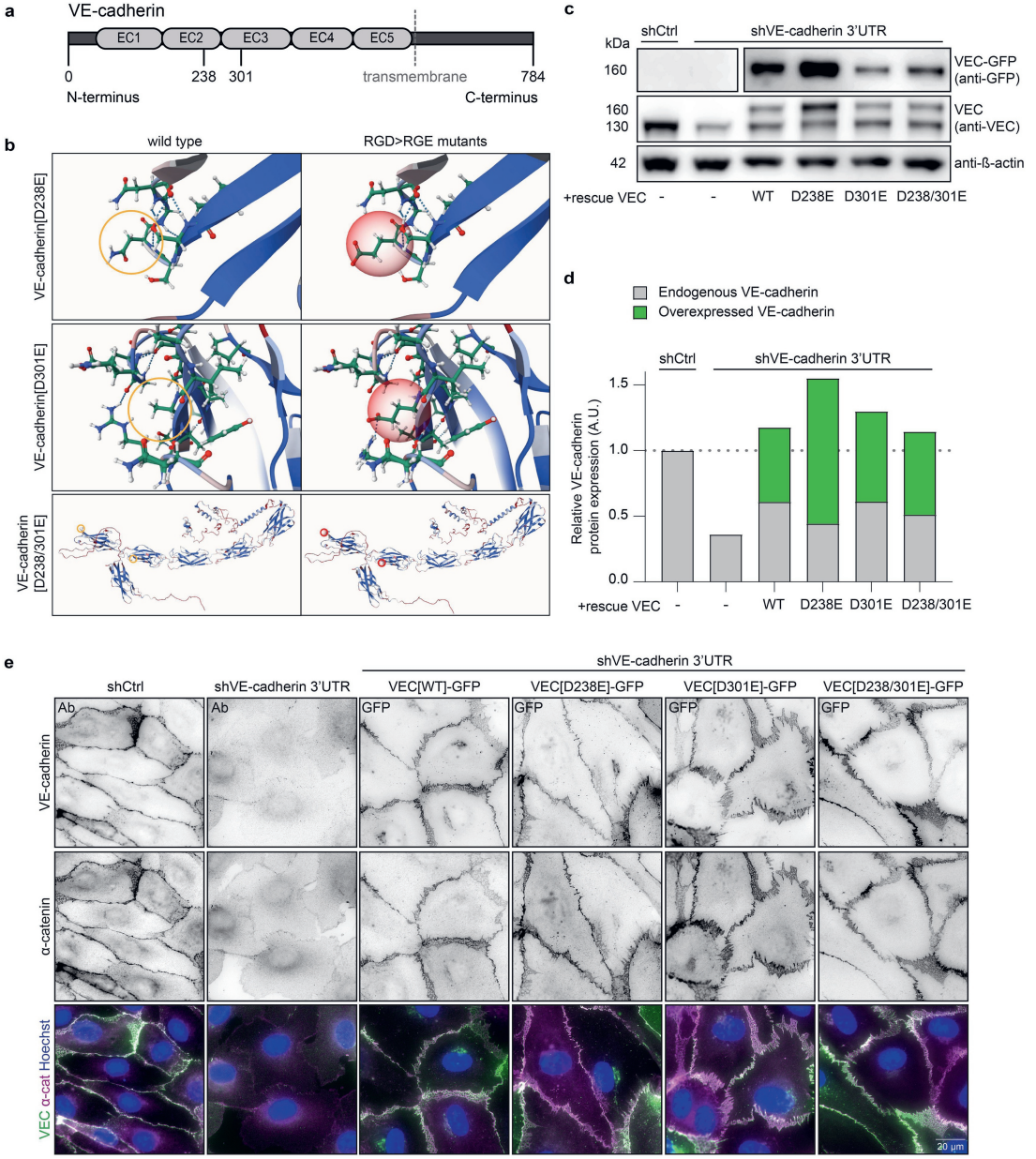


Figure 1. Replacing endogenous VE-cadherin with VE-cadherin-[RGD>RGE] variants in endothelial cells. (a) Human VE-cadherin contains two RGD sites in its extracellular EC2 and EC3 domains. The locations of the D>E mutations in the RGD domains are at amino acid positions 238 and 301. (b) 3D visualization of the amino acid substitution using the MutationExplorer web tool.[38] (c) Representative Western blot analysis of lysates derived from wild-type BOECs and cells transduced with control shRNA or shVE-cadherin-3'UTR and subsequent rescue lines. Blots are probed for VE-cadherin, GFP and ß-actin as loading control. See Supplemental Figure S2 for corresponding full scans of the blots. (d) Analysis of VE-cadherin blot from (C). Graph shows VE-cadherin expression levels, signal corrected for background and relative to expression of endogenous VE-cadherin in control shRNA-treated cells. (e) Representative immunofluorescence images of BOECs transduced shVE-cadherin-3'UTR to deplete endogenous VE-cadherin and rescued with the indicated VE-cadherin-GFP variants (GFP, green). shCtrl and shVE-cadherin cells were stained for endogenous VE-cadherin (Ab, green). All cells were stained for α-catenin (magenta) and Hoechst (blue).

The VE-cadherin RGD motifs are dispensable for endothelial barrier function

VE-cadherin mediates homotypic binding in trans between adjacent endothelial cells through the first extracellular cadherin (EC) domain.[40] The RGD motifs are located within the second and third EC domains, potentially affecting the adhesive function of VE-cadherin. In addition, we hypothesized that the RGD motifs may contribute to barrier function through heterotypic interactions between endothelial cells binding to endothelial ß1 and ß3 integrins. To examine barrier function in the RGD>RGE cell lines we performed electric cell-substrate impedance sensing (ECIS) measurements at different frequencies: 4,000 hz to assess the tightness of cell–cell junctions in the respective endothelial monolayers, and 16,000 hz to assess cell adhesion to the substrate.[31,34,35] These experiments showed that the VE-cadherin-depleted cells show severely impaired barrier function as expected (Supplemental Figure S1C-E), while cell lines rescued with VE-cadherin WT or RGD>RGE variants form stable barriers (Figure 2(a)). Cells expressing VE-cadherin RGD>RGE, in particular VE-cadherin [D238/301E], display a slight delay in the initial phase of endothelial barrier formation when compared to VE-cadherin [WT] (Figure 2(a)). At 24 h after seeding, all cell lines reached maximal barrier function, indicating the establishment of confluent monolayers (Figure 2(b)). We observed that monolayers formed by VE-cadherin [D238E] and VE-cadherin [D238/D301E] were slightly less resistant compared to the control. However, no significant differences in the barrier function of the endothelial monolayers were detected at 48 h post-cell seeding (Figure 2(c)). Endothelial cells expressing VE-cadherin RGD>RGE displayed only a minor delay in initial cell-substrate adhesion within 2–4 h post-seeding, based on impedance sensing at a frequency of 16,000 hz (Figure 2(d)), but no significant differences were measured at 24 and 48 h after seeding (Figure 2(e,f)). To further test the role of the RGD motifs in adherens junction dynamics, we next challenged endothelial monolayers with the permeability factor thrombin.[31,41] These experiments showed that VE-cadherin [D238/301E] expressing monolayers responded normally to thrombin stimulation, as visualized by the temporary loss of barrier function (Figure 3(a)). There was a minor delay in the barrier recovery phase at 30 min after thrombin treatment (Figure 3(b)). Hence, we conclude that the extracellular RGD motifs might minimally support VE-cadherin-based junction formation, but do not contribute substantially to cell–cell junction stability over time, nor are they critical for adhesion of endothelial cells to the basal substrate.

VE-cadherin's RGD motifs do not regulate monocyte adhesion and transendothelial migration

As the RGD motif is a recognition site for various integrins that are expressed by monocytes,[23] we next investigated whether VE-cadherin might control the adhesion and/or transendothelial migration of these leukocytes via its RGD motifs. To assess this, the VE-cadherin variant endothelial monolayers were grown in fibronectin-coated channel slides and stimulated with inflammatory mediator tumor necrosis factor (TNF)α. Next, monocytes isolated from healthy donor blood were allowed to transmigrate across the inflamed monolayers under physiological flow of 0.8 dyne/cm^2 (Figure 4(a)). These experiments indicate that endothelial cells expressing VE-cadherin RGD>RGE-mutants retained their ability to facilitate capture and rolling of monocytes (Figure 4(a,b)). Moreover, monocytes transmigrated with equal efficiency across the different endothelial monolayers (Figure 4(c)). Together, these data imply no major role for the RGD motifs of VE-cadherin in monocyte recruitment or transmigration.

Discussion

The presence of the RGD motifs in the extracellular domain of VE-cadherin is a seemingly overlooked molecular property with a possible role in endothelial cells. In this study, we replaced the endogenous VE-cadherin protein with RGD>RGE nonfunctional variants to investigate this aspect. Our results show that the VE-cadherin RGD motifs are not crucial for key endothelial functions such as adherens junction formation, maintenance of endothelial barrier function and monocyte transendothelial migration.

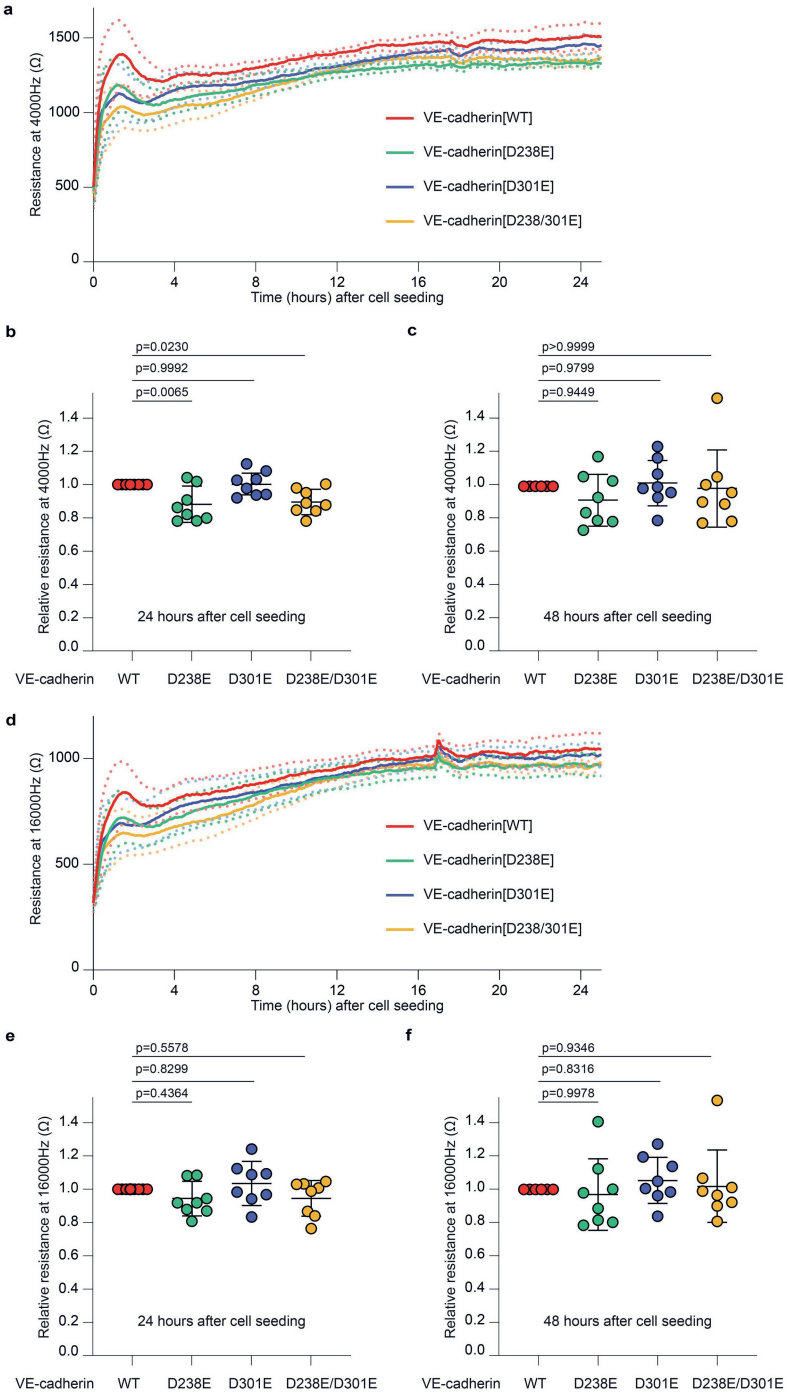


Figure 2. VE-cadherin RGD motifs are dispensable for endothelial barrier function. (a) Line graph showing the average resistance (±SEM, dotted lines) measured with ECIS at 4,000 hz of indicated BOEC monolayers over time. Data from $n = 8$ independent experiments. (b,c) Graphs showing the relative, compared to VE-cadherin[WT], resistance at 4,000 hz 24 (b) and 48 (c) hours after cell seeding. Data from $n = 8$ independent experiments, mean and SD shown, ANOVA with Dunnett's multiple comparison test, p-values indicated. (d) Line graph showing the average resistance (±SEM, dotted lines) measured with ECIS at 16,000 hz of BOEC monolayers over time. Data from $n = 8$ independent experiments. (e,f) Graphs showing the relative, compared to VE-cadherin[WT], resistance at 16,000 hz 24 (e) and 48 (f) hours after cell seeding data from $n = 8$ independent experiments, mean and SD shown, ANOVA with Dunnett's multiple comparison test, p-values indicated.

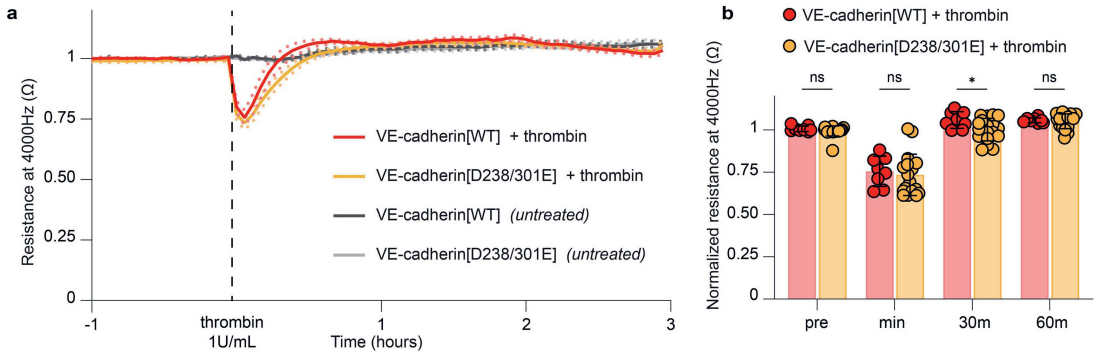


Figure 3. Normal thrombin-induced permeability response in VE-cadherin [D238/301E] cells. (a) Line graph showing the average resistance (±SEM, dotted lines) measured with ECIS at 4,000 hz of indicated BOEC monolayers over time following treatment with the permeability factor human plasma-derived thrombin (used at 1 U/mL). Data are normalized to the baseline values prior to thrombin treatment and are derived from $n = 4$ independent experiments. (b) Graphs showing the relative, compared to VE-cadherin[WT], resistance at 4,000 hz at baseline before thrombin stimulation (*pre*), at the lowest barrier level after thrombin treatment (*min*), and 30 and 60 minutes after thrombin treatment. Data from $n = 4$ independent experiments performed in duplo, mean and SD shown, ANOVA with Dunnett's multiple comparison test, $^*p < 0.05$.

The presence of the RGD motif in various extracellular ligands promotes cell adhesion, migration, and signaling in a multitude of cell types, including endothelial cells and leukocytes, monocytes in particular.[20,22,39,42] The RGD motif, often part of extracellular matrix components such as fibronectin, vitronectin and fibrinogen, mediates adhesion by ß1 and ß3 integrins. Other integrin subtypes are well known to control the rolling, adhesion and transendothelial migration cascade of leukocytes. These steps rely for instance on the function of leukocyte-expressed LFA-1 and Mac-1, which both contain the ß2 integrin subunit, but do not interact to ligands through RGD. Our data show that the RGD motifs of VE-cadherin do not significantly alter the interaction between monocytes and endothelial cells. This indicates that RGD-binding integrins on monocytes, such as αvβ3 or α5β1, do not use VE-cadherin's RGD motifs during transmigration. An explanation for why these RGD motifs do not affect monocyte adhesion might be the potential steric inaccessibility of the peptide sequence within the VE-cadherin extracellular domain through posttranslational modifications in the extracellular domain. For instance, decreasing VE-cadherin N-glycosylation has been shown to promote the adhesion of monocytes.[43] The RGD motifs might also be inaccessible as a result of the tertiary structure of the folded VE-cadherin protein within the adhesion complex, or because of the tight cell–cell contact organization. Adherens junctions are formed by VE-cadherin *trans*-dimerization through the first cadherin domain of proteins on adjacent cells,[44] as well as *cis*-dimerization between proteins of the same cell via the fourth cadherin domain[40] resulting in the formation of cadherin clusters.[45] Cluster density might also shield the RGD motifs from passing leukocytes, hence preventing specific monocyte recruitment.

Another explanation for the dispensable role of VE-cadherin's RGD motifs is that for optimal adhesion the RGD needs synergistic domains to bind to integrins. In the field of functionalized biomaterials, it has been reported that the isolated RGD motif is less potent to induce integrin-signaling compared to RGD within the context of native proteins.[46] The cooperation with other protein domains also explains how the RGD peptide can bind different integrins and induce differential signaling.[47] Examples of such co-motifs are the amino acid sequence PHSRN that allows fibronectin-RGD to specifically activate integrin α5ß1,[48,49] and the sequence NGR that specifically binds αvß3.[50] Furthermore, larger protein chains like the 140 amino acid FAS1 domain promote RGD-αvß3 binding.[51] Altogether, our data suggest that VE-cadherin does not contain the proper protein structure and composition to unlock the adhesive potential of its extracellular RGD sites.

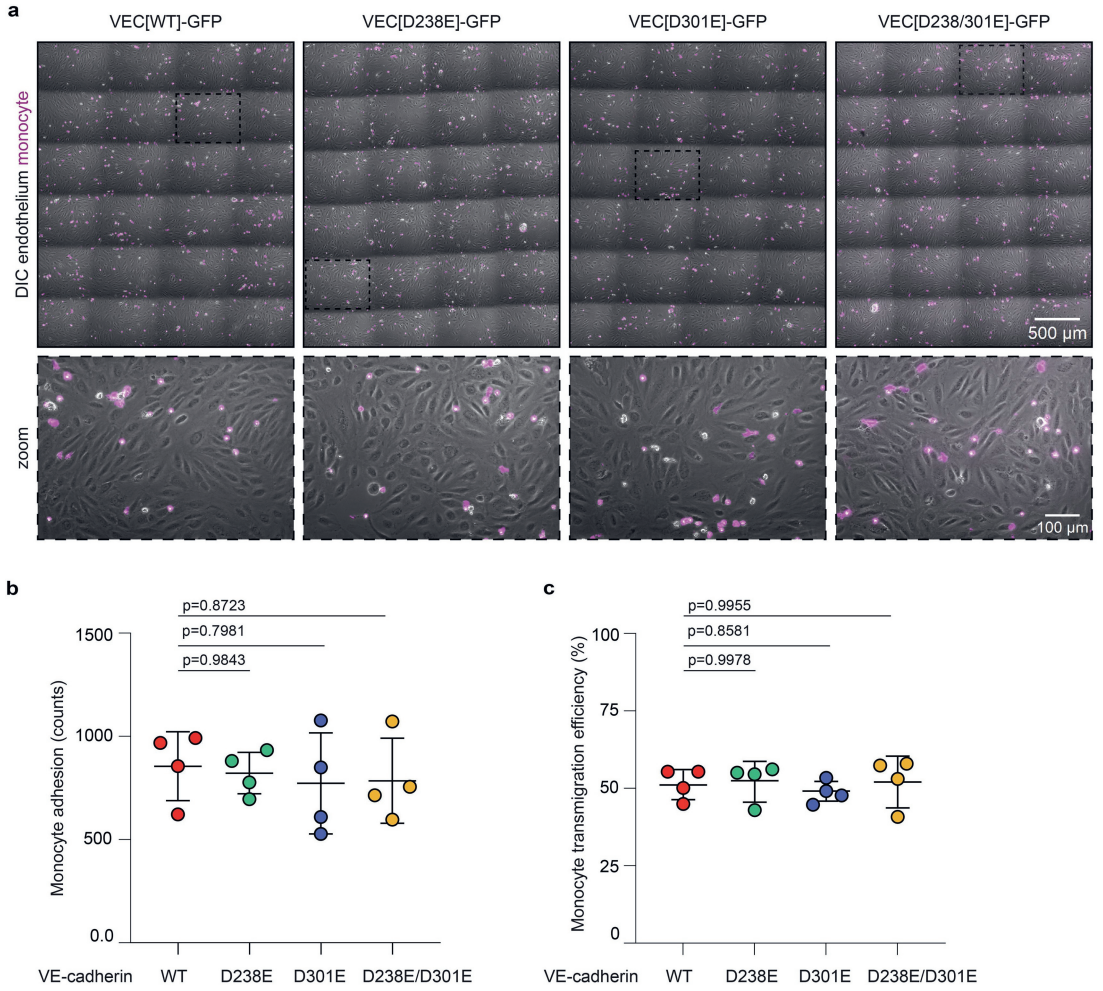


Figure 4. VE-cadherin's RGD motifs do not regulate monocyte adhesion and transendothelial migration. (a) Representative images (4×6 stitched together) taken after 10 minutes of flowing monocytes (magenta) over TNFα-stimulated inflamed wild type and RGD>RGE mutant VE-cadherin-expressing BOEC monolayers (gray) under physiological flow. (b) Graph indicating absolute monocyte adhesion to wild type and RGD>RGE mutant VE-cadherin-expressing BOEC monolayers under physiological flow. Data from $n = 4$ independent experiments, mean and SD shown, ANOVA with Dunnett's multiple comparison test, p-values indicated. (c) Graph showing monocyte transendothelial migration efficiency as the percentage of all adhered monocytes. Data from $n = 4$ independent experiments, ANOVA with Dunnett's multiple comparison test, p-values indicated.

In summary, by using mutagenesis to disrupt the RGD motifs, combined with assays that examined cell–cell junctions, cell adhesion, endothelial barrier function and monocyte transmigration, our results suggest that there is no major role for VE-cadherin's RGD motifs in in vitro endothelial cells. To fully rule out a possible function of VE-cadherin's RGD motifs in the vasculature one could generate transgenic zebrafish or mouse models. Using such transgenic models one can determine whether the RGD motifs of VE-cadherin are needed for vascular development or vascular maintenance within a physiologically perfused organism. However, with the obtained insights from the in vitro cells generated in this study, it currently lacks sufficient rationale to make that effort.

Disclosure statement

No potential conflict of interest was reported by the author(s).

That could have appeared to influence the work reported in this article.

Funding

This work is financially supported by the Netherlands Organization of Scientific Research (ZonMw VIDI grant 016.156.327, ZonMw Vici grant 09150182310041 to S.H. and ZonMW Vici grant 91819632 to J.D.v.B.), the Dutch Heart Foundation (03-002-2021-T087 Established Investigator Dekker grant to S.H.) and a grant from the Rembrandt Institute for Cardiovascular Sciences to S.H. and J.D.v.B.).

ORCID

Stephan Huveneers http://orcid.org/0000-0002-1091-475X

References

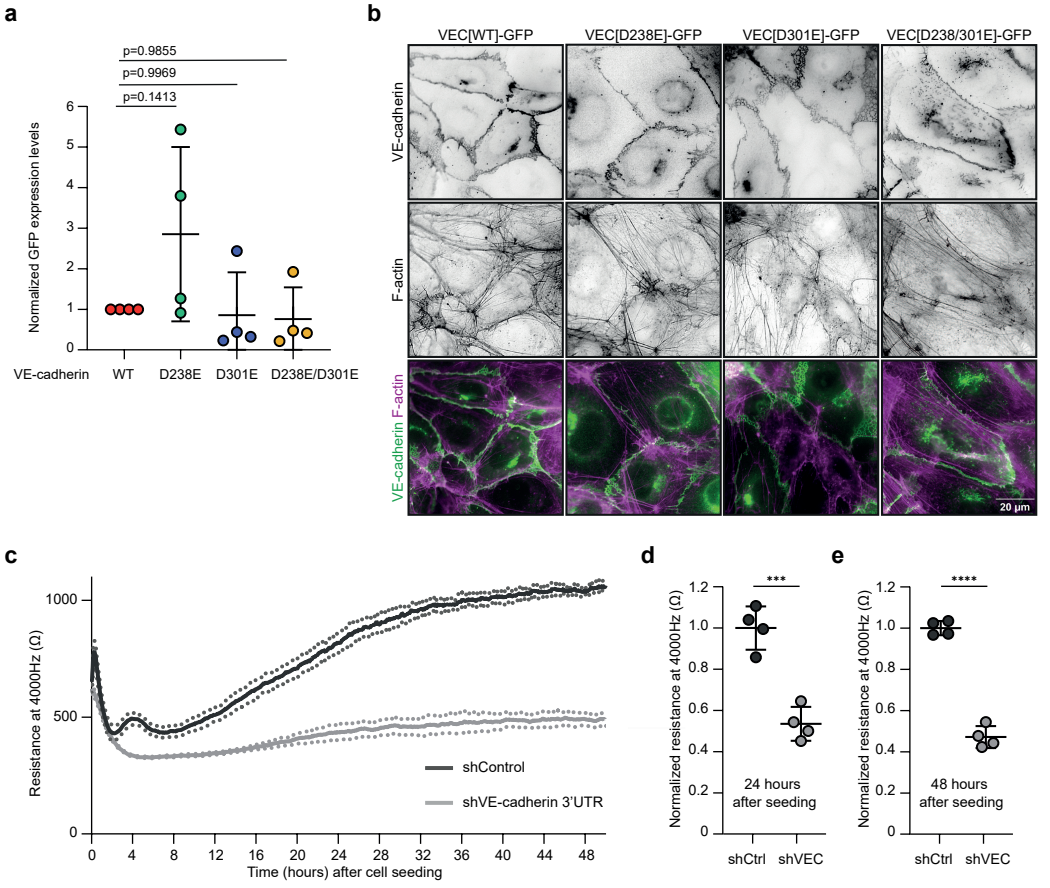
1. Bazzoni G, Dejana E. Endothelial cell-to-cell junctions: molecular organization and role in vascular homeostasis. Physiol Rev. 2004;84:869–901. doi:10.1152/physrev.00035.2003.
2. Hartsock A, Nelson WJ. Adherens and tight junctions: structure, function and connections to the actin cytoskeleton. Biochim et Biophys Acta (BBA) - Biomembr. 2008;1778:660–669. doi:10.1016/j.bbamem.2007.07.012.
3. Dejana E, Orsenigo F, Lampugnani MG. The role of adherens junctions and ve-cadherin in the control of vascular permeability. J Cell Sci. 2008;121:2115–2122. doi:10.1242/jcs.017897.
4. Ley K, Laudanna C, Cybulsky MI, Nourshargh S. Getting to the site of inflammation: the leukocyte adhesion cascade updated. Nat Rev Immunol. 2007;7:678–689. doi:10.1038/nri2156.
5. Nourshargh S, Alon R. Leukocyte migration into inflamed tissues. Immunity. 2014;41:694–707. doi:10.1016/j.immuni.2014.10.008.
6. Vestweber D. How leukocytes cross the vascular endothelium. Nat Rev Immunol. 2015;15:692–704. doi:10.1038/nri3908.
7. Aman J, Margadant C. Integrin-dependent cell–matrix adhesion in endothelial health and disease. Circ Res. 2023;132:355–378. doi:10.1161/CIRCRESAHA.122.322332.
8. Dejana E, Raiteri M, Resnati M, Lampugnani MG. Endothelial integrins and their role in maintaining the integrity of the vessel wall. Kidney Int. 1993;43:61–65. doi:10.1038/ki.1993.11.
9. Mitroulis I, Alexaki VI, Kourtzelis I, Ziogas A, Hajishengallis G, Chavakis T. Leukocyte integrins: role in leukocyte recruitment and as therapeutic targets in inflammatory disease. Pharmacol Ther. 2015;147:123–135. doi:10.1016/j.pharmthera.2014.11.008.
10. Arif N, Zinnhardt M, Nyamay'antu A, Teber D, Brückner R, Schaefer K, Li Y, Trappmann B, Grashoff C, Vestweber D. PECAM-1 supports leukocyte diapedesis by tension-dependent dephosphorylation of ve-cadherin. EMBO J. 2021;40:e106113. doi:10.15252/embj.2020106113.
11. Wessel F, Winderlich M, Holm M, Frye M, Rivera-Galdos R, Vockel M, Linnepe R, Ipe U, Stadtmann A, Zarbock A, et al. Leukocyte extravasation and vascular permeability are each controlled in vivo by different tyrosine residues of ve-cadherin. Nat Immunol. 2014;15:223–230. doi:10.1038/ni.2824.
12. Wilkens M, Holtermann L, Stahl A-K, Stegmeyer RI, Nottebaum AF, Vestweber D. Ubiquitination of ve-cadherin regulates inflammation-induced vascular permeability in vivo. EMBO Rep. 2024;25:4013–4032. doi:10.1038/s44319-024-00221-7.
13. Arts JJ, Mahlandt EK, Grönloh ML, Schimmel L, Noordstra I, Gordon E, Van Steen AC, Tol S, Walzog B, Van Rijssel J, et al. Endothelial junctional membrane protrusions serve as hotspots for neutrophil transmigration. eLife. 2021;10:e66074. doi:10.7554/eLife.66074.
14. Liu Y, Shaw SK, Ma S, Yang L, Luscinskas FW, Parkos CA. Regulation of leukocyte transmigration: cell surface interactions and signaling events. J Immunol. 2004;172:7–13. doi:10.4049/jimmunol.172.1.7.
15. Van Buul JD, Voermans C, Van Den Berg V, Anthony EC, Mul FPJ, Van Wetering S, Van Der Schoot CE, Hordijk PL. Migration of human hematopoietic progenitor cells across bone marrow endothelium is regulated by vascular endothelial cadherin. J Immunol. 2002;168:588–596. doi:10.4049/jimmunol.168.2.588.
16. Martinelli R, Kamei M, Sage PT, Massol R, Varghese L, Sciuto T, Toporsian M, Dvorak AM, Kirchhausen T, Springer TA, et al. Release of cellular tension signals self-restorative ventral lamellipodia to heal barrier micro-wounds. J Cell Biol. 2013;201:449–465. doi:10.1083/jcb.201209077.
17. Schulte D, Küppers V, Dartsch N, Broermann A, Li H, Zarbock A, Kamenyeva O, Kiefer F, Khandoga A, Massberg S, et al. Stabilizing the ve-cadherin-catenin complex blocks leukocyte extravasation and vascular permeability: necessity of paracellular diapedesis in vivo. EMBO J. 2011;30:4157–4170. doi:10.1038/emboj.2011.304.
18. Bartolomé RA, Torres S, De Val SI, Escudero-Paniagua B, Calviño E, Teixidó J, Casal JI. Ve-cadherin RGD motifs promote metastasis and constitute a potential therapeutic target in melanoma and breast cancers. Oncotarget. 2017;8:215–227. doi:10.18632/oncotarget.13832.

19. Casal JI, Bartolomé RA. Beyond N-Cadherin, relevance of cadherins 5, 6 and 17 in cancer progression and metastasis. IJMS. 2019;20:3373. doi:10.3390/ijms20133373.
20. Benelli R, Mortarini R, Anichini A, Giunciuglio D, Noonan DM, Montalti S, Tacchetti C, Albini A. Monocyte-derived dendritic cells and monocytes migrate to HIV-Tat RGD and basic peptides. AIDS. 1998;12:261–268. doi:10.1097/00002030-199803000-00003.
21. Pytela R, Pierschbacher MD, Argraves S, Suzuki S, Ruoslahti E. [27] arginine-glycine-aspartic acid adhesion receptors, in: methods in Enzymology. Elsevier; 1987. p. 475–489. doi:10.1016/0076-6879(87)44196-7.
22. Ruoslahti E, Pierschbacher MD. New perspectives in cell adhesion: RGD and Integrins. Science. 1987;238:491–497. doi:10.1126/science.2821619.
23. Languino LR, Ruoslahti E. An alternative form of the integrin beta 1 subunit with a variant cytoplasmic domain. J Biol Chem. 1992;267:7116–7120. doi:10.1016/S0021-9258(19)50545-2.
24. Amschler K, Kossmann E, Erpenbeck L, Kruss S, Schill T, Schön M, Möckel SMC, Spatz JP, Schön MP. Nanoscale tuning of VCAM-1 determines VLA-4–dependent melanoma cell plasticity on RGD motifs. Mol Cancer Res. 2018;16:528–542. doi:10.1158/1541-7786.MCR-17-0272.
25. Yusuf-Makagiansar H, Anderson ME, Yakovleva TV, Murray JS, Siahaan TJ. Inhibition of LFA-1/ICAM-1 and VLA-4/VCAM-1 as a therapeutic approach to inflammation and autoimmune disease. Med Res Rev. 2002;22(2):146–167. doi:10.1002/med.10001.
26. Yamamoto H, Ehling M, Kato K, Kanai K, Van Lessen M, Frye M, Zeuschner D, Nakayama M, Vestweber D, Adams RH. Integrin β1 controls ve-cadherin localization and blood vessel stability. Nat Commun. 2015;6:6429. doi:10.1038/ncomms7429.
27. Ingram DA, Mead LE, Tanaka H, Meade V, Fenoglio A, Mortell K, Pollok K, Ferkowicz MJ, Gilley D, Yoder MC. Identification of a novel hierarchy of endothelial progenitor cells using human peripheral and umbilical cord blood. Blood. 2004;104:2752–2760. doi:10.1182/blood-2004-04-1396.
28. Lin Y, Banno K, Gil C-H, Myslinski J, Hato T, Shelley WC, Gao H, Xuei X, Liu Y, Basile DP, et al. Origin, prospective identification, and function of circulating endothelial colony-forming cells in mice and humans. JCI Insight. 2023;8:e164781. doi:10.1172/jci.insight.164781.
29. Martin-Ramirez J, Hofman M, Van Den Biggelaar M, Hebbel RP, Voorberg J. Establishment of outgrowth endothelial cells from peripheral blood. Nat Protoc. 2012;7:1709–1715. doi:10.1038/nprot.2012.093.
30. Malinova TS, Angulo-Urarte A, Nüchel J, Tauber M, van der Stoel MM, Janssen V, de Haan A, Groenen AG, Tebbens M, Graupera M, et al. A junctional PACSIN2/EHD4/MICAL-L1 complex coordinates ve-cadherin trafficking for endothelial migration and angiogenesis. Nat Commun. 2021;12(1):2610. doi:10.1038/s41467-021-22873-y.
31. Van Der Stoel MM, Kotini MP, Schoon RM, Affolter M, Belting H-G, Huveneers S. Vinculin strengthens the endothelial barrier during vascular development. Vasc Biol. 2022;5(1):e220012. doi:10.1530/VB-22-0012.
32. Benson K, Cramer S, Galla H-J. Impedance-based cell monitoring: barrier properties and beyond. Fluids Barriers CNS. 2013;10:5. doi:10.1186/2045-8118-10-5.
33. Luong JHT, Xiao C, Lachance B, Leabu ŠM, Li X, Uniyal S, Chan BMC. Extended applications of electric cell-substrate impedance sensing for assessment of the structure–function of α2β1 integrin. Analytica (Rome) Acta. 2004;501:61–69. doi:10.1016/j.aca.2003.09.016.
34. Robilliard LD, Kho DT, Johnson RH, Anchan A, O'Carroll SJ, Graham ES. The importance of multifrequency impedance sensing of endothelial barrier formation using ECIS technology for the generation of a strong and durable paracellular barrier. Biosensors. 2018;8:64. doi:10.3390/bios8030064.
35. Tiruppathi C, Malik AB, Vecchio PJD, GIAEVERt I, Giaever I. Electrical method for detection of endothelial cell shape change in real time: assessment of endothelial barrier function. Proc Natl Acad Sci USA. 1992;89(17):7919–7923. doi:10.1073/pnas.89.17.7919.
36. Zhang Z, Huang X, Liu K, Lan T, Wang Z, Zhu Z. Recent advances in electrical impedance sensing technology for single-cell analysis. Biosensors. 2021;11:470. doi:10.3390/bios11110470.
37. Grönloh MLB, Arts JJG, Mahlandt EK, Nolte MA, Goedhart J, Van Buul JD. Primary adhered neutrophils increase JNK1-MARCKSL1-mediated filopodia to promote secondary neutrophil transmigration. iScience. 2023;26:107406. doi:10.1016/j.isci.2023.107406.
38. Philipp M, Moth CW, Ristic N, Tiemann JKS, Seufert F, Panfilova A, Meiler J, Hildebrand PW, Stein A, Wiegreffe D, et al. MutationExplorer: a webserver for mutation of proteins and 3D visualization of energetic impacts. Nucleic Acids Res. 2024;52:W132–W139. doi:10.1093/nar/gkae301.
39. Pierschbacher MD, Ruoslahti E. Cell attachment activity of fibronectin can be duplicated by small synthetic fragments of the molecule. Nature. 1984;309:30–33. doi:10.1038/309030a0.
40. Brasch J, Harrison OJ, Ahlsen G, Carnally SM, Shapiro B, Honig L, Shapiro L. Structure and binding mechanism of vascular endothelial cadherin, a divergent classical cadherin. J Mol Biol. 2011;408(1):57–73. doi:10.1016/j.jmb.2011.01.031.
41. Rabiet M-J, Plantier J-L, Rival Y, Genoux Y, Lampugnani M-G, Dejana E. Thrombin-induced Increase in endothelial permeability is associated with changes in cell-to-cell junction organization. ATVB. 1996;16:488–496. doi:10.1161/01.ATV.16.3.488.
42. Kamoshida G, Matsuda A, Sekine W, Mizuno H, Oku T, Itoh S, Irimura T, Tsuji T. Monocyte differentiation

induced by co-culture with tumor cells involves rgd-dependent cell adhesion to extracellular matrix. Cancer Lett. 2012;315:145–152. doi:10.1016/j.canlet.2011.09.029.

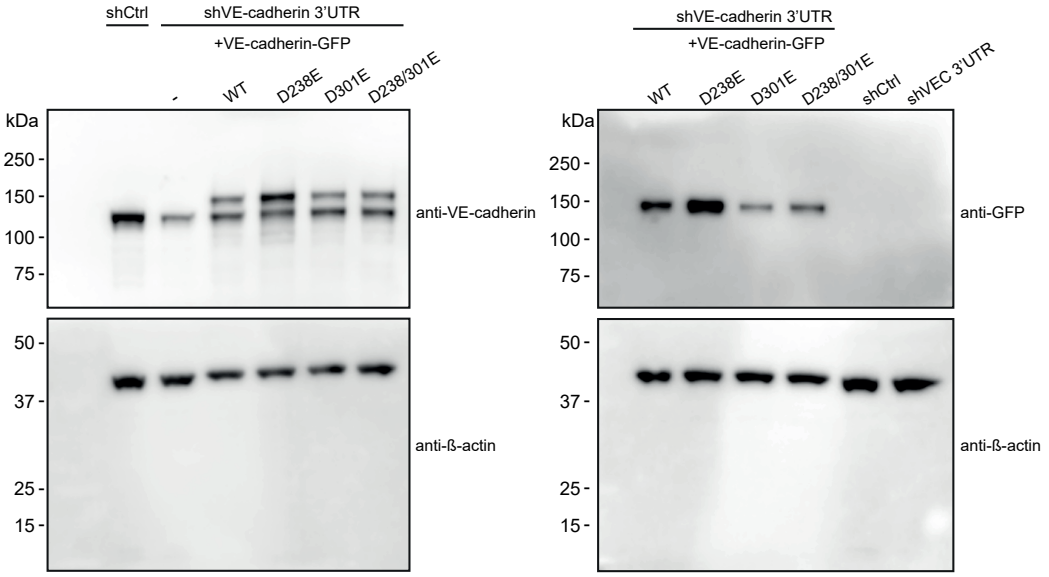
43. Zhang L, Ma L, Li J, Lei J, Chen J, Yu C. Ve-cadherin N-glycosylation modified by N-acetylglucosamin yltransferase V regulates ve-cadherin–β-catenin interaction and monocyte adhesion. Exp Phys. 2021;106(9):1869–1877. doi:10.1113/EP089617.
44. Navarro P, Caveda L, Breviario F, Mândoteanu I, Lampugnani M-G, Dejana E. Catenin-dependent and -independent functions of vascular endothelial cadherin. J Biol Chem. 1995;270:30965–30972. doi:10.1074/jbc.270.52.30965.
45. Troyanovsky SM. Adherens junction: the ensemble of specialized cadherin clusters. Trends In Cell Biol. 2023;33:374–387. doi:10.1016/j.tcb.2022.08.007.
46. Hautanen A, Gailit J, Mann DM, Ruoslahti E. Effects of modifications of the RGD sequence and its context on recognition by the fibronectin receptor. J Biol Chem. 1989;264:1437–1442. doi:10.1016/S0021-9258(18)94206-7.
47. Mao Y, Schwarzbauer JE. Accessibility to the fibronectin synergy site in a 3D matrix regulates engagement of α 5β 1 versus α vβ 3 integrin receptors. Cell Commun Adhes. 2006;13(5–6):267–277. doi:10.1080/15419060601072215.
48. Altroff H, Schlinkert R, Van Der Walle CF, Bernini A, Campbell ID, Werner JM, Mardon HJ. Interdomain tilt angle determines integrin-dependent function of the ninth and tenth FIII domains of human fibronectin. J Biol Chem. 2004;279:55995–56003. doi:10.1074/jbc.M406976200.
49. Aota S, Nomizu M, Yamada KM. The short amino acid sequence pro-his-ser-arg-asn in human fibronectin enhances cell-adhesive function. J Biol Chem. 1994;269:24756–24761. doi:10.1016/S0021-9258(17)31456-4.
50. Leiss M, Beckmann K, Girós A, Costell M, Fässler R. The role of integrin binding sites in fibronectin matrix assembly in vivo. Curr Opin In Cell Biol. 2008;20:502–507. doi:10.1016/j.ceb.2008.06.001.
51. Son H-N, Nam J-O, Kim S, Kim I-S. Multiple FAS1 domains and the RGD motif of TGFBI act cooperatively to bind αvβ3 integrin, leading to anti-angiogenic and anti-tumor effects. Biochim et Biophys Acta (BBA) - Mol Cell Res. 2013;1833:2378–2388. doi:10.1016/j.bbamcr.2013.06.012.

Supplemental Figure S1.



Supplementary Figure S1. VE-cadherin endogenous knock-down impairs the endothelial barrier. a) Quantification of the total expression levels of the VE-cadherin-GFP variants normalized to WT-VE-cadherin-GFP. Data from n=4 independent Western blot experiments. **b)** BOECs transduced with shVE-cadherin-3'UTR, rescued with indicated VE-cadherin variants (green), stained for F-actin using phalloidin (magenta). **c)** Line graph showing the average resistance (±SEM, dotted lines) measured with ECIS at 4000Hz of shControl and shVE-cadherin-3'UTR BOEC monolayers over time. **d-e)** Graphs showing the relative resistance of shVE-cadherin-3'UTR monolayers, compared to shControl, at 4000Hz 24 (d) and 48 (e) hours after cell seeding Data from n=4 independent experiments, mean and SD shown, Student's t-test, ***p<0.001, ****p<0.0001.

Supplemental Figure S2.



Supplementary Figure S2. Full scans of Western blots from Figure 1c.



Chapter 5

Vinculin strengthens the endothelial barrier during vascular development

Vascular Biology, (2023)

RESEARCH

Vinculin strengthens the endothelial barrier during vascular development

Miesje M van der Stoel[1,*], Maria P Kotini[2,*], Rianne M Schoon[1], Markus Affolter[2], Heinz-Georg Belting[2,†] and Stephan Huveneers[1,†]

[1]Amsterdam UMC, University of Amsterdam, location AMC, Amsterdam Cardiovascular Sciences, Department of Medical Biochemistry, Meibergdreef, Amsterdam, The Netherlands
[2]Biozentrum der Universität Basel, Spitalstrasse, Basel, Switzerland

Correspondence should be addressed to H Belting or S Huveneers: heinz-georg.belting@unibas.ch or s.huveneers@amsterdamumc.nl

*(M M van der Stoel and M P Kotini contributed equally to this work)
†(H-G Belting and S Huveneers contributed equally as senior authors)

Abstract

Remodelling of cell–cell junctions is crucial for proper tissue development and barrier function. The cadherin-based adherens junctions anchor via β-catenin and α-catenin to the actomyosin cytoskeleton, together forming a junctional mechanotransduction complex. Tension-induced conformational changes in the mechanosensitive α-catenin protein induce junctional vinculin recruitment. In endothelial cells, vinculin protects the remodelling of VE–cadherin junctions. In this study, we have addressed the role of vinculin in endothelial barrier function in the developing vasculature. *In vitro* experiments, using endothelial cells in which α-catenin was replaced by a vinculin-binding-deficient mutant, showed that junctional recruitment of vinculin promotes endothelial barrier function. To assess the role of vinculin within blood vessels *in vivo*, we next investigated barrier function in the vasculature of *vcl* knockout zebrafish. In the absence of vinculin, sprouting angiogenesis and vessel perfusion still occurred. Intriguingly, the absence of vinculin made the blood vessels more permeable for 10 kDa dextran molecules but not for larger tracers. Taken together, our findings demonstrate that vinculin strengthens the endothelial barrier and prevents vascular leakage in developing vessels.

Keywords

- vinculin
- endothelial barrier
- mechanotransduction
- adherens junction
- zebrafish
- vascular leakage
- extravasation

Introduction

The semi-permeable vascular barrier between the blood and the surrounding tissue is maintained by a monolayer of endothelial cells (1). The endothelial barrier regulates the extravasation of leukocytes and fluid (2, 3). Changes in permeability induced by angiogenic growth factors or inflammatory cytokines are often temporal and reversible, ensuring recovery of the vascular barrier (4). Chronic disruptions of the endothelial barrier however, perturb vascular homeostasis and contribute to a multitude of pathologies, including atherosclerosis, cancer and inflammatory diseases (1, 5). Hence, maintaining a tight, yet adaptable, endothelial barrier is important.

The endothelium in the developing vasculature is exposed to multiple forces that are derived from the mural cells, blood pressure and hemodynamic forces from the bloodstream (6, 7, 8, 9). Endothelial cells sense and transmit such mechanical cues via their cell–cell contacts, which evoke proportional cellular responses to maintain the endothelial barrier (10). VE–cadherin-based adherens

https://vb.bioscientifica.com
https://doi.org/10.1530/VB-22-0012
© 2023 The authors
Published by Bioscientifica Ltd

This work is licensed under a Creative Commons Attribution-NonCommercial 4.0 International License.
Downloaded from Bioscientifica.com at 10/13/2025 03:21:18PM
via Open Access. This work is licensed under a Creative Commons Attribution-NonCommercial 4.0 International License.
https://creativecommons.org/licenses/by-nc/4.0/

junctions (AJs) are crucial adhesion structures that form endothelial cell–cell contacts (11, 12). Endothelial junction remodelling is required for collective endothelial migration during sprouting angiogenesis (13, 14). The cytoplasmic domain of the transmembrane VE–cadherin protein binds to β-catenin and α-catenin, which in turn couples to the actomyosin cytoskeleton and forms the core junctional mechanotransduction complex (15, 16, 17, 18). The interaction of the VE–cadherin–catenin complex with the actin cytoskeleton stabilises the AJs and maintains endothelial monolayer integrity (19, 20, 21).

Tension on the VE–cadherin complex results in unfolding of α-catenin, which enhances its actin-binding affinity and exposes a cryptic binding site for vinculin (16, 22, 23, 24, 25, 26, 27). The vinculin–α-catenin interaction drives α-catenin-mediated mechanotransduction and preserves junctional integrity during force-dependent remodelling in cultured endothelial and epithelial cells (22, 25, 28, 29, 30, 31). Vinculin recruitment to AJs occurs to different extents during agonist-induced endothelial barrier enhancing and disrupting processes (22, 32, 33). In zebrafish embryos, vinculin associates with endothelial junctions that are remodelled by changes in blood flow (34) and endothelial expression of vinculin is important for angiogenesis in the postnatal mouse retina (35). Whether junctional vinculin has a role in endothelial barrier function remains unclear.

In this study, we found that junctional vinculin recruitment facilitates endothelial barrier function *in vitro*. To define the importance of vinculin for endothelial tissue integrity in vivo, we examined the vasculature of *vcl*-knockout zebrafish. We found that the endothelial cells still generated a functional and perfused vasculature in the absence of vinculin. Interestingly, the developed blood vessels in *vcl* mutant zebrafish were more permeable for small dextran molecules, whereas large dextran molecules did not extravasate. Taken together, these results point to a role for vinculin in strengthening the endothelial barrier in the vasculature.

Materials and methods

Antibodies and reagents

Rabbit polyclonal anti-VE–cadherin (Cat# 36-1900, diluted 1:200 for immunofluorescence (IF)) was from Thermo Fischer Scientific. Purified mouse anti-vinculin (clone hVIN-1, Cat# V9131, diluted 1:400 for IF) was from Sigma Aldrich. Rabbit polyclonal anti-β-actin (Cat# 4867S, diluted 1:1000 for Western blot (WB)) and rabbit polyclonal anti-phospho-paxillin-Tyr118 (Cat# 69363, diluted 1:200 for IF) were from Cell Signaling. Mouse monoclonal anti-α-catenin (Cat# 13-9700; diluted 1:1000 for WB) was from Invitrogen/Zymed and mouse monoclonal anti-GFP (B-2, Cat# sc-9996, diluted 1:1000 for WB) was from Santa Cruz Biotechnology. Promofluor 415 Phalloidin (Promokine, Cat# PK-PF415-7-01, diluted 1:200 for IF) was used for IF of F-actin. Alexa Fluor 488 or 594-coupled secondary antibodies were from Invitrogen (diluted 1:250 for IF). Secondary antibodies coupled to horseradish peroxidase (HRP) were from Bio-Rad (diluted 1:1000 for WB). Human plasma-derived thrombin (used at 1 U/mL) was purchased from Sigma–Aldrich.

Cell culture

Pooled primary human umbilical vein endothelial cells (HUVECs) from different donors (Lonza) were cultured in endothelial cell growth medium 2 (EGM-2) culture medium supplemented with the growth medium 2 supplement pack (PromoCell) on gelatin-coated tissue flasks. HEK293T cells (ATCC) were cultured in Dulbecco's modified Eagle's medium with L-glutamine and supplemented with 10% FCS and 1% pen/strep. Cells were recently authenticated and tested for contamination.

DNA plasmids and lentivirus production

To silence α-catenin expression in HUVECs, pLKO.1-shRNA plasmid targeting human α-catenin mRNA was used (TRCN0000062653). ShC002 was used as shRNA control (Sigma–Aldrich mission library). The mouse α-catenin–GFP and α-catenin–ΔVBS–GFP lentiviral plasmids were previously described (22). Lentivirus was generated by transfecting HEK293T cells with the lentiviral expression plasmids and third-generation packaging plasmids using Trans-IT-LTI transfection reagents (Mirus) as described previously (42). To transduce HUVECs, the supernatant containing the lentiviral particles was mixed at a 5:1 ratio with EGM-2 and incubated with the HUVECs for 16 h. Subsequently, transduced HUVECs were selected for expression of the shRNA with 2.5 μg/mL puromycin (Sigma). shRNA-based knockdown levels were analysed at least 72 h after transduction.

ECIS

To measure endothelial barrier resistance, we used electric-cell impedance sensing as previously described (43). Gold electrode arrays (8W10E, Applied Biophysics) were

https://vb.bioscientifica.com
https://doi.org/10.1530/VB-22-0012
© 2023 The authors
Published by Bioscientifica Ltd

This work is licensed under a Creative Commons Attribution-NonCommercial 4.0 International License.
Downloaded from Bioscientifica.com at 10/13/2025 03:21:18PM
via Open Access. This work is licensed under a Creative Commons Attribution-NonCommercial 4.0 International License.
https://creativecommons.org/licenses/by-nc/4.0/

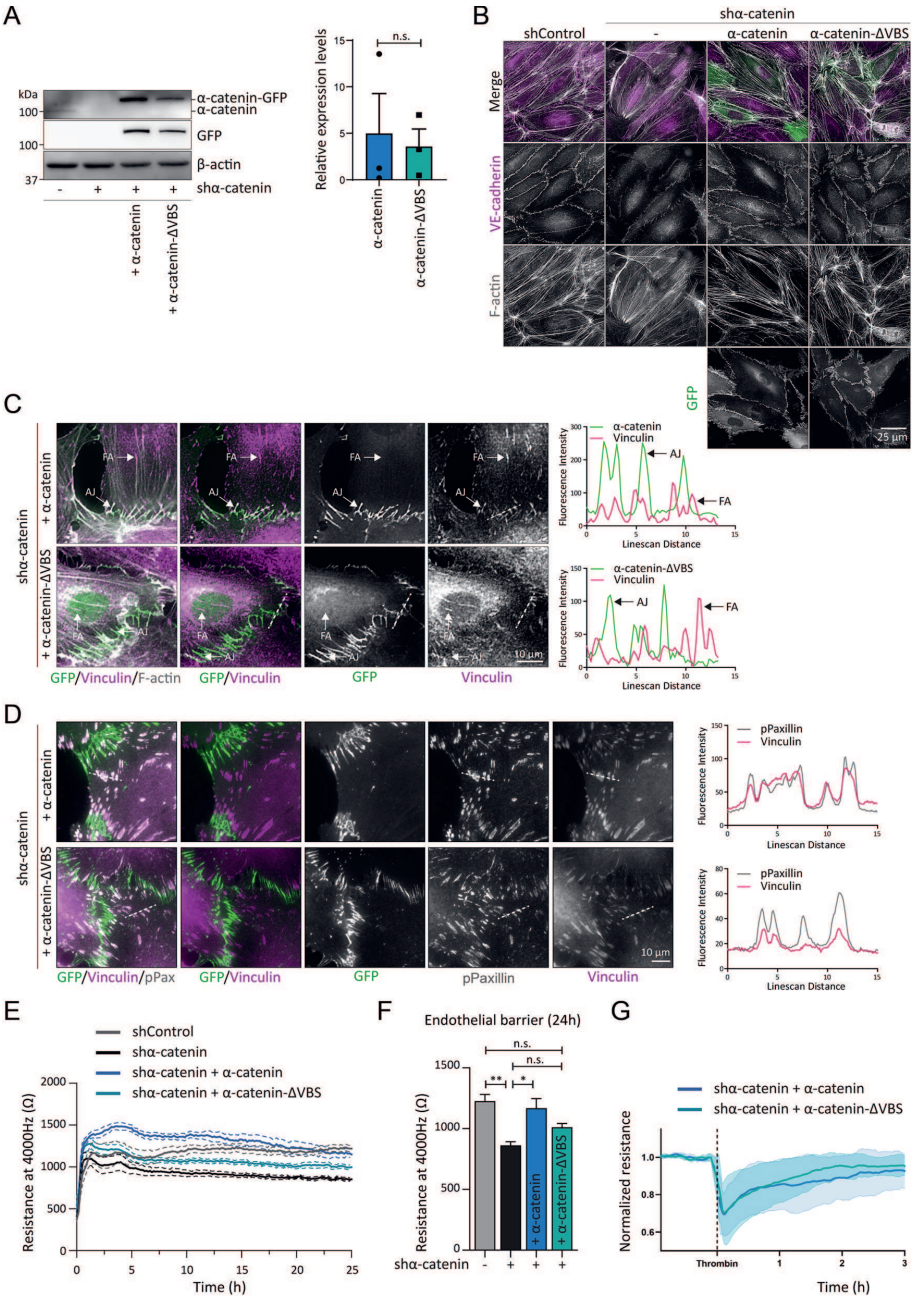


Figure 1

Junctional vinculin strengthens the endothelial barrier in vitro. (A) Representative Western blot analysis of shControl and shα-catenin transduced HUVECs rescued with lentiviral expression of α-catenin–GFP or α-catenin–ΔVBS–GFP. Blotted for α-catenin, GFP or β-actin. Bar graphs indicate the average ± s.e. expression levels of α-catenin–GFP and α-catenin–ΔVBS–GFP in shα-catenin-transduced HUVECs relative to endogenous α-catenin levels in shControl

https://vb.bioscientifica.com
https://doi.org/10.1530/VB-22-0012
© 2023 The authors
Published by Bioscientifica Ltd

This work is licensed under a Creative Commons Attribution-NonCommercial 4.0 International License.
Downloaded from Bioscientifica.com at 10/13/2025 03:21:18PM
via Open Access. This work is licensed under a Creative Commons Attribution-NonCommercial 4.0 International License.
https://creativecommons.org/licenses/by-nc/4.0/

Figure 1 (Continued)

HUVECs. n.s., non-significant (non-parametric Wilcoxon matched-pairs signed-rank test). Data are from three independent experiments. (B) Representative immunofluorescent images of shControl and shα-catenin-transduced HUVECs rescued with lentiviral expression of α-catenin–GFP or α-catenin–ΔVBS–GFP. Stained for F-actin (grey) and VE-cadherin (magenta). (C) Representative IF images of shα-catenin HUVECs rescued with α-catenin–GFP or α-catenin–ΔVBS–GFP (green) that were stained for vinculin (magenta) and F-actin (grey). Colocalisation of vinculin with α-catenin–GFP or α-catenin–ΔVBS–GFP was analysed by line scans displaying signal intensity (arbitrary units) across the AJs and FAs as indicated. Scale bar, 10 µm. (D) Representative IF images of shα-catenin HUVECs rescued with α-catenin–GFP or α-catenin–ΔVBS–GFP (green) that were stained for vinculin (magenta) and phosphor-Paxillin Tyr118 (grey). Colocalisation of vinculin with pPaxillin was analysed by line scans displaying signal intensity (arbitrary units) across FAs as indicated. Scale bar, 10 µm. (E) Line graph showing the average resistance ± S.E. measured with ECIS at 4000 Hz of indicated endothelial monolayers over time. Data are from three independent experiments. (F) Bar graphs representing the average resistance ± S.E. measured with ECIS at 4000 Hz of indicated endothelial monolayers after 24 h. Data are from three independent experiments. n.s., non-significant, $^{*}P < 0.05$, $^{**}P < 0.01$, $^{***}P < 0.001$ (one-Way ANOVA with Tukey's post hoc test for multiple comparisons). (G) Line graph showing the average resistance ± S.D. measured with ECIS at 4000 Hz of indicated endothelial monolayers over time following treatment with the permeability factor thrombin. Data are normalised to the baseline values prior to thrombin treatment and are derived from two independent experiments.

treated with 10 mM L-cysteine (Sigma) for 15 min at room temperature. After washing with MQ water, the wells were coated with 5 µg/mL fibronectin in MQ for 1 h at 37°C and 5% CO_2. Subsequently, 120,000 cells per well were seeded on the arrays and the impedance was measured during monolayer formation at 4000 Hz using the ECIS model ZTheta (Applied BioPhysics).

Immunofluorescence stainings

For immunofluorescence stainings, HUVECs were cultured on 5 µg/mL fibronectin-coated coverslips and later fixed for 15 min at room temperature with 4% paraformaldehyde in PBS^{++} (PBS supplemented with 1 mM $CaCl_2$ and 0.5 mM $MgCl_2$). The fixed cells were permeabilised for 5 min at room temperature with 0.5% Triton X-100 in PBS and blocked for 15 min in 2% BSA in PBS. Primary and secondary antibodies were diluted in 0.5% BSA in PBS and incubated for 45 min. Between incubations, fixed cells were washed three times with 0.5% BSA in PBS. Coverslips were mounted in Mowiol4-88/DABCO solution (Sigma).

Immunoblot analysis

HUVECs were lysed using reduced sample buffer containing 4% β-mercaptoethanol. Samples were denatured at 95°C for 5 min and subsequently loaded on a 10% SDS page gel. Gel running was performed in SDS-page running buffer (25 mM Tris–HCl, pH 8.3, 192 mM glycine and 0.1% SDS) and blotted on ethanol-activated PVDF membranes using full-wet transfer blot buffer (25 mM Tris–HCl, pH 8.3, 192 mM glycine and 20% (v/v) ethanol). Blots were blocked in 5% milk powder in tris-buffered saline (TBS) for 30 min and subsequently incubated with the primary antibodies in 5% milk powder in TBS supplemented with Tween-20 (TBS-t) overnight at 4°C. The secondary antibodies, coupled to HRP, were incubated for 45 min at room temperature. Between antibody incubations, blots were washed three times with TBS-t. As a final step before visualisation, blots were washed one time with TBS. HRP signal was visualised using enhanced chemiluminescence (ECL) detection (Supersignal West Pico PLUS, Thermo Fischer) with an ImageQuant LAS 4000 (GE Healthcare).

Zebrafish lines and maintenance

Zebrafish were maintained in standard housing conditions according to FELASA guidelines (44). All experiments were performed in accordance with federal guidelines and were approved by the Kantonales Veterinäramt of Kanton Basel-Stadt (1027H, 1014HE2, 1014G). The vcla^{hu10818}; vclb^{hu11202} zebrafish lines (38) were crossed into the transgenic *Tg(fli1a:EGFP)*^{y1} line, which labels all endothelial cells (45) as described in (34).

Genotyping of the vinculin (*vcl*)-mutant lines

For genotyping of the vinculin-mutant alleles, genomic DNA was extracted from adult fish fin biopsies or from whole embryos using a standard protocol (46) with addition of proteinase K to the sample. The extracted genomic DNA was then used to genotype the *vcla* and *vclb* loci. Genotyping protocol for *vcla* or *vclb* alleles was performed as described previously (34).

Microangiography

48 hpf zebrafish embryos were anaesthetised with 1× tricaine (0.08%, Sigma) and were injected with 250 µg/mL of 10 kDa or 70 kDa rhodamine-dextran (Molecular Probes) in the duct of Cuvier using glass needles (Biomedical Instruments) and standard microinjection protocols (47, 48). The injected embryos were transferred back to embryo media (5 mM NaCl, 0.17 mM KCl, 0.33 mM $CaCl_2$, 0.33 mM $MgSO_4$, pH 7.4) to recover and subsequently imaged 1 h

https://vb.bioscientifica.com
https://doi.org/10.1530/VB-22-0012
© 2023 The authors
Published by Bioscientifica Ltd

This work is licensed under a Creative Commons Attribution-NonCommercial 4.0 International License.
Downloaded from Bioscientifica.com at 10/13/2025 03:21:18PM
via Open Access. This work is licensed under a Creative Commons Attribution-NonCommercial 4.0 International License.
https://creativecommons.org/licenses/by-nc/4.0/

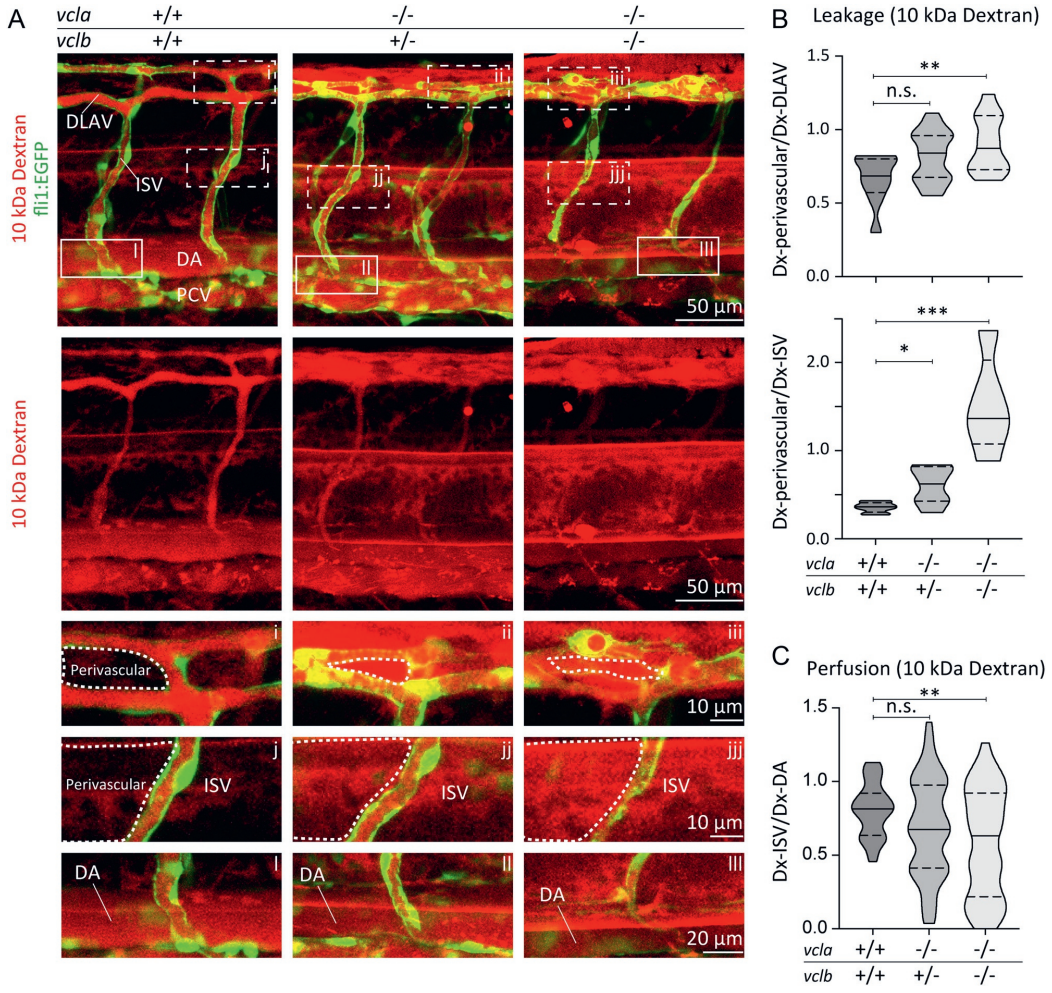


Figure 2
Vinculin ensures vascular barrier function for 10 kDa dextran. (A) Images of ISVs from 48 hpf Tg(*fli1:EGFP*) *vcla*$^{+/+}$;*vclb*$^{+/+}$, *vcla*$^{-/-}$;*vclb*$^{+/-}$ or *vcla*$^{-/-}$;*vclb*$^{-/-}$ embryos injected with 10 kDa rhodamine-dextran (red). Lower panels are single-channel images of the rhodamine signal. Scale bars, 50 µm. (A, i-iii) Corresponding close-up images showing the dextran leakage in the perivascular area around the dorsal longitudinal anastomotic vessel (DLAV). (A, j-jjj) Corresponding close-up images showing the dextran leakage in the perivascular area around an intersegmental vessel (ISV). Scale bars, 10 µm. (A, I-III) Close-up images of an ISV and the dorsal aorta (DA) showing the rhodamine signal within these vessels. Scale bar, 20 µm. (B) Violin plots showing the average leakage ± s.e. of 10 kDa dextran into the perivascular area of the DLAV or ISVs normalised to the dextran inside the DLAV or ISVs from 48 hpf embryos. The dotted lines represent the quartiles and the straight lines represent the median, n = 10 *vcla*$^{+/+}$;*vclb*+/+, n = 25 *vcla*$^{-/-}$;*vclb*$^{+/-}$ and n = 13 *vcla*$^{-/-}$;*vclb*$^{-/-}$ embryos, n.s., non-significant, $^{*}P < 0.05$, $^{**}P < 0.01$, $^{***}P < 0.001$ (one-way ANOVA and Dunnett's post-test). PCV, posterior cardinal vein. (C) Violin plot showing the ISV perfusion determined as the ratio between fluorescent dextran levels inside the ISV ± s.e. and dextran inside the dorsal aorta (DA) from 48 hpf embryos. The dotted lines represent the quartiles, the straight lines represent the median. n = 10 *vcla*$^{+/+}$;*vclb*$^{+/+}$, n = 25 *vcla*$^{-/-}$;*vclb*$^{+/-}$ and n = 13 *vcla*$^{-/-}$;*vclb*$^{-/-}$ embryos.

after microinjections. For visualisation of vascular leakage, embryos were mounted in 0.7% low-melting-point agarose (Sigma) and imaged with the Zeiss Axioplan Airy (25× oil/0.8 NA objective, confocal mode).

Imaging and image analysis

Fixed HUVECs were imaged using widefield microscopy on a NIKON Eclipse TI, with a SOLA SE II light source, 60× 1.49

https://vb.bioscientifica.com
https://doi.org/10.1530/VB-22-0012
© 2023 The authors
Published by Bioscientifica Ltd

This work is licensed under a Creative Commons Attribution-NonCommercial 4.0 International License.
Downloaded from Bioscientifica.com at 10/13/2025 03:21:18PM
via Open Access. This work is licensed under a Creative Commons Attribution-NonCommercial 4.0 International License.
https://creativecommons.org/licenses/by-nc/4.0/

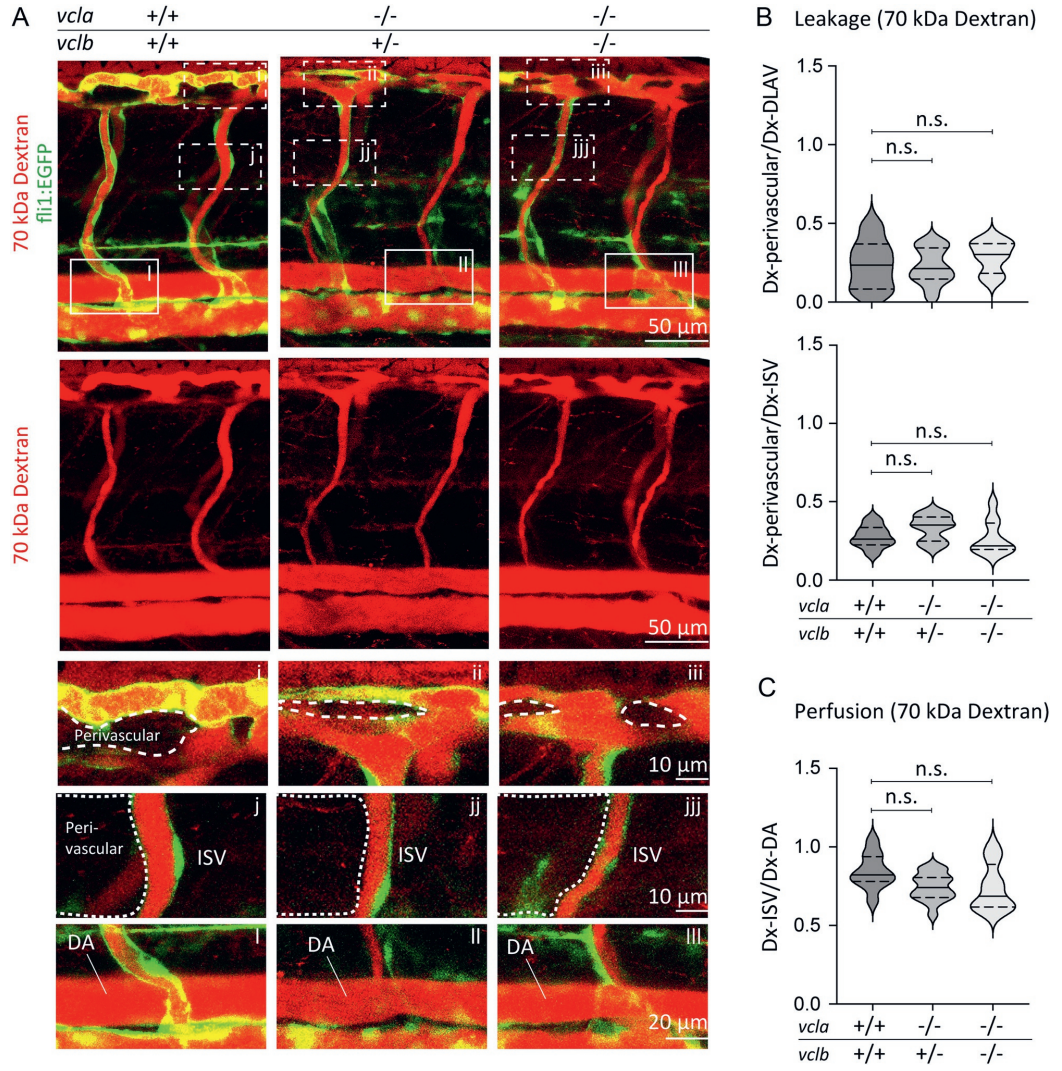


Figure 3

Loss of vinculin does not impair vascular barrier function for 70 kDa dextran. (A) Images of ISVs from 48 hpf Tg*(fli1:EGFP) vcla*$^{+/+}$;*vclb*$^{+/+}$, *vcla*$^{-/-}$;*vclb*$^{+/-}$ or *vcla*$^{-/-}$;*vclb*$^{-/-}$ embryos injected with 70 kDa rhodamine-dextran (red). Lower panels are single channel images of the rhodamine signal. Scale bars, 50 µm. (A, i-iii) Corresponding close-up images showing the dextran levels in the perivascular area around the dorsal longitudinal anastomotic vessel (DLAV). (A, j-jjj) Corresponding close-up images showing the dextran levels in the perivascular area around an intersegmental vessel (ISV). Scale bars, 10 µm. (A, I-III) Close-up images of an ISV and the dorsal aorta (DA) showing the rhodamine signal within these vessels. Scale bar, 20 µm. (B) Violin plot showing the average leakage ± s.e. of 70 kDa dextran into the perivascular area of the DLAV or ISVs normalised to the dextran inside the DLAV or ISVs from 48 hpf embryos. The dotted lines represent the quartiles, the straight lines represent the median, $n = 7$ *vcla*$^{+/+}$;*vclb*$^{+/+}$, $n = 16$ *vcla*$^{-/-}$;*vclb*$^{+/-}$ and $n = 7$ *vcla*$^{-/-}$;*vclb*$^{-/-}$ embryos, n.s. non-significant, one-way ANOVA and Dunnett's post-test. (C) Violin plot showing the ISV perfusion determined as the ratio between fluorescent dextran levels inside the ISV ± s.e. and dextran inside the dorsal aorta (DA) from 48 hpf embryos. The dotted lines represent the quartiles, the straight lines represent the median, $n = 10$ *vcla*$^{+/+}$;*vclb*$^{+/+}$, $n = 16$ *vcla*$^{-/-}$;*vclb*$^{+/-}$ and $n = 8$ *vcla*$^{-/-}$;*vclb*$^{-/-}$ embryos.

https://vb.bioscientifica.com
https://doi.org/10.1530/VB-22-0012
© 2023 The authors
Published by Bioscientifica Ltd

This work is licensed under a Creative Commons Attribution-NonCommercial 4.0 International License.
Downloaded from Bioscientifica.com at 10/13/2025 03:21:18PM
via Open Access. This work is licensed under a Creative Commons Attribution-NonCommercial 4.0 International License.
https://creativecommons.org/licenses/by-nc/4.0/

NA Apo TIRF (oil) objective and Andor Zyla 4.2 plus sCMOS camera and standard CFP, GFP or mCherry filter cubes (NIKON). For live imaging of zebrafish, a Zeiss LSM880 Airyscan inverted confocal microscope, with a 25× 0.8 NA oil objective was used. First, live embryos were selected for fluorescence signal and subsequently anaesthetised with 1× tricaine (0.08%) in E3 fish water and mounted in glass bottom Petri dishes (MatTek) using 0.7% low-melting-point agarose (Sigma) containing 1× tricaine. For live imaging, E3 with 1× tricaine and 0.003% 1-phenyl-2-thiourea (PTU, Sigma) was added to avoid pigmentation. Images were acquired with a zoom of 1–1.6 and z-stack step size of 0.5–1.0 µm, with a time interval of 25–30 min. Vascular perfusion and vascular leakage were analysed based on the fluorescent dextran levels in zebrafish embryos at 48 hpf. Vascular perfusion was defined as the ratio of fluorescent dextran levels in the ISVs to the levels of dextran inside the dorsal aorta (DA). Vascular leakage was defined as the ratio of the dextran fluorescent levels at the perivascular area of the vessels to the dextran levels inside the vessels. For this analysis, DLAV and its perivascular areas were analysed.

Statistical analysis

Graphpad Prism was used for the statistical analysis of the data. All violin plots represent data distribution, with the dashed line representing the quartiles and the straight line representing the median. When two groups were compared, a Wilcoxon test was used. When two or more groups were compared to the control, a one-way ANOVA was used, in combination with Tukey's or Dunnett's post hoc test for multiple comparisons and a D'Agostino–Pearson test for normality. Asterisks indicate *P* values and are defined as n.s., non-significant, * $P<0.05$, ** $P<0.01$, *** $P<0.001$.

Results

Junctional vinculin strengthens the endothelial barrier *in vitro*

Vinculin is recruited to tensile AJs by α-catenin. In addition, vinculin localises at integrin-based focal adhesions (FAs) through its force-dependent interaction with talin (36). To specifically investigate the role of junctional vinculin, we used lentiviral shRNA transductions that deplete endogenous α-catenin from human umbilical vein endothelial cells (HUVECs). Subsequently, we lentivirally expressed mouse α-catenin–GFP (green fluorescent protein) or α-catenin–ΔVBS–GFP, a modified α-catenin protein in which the binding to vinculin is prevented (22). Western blot analysis confirmed the depletion of endogenous α-catenin and expression of the α-catenin–GFP and α-catenin–ΔVBS–GFP in the rescued cells (Fig. 1A). Immunofluorescent (IF) stainings for VE–cadherin were performed to assess AJs in the different experimental conditions. Knockdown of α-catenin led to disassembly of AJs. The expression of α-catenin–GFP and α–catenin–ΔVBS–GFP restored the AJs in shα–catenin HUVECs (Fig. 1B), as shown previously (22). Next, we examined junctional vinculin recruitment by performing IF analysis. Vinculin localised at both FAs and AJs in wild type α-catenin rescued HUVECs (Fig. 1C and D). Analysis of α-catenin–ΔVBS-based junctions showed efficient preclusion of vinculin from the tensile AJs, while vinculin localisation at the FAs was maintained (Fig. 1C and D). This confirms the junction-specific depletion of vinculin in the α-catenin–ΔVBS-expressing cells. To examine whether junctional vinculin controls endothelial barrier function, we next performed electric cell-substrate impedance sensing (ECIS) as readout for the tightness of the endothelial cell monolayers. Silencing of endogenous α-catenin expression led to a decrease in transendothelial resistance, indicating an impairment of endothelial barrier function (Fig. 1E). Restoring α-catenin levels by α-catenin–GFP re-established endothelial monolayer integrity; however, α–catenin–ΔVBS–GFP expression, the mutated form lacking the vinculin binding site did not fully restore barrier function (Fig. 1E and F). To investigate whether the junctional depletion of vinculin might affect barrier loss upon physiological remodelling conditions, we performed ECIS experiments following treatment with the permeability factor Thrombin. These experiments showed that thrombin-induced barrier loss occurs similarly in α-catenin–GFP or α-catenin–ΔVBS–GFP rescued endothelial monolayers (Fig. 1G). Taken together, these results indicate that junctional vinculin promotes basal endothelial barrier function.

Vinculin mediates vascular barrier function for small molecules

Since junctional vinculin strengthens the barrier function of cultured endothelial monolayers, we next investigated the consequence of vinculin ablation on the vascular barrier *in vivo*. We recently showed that vinculin is important for the formation of junctional fingers in response to blood flow in the developing vessels of zebrafish (34). The zebrafish genome encodes two vinculin isoforms, vinculin a (*vcla*) and vinculin

https://vb.bioscientifica.com
https://doi.org/10.1530/VB-22-0012
© 2023 The authors
Published by Bioscientifica Ltd

This work is licensed under a Creative Commons Attribution-NonCommercial 4.0 International License.
Downloaded from Bioscientifica.com at 10/13/2025 03:21:18PM
via Open Access. This work is licensed under a Creative Commons Attribution-NonCommercial 4.0 International License.
https://creativecommons.org/licenses/by-nc/4.0/

b (*vclb*) (37, 38). The genetic ablation of both vinculin isoforms delays sprouting angiogenesis during early vascular development (34). Nevertheless, the *vcl*-KO embryos develop functional blood vessels and no evident haemorrhages were observed (34). To assess the permeability of the endothelial barrier, the 10 kDa rhodamine-dextran tracer was injected into the duct of Cuvier at 48 hpf of control or *vcl*-KO Tg(*fli1a:EGFP*)^{y1} embryos, in which the *fli1a* promoter drives the endothelial-specific expression of EGFP. One hour after dextran-microinjections, we examined vascular perfusion and leakage by imaging the blood vessels of the zebrafish trunk, namely the intersegmental vessels (ISVs), the DLAV and their perivascular areas. The ISVs of control embryos were perfused, as shown by the presence of the 10 kDa rhodamine-dextran tracer in the lumen of blood vessels. In control zebrafish, the tracer was maintained in the blood vessel lumen of the DLAV and the ISVs and did not extravasate into the perivascular regions (Fig. 2A-C), which indicates that endothelial junctions are sufficiently tight to prevent leakage of small molecular such as 10 kDa rhodamine-dextran. Conversely, in *vcl* mutants, we observed extensive leakage of the tracer dye into the surrounding tissues (Fig. 2A and B). In *vcla*$^{-/-}$*;vclb*$^{+/-}$, and in particular, in *vcl* full-KO embryos, the 10 kDa rhodamine-dextran intensities were lower within the perfused ISVs, suggesting that dextran molecules extravasated from the circulation (Fig. 2C). Our analysis shows that *vcla*$^{-/-}$*; vclb*$^{+/-}$ and *vcl* full-KO embryos exhibited increased perivascular dextran levels (Fig. 2A and B). To examine the requirement of vinculin for vascular barrier function of larger molecules, we next injected 70 kDa rhodamine-dextran in *fli1:EGFP* control and *vcl* KO embryos. An hour after dextran-microinjections, no differences in vascular permeability and perfusion between control and *vcl* heterozygous or homozygous KO embryos were observed (Fig. 3A-C). Taken together, these experiments demonstrate that vinculin is required for the strengthening of the endothelial barrier in newly developed blood vessels to prevent leakage of small molecules.

Discussion

Endothelial barrier function is tightly regulated through force-dependent remodelling of cell–cell contacts. Failure of the endothelial junctions to adapt to subjected forces leads to vascular leakage and inflammation in cardiovascular disease (1). In this study, we examined the importance of the mechanotransduction protein vinculin for the endothelial barrier using both *in vitro* and *in vivo* functional approaches. These results reveal that recruitment of vinculin to AJs strengthens the endothelial cell–cell junctions in blood vessels.

Vinculin knockout mice are embryonically lethal due to neuronal and cardiovascular defects at E10.5 (39), demonstrating the importance of vinculin for mammalian development. In addition, endothelial-specific vinculin depletion constrains collective endothelial migration during retinal angiogenesis in mice (35), indicating that endothelial vinculin contributes to vascular development. Endothelial vinculin is recruited to both integrin-based FAs and cadherin-based AJs in a force-dependent manner (29, 36). When tensile forces remodel AJs, vinculin-mediated mechanotransduction occurs via the VE–cadherin complex (22). By generating endothelial cells that form junctions through the vinculin-binding-deficient α-catenin mutant (α-catenin–ΔVBS), we now specifically showed that junctional vinculin recruitment supports strengthening of monolayer integrity in cultured endothelial cells. Single *vcla* or *vclb* mutant zebrafish display mild developmental defects (38, 40). We find that the *vcla*$^{-/-}$*;vclb*$^{-/-}$ double knockout zebrafish exhibit mild defects in vascular morphogenesis and eventually the morphogenetic process gives rise to a functional vasculature (34). In line with the expectation that vinculin modulates, rather than being needed for, endothelial cell–cell junctions (22, 27, 28), we observed vascular leakage specifically for small molecules, 10 kDa, in vinculin knockout zebrafish, whereas the vasculature still acted as a barrier for larger molecules. This result is corroborated by the notion that recruitment of vinculin to VE–cadherin-based junctions does not affect histamine-induced vascular leakage of Evans Blue in mice, which is a measure for the extravasation of large molecules (27). Even though the measured resistance formed by cultured endothelial cells expressing α-catenin–ΔVBS indicated minor barrier differences upon the junctional depletion of vinculin, the knockout of vinculin in vivo resulted in significant leakage of small molecules. This indicates that the endothelial dysfunction upon vinculin depletion becomes aggravated in pressurised vascular conditions. Potentially, the mild phenotype of the vinculin knockout zebrafish might be aggravated under pathological conditions that weaken the endothelial barrier, such as during inflammation or sepsis. Together, the data show that vinculin tightens endothelial junctions in blood vessels.

We expect that the depletion of the junctional vinculin pool underlies the vascular phenotype of the vinculin KO zebrafish. Cultured endothelial cells that form junctions through α-catenin–ΔVBS fail to sprout in collagen gels

https://vb.bioscientifica.com
https://doi.org/10.1530/VB-22-0012
© 2023 The authors
Published by Bioscientifica Ltd

This work is licensed under a Creative Commons Attribution-NonCommercial 4.0 International License.
Downloaded from Bioscientifica.com at 10/13/2025 03:21:18PM
via Open Access. This work is licensed under a Creative Commons Attribution-NonCommercial 4.0 International License.
https://creativecommons.org/licenses/by-nc/4.0/

(data not shown). This suggests that the junctional pool of vinculin controls endothelial dynamics within angiogenic sprouts, an effect that has also been observed in endothelial-specific knockout mice (35). Moreover, we recently observed differences in flow-induced endothelial junction dynamics in the ISVs of control and vinculin KO zebrafish, whereas integrin-dependent filopodia still formed equally (34). Other groups showed that juvenile *Vclb*-mutant zebrafish display epicardial defects and pericardial edema (38, 40, 41). Recruitment of vinculin was observed during the maturation of cell–cell junctions between cardiomyocytes in vivo (41). These findings suggest that *in vivo,* vinculin's role in cell–cell junctions is prominent. Nevertheless, a potential contribution of vinculin's role in integrin-based adhesion cannot be fully ruled out in this model system.

Finally, we surmise that junctional vinculin recruitment fortifies the endothelial barrier for small molecules upon vascular remodelling. Future work targeting the protective function of vinculin using pharmacological approaches, for instance by enhancing its interaction with the junctions, may provide a strategy to treat pathologies that entail vascular permeability.

Declaration of interest

The authors declare that there is no conflict of interest.

Funding

This work has been supported by the Kantons Basel-Stadt and Basel-Land and by a grant from the Swiss National Science Foundation to M.A.. S.H. is financially supported by the Netherlands Organization of Scientific Research (ZonMw VIDI grant 016.156.327) and the Rembrandt Institute for Cardiovascular Sciences. M.S. was financially supported by (EUFish, UvA365, Amsterdam UMC).

Author contribution statement

MvdS, MK and RS designed and performed experiments. SH and HGB conceived and supervised the study. MvdS, MK, RS, HGB and SH analysed the data. MvdS, MK, HGB and SH wrote the manuscript. All authors reviewed the manuscript.

Data availability

Data are available from the authors upon reasonable request.

References

1 Claesson-Welsh L, Dejana E & McDonald DM. Permeability of the endothelial barrier: identifying and reconciling controversies. *Trends in Molecular Medicine* 2021 **27** 314–331. (https://doi.org/10.1016/j.molmed.2020.11.006)

2 Wettschureck N, Strilic B & Offermanns S. Passing the vascular barrier: endothelial signaling processes controlling extravasation. *Physiological Reviews* 2019 **99** 1467–1525. (https://doi.org/10.1152/physrev.00037.2018)

3 Schimmel L, Heemskerk N & van Buul JD. Leukocyte transendothelial migration: a local affair. *Small GTPases* 2017 **8** 1–15. (https://doi.org/10.1080/21541248.2016.1197872)

4 Weis SM & Cheresh DA. Pathophysiological consequences of VEGF-induced vascular permeability. *Nature* 2005 **437** 497–504. (https://doi.org/10.1038/nature03987)

5 Radeva MY & Waschke J. Mind the gap: mechanisms regulating the endothelial barrier. *Acta Physiologica* 2018 **222** e12860. (https://doi.org/10.1111/apha.12860)

6 Liu HB, Zhang J, Xin SY, Liu C, Wang CY, Zhao D & Zhang ZR. Mechanosensitive properties in the endothelium and their roles in the regulation of endothelial function. *Journal of Cardiovascular Pharmacology* 2013 **61** 461–470. (https://doi.org/10.1097/FJC.0b013e31828c0933)

7 Hahn C & Schwartz MA. Mechanotransduction in vascular physiology and atherogenesis. *Nature Reviews. Molecular Cell Biology* 2009 **10** 53–62. (https://doi.org/10.1038/nrm2596)

8 Dessalles CA, Leclech C, Castagnino A & Barakat AI. Integration of substrate- and flow-derived stresses in endothelial cell mechanobiology. *Communications Biology* 2021 **4** 764. (https://doi.org/10.1038/s42003-021-02285-w)

9 Phng LK & Belting HG. Endothelial cell mechanics and blood flow forces in vascular morphogenesis. *Seminars in Cell and Developmental Biology* 2021 **120** 32–43. (https://doi.org/10.1016/j.semcdb.2021.06.005)

10 Dorland YL & Huveneers S. Cell–cell junctional mechanotransduction in endothelial remodeling. *Cellular and Molecular Life Sciences* 2017 **74** 279–292. (https://doi.org/10.1007/s00018-016-2325-8)

11 Dejana E, Orsenigo F & Lampugnani MG. The role of adherens junctions and VE-cadherin in the control of vascular permeability. *Journal of Cell Science* 2008 **121** 2115–2122. (https://doi.org/10.1242/jcs.017897)

12 Dejana E & Vestweber D. The role of VE-cadherin in vascular morphogenesis and permeability control. *Progress in Molecular Biology and Translational Science* 2013 **116** 119–144. (https://doi.org/10.1016/B978-0-12-394311-8.00006-6)

13 Cao J, Ehling M, März S, Seebach J, Tarbashevich K, Sixta T, Pitulescu ME, Werner AC, Flach B, Montanez E *et al.* Polarized actin and VE-cadherin dynamics regulate junctional remodelling and cell migration during sprouting angiogenesis. *Nature Communications* 2017 **8** 2210. (https://doi.org/10.1038/s41467-017-02373-8)

14 Bentley K, Franco CA, Philippides A, Blanco R, Dierkes M, Gebala V, Stanchi F, Jones M, Aspalter IM, Cagna G *et al.* The role of differential VE-cadherin dynamics in cell rearrangement during angiogenesis. *Nature Cell Biology* 2014 **16** 309–321. (https://doi.org/10.1038/ncb2926)

15 Angulo-Urarte A, van der Wal T & Huveneers S. Cell-cell junctions as sensors and transducers of mechanical forces. *Biochimica et Biophysica Acta. Biomembranes* 2020 **1862** 183316. (https://doi.org/10.1016/j.bbamem.2020.183316)

16 Pannekoek W-J, de Rooij J & Gloerich M. Force transduction by cadherin adhesions in morphogenesis. *F1000Research* 2019 **8** F1000. (https://doi.org/10.12688/f1000research.18779.1)

17 Mège RM & Ishiyama N. Integration of cadherin adhesion and cytoskeleton at adherens junctions. *Cold Spring Harbor Perspectives in Biology* 2017 **9** a028738. (https://doi.org/10.1101/cshperspect.a028738)

18 Charras G & Yap AS. Tensile forces and mechanotransduction at cell–cell junctions. *Current Biology* 2018 **28** R445–R457. (https://doi.org/10.1016/j.cub.2018.02.003)

19 Buckley CD, Tan J, Anderson KL, Hanein D, Volkmann N, Weis WI, Nelson WJ & Dunn AR. Cell adhesion. The minimal cadherin-catenin complex binds to actin filaments under force. *Science* 2014 **346** 1254211. (https://doi.org/10.1126/science.1254211)

20 Noda K, Zhang J, Fukuhara S, Kunimoto S, Yoshimura M & Mochizuki N. Vascular endothelial-cadherin stabilizes at cell-cell junctions by anchoring to circumferential actin bundles through alpha- and beta-catenins in cyclic AMP-Epac-Rap1 signal-activated endothelial cells. *Molecular Biology of the Cell* 2010 **21** 584–596. (https://doi.org/10.1091/mbc.e09-07-0580)

© 2023 The authors
Published by Bioscientifica Ltd

This work is licensed under a Creative Commons Attribution-NonCommercial 4.0 International License.
Downloaded from Bioscientifica.com at 10/13/2025 03:21:18PM
via Open Access. This work is licensed under a Creative Commons Attribution-NonCommercial 4.0 International License.
https://creativecommons.org/licenses/by-nc/4.0/

21 Schulte D, Küppers V, Dartsch N, Broermann A, Li H, Zarbock A, Kamenyeva O, Kiefer F, Khandoga A, Massberg S *et al.* Stabilizing the VE-cadherin-catenin complex blocks leukocyte extravasation and vascular permeability. *EMBO Journal* 2011 **30** 4157–4170. (https://doi.org/10.1038/emboj.2011.304)

22 Huveneers S, Oldenburg J, Spanjaard E, van der Krogt G, Grigoriev I, Akhmanova A, Rehmann H & de Rooij J. Vinculin associates with endothelial VE-cadherin junctions to control force-dependent remodeling. *Journal of Cell Biology* 2012 **196** 641–652. (https://doi.org/10.1083/jcb.201108120)

23 Liu Z, Tan JL, Cohen DM, Yang MT, Sniadecki NJ, Ruiz SA, Nelson CM & Chen CS. Mechanical tugging force regulates the size of cell-cell junctions. *Proceedings of the National Academy of Sciences of the United States of America* 2010 **107** 9944–9949. (https://doi.org/10.1073/pnas.0914547107)

24 Yonemura S, Wada Y, Watanabe T, Nagafuchi A & Shibata M. α-Catenin as a tension transducer that induces adherens junction development. *Nature Cell Biology* 2010 **12** 533–542. (https://doi.org/10.1038/ncb2055)

25 le Duc Q, Shi Q, Blonk I, Sonnenberg A, Wang N, Leckband D & de Rooij J. Vinculin potentiates E-cadherin mechanosensing and is recruited to actin-anchored sites within adherens junctions in a myosin II–dependent manner. *Journal of Cell Biology* 2010 **189** 1107–1115. (https://doi.org/10.1083/jcb.201001149)

26 Ishiyama N, Sarpal R, Wood MN, Barrick SK, Nishikawa T, Hayashi H, Kobb AB, Flozak AS, Yemelyanov A, Fernandez-Gonzalez R *et al.* Force-dependent allostery of the α-catenin actin-binding domain controls adherens junction dynamics and functions. *Nature Communications* 2018 **9** 5121. (https://doi.org/10.1038/s41467-018-07481-7)

27 Duong CN, Brückner R, Schmitt M, Nottebaum AF, Braun LJ, zu Brickwedde MM, Ipe U, Vom Bruch H, Schöler HR, Trapani G *et al.* Force-induced changes of α-catenin conformation stabilize vascular junctions independent of vinculin. *Journal of Cell Science* 2021 **134**. (https://doi.org/10.1242/jcs.259012)

28 Twiss F, Le Duc Q, Van Der Horst S, Tabdili H, Van Der Krogt G, Wang N, Rehmann H, Huveneers S, Leckband DE & De Rooij J. Vinculin-dependent cadherin mechanosensing regulates efficient epithelial barrier formation. *Biology Open* 2012 **1** 1128–1140. (https://doi.org/10.1242/bio.20122428)

29 Yao M, Qiu W, Liu R, Efremov AK, Cong P, Seddiki R, Payre M, Lim CT, Ladoux B, Mège RM *et al.* Force-dependent conformational switch of α-catenin controls vinculin binding. *Nature Communications* 2014 **5** 4525. (https://doi.org/10.1038/ncomms5525)

30 Seddiki R, Narayana GHNS, Strale PO, Balcioglu HE, Peyret G, Yao M, Le AP, Teck Lim C, Yan J, Ladoux B *et al.* Force-dependent binding of vinculin to α-catenin regulates cell-cell contact stability and collective cell behavior. *Molecular Biology of the Cell* 2018 **29** 380–388. (https://doi.org/10.1091/mbc.E17-04-0231)

31 Barry AK, Wang N & Leckband DE. Local VE-cadherin mechanotransduction triggers long-ranged remodeling of endothelial monolayers. *Journal of Cell Science* 2015 **128** 1341–1351. (https://doi.org/10.1242/jcs.159954)

32 Birukova AA, Shah AS, Tian Y, Moldobaeva N & Birukov KG. Dual role of vinculin in barrier-disruptive and barrier-enhancing endothelial cell responses. *Cellular Signalling* 2016 **28** 541–551. (https://doi.org/10.1016/j.cellsig.2016.02.015)

33 Kugelmann D, Rotkopf LT, Radeva MY, Garcia-Ponce A, Walter E & Waschke J. Histamine causes endothelial barrier disruption via Ca2+-mediated RhoA activation and tension at adherens junctions. Sci Rep. *Scientific Reports* 2018 **8** 13229. (https://doi.org/10.1038/s41598-018-31408-3)

34 Kotini MP, van der Stoel MM, Yin J, Han MK, Kirchmaier B, de Rooij J, Affolter M, Huveneers S & Belting HG. Vinculin controls endothelial cell junction dynamics during vascular lumen formation. *Cell Reports* 2022 **39** 110658. (https://doi.org/10.1016/j.celrep.2022.110658)

35 Carvalho JR, Fortunato IC, Fonseca CG, Pezzarossa A, Barbacena P, Dominguez-Cejudo MA, Vasconcelos FF, Santos NC, Carvalho FA & Franco CA. Non-canonical Wnt signaling regulates junctional mechanocoupling during angiogenic collective cell migration. *eLife* 2019 **8** e45853. (https://doi.org/10.7554/eLife.45853)

36 Yao M, Goult BT, Chen H, Cong P, Sheetz MP & Yan J. Mechanical activation of vinculin binding to talin locks talin in an unfolded conformation. *Scientific Reports* 2014 **4** 4610. (https://doi.org/10.1038/srep04610)

37 Pascoal S, Esteves de Lima J, Leslie JD, Hughes SM & Saúde L. Notch signalling is required for the formation of structurally stable muscle fibres in zebrafish. *PLOS ONE* 2013 **8** e68021. (https://doi.org/10.1371/journal.pone.0068021)

38 Han MKL, van der Krogt GNM & de Rooij J. Zygotic vinculin is not essential for embryonic development in zebrafish. *PLoS One* 2017 **12** e0182278. (https://doi.org/10.1371/journal.pone.0182278)

39 Xu W, Baribault H & Adamson ED. Vinculin knockout results in heart and brain defects during embryonic development. *Development* 1998 **125** 327–337. (https://doi.org/10.1242/dev.125.2.327)

40 Cheng F, Miao L, Wu Q, Gong X, Xiong J & Zhang J. Vinculin b deficiency causes epicardial hyperplasia and coronary vessel disorganization in zebrafish. *Development* 2016 **143** 3522–3531. (https://doi.org/10.1242/dev.132936)

41 Fukuda R, Gunawan F, Ramadass R, Beisaw A, Konzer A, Mullapudi ST, Gentile A, Maischein HM, Graumann J & Stainier DYR. Mechanical forces regulate cardiomyocyte myofilament maturation via the VCL-SSH1-CFL axis. *Developmental Cell* 2019 **51** 62–77.e5. (https://doi.org/10.1016/j.devcel.2019.08.006)

42 van der Stoel M, Schimmel L, Nawaz K, van Stalborch AM, de Haan A, Klaus-Bergmann A, Valent ET, Koenis DS, van Nieuw Amerongen GP, de Vries CJ *et al.* DLC1 is a direct target of activated YAP/TAZ that drives collective migration and sprouting angiogenesis. *Journal of Cell Science* 2020 **133** jcs239947. (https://doi.org/10.1242/jcs.239947)

43 Dorland YL, Malinova TS, van Stalborch AM, Grieve AG, van Geemen D, Jansen NS, de Kreuk BJ, Nawaz K, Kole J, Geerts D *et al.* The F-BAR protein pacsin2 inhibits asymmetric VE-cadherin internalization from tensile adherens junctions. *Nature Communications* 2016 **7** 12210. (https://doi.org/10.1038/ncomms12210)

44 Aleström P, D'Angelo L, Midtlyng PJ, Schorderet DF, Schulte-Merker S, Sohm F & Warner S. Zebrafish: housing and husbandry recommendations. *Laboratory Animals* 2020 **54** 213–224. (https://doi.org/10.1177/0023677219869037)

45 Lawson ND & Weinstein BM. In vivo imaging of embryonic vascular development using transgenic zebrafish. *Developmental Biology* 2002 **248** 307–318. (https://doi.org/10.1006/dbio.2002.0711)

46 Meeker ND, Hutchinson SA, Ho L & Trede NS. Method for isolation of PCR-ready genomic DNA from zebrafish tissues. *BioTechniques* 2007 **43** 610–614. (https://doi.org/10.2144/000112619)

47 Lenard A, Ellertsdottir E, Herwig L, Krudewig A, Sauteur L, Belting HG & Affolter M. In vivo analysis reveals a highly stereotypic morphogenetic pathway of vascular anastomosis. *Developmental Cell* 2013 **25** 492–506. (https://doi.org/10.1016/j.devcel.2013.05.010)

48 Weinstein BM, Stemple DL, Driever W & Fishman MC. Gridlock, a localized heritable vascular patterning defect in the zebrafish. *Nature Medicine* 1995 **1** 1143–1147. (https://doi.org/10.1038/nm1195-1143)

Received 12 May 2022
Accepted 19 October 2022
Available online 19 October 2022
Version of Record published 27 January 2023

© 2023 The authors
Published by Bioscientifica Ltd

This work is licensed under a Creative Commons Attribution-NonCommercial 4.0 International License.
Downloaded from Bioscientifica.com at 10/13/2025 03:21:18PM
via Open Access. This work is licensed under a Creative Commons Attribution-NonCommercial 4.0 International License.
https://creativecommons.org/licenses/by-nc/4.0/



Chapter 6

Breaking barriers in inflammation: Mechanotransduction at the leukocyte-endothelial interface

Breaking barriers in inflammation: Mechanotransduction at the leukocyte-endothelial interface

Rianne M. Schoon[1] & Stephan Huveneers[1]

[1] Amsterdam UMC, University of Amsterdam, Department of Medical Biochemistry, Amsterdam Cardiovascular Sciences, Amsterdam, The Netherlands.

Abstract

Endothelial cells maintain vascular integrity under homeostatic conditions. During inflammation, however, leukocytes migrate from the bloodstream across the endothelium into tissues. This transendothelial migration depends on mechanical cues at the leukocyte-endothelial interface that regulate immune cell recruitment, vascular function, and the progression of inflammatory processes and cardiovascular disease. Mechanotransduction in transmigration has been extensively studied in neutrophils and monocytes, which play key roles in acute inflammation and rolling/adhesion dynamics. These studies demonstrate that biomechanical forces, including shear stress, integrin activation, cytoskeletal responses, and endothelial stiffness sensing, are central to the transmigration process. T-cell trafficking to solid tumors or inflamed tissues also relies on these force-dependent mechanisms. Unlike innate immune cells, T-cells engage the endothelium through distinct integrin interactions and can uniquely establish a mechanosensitive immune synapse mediated by the T-cell receptor. In this review, we highlight the forces at play during T-cell-endothelium interactions, emphasizing the central role of mechanotransduction and the underlying biophysical principles that shape immune cell behavior within the inflamed vascular microenvironment.

1. Introduction

Mechanobiology in cardiovascular disease

Cardiovascular disease is a diverse group of disorders that involve the heart and blood vessels, and it is the leading cause of death worldwide (World Health Organization). One key cause for stroke or heart attack is atherosclerosis, an age- and lifestyle-related condition in which the blood vessel wall is stiffened and inflamed [1]. Mechanical cues play an important role in atherosclerosis: for instance, vascular stiffening impairs the ability of endothelial cells lining the vessel wall to maintain the barrier between blood and tissue, disrupting the regulation of selective transport of fluid, molecules, and cells [2-5]. The affected endothelium becomes increasingly susceptible to chronic inflammation and allows abnormal invasion of immune cells into the surrounding tissue [6-8]. During immune cell extravasation, the endothelial cells experience physical forces exerted by rolling, adhering, and transmigrating leukocytes, with emerging evidence demonstrating that these forces influence both endothelial function and T-cell behavior [9-12]. Mechanosensing plays a specifically important role in triggering the effector function the T-cell antigen receptor [11,13-15]. It is becoming clear that biomechanical forces in the vasculature integrate with molecular signaling to regulate cell adhesion, migration, and communication during immune surveillance and inflammation. This review aims to overview the role of mechanotransduction at the T-cell-endothelial interface, discussing the extent as well as the molecular basis of these processes, providing a biomechanical perspective to better understand the development of cardiovascular diseases.

Function of the endothelium in immune surveillance

The luminal surface of arteries and veins is lined with a monolayer of vascular endothelial cells (ECs) that selectively allow the exchange of cells and solutes between blood and tissue [16,17]. In addition, the endothelium is a central player in the immune response. When activated by inflammatory signals (pathogen- or damage-associated molecular patterns) from surrounding tissues, tissue resident innate immune cells activate the endothelium via pro-inflammatory cues like tumor necrosis factor α (TNFα) [18,19]. Activated ECs recruit more immune cells from the circulation to the site of infection via expression of chemoattractants and upregulation of surface adhesion molecules, and facilitate their extravasation while simultaneously minimizing vascular leakage [20-22]. Interestingly, endothelial cells can function as antigen-presenting cells to (re-)stimulate T-cells [23-25]. By combining these functions, the endothelium is vital for maintaining vascular integrity while contributing to immune surveillance as well as appropriate innate and adaptive immunity.

Endothelial and T-cell mechano-interactions

The endothelial-T-cell interface is a biomechanically dynamic site where physical forces arrange reciprocal signaling between these cells. While blood flow imposes shear stress on both endothelial and circulating immune cells, traction and peeling forces arise as T-cells tether, arrest, and transmigrate across the endothelium. The T-cells deform the apical endothelial membrane and engage through membrane-tethered mechanosensitive adhesion proteins [22,26]. The resulting load-dependent conformational changes in the adhesion receptors induce catch or slip bond dynamics with ligands and trigger intracellular pathways that remodel cytoskeletal and transcriptional programs [27,28]. The magnitude, vector, and duration of these forces, together with mechanical compliance of both cell types, influence transmigration outcomes, eliciting distinct mechanosignals via context-dependent receptor-ligand engagement that includes integrins, selectins, cadherins, and ion-channels. Together, these components at the endothelial-T-cell interface form a tightly integrated biomechanical signaling scaffold.

This review outlines the molecular mechanisms underlying the force-dependent interactions between endothelial cells and T-cells. We first discuss mechanosensitive pathways and molecules in endothelial cells and explore how hemodynamic forces govern endothelial pro-inflammatory signaling. We then turn to the mechanical properties and force-responsiveness of T-cells, addressing their migratory behavior, immune synapse formation, and force-induced activation. The core of the review focuses on the endothelial-T-cell interface itself, dissecting the involved physical forces, force-transducing receptor systems, and mechanical modulation of adhesion and transmigration.

2. Mechanotransduction in endothelial cells

Mechanosensitive pathways and molecules

Endothelial cells are rapid sensors and responders to changes in (hemodynamic) forces within the vasculature [29]. For instance, the endothelium senses shear stress through various mechanosensors, including membrane receptor kinases, integrins, G-coupled protein receptors, ion channels, glycoproteins and intercellular junction proteins which, in turn, activate downstream signaling [30,31]. Here, we briefly introduce general mechanotransduction pathways that explain how endothelial cells sense and adapt to their physical surroundings. Note that later sections will provide in-depth discussion of the specific integrins and adhesion molecules that are active during force sensing at the endothelial-T-cell-interface.

The connections between ECs are formed by transmembrane cell-cell junctions that tightly link adjacent cells and their cytoskeletons to provide vascular barrier integrity [32-34]. Endothelial intercellular adhesion is mediated through homotypic adhesion of transmembrane vascular

endothelial-cadherin (VE-cadherin) molecules, which on the intracellular side interact via β-catenin and α-catenin with the actin cytoskeleton. When VE-cadherin-based adherens junctions (AJs) are dysregulated, this results in hyperpermeability and aberrant leukocyte extravasation, contributing to inflammation as well as the progression of cardiovascular disease and cancer [35-37]. Connections between ECs and the extracellular matrix (ECM) are formed by basal cellular anchors called focal adhesions (FAs), where ECM-binding integrins tether the cytoskeleton [38,39]. Based on their adhesive function, both endothelial AJs and FAs serve as ideal molecular complexes for mechanosensing and -transduction, converting biomechanical cues such as shear stress, stiffness, tension, and stretch into coordinated biochemical and transcriptional responses [40]. At AJs, a junctional complex consisting of VE-cadherin, PECAM1, and VEGFR-2 detects flow-derived forces and activates PI3K and RhoA/ROCK-dependent signaling cascades that modulate actomyosin contractility and cytoskeletal remodeling [41]. These flow-induced signaling pathways in turn activate integrins, leading to remodeling of the FAs [42]. In addition, within the VE-cadherin complex, α-catenin acts as a key mechanotransducer: when stretched under tension, it undergoes a conformational change that exposes a binding site for vinculin [43]. Vinculin recruitment reinforces tensile junctions following increased blood pressure and promotes vascular barrier function [44,45].

Endothelial mechanotransduction is further modulated by membrane-localized ion channels such as PIEZO1, which directly sense membrane stretch and trigger calcium influx, thereby regulating endothelial responses including nitric oxide (NO) production, permeability, and cytoskeletal dynamics [46-48]. During leukocyte adhesion and transmigration, force-dependent cytoskeletal remodeling and changes in membrane tension facilitates the recruitment of tyrosine phosphatases such as SHP-2 to PECAM1, modulating local phosphorylation of receptors and junctional disassembly [35]. In addition, when leukocytes engage with PECAM1, another force-activated ion channel TRPC6, which, like PIEZO, increases intracellular calcium signaling in the endothelium [49].

Finally, a complementary class of endothelial shear-stress sensing molecules are the G protein-coupled receptors (GPCRs). A subset of endothelial GPCRs, including GPR68, H1R, B2R, S1PR1, and GPR116, respond to mechanical forces via ligand-independent conformational changes [50]. Upon mechanical activation, these receptors trigger downstream signaling cascades involving G proteins, β-arrestins, PI3K/AKT, and eNOS, ultimately promoting responses such as cytoskeletal reorganization, expression of flow-sensitive transcription factors like KLF2, and vasodilation [50,51].

Collectively, these general mechanotransduction systems allow endothelial cells to convert diverse mechanical stimuli from the vascular environment into adaptive responses that maintain vascular homeostasis and allow for normal immune surveillance.

Shear stress, mechanosignaling, and its impact on endothelial cell state

Endothelial cells are continuously exposed to hemodynamic shear stress, which levels vary across vascular beds depending on vessel diameter, wall structure, and flow velocity. The shear stress-induced tangential, frictional forces on the endothelium define their cell state [52,53]. In general, laminar, unidirectional flow promotes endothelial quiescence, alignment of endothelial cells in the direction of flow, and suppression of inflammatory signaling, largely via KLF2-mediated inhibition of NF-κB signaling [54]. In contrast, disturbed or oscillatory flow, often found at bifurcations in the vasculature or in postcapillary venules, drives a pro-inflammatory endothelial cell state: it enhances NF-κB activation, increases reactive oxygen species, and reduces nitric oxide bioavailability, together predisposing the endothelium to dysfunction [5,55]. Consequently, NF-κB activation upregulates pro-inflammatory genes, including ICAM-1 and VCAM-1, key adhesion molecules that facilitate leukocyte tethering and transmigration. NF-κB also induces AP1 signaling, which further upregulates pro-inflammatory cytokines and chemokines such as TNF-α, interleukins, interferon-γ, and chemokine (C-X-C motif) ligands [52,56-58]. In addition, endothelial cells require a basal level of flow for optimal healthy functioning: too low blood flow, resulting in shear stress on endothelium below 0.2N/m^2, leads to endothelial dysfunction by activation of angiogenic and endothelial-to-mesenchymal pathways [52,53]. A key example of a mechanosensor that safeguards healthy endothelial functioning is PIEZO1, since it acts as a membrane stretch-activated ion channel that is responsive to moderate shear stress (0.5-1N/m²) [53,59,60]. Force-activated PIEZO1 promotes calcium influx leading to calpain protease activity which degrades Src kinase, ultimately preventing VE-cadherin lysosomal degradation [61,62], thereby promoting vascular barrier function. This likely explains why in venules, which experience shear stress levels under PIEZO1's sensing range, the endothelial barrier is less tight and more permissive of fluid and leukocyte extravasation [63].

Hemodynamic forces in the postcapillary venules direct T-cell extravasation

Postcapillary venules (PVs, vessels 10-100mm in diameter located immediately downstream of capillaries) form a specialized site for T-cell extravasation. Unlike arteries and arterioles, PVs are shielded from the pulsatile stretch and compression caused by cardiac output, creating a stable biomechanical setting where shear stress is the dominant hemodynamic force acting on both endothelium and circulating T-cells. Here, blood pressure is low and wall shear stress (WSS) can drop from capillary levels of around 9.55N/m2 to 0.28N/m^2 [63]. This low-shear, low-resistance environment is essential for vascular bed-specific endothelial functions and supports coordinated T-cell arrest [64-67]. Although T-cells flow through PVs at relatively low velocities (0.6-1.8mm/s), their capture still requires finely tuned shear-dependent interactions. Studies have shown enhanced leukocyte adhesion at the transition region from collecting venules to PVs, potentially due to flow-induced reorientation of the endothelium [68-70]. Under homeostatic conditions, constitutive adhesion

molecule expression allows for basal immune surveillance; during inflammation, these molecules are upregulated in combination with local chemokine release, promoting efficient and selective T-cell recruitment [21]. Moreover, high endothelial venules (HEVs) are a specialized PV subtype found in lymphoid organs that are morphologically adapted to support even greater levels of T-cell extravasation [71,72]. Taken together, the PV microenvironment integrates anatomical and mechanical properties into a permissive and highly responsive niche for T-cell arrest, adhesion, and diapedesis.

3. Interplay between mechanobiology and T-cells

Mechanical properties of T-cells

Now that we have insight into endothelial mechanosensitive pathways, this section introduces the T-cell as another mechano-adaptable component in the (inflamed) vasculature. While distinct T-cell subsets display specialized effector functions, we will refer to T-cells in general throughout this review, since the biomechanical principles underlying their activation, migration, and interaction with the endothelium are often shared across lineages. T-cells are both subject to forces and are exerting forces onto their direct environment. We will discuss how T-cells deal with the strongly varying forces during immune surveillance, antigen recognition, the interplay between the T-cell receptor (TCR) and antigen-presenting cells (APCs), and during diapedesis. This will set the stage for understanding how biomechanical cues at the T-cell-endothelial interface affect T-cells and govern immune surveillance, effector function, and extravasation.

Role of mechanosensing in T-cell activation and migration

Memory and effector T-cells circulate through the blood and lymphoid tissues until the TCR recognizes their specific antigen on the surface of an antigen-presenting cell (APC) [15]. Endothelial cells, functioning as “semi-professional” APCs, can present antigens to, and restimulate, T-cells [23-25]. The binding between the TCR and its corresponding antigen peptide presented on the APC by a major histocompatibility complex (MHC) molecule is a mechanosensitive process that depends on binding affinity and specificity [73,74]. In addition to this TCR-MHC complex, forces are exchanged between the interacting T-cell and the endothelium via integrins, which contribute to the formation of a strong immune synapse [14].

Much research in immuno-mechanobiology has focused on the role of force in TCR-MHC recognition and immunological synapse structure [15]. T-cells sense mechanical cues from the APC, with cytoskeleton-generated pulling forces on TCRs acting as critical determinants for signal strength and specificity [13,75,76]. Interestingly, endothelial cells are much stiffer than classical APCs: atomic force measurements have shown that dendritic cells have elastic moduli ranging from 0.5-1kPa [77], whereas the stiffness of endothelial cells lies within a 1-5kPa range [78,79]. This implies that the interaction of the

immune synapse with professional APCs is more stable than with endothelial cells. The exact forces transmitted through LFA-1/ICAM-1 and TCR/antigen complexes have been spatially mapped using high-resolution force spectroscopy and spectrally encoded DNA tension probes [80]. These studies showed that pulling forces exceeding 12pN at individual LFA-1/ICAM-1 bonds significantly enhance antigen-dependent T-cell activation by increasing T-cell engagement with the substrate; these forces are transduced through cytoskeleton remodeling, which organizes TCRs into microclusters [80,81]. Further TCR-mediated T-cell activation (T-cell spreading and cytokine upregulation) depends on 5-19pN forces transduced across LFA-1/ICAM-1 bonds, which propagate interaction between these proteins via feedback mechanisms [14]. Moreover, changes in the endothelial cytoskeleton and its associated adhesion receptors such as ICAM-1, influence force transduction onto the T-cell, potentially affecting synapse stability, polarization, and the onset of transmigration.

Once efficiently adhered to the endothelium, T-cells migrate over and extravasate through the vessel wall into the inflamed tissue. When adhesion between T-cells and the endothelium is formed, the T-cell membrane gets stretched. The stretch-induced forces result in opening of PIEZO1 (who we met previously in endothelial context) and rapid calcium influx that activates the cytosolic protease calpain [11]. In turn, calpain drives localized actin polymerization and recruitment of LFA-1 integrins at the leading edge to promote T-cell migration.

Both during migration and during its squeezing through the vessel wall, the T-cell cytoskeleton extensively reorganizes. Force transduction through firm LFA1-ICAM-1 adhesions promotes T-cell lamellipodia formation through ARP2/3-mediated actin polarization, nucleation, and branching at the leading edge. At the same time, actomyosin contractility at the trailing end of the migrating T-cell is driven by non-muscle myosin II activity. Actomyosin contraction supports migration by first elongating the T-cell body to squeeze through the endothelium, next by pushing the nucleus forward, and finally retracting the trailing end of the T-cell to enable forward movement. Especially passaging the nucleus through the endothelium is a physical hurdle: although the leukocyte membrane itself is quite elastic (Young modulus 0.1-0.4kPa [82]), the nucleus is large and way stiffer (1-5kPa, [83]). To constrict it through the vessel wall, actomyosin contractility is complemented by the activity of actin assembly proteins such as formin family members [81,84 85]. Together, these actin remodeling pathways allow for cytoskeletal resilience to promote T-cell migration under confinement [86]. Overall, the T-cell actin cytoskeleton needs to be tightly, yet flexibly regulated, integrating both mechanical and molecular signals for transmigration.

4. Endothelium-T-cell interface: a dynamic interaction

Mechanisms of adhesion and transmigration

The transendothelial migration of T-cells consists of several sequential steps, as summarized in previous reviews [87-89]. During this process physical forces are transmitted between the endothelium and the transmigrating leukocytes [10,11,90]. In the following parts, we will describe how forces allow T-cells to adhere, roll, and transmigrate through the endothelium. To envision these forces, it helps to imagine the system as a round T-cell sticking to the flat endothelial surface. Shear flow generates both a **drag** force (horizontal pulling force, like wind on a kite) and a **torque** (twisting force that tries to roll the cell off) on an adherent spherical cell. These forces would cause the T-cell to rotate or to be ripped off, if not counterbalanced by a **peeling** force at the cell's trailing edge (like pulling on tape) and a vertical **impingement stress** across the adhesion interface (also called contact stress, which presses the T-cell against the endothelium). By representing the T-cell as a rigid sphere and assuming uniform stress distribution across the contact zone, theoretical models have been developed to quantify how cell geometry and adhesion strength determine whether the cell rolls, arrests, or [91,92]. This biophysical framework also provides insight into the physical limits that adhesion molecules, or molecular complexes, need to resist during immune cell trafficking within blood vessels, complementing biological observations with understanding from a mechanical perspective.

BOX 1 – Overall forces at play at the T-cell endothelial interface

Immune surveillance through the vessels, the formation of an immune synapse between EC and T-cell, and leukocyte extravasation into the tissue: these are all multistep processes that involve coordinated transitions between hemodynamic-, intracellular-, and extracellular forces [13,14,89]. Everywhere in the vasculature, cells deal with **shear force** from blood flow, which in postcapillary venules is particularly conducive to the extravasation [68]. During adhesion **dragging**, **twisting**, and **peeling forces** have to be resisted as circulating T-cells are captured from the flow through selectin-mediated tethering and crawling [93-95]. These forces also play a role in immune synapse formation [13,14] and in the modulation of **contact stress** that presses the T-cell against the endothelial surface [12,22,96,97]. Meanwhile, both endothelial and T-cell cytoskeletons exert **protrusive force** resulting in actin-rich protrusions to respectively flag down leukocytes from the lumen, and to probe the endothelial membrane to find a suitable extravasation spot [98-100]. In turn, the probed endothelial cell resists membrane deformation by meeting these protrusions with **contractile force** [101]. Actomyosin contraction is also necessary to elongate the T-cell body and nucleus to squeeze through the endothelium, while the ECs contract to wrap around the transmigrating T-cell and prevent vascular leakage [66]. Dissecting the mechanobiological dynamics of immune-vascular interactions is promising for both basic research and potentially therapeutic innovation in inflammatory cardiovascular disease.

Adhesion of surface receptors and their ligands in mechanosensing

Adhesion of T-cells to the endothelium begins with selectin-mediated tethering and rolling [93-95]. Selectins are transmembrane glycoproteins expressed on endothelial cells that bind to ligands on T-cells. These interactions not only *resist* shear forces imposed by blood flow but are paradoxically *stabilized* by them due to the formation of force-dependent catch-bonds. Catch-bonds are non-covalent receptor-ligand interactions whose lifetimes increase under tensile load up to an optimal force, contrasting with so-called slip-bonds that destabilize under stress [102,103]. This property enables selectin-mediated adhesions to become more stable under moderate shear, which facilitates T-cell capture and firm adhesion.

Selectin-adhesions & shear-dependent binding kinetics

Inflammatory cytokines regulate the surface availability of selectins: for instance interleukin-4 induces P-selectin mobilization from Weibel-Palade bodies, the storage units of endothelial cells, whereas TNF-α induces *de novo* E-selectin synthesis [104-108]. These endothelial selectins engage with T-cells-expressed L-selectin and PSGL1 ligands [93-95,108,109]. Selectin-ligand interactions are stabilized by a conserved lectin domain that recognizes specific carbohydrate residues, and which displays shear-dependent binding kinetics. Below a threshold shear of 0.3-0.5N/m², bond lifetimes are too short to mediate rolling, while optimal shear levels induce catch-bond stabilization and downstream signaling [102,103,110,111]. Flow-enhanced catch-bonding of E- and P-selectin binding with T-cell L-selectin and PSGL1 ligands triggers upregulation of ß2-integrins lymphocyte function-associated antigen 1 (LFA1) and macrophage antigen 1 (Mac1) on the T-cell surface, converting them into high-affinity, shear-resistant states [20,103,112,113]. As the rolling T-cell slows down, the contact area with the endothelium increases, further stabilizing adhesion between the cells through integrins.

Integrins enhance adhesion

Integrin-mediated adhesions are functionally stronger and longer-lived than selectin-based contacts, which supports stable T-cell arrest and transmigration [114]. Inflammatory signaling promotes endothelial ICAM-1 clustering and the formation of ICAM-1-rich membrane protrusions [115]. The T-cell integrins Mac1 and LFA1 bind to endothelial ICAM-1 to mediate rolling and firm adhesion to the vessel wall [116-119]. As T-cells roll under flow, they experience torque across the contact zone with the endothelium, generating a combination of tangential and impingement stresses at the leading edge and tensile peeling forces at the trailing edge [92,107,120]. Interestingly, experiments have shown that the integrin density at the interface increases 5-10-fold under these force conditions and further increases the cell-cell contact area [92]. Altogether, the process of rolling thus self-propagates integrin availability and clustering, thereby rapidly promoting cellular adhesion.

Biomechanical properties during T-cell rolling

Theoretical models based on [121] predict that under physiological shear stresses (0.1-1nN/μm²), a T-cell with a 2-4μm radius contact zone experiences tensile peeling forces of ~100-1500pN at the trailing edge, counterbalanced by compressive contact stresses of ~5-50mN/μm² at the leading edge [122,123]. These calculations align with experimental measurements: single-molecule force probes report LFA1-ICAM-1 resting loads around 2pN [124], with rupture forces around 12-56pN [14], or up to 30-70pN in micropipette assays. Adhesive strength across the interface has been measured to be 28-38pN/μm² for LFA1 and Mac1-mediated contacts, supporting cumulative loads exceeding 50-100pN across the contact area [123]. In torque-based models [92], a shear force of 0.2N/m² applied to a 4μm-radius cell generates a torque of 4×10^{-16}Nm, balanced by a reaction force of 125pN across a contact area of 35μm². Taken together, these calculations and measurements support the notion that physiologically relevant flow-generated forces are sufficient to drive the integrin clustering observed experimentally, providing a mechanical mechanism for the amplification of adhesion strength during rolling.

To migrate over the endothelium, T-cells engage in a coordinated cycle of adhesion at the front and rear detachment, organized by external shear and internal cytoskeletal dynamics. As the cell advances, membrane tension and contractile forces rise at the trailing edge, focusing stress on mature adhesions. Rear detachment primarily proceeds via peeling forces, which mechanically unzip bonds under tensile load. Under physiological flow, peeling forces at the trailing edge can approach hundreds of piconewtons [121,123]. This mechanical release is complemented by cytoskeletal disassembly of the adhesion complex, ensuring forward motility. Selectin-mediated adhesions can withstand shear stresses up to 15.2dynes/cm² (1.52N/m²) of twisting forces before breaking [125], while membrane tethers formed under flow maintain adhesions through stretched L-selectin and PSGL1 bonds [126]. Force measurements indicate that L-selectin tethers experience 45pN tensile forces, while integrin-β2 interactions sustain forces up to 120pN [127,128]. This indicates strong T-cell-endothelial adhesion through these molecules within shear ranges as found in the PV and HEV. When shear levels exceeds the catch-bond optimum of these interactions, they switch to slip-bond behavior, resulting in reduced adhesion lifetime and facilitating T-cell detachment [102,103]. As the rear of the migrating T-cell needs to let go, the molecular interactions rupture with a force-dependent rate [129]. Thus, rear-detachment is not governed by passive rupture-rates alone, but by a finely tuned balance between cytoskeletal force generation, receptor mechanics, and the distribution of forces imposed by migration and shear flow.

Endothelial cell-cell junctions as mechanosensitive gateways for leukocytes

Endothelial cells form a tightly regulated barrier through the formation of adherens junctions (AJs) and tight junctions (TJs), both of which anchor the intercellular contacts to the actin cytoskeleton [130,131]. Both junction types are mechanically sensitive, and their structural integrity is modulated by inflammatory and hemodynamic stimuli [26,132-135]. TJs, located apically, are based on adhesion of claudins, occludins, and junctional adhesion molecules (JAMs) that link to actin through scaffolding proteins such as ZO-1 [136,137]. AJs locate more basally on the lateral membrane and are based on adhesion through VE-cadherin [43,138-140]. VE-cadherin is a principal component of a force-sensitive junctional signaling complex. It forms mechanically resilient intercellular bonds and links to the actin cytoskeleton via a multiprotein complex including p120-catenin, β/γ-catenin, α-catenin, and vinculin. This arrangement enables the transmission of cytoskeletal tension across cells in the endothelial monolayer and enables the junction's responsiveness to biomechanical signals [43,138]. FRET-based molecular tension sensors have shown that VE-cadherin experiences baseline myosin-dependent tension, which decreases in response to fluid shear, with forces approximating ~2.5nN per molecule [141,142]. These findings illustrate the role of AJs in integrating biomechanical signals and modulating endothelial responses accordingly.

Inflammatory cytokines further modulate the structure and permeability of junctions [37,67,143-146]. TNF-α promotes phosphorylation of VE-cadherin at Y685, weakening barrier integrity and facilitating leukocyte extravasation [147,148]. Conversely, engagement of leukocyte adhesion molecules such as ICAM-1 and PECAM1 triggers dephosphorylation of VE-cadherin at Y731, promoting clathrin-mediated endocytosis and local disassembly of the junction [36,149,150]. Interestingly, the dephosphorylation of VE-cadherin depends on actomyosin-derived pulling forces, which unmask the Y731 for the phosphatase SHP2 [35]. Thus, VE-cadherin integrates both biochemical and mechanical signals to regulate paracellular transmigration of leukocytes.

Junctional force integration during T-cell transmigration

T-cell diapedesis, in the case of paracellular transmigration, requires localized remodeling of the endothelial junctions and cytoskeleton to accommodate the passage. Live-cell imaging and traction force microscopy have shown that transmigrating leukocytes locally disrupt VE-cadherin at junctions, with pronounced displacement and force generation at the point where the leukocyte inserts between endothelial cells [151,152]. The latter group found that VE-cadherin disassembly began upon leukocyte arrival at the junction, even before a significant increase in traction force was detected. Only when the bulk of the T-cell has squeezed through did forces jump from baseline (~3-4 nN per pillar) to over 100 nN per pillar, in a radial outward orientation from the diapedesis site, coinciding with marked VE-cadherin loss at those foci. These findings suggest that early VE-cadherin weakening may be initiated

by inflammatory signaling, while subsequent force spikes, induced by the transmigrating leukocytes, contribute to more extensive junctional opening.

Experimental fusion of VE-cadherin to α-catenin in mice, which stabilizes the junctional complex through strong anchoring with the actin cytoskeleton, significantly reduced leukocyte extravasation, highlighting the necessity of junctional weakening or uncoupling from the cytoskeleton during diapedesis [153]. Leukocyte-induced remodeling of the endothelial actin cytoskeleton is also important for the generation of diapedesis pores [154]. In turn, actomyosin contractility is needed to maintain endothelial barrier integrity during the transmigration process: VE-cadherin localizes to the edges of a contractile, F-actin-rich endothelial pore that forms around the transmigrating leukocyte, restricts the pore size and prevents fluid leakage while facilitating passage at the same time [66,108]. Actin remodeling and actomyosin-generated contractile forces together thus drive the cytoskeletal remodeling in endothelial cells during leukocyte diapedesis. The junctional VE-cadherin complex not only senses such mechanical changes but also coordinates appropriate cytoskeletal responses that maintain vascular integrity during inflammatory and transmigratory events [13,155,156].

Besides VE-cadherin, other junction-associated receptors such as PECAM1 control transmigration. PECAM1 is expressed on both endothelial cells and T-cells, enabling transient homophilic interactions that guide leukocytes through junctional openings [157-159]. Its expression is upregulated during inflammation and enriched at wider junctions, which may favor leukocyte passage [18,160,161]. PECAM1 was one of the first mammalian molecules that was identified as directly mechanosensitive: force applied via magnetic beads triggered conformational responses, and PECAM1 was shown to respond to shear stress [162]. Subsequent studies using FRET-based molecular tension sensors confirmed that PECAM1 experiences cytoskeleton-linked tension only under flow conditions, with the intermediate filament component vimentin as mediator of force transmission [142]. Furthermore, other junctional molecules like CD99 and occludin control leukocyte passage via homophilic interactions [109,163,164], but it is as of yet unclear whether these involve force-dependent regulation.

Altogether, these studies indicate that junction remodeling during diapedesis is a force-coordinated process in which VE-cadherin and PECAM1-based adhesions actively integrate forces and cytoskeletal adaptation upon T-cell transmigration. Here, external forces are integrated with inflammatory signals to coordinate local cytoskeletal responses, modulate adhesion molecule dynamics, and maintain barrier function while allowing controlled leukocyte passage.

T-cell protrusive forces in endothelial junction remodeling

During the final step of transendothelial migration (TEM), leukocytes traverse the endothelium either transcellularly or paracellularly, with the latter being the predominant route (90%) [165-167]. This section discusses the paracellular route, which requires remodeling of inter-endothelial junctions. T-cells exert mechanical force on the endothelium to disrupt junctions [152] and use force-generating actin-rich protrusions to probe the endothelial surface before crossing the endothelial barrier [99,168-170]. The studies of these T-cell protrusions led to the hypothesis of 'tenertaxis', which proposed that leukocytes transmigrate through the path of least resistance [165]. Diapedesis often occurs at locations with lower cortical F-actin density in the endothelium [171] and breaching efficiency inversely correlates with local actin density and stiffness [99]. Efficient transmigration thus requires not only a permissive endothelial cell state but also T-cell probing activity to detect optimal locations for transmigration.

In addition, leukocyte transmigration occurs most frequently at ICAM-1 rich and ruffling endothelial areas [21,100]. Clearly, T-cells appear to be able to select transmigration hotspots based on mechanical and biochemical cues [172]. Such hotspots typically localize at the poles of elongated endothelial cells [67], where F-actin stress fibers terminate and caveolae are abundant [108]. Moreover, leukocyte protrusions frequently target tricellular junctions: locations where three endothelial cells converge [8,137,161].

T-cells use LFA1-rich extensions to navigate across the endothelium [173], while lamellipodia aid in probing for optimal transmigration sites [99]. Despite the global distribution of selectins on endothelial surfaces [108], leukocytes exhibit directional migration toward specific sites before diapedesis. Inflammatory conditions induce elongation of endothelial cells, creating mechanical polarity and guiding leukocytes to favorable transmigration zones. Quantitative observations confirm that leukocytes migrate across distances up to 30μm on top of the endothelium before transmigration [174].

Experimental data confirm that leukocytes exert measurable forces during endothelial probing. T-cells apply forces in the range of 1-100pN through podosome-like structures [12], enabling them to sense local endothelial stiffness and cytoskeletal organization [96]. Podosome formation and function appear sensitive to the nanoscale distribution of ICAM-1, further underscoring the importance of spatial molecular organization in mechanosensing [175]. Mechanistically, podosomes transmit two opposing forces: a protrusive force from the T-cell's actin cytoskeleton toward the endothelium, and a reciprocal compressive force transmitted through the endothelial integrin ligands, membrane, and cortical actin. Protrusion force microscopy showed that individual leukocyte podosomes can exert forces in the 1-100pN range, depending on substrate stiffness [176]. This work was extended by studies combining atomic force microscopy with 3D super-resolution imaging and computational modeling to

show that podosomes exert forces up to 10nN, balanced by tractional components within the same structure [98]. The integrin-related proteins talin, vinculin, and paxillin were identified as essential components for sustaining these forces and enabling protrusive activity.

Overall, leukocytes are not passive players in transmigration but actively probe and deform the endothelium using nanoscale forces. These biomechanical interactions (see Table 1) help locate mechanically permissive sites and facilitate endothelial junction opening, acting in concert with inflammatory signaling pathways to enable efficient diapedesis.

5. Summary and perspective

Forces play a central role in the interaction between T-cells and the endothelium within inflamed vasculature. Transendothelial migration involves tightly coordinated mechanical and molecular interactions between immune cells and endothelial cells. Increasing evidence highlights the fundamental role of mechanobiology in regulating vascular barrier function and transmigration. As interest in interdisciplinary biophysical research continues to grow, so too does the range and sophistication of tools available to address outstanding questions in this field. Ultimately, advancing these research tools and deepening our understanding of mechanotransduction will provide insights into the biomechanics of the immune response at the endothelial interface. Currently, mechanotransduction cascades are not yet widely recognized as potential therapeutic targets for inflammatory or cardiovascular diseases. However, the activation of mechanosensitive proteins, ion channels, and adhesion complexes represents a promising avenue for drug development in conditions such as hypertension and atherosclerosis, where the vascular environment becomes stiffened.

Table 1: Existing literature regarding forces at the leukocyte-endothelial interface

Legend vessel/cellular/molecular scale

Vessels
Cells
Individual intermolecular bonds

† SD: standard deviation; SE: standard error.
* Conversion Between CGS and SI Units of Pressure: 10 dyn/cm^2 = 1N/m^2 = 1Pascal

Tissue scale	Force type	Force level *	Readout	Source
Endothelial surface (healthy)	Shear from fluid flow	>0.2N/m^2	Laminar / oscillatory flow in vitro	177
Capillary venule endothelium	Blood pressure	33.2 ± 1.5mmHg (SE †)	Servo-nulling pressure recording through a micropipette in live human lip vessels	178
	Wall shear stress	9.55N/m2	Calculated from erythrocyte velocity (which is measured by imaging) in live human bulbar conjunctiva	63
Postcapillary venule (PV) endothelium	Blood pressure	18.9 ± 1.6mmHg (SE)	Servo-nulling pressure recording through a micropipette in live human lip vessels	178
	Wall shear stress	0.28N/m^2	Calculated from erythrocyte velocity (which is measured by imaging) in live human bulbar conjunctiva	63
Dendritic cell surface	Stiffness (Young's elastic modulus)	0.799 ± 0.260kPa (SD †)	Real-time fluorescence deformability cytometry	77
		2-8kPa	Atomic force microscopy (AFM)	179
Endothelial cell surface	Stiffness (Young's elastic modulus)	0.7-3kPa	AFM	180
Leukocyte surface	Stiffness (Young's elastic modulus)	Tens of Pa	AFM	82
		Triple digits of Pa	AFM	181

Leukocyte nucleus	Stiffness (Young's elastic modulus)	1-5kPa	AFM	[181]
		0.6-0.8kPa	AFM	[83]
Lymphocyte	Stiffness (Young's elastic modulus)	Resting: 11kPa Activated: 20kPa	AFM	[182]
T-cell with a 2-4μm radius under physiological shear stress from blood flow	Physiological shear stress from blood flow	0.1-1nN/μm²	Calculations	[121, 122,123]
	Tensile peeling force at trailing edge	~100-1500pN		
	Compressive contact stress at the leading edge	~5-50mN/μm²		
T-cell with 4μm radius under 0.2N/m² flow shear	Torque	4×10^{-16}Nm	Torque-based models	[121, 92]
	Reaction force across a contact area of 35μm²	125pN		
Endothelial traction force on extracellular matrix during diapedesis	During monocyte adhesion	~13nN	Pillar-based traction force microscopy	[183]
TCR - antigen	Threshold contractile force (generated by T-cell cytoskeleton) to activate T-cell	12-19pN	Micropipette	[184]
LFA1-ICAM1	Threshold tensile force to activate T-cell	12pN	DNA-based tension probes that mechanically rupture at defined tensions	[80]
		5-19pN		[14]
	Resting loads	2pN	Single-molecule force probes	[124]
	Rupture forces	12-56pN	Single-molecule force probes	[14]
		30-100pN	Micropipette assays	[185]
			AFM	[186]
LFA1-Mac1	Adhesive strength across the interface	28-38pN/μm²	Total internal reflection fluorescence (TIRF) microscopy of cells on	[123]

	Maximum force across the contact area before rupture	50-100pN	microvillar ruffles and micropipette manipulation	
P/L/E-selectin-PSGL1	Shear forces threshold for conversion slip>catch bonds	0.5-2dyn/cm²	Microsphere perfusion in different flow viscosities	102
	Tether forces per unit wall shear stress	125pN	Microsphere perfusion in different flow viscosities	102
		25pN	TIRF and quantitative dynamic footprinting (qDF)	103
	Shear forces for optimal adhesion	0.8 dyne/cm²	TIRF + qDF	103
	Tensile load to induce peak bond lifetime	30pN	Optical bead trapping	187
	Shear stress-induced of twisting forces before breaking	15.2dyn/cm²	Micropipette aspiration + optical traps	125
			Special flow chamber to be imaged from the side	126
	Maximum twisting force load	25-45pN	Micropipette aspiration	127,128
Integrin-β2-interactions	Maximum twisting force load	60-130pN	Micropipette aspiration	127,128
PIEZO1	Shear stress to activate	5-10dyn/cm²	Readout is Ca2+ mobilization into the endoplasmic reticulum	53
		>20dyn/cm²	Electrophysiology for PIEZO1 activation, with particle image velocimetry to estimate the shear stress intensity at cell surface	47
		2-10dyn/cm²	Calcium-sensitive dye Fluo-4 AM coupled with confocal microscopy	188
VE-cadherin	Baseline tension	~2.5nN	FRET-based molecular tension sensors	141,142
		~3-4nN	Traction force microscopy with pillars	152
	Tension induced by T-cell insertion in junction	>100nN radially outward from the diapedesis site	Traction force microscopy with pillars	152
PECAM1	Shear threshold for activation	3dyn/cm²	Laminar flow and Western blot	189
			Magnetic beads	190

References

1. Gimbrone, M.A., Jr., and Garcia-Cardena, G. (2016). Endothelial Cell Dysfunction and the Pathobiology of Atherosclerosis. Circ Res *118*, 620–636. 10.1161/CIRCRESAHA.115.306301.
2. Andresen Eguiluz, R.C., Kaylan, K.B., Underhill, G.H., and Leckband, D.E. (2017). Substrate stiffness and VE-cadherin mechano-transduction coordinate to regulate endothelial monolayer integrity. Biomaterials *140*, 45–57. 10.1016/j.biomaterials.2017.06.010.
3. Birukova, A.A., Tian, X., Cokic, I., Beckham, Y., Gardel, M.L., and Birukov, K.G. (2013). Endothelial barrier disruption and recovery is controlled by substrate stiffness. Microvasc Res *87*, 50–57. 10.1016/j.mvr.2012.12.006.
4. VanderBurgh, J.A., Potharazu, A.V., Schwager, S.C., and Reinhart-King, C.A. (2020). A discrete interface in matrix stiffness creates an oscillatory pattern of endothelial monolayer disruption. J Cell Sci *133*. 10.1242/jcs.244533.
5. Zhou, M., Yu, Y., Chen, R., Liu, X., Hu, Y., Ma, Z., Gao, L., Jian, W., and Wang, L. (2023). Wall shear stress and its role in atherosclerosis. Front Cardiovasc Med *10*, 1083547. 10.3389/fcvm.2023.1083547.
6. Carman, C.V., and Martinelli, R. (2015). T Lymphocyte-Endothelial Interactions: Emerging Understanding of Trafficking and Antigen-Specific Immunity. Front Immunol *6*, 603. 10.3389/fimmu.2015.00603.
7. He, P. (2010). Leucocyte/endothelium interactions and microvessel permeability: coupled or uncoupled? Cardiovasc Res *87*, 281–290. 10.1093/cvr/cvq140.
8. Huynh, J., Nishimura, N., Rana, K., Peloquin, J.M., Califano, J.P., Montague, C.R., King, M.R., Schaffer, C.B., and Reinhart-King, C.A. (2011). Age-related intimal stiffening enhances endothelial permeability and leukocyte transmigration. Sci Transl Med *3*, 112ra122. 10.1126/scitranslmed.3002761.
9. Colin-York, H., Javanmardi, Y., Skamrahl, M., Kumari, S., Chang, V.T., Khuon, S., Taylor, A., Chew, T.L., Betzig, E., Moeendarbary, E., et al. (2019). Cytoskeletal Control of Antigen-Dependent T Cell Activation. Cell Rep *26*, 3369–3379 e3365. 10.1016/j.celrep.2019.02.074.
10. Kumari, S., Colin-York, H., Irvine, D.J., and Fritzsche, M. (2019). Not All T Cell Synapses Are Built the Same Way. Trends Immunol *40*, 977–980. 10.1016/j.it.2019.09.009.
11. Liu, C.S.C., and Ganguly, D. (2019). Mechanical Cues for T Cell Activation: Role of Piezo1 Mechanosensors. Crit Rev Immunol *39*, 15–38. 10.1615/CritRevImmunol.2019029595.
12. Schwartz, A.B., Campos, O.A., Criado-Hidalgo, E., Chien, S., Del Alamo, J.C., Lasheras, J.C., and Yeh, Y.T. (2021). Elucidating the Biomechanics of Leukocyte Transendothelial Migration by Quantitative Imaging. Front Cell Dev Biol *9*, 635263. 10.3389/fcell.2021.635263.
13. Harrison, D.L., Fang, Y., and Huang, J. (2019). T-Cell Mechanobiology: Force Sensation, Potentiation, and Translation. Front Phys *7*. 10.3389/fphy.2019.00045.
14. Ma, V.P.-Y., Hu, Y., Kellner, A.V., Brockman, J.M., Velusamy, A., Blanchard, A.T., Evavold, B.D., Alon, R., and Salaita, K. (2022). The magnitude of LFA-1/ICAM-1 forces fine-tune TCR-triggered T cell activation. Science Advances *8*, eabg4485. doi:10.1126/sciadv.abg4485.
15. Zhu, C., Chen, W., Lou, J., Rittase, W., and Li, K. (2019). Mechanosensing through immunoreceptors. Nat Immunol *20*, 1269–1278. 10.1038/s41590-019-0491-1.
16. Bazzoni, G., and Dejana, E. (2004). Endothelial Cell-to-Cell Junctions: Molecular Organization and Role in Vascular Homeostasis. Physiological Reviews *84*, 869–901. 10.1152/physrev.00035.2003.
17. Hartsock, A., and Nelson, W.J. (2008). Adherens and tight junctions: structure, function and connections to the actin cytoskeleton. Biochim Biophys Acta *1778*, 660–669. 10.1016/j.bbamem.2007.07.012.
18. Jaczewska, J., Abdulreda, M.H., Yau, C.Y., Schmitt, M.M., Schubert, I., Berggren, P.O., Weber, C., Koenen, R.R., Moy, V.T., and Wojcikiewicz, E.P. (2014). TNF-alpha and IFN-gamma promote lymphocyte adhesion to endothelial junctional regions facilitating transendothelial migration. J Leukoc Biol *95*, 265–274. 10.1189/jlb.0412205.
19. Zindel, J., and Kubes, P. (2020). DAMPs, PAMPs, and LAMPs in Immunity and Sterile Inflammation. Annu Rev Pathol *15*, 493–518. 10.1146/annurev-pathmechdis-012419-032847.
20. Dunne, J.L., Ballantyne, C.M., Beaudet, A.L., and Ley, K. (2002). Control of leukocyte rolling velocity in TNF-alpha-induced inflammation by LFA-1 and Mac-1. Blood *99*, 336–341. 10.1182/blood.v99.1.336.
21. Gronloh, M.L.B., Arts, J.J.G., Mahlandt, E.K., Nolte, M.A., Goedhart, J., and van Buul, J.D. (2023). Primary adhered neutrophils increase JNK1-MARCKSL1-mediated filopodia to promote secondary neutrophil transmigration. iScience *26*, 107406. 10.1016/j.isci.2023.107406.
22. Gronloh, M.L.B., Arts, J.J.G., Palacios Martinez, S., van der Veen, A.A., Kempers, L., van Steen, A.C.I., Roelofs, J., Nolte, M.A., Goedhart, J., and van Buul, J.D. (2023). Endothelial transmigration hotspots limit vascular leakage through heterogeneous expression of ICAM-1. EMBO Rep *24*, e55483. 10.15252/embr.202255483.
23. Amersfoort, J., Eelen, G., and Carmeliet, P. (2022). Immunomodulation by endothelial cells - partnering up with the immune system? Nat Rev Immunol *22*, 576–588. 10.1038/s41577-022-00694-4.
24. Knolle, P.A., and Wohlleber, D. (2016). Immunological functions of liver sinusoidal endothelial cells. Cell Mol Immunol *13*, 347–353. 10.1038/cmi.2016.5.
25. Young, M.R. (2012). Endothelial cells in the eyes of an immunologist. Cancer Immunol Immunother *61*, 1609–1616. 10.1007/s00262-012-1335-0.
26. Charbonier, F.W., Zamani, M., and Huang, N.F. (2019). Endothelial Cell Mechanotransduction in the Dynamic Vascular Environment. Adv Biosyst *3*, e1800252. 10.1002/adbi.201800252.

27. Chen, Y., Ju, L., Rushdi, M., Ge, C., and Zhu, C. (2017). Receptor-mediated cell mechanosensing. Mol Biol Cell *28*, 3134–3155. 10.1091/mbc.E17-04-0228.
28. Puech, P.H., and Bongrand, P. (2021). Mechanotransduction as a major driver of cell behaviour: mechanisms, and relevance to cell organization and future research. Open Biol *11*, 210256. 10.1098/rsob.210256.
29. Barakat, A.I., and Davies, P.F. (1998). Mechanisms of shear stress transmission and transduction in endothelial cells. Chest *114*, 58s–63s. 10.1378/chest.114.1_supplement.58s.
30. Ahmed, M.E., Leistner, D.M., Hakim, D., Abdelwahed, Y., Coskun, A.U., Maynard, C., Seppelt, C., Nelles, G., Meteva, D., Cefalo, N.V., et al. (2024). Endothelial Shear Stress Metrics Associate With Proinflammatory Pathways at the Culprit Site of Coronary Erosion. JACC Basic Transl Sci *9*, 1269–1283. 10.1016/j.jacbts.2024.07.008.
31. Davies, H.S., Baranova, N.S., El Amri, N., Coche-Guerente, L., Verdier, C., Bureau, L., Richter, R.P., and Debarre, D. (2019). An integrated assay to probe endothelial glycocalyx-blood cell interactions under flow in mechanically and biochemically well-defined environments. Matrix Biol *78-79*, 47–59. 10.1016/j.matbio.2018.12.002.
32. Dejana, E. (2004). Endothelial cell-cell junctions: happy together. Nat Rev Mol Cell Biol *5*, 261–270. 10.1038/nrm1357.
33. Dejana, E., Tournier-Lasserve, E., and Weinstein, B.M. (2009). The control of vascular integrity by endothelial cell junctions: molecular basis and pathological implications. Dev Cell *16*, 209–221. 10.1016/j.devcel.2009.01.004.
34. Vincent, P.A., Xiao, K., Buckley, K.M., and Kowalczyk, A.P. (2004). VE-cadherin: adhesion at arm's length. American Journal of Physiology-Cell Physiology *286*, C987–C997. 10.1152/ajpcell.00522.2003.
35. Arif, N., Zinnhardt, M., Nyamay'Antu, A., Teber, D., Bruckner, R., Schaefer, K., Li, Y.T., Trappmann, B., Grashoff, C., and Vestweber, D. (2021). PECAM-1 supports leukocyte diapedesis by tension-dependent dephosphorylation of VE-cadherin. EMBO J *40*, e106113. 10.15252/embj.2020106113.
36. Wessel, F., Winderlich, M., Holm, M., Frye, M., Rivera-Galdos, R., Vockel, M., Linnepe, R., Ipe, U., Stadtmann, A., Zarbock, A., et al. (2014). Leukocyte extravasation and vascular permeability are each controlled in vivo by different tyrosine residues of VE-cadherin. Nat Immunol *15*, 223–230. 10.1038/ni.2824.
37. Wilkens, M., Holtermann, L., Stahl, A.K., Stegmeyer, R.I., Nottebaum, A.F., and Vestweber, D. (2024). Ubiquitination of VE-cadherin regulates inflammation-induced vascular permeability in vivo. EMBO Rep *25*, 4013–4032. 10.1038/s44319-024-00221-7.
38. Changede, R., and Sheetz, M. (2017). Integrin and cadherin clusters: A robust way to organize adhesions for cell mechanics. Bioessays *39*, 1–12. 10.1002/bies.201600123.
39. Aman, J., and Margadant, C. (2023). Integrin-Dependent Cell-Matrix Adhesion in Endothelial Health and Disease. Circ Res *132*, 355–378. 10.1161/CIRCRESAHA.122.322332.
40. Hooglugt, A., van der Stoel, M.M., Shapeti, A., Neep, B.F., de Haan, A., van Oosterwyck, H., Boon, R.A., and Huveneers, S. (2024). DLC1 promotes mechanotransductive feedback for YAP via RhoGAP-mediated focal adhesion turnover. J Cell Sci *137*. 10.1242/jcs.261687.
41. Tzima, E., Irani-Tehrani, M., Kiosses, W.B., Dejana, E., Schultz, D.A., Engelhardt, B., Cao, G., DeLisser, H., and Schwartz, M.A. (2005). A mechanosensory complex that mediates the endothelial cell response to fluid shear stress. Nature *437*, 426–431. 10.1038/nature03952.
42. Jalali, S., del Pozo, M.A., Chen, K., Miao, H., Li, Y., Schwartz, M.A., Shyy, J.Y., and Chien, S. (2001). Integrin-mediated mechanotransduction requires its dynamic interaction with specific extracellular matrix (ECM) ligands. Proc Natl Acad Sci U S A *98*, 1042–1046. 10.1073/pnas.98.3.1042.
43. Huveneers, S., Oldenburg, J., Spanjaard, E., van der Krogt, G., Grigoriev, I., Akhmanova, A., Rehmann, H., and de Rooij, J. (2012). Vinculin associates with endothelial VE-cadherin junctions to control force-dependent remodeling. J Cell Biol *196*, 641–652. 10.1083/jcb.201108120.
44. van der Stoel, M.M., Kotini, M.P., Schoon, R.M., Affolter, M., Belting, H.G., and Huveneers, S. (2023). Vinculin strengthens the endothelial barrier during vascular development. Vasc Biol *5*. 10.1530/VB-22-0012.
45. Kotini, M.P., van der Stoel, M.M., Yin, J., Han, M.K., Kirchmaier, B., de Rooij, J., Affolter, M., Huveneers, S., and Belting, H.G. (2022). Vinculin controls endothelial cell junction dynamics during vascular lumen formation. Cell Rep *39*, 110658. 10.1016/j.celrep.2022.110658.
46. Chuntharpursat-Bon, E., Povstyan, O.V., Ludlow, M.J., Carrier, D.J., Debant, M., Shi, J., Gaunt, H.J., Bauer, C.C., Curd, A., Simon Futers, T., et al. (2023). PIEZO1 and PECAM1 interact at cell-cell junctions and partner in endothelial force sensing. Commun Biol *6*, 358. 10.1038/s42003-023-04706-4.
47. Ranade, S.S., Qiu, Z., Woo, S.-H., Hur, S.S., Murthy, S.E., Cahalan, S.M., Xu, J., Mathur, J., Bandell, M., Coste, B., et al. (2014). Piezo1, a mechanically activated ion channel, is required for vascular development in mice. Proceedings of the National Academy of Sciences *111*, 10347–10352. doi:10.1073/pnas.1409233111.
48. Lhomme, A., Gilbert, G., Pele, T., Deweirdt, J., Henrion, D., Baudrimont, I., Campagnac, M., Marthan, R., Guibert, C., Ducret, T., et al. (2019). Stretch-activated Piezo1 Channel in Endothelial Cells Relaxes Mouse Intrapulmonary Arteries. Am J Respir Cell Mol Biol *60*, 650–658. 10.1165/rcmb.2018-0197OC.
49. Fu, T., Sullivan, D.P., Gonzalez, A.M., Haynes, M.E., Dalal, P.J., Rutledge, N.S., Tierney, A.L., Yescas, J.A., Weber, E.W., and Muller, W.A. (2023). Mechanotransduction via endothelial adhesion molecule CD31 initiates transmigration and reveals a role for VEGFR2 in diapedesis. Immunity *56*, 2311–2324.e2316. 10.1016/j.immuni.2023.08.001.
50. Xiao, R., Liu, J., and Xu, X.Z.S. (2023). Mechanosensitive GPCRs and ion channels in shear stress sensing. Curr Opin Cell Biol *84*, 102216. 10.1016/j.ceb.2023.102216.

51. Erdogmus, S., Storch, U., Danner, L., Becker, J., Winter, M., Ziegler, N., Wirth, A., Offermanns, S., Hoffmann, C., Gudermann, T., and Mederos, Y.S.M. (2019). Helix 8 is the essential structural motif of mechanosensitive GPCRs. Nat Commun *10*, 5784. 10.1038/s41467-019-13722-0.
52. Mo, F.E. (2021). Shear-Regulated Extracellular Microenvironments and Endothelial Cell Surface Integrin Receptors Intertwine in Atherosclerosis. Front Cell Dev Biol *9*, 640781. 10.3389/fcell.2021.640781.
53. Santana Nunez, D., Malik, A.B., Lee, Q., Ahn, S.J., Coctecon-Murillo, A., Lazarko, D., Levitan, I., Mehta, D., and Komarova, Y.A. (2023). Piezo1 induces endothelial responses to shear stress via soluble adenylyl Cyclase-IP(3)R2 circuit. iScience *26*, 106661. 10.1016/j.isci.2023.106661.
54. Hahn, C., and Schwartz, M.A. (2009). Mechanotransduction in vascular physiology and atherogenesis. Nat Rev Mol Cell Biol *10*, 53–62. 10.1038/nrm2596.
55. Albarran-Juarez, J., Iring, A., Wang, S., Joseph, S., Grimm, M., Strilic, B., Wettschureck, N., Althoff, T.F., and Offermanns, S. (2018). Piezo1 and G(q)/G(11) promote endothelial inflammation depending on flow pattern and integrin activation. J Exp Med *215*, 2655–2672. 10.1084/jem.20180483.
56. Liu, G., Ye, X., Miller, E.J., and Liu, S.F. (2014). NF-kappaB-to-AP-1 switch: a mechanism regulating transition from endothelial barrier injury to repair in endotoxemic mice. Sci Rep *4*, 5543. 10.1038/srep05543.
57. Nourshargh, S., Larkin, S.W., Das, A., and Williams, T.J. (1995). Interleukin-1-induced leukocyte extravasation across rat mesenteric microvessels is mediated by platelet-activating factor. Blood *85*, 2553–2558. 10.1182/blood.V85.9.2553.bloodjournal8592553.
58. Rival, Y., Del Maschio, A., Rabiet, M.J., Dejana, E., and Duperray, A. (1996). Inhibition of platelet endothelial cell adhesion molecule-1 synthesis and leukocyte transmigration in endothelial cells by the combined action of TNF-alpha and IFN-gamma. The Journal of Immunology *157*, 1233–1241. 10.4049/jimmunol.157.3.1233.
59. Beech, D.J., and Kalli, A.C. (2019). Force Sensing by Piezo Channels in Cardiovascular Health and Disease. Arterioscler Thromb Vasc Biol *39*, 2228–2239. 10.1161/ATVBAHA.119.313348.
60. Douguet, D., Patel, A., Xu, A., Vanhoutte, P.M., and Honore, E. (2019). Piezo Ion Channels in Cardiovascular Mechanobiology. Trends Pharmacol Sci *40*, 956–970. 10.1016/j.tips.2019.10.002.
61. Friedrich, E.E., Hong, Z., Xiong, S., Zhong, M., Di, A., Rehman, J., Komarova, Y.A., and Malik, A.B. (2019). Endothelial cell Piezo1 mediates pressure-induced lung vascular hyperpermeability via disruption of adherens junctions. Proc Natl Acad Sci U S A *116*, 12980–12985. 10.1073/pnas.1902165116.
62. Zhong, M., Wu, W., Kang, H., Hong, Z., Xiong, S., Gao, X., Rehman, J., Komarova, Y.A., and Malik, A.B. (2020). Alveolar Stretch Activation of Endothelial Piezo1 Protects Adherens Junctions and Lung Vascular Barrier. Am J Respir Cell Mol Biol *62*, 168–177. 10.1165/rcmb.2019-0024OC.
63. Koutsiaris, A.G., Tachmitzi, S.V., Batis, N., Kotoula, M.G., Karabatsas, C.H., Tsironi, E., and Chatzoulis, D.Z. (2007). Volume flow and wall shear stress quantification in the human conjunctival capillaries and post-capillary venules in vivo. Biorheology *44*, 375–386.
64. Baluk, P., Fuxe, J., Hashizume, H., Romano, T., Lashnits, E., Butz, S., Vestweber, D., Corada, M., Molendini, C., Dejana, E., and McDonald, D.M. (2007). Functionally specialized junctions between endothelial cells of lymphatic vessels. J Exp Med *204*, 2349–2362. 10.1084/jem.20062596.
65. Eskin, S.G., Ives, C.L., McIntire, L.V., and Navarro, L.T. (1984). Response of cultured endothelial cells to steady flow. Microvasc Res *28*, 87–94. 10.1016/0026-2862(84)90031-1.
66. Heemskerk, N., Schimmel, L., Oort, C., van Rijssel, J., Yin, T., Ma, B., van Unen, J., Pitter, B., Huveneers, S., Goedhart, J., et al. (2016). F-actin-rich contractile endothelial pores prevent vascular leakage during leukocyte diapedesis through local RhoA signalling. Nat Commun *7*, 10493. 10.1038/ncomms10493.
67. Marcos-Ramiro, B., Garcia-Weber, D., and Millan, J. (2014). TNF-induced endothelial barrier disruption: beyond actin and Rho. Thromb Haemost *112*, 1088–1102. 10.1160/TH14-04-0299.
68. Benson, B.L., Li, L., Myers, J.T., Dorand, R.D., Gurkan, U.A., Huang, A.Y., and Ransohoff, R.M. (2018). Biomimetic post-capillary venule expansions for leukocyte adhesion studies. Sci Rep *8*, 9328. 10.1038/s41598-018-27566-z.
69. Nash, G.B. (2024). The rheology of interactions between leukocytes, platelets and the vessel wall in thrombo-inflammation. Biorheology *59*, 63–80. 10.3233/BIR-230040.
70. Yan, W.W., Cai, B., Liu, Y., and Fu, B.M. (2012). Effects of wall shear stress and its gradient on tumor cell adhesion in curved microvessels. Biomech Model Mechanobiol *11*, 641–653. 10.1007/s10237-011-0339-6.
71. Blanchard, L., and Girard, J.P. (2021). High endothelial venules (HEVs) in immunity, inflammation and cancer. Angiogenesis *24*, 719–753. 10.1007/s10456-021-09792-8.
72. Sawada, J., Perrot, C.Y., Chen, L., Fournier-Goss, A.E., Oyer, J., Copik, A., and Komatsu, M. (2021). High Endothelial Venules Accelerate Naive T Cell Recruitment by Tumor Necrosis Factor-Mediated R-Ras Upregulation. Am J Pathol *191*, 396–414. 10.1016/j.ajpath.2020.10.009.
73. Kim, S.T., Shin, Y., Brazin, K., Mallis, R.J., Sun, Z.Y., Wagner, G., Lang, M.J., and Reinherz, E.L. (2012). TCR Mechanobiology: Torques and Tunable Structures Linked to Early T Cell Signaling. Front Immunol *3*, 76. 10.3389/fimmu.2012.00076.
74. Liu, Y., Blanchfield, L., Ma, V.P., Andargachew, R., Galior, K., Liu, Z., Evavold, B., and Salaita, K. (2016). DNA-based nanoparticle tension sensors reveal that T-cell receptors transmit defined pN forces to their antigens for enhanced fidelity. Proc Natl Acad Sci U S A *113*, 5610–5615. 10.1073/pnas.1600163113.
75. Sawicka, A., Babataheri, A., Dogniaux, S., Barakat, A.I., Gonzalez-Rodriguez, D., Hivroz, C., and Husson, J. (2017). Micropipette force probe to quantify single-cell force generation: application to T-cell activation. Mol Biol Cell *28*, 3229–3239. 10.1091/mbc.E17-06-0385.

76. Hu, K.H., and Butte, M.J. (2016). T cell activation requires force generation. J Cell Biol *213*, 535–542. 10.1083/jcb.201511053.
77. Lühr, J.J., Alex, N., Amon, L., Kräter, M., Kubánková, M., Sezgin, E., Lehmann, C.H.K., Heger, L., Heidkamp, G.F., Smith, A.-S., et al. (2020). Maturation of Monocyte-Derived DCs Leads to Increased Cellular Stiffness, Higher Membrane Fluidity, and Changed Lipid Composition. Frontiers in Immunology *Volume 11 - 2020*. 10.3389/fimmu.2020.590121.
78. Silvani, G., Romanov, V., Cox, C.D., and Martinac, B. (2021). Biomechanical Characterization of Endothelial Cells Exposed to Shear Stress Using Acoustic Force Spectroscopy. Frontiers in Bioengineering and Biotechnology *Volume 9 - 2021*. 10.3389/fbioe.2021.612151.
79. Xie, L., Sun, Z., Brown, N.J., Glinskii, O.V., Meininger, G.A., and Glinsky, V.V. (2022). Changes in dynamics of tumor/endothelial cell adhesive interactions depending on endothelial cell growth state and elastic properties. PLOS ONE *17*, e0269552. 10.1371/journal.pone.0269552.
80. Hu, Y., Li, H., Zhang, C., Feng, J., Wang, W., Chen, W., Yu, M., Liu, X., Zhang, X., and Liu, Z. (2024). DNA-based ForceChrono probes for deciphering single-molecule force dynamics in living cells. Cell *187*, 3445–3459.e3415. 10.1016/j.cell.2024.05.008.
81. Murugesan, S., Hong, J., Yi, J., Li, D., Beach, J.R., Shao, L., Meinhardt, J., Madison, G., Wu, X., Betzig, E., and Hammer, J.A. (2016). Formin-generated actomyosin arcs propel T cell receptor microcluster movement at the immune synapse. Journal of Cell Biology *215*, 383–399. 10.1083/jcb.201603080.
82. Li, M., Liu, L., Xi, N., and Wang, Y. (2018). Atomic force microscopy studies on cellular elastic and viscoelastic properties. Science China Life Sciences *61*, 57–67. 10.1007/s11427-016-9041-9.
83. Hobson, C.M., Kern, M., O'Brien, E.T., Stephens, A.D., Falvo, M.R., and Superfine, R. (2020). Correlating nuclear morphology and external force with combined atomic force microscopy and light sheet imaging separates roles of chromatin and lamin A/C in nuclear mechanics. Molecular Biology of the Cell *31*, 1788–1801. 10.1091/mbc.E20-01-0073.
84. Thompson, S.B., Sandor, A.M., Lui, V., Chung, J.W., Waldman, M.M., Long, R.A., Estin, M.L., Matsuda, J.L., Friedman, R.S., and Jacobelli, J. (2020). Formin-like 1 mediates effector T cell trafficking to inflammatory sites to enable T cell-mediated autoimmunity. Elife *9*. 10.7554/eLife.58046.
85. Simao, M., Régnier, F., Taheraly, S., Fraisse, A., Tacine, R., Fraudeau, M., Benabid, A., Feuillet, V., Lambert, M., Delon, J., and Randriamampita, C. (2021). cAMP Bursts Control T Cell Directionality by Actomyosin Cytoskeleton Remodeling. Front Cell Dev Biol *9*, 633099. 10.3389/fcell.2021.633099.
86. Lam, T.T., and Chong, M.M.W. (2025). Regulation of actin cytoskeletal dynamics in T cell development and function. Frontiers in Immunology *Volume 16 - 2025*. 10.3389/fimmu.2025.1622928.
87. Nourshargh, S., Hordijk, P.L., and Sixt, M. (2010). Breaching multiple barriers: leukocyte motility through venular walls and the interstitium. Nat Rev Mol Cell Biol *11*, 366–378. 10.1038/nrm2889.
88. Grönloh, M.L.B., van der Meer, W.J., Tebbens, M.E., and van Buul, J.D. (2025). Leukocyte transendothelial migration hotspots at a glance. J Cell Sci *138*. 10.1242/jcs.263862.
89. Vestweber, D. (2015). How leukocytes cross the vascular endothelium. Nat Rev Immunol *15*, 692–704. 10.1038/nri3908.
90. Colin-York, H., Javanmardi, Y., Barbieri, L., Li, D., Korobchevskaya, K., Guo, Y., Hall, C., Taylor, A., Khuon, S., Sheridan, G.K., et al. (2019). Spatiotemporally Super-Resolved Volumetric Traction Force Microscopy. Nano Lett *19*, 4427–4434. 10.1021/acs.nanolett.9b01196.
91. Lomakina, E.B., Spillmann, C.M., King, M.R., and Waugh, R.E. (2004). Rheological analysis and measurement of neutrophil indentation. Biophys J *87*, 4246–4258. 10.1529/biophysj.103.031765.
92. Spillmann, C.M., Lomakina, E., and Waugh, R.E. (2004). Neutrophil adhesive contact dependence on impingement force. Biophys J *87*, 4237–4245. 10.1529/biophysj.103.031773.
93. Abadier, M., and Ley, K. (2017). P-selectin glycoprotein ligand-1 in T cells. Curr Opin Hematol *24*, 265–273. 10.1097/MOH.0000000000000331.
94. Ivetic, A., Hoskins Green, H.L., and Hart, S.J. (2019). L-selectin: A Major Regulator of Leukocyte Adhesion, Migration and Signaling. Front Immunol *10*, 1068. 10.3389/fimmu.2019.01068.
95. Rahman, I., Collado Sanchez, A., Davies, J., Rzeniewicz, K., Abukscem, S., Joachim, J., Hoskins Green, H.L., Killock, D., Sanz, M.J., Charras, G., et al. (2021). L-selectin regulates human neutrophil transendothelial migration. J Cell Sci *134*. 10.1242/jcs.250340.
96. Kameritsch, P., and Renkawitz, J. (2020). Principles of Leukocyte Migration Strategies. Trends Cell Biol *30*, 818–832. 10.1016/j.tcb.2020.06.007.
97. Yeh, Y.T., Serrano, R., Francois, J., Chiu, J.J., Li, Y.J., Del Alamo, J.C., Chien, S., and Lasheras, J.C. (2018). Three-dimensional forces exerted by leukocytes and vascular endothelial cells dynamically facilitate diapedesis. Proc Natl Acad Sci U S A *115*, 133–138. 10.1073/pnas.1717489115.
98. Bouissou, A., Proag, A., Bourg, N., Pingris, K., Cabriel, C., Balor, S., Mangeat, T., Thibault, C., Vieu, C., Dupuis, G., et al. (2017). Podosome Force Generation Machinery: A Local Balance between Protrusion at the Core and Traction at the Ring. ACS Nano *11*, 4028–4040. 10.1021/acsnano.7b00622.
99. Martinelli, R., Zeiger, A.S., Whitfield, M., Sciuto, T.E., Dvorak, A., Van Vliet, K.J., Greenwood, J., and Carman, C.V. (2014). Probing the biomechanical contribution of the endothelium to lymphocyte migration: diapedesis by the path of least resistance. J Cell Sci *127*, 3720–3734. 10.1242/jcs.148619.
100. Arts, J.J., Mahlandt, E.K., Gronloh, M.L., Schimmel, L., Noordstra, I., Gordon, E., van Steen, A.C., Tol, S., Walzog, B., van Rijssel, J., et al. (2021). Endothelial junctional membrane protrusions serve as hotspots for neutrophil transmigration. Elife *10*. 10.7554/eLife.66074.

101. De Belly, H., Yan, S., Borja da Rocha, H., Ichbiah, S., Town, J.P., Zager, P.J., Estrada, D.C., Meyer, K., Turlier, H., Bustamante, C., and Weiner, O.D. (2023). Cell protrusions and contractions generate long-range membrane tension propagation. Cell *186*, 3049–3061 e3015. 10.1016/j.cell.2023.05.014.
102. Yago, T., Wu, J., Wey, C.D., Klopocki, A.G., Zhu, C., and McEver, R.P. (2004). Catch bonds govern adhesion through L-selectin at threshold shear. J Cell Biol *166*, 913–923. 10.1083/jcb.200403144.
103. Morikis, V.A., Chase, S., Wun, T., Chaikof, E.L., Magnani, J.L., and Simon, S.I. (2017). Selectin catch-bonds mechanotransduce integrin activation and neutrophil arrest on inflamed endothelium under shear flow. Blood *130*, 2101–2110. 10.1182/blood-2017-05-783027.
104. Hahne, M., Jäger, U., Isenmann, S., Hallmann, R., and Vestweber, D. (1993). Five tumor necrosis factor-inducible cell adhesion mechanisms on the surface of mouse endothelioma cells mediate the binding of leukocytes. J Cell Biol *121*, 655–664. 10.1083/jcb.121.3.655.
105. Koedam, J.A., Cramer, E.M., Briend, E., Furie, B., Furie, B.C., and Wagner, D.D. (1992). P-selectin, a granule membrane protein of platelets and endothelial cells, follows the regulated secretory pathway in AtT-20 cells. J Cell Biol *116*, 617–625. 10.1083/jcb.116.3.617.
106. Liu, Z., Miner, J.J., Yago, T., Yao, L., Lupu, F., Xia, L., and McEver, R.P. (2010). Differential regulation of human and murine P-selectin expression and function in vivo. J Exp Med *207*, 2975–2987. 10.1084/jem.20101545.
107. McEver, R.P. (2015). Selectins: initiators of leucocyte adhesion and signalling at the vascular wall. Cardiovasc Res *107*, 331–339. 10.1093/cvr/cvv154.
108. Millan, J., Hewlett, L., Glyn, M., Toomre, D., Clark, P., and Ridley, A.J. (2006). Lymphocyte transcellular migration occurs through recruitment of endothelial ICAM-1 to caveola- and F-actin-rich domains. Nat Cell Biol *8*, 113–123. 10.1038/ncb1356.
109. Watson, H.A., Durairaj, R.R.P., Ohme, J., Alatsatianos, M., Almutairi, H., Mohammed, R.N., Vigar, M., Reed, S.G., Paisey, S.J., Marshall, C., et al. (2019). L-Selectin Enhanced T Cells Improve the Efficacy of Cancer Immunotherapy. Front Immunol *10*, 1321. 10.3389/fimmu.2019.01321.
110. Rosen, S.D. (2004). Ligands for L-selectin: homing, inflammation, and beyond. Annu Rev Immunol *22*, 129–156. 10.1146/annurev.immunol.21.090501.080131.
111. Somers, W.S., Tang, J., Shaw, G.D., and Camphausen, R.T. (2000). Insights into the molecular basis of leukocyte tethering and rolling revealed by structures of P- and E-selectin bound to SLe(X) and PSGL-1. Cell *103*, 467–479. 10.1016/s0092-8674(00)00138-0.
112. Auffray, C., Fogg, D., Garfa, M., Elain, G., Join-Lambert, O., Kayal, S., Sarnacki, S., Cumano, A., Lauvau, G., and Geissmann, F. (2007). Monitoring of blood vessels and tissues by a population of monocytes with patrolling behavior. Science *317*, 666–670. 10.1126/science.1142883.
113. Chesnutt, B.C., Smith, D.F., Raffler, N.A., Smith, M.L., White, E.J., and Ley, K. (2006). Induction of LFA-1-dependent neutrophil rolling on ICAM-1 by engagement of E-selectin. Microcirculation *13*, 99–109. 10.1080/10739680500466376.
114. Siegelman, M.H., Stanescu, D., and Estess, P. (2000). The CD44-initiated pathway of T-cell extravasation uses VLA-4 but not LFA-1 for firm adhesion. J Clin Invest *105*, 683–691. 10.1172/JCI8692.
115. Schimmel, L., van der Stoel, M., Rianna, C., van Stalborch, A.M., de Ligt, A., Hoogenboezem, M., Tol, S., van Rijssel, J., Szulcek, R., Bogaard, H.J., et al. (2018). Stiffness-Induced Endothelial DLC-1 Expression Forces Leukocyte Spreading through Stabilization of the ICAM-1 Adhesome. Cell Rep *24*, 3115–3124. 10.1016/j.celrep.2018.08.045.
116. Phillipson, M., Heit, B., Colarusso, P., Liu, L., Ballantyne, C.M., and Kubes, P. (2006). Intraluminal crawling of neutrophils to emigration sites: a molecularly distinct process from adhesion in the recruitment cascade. J Exp Med *203*, 2569–2575. 10.1084/jem.20060925.
117. Hogg, N., Laschinger, M., Giles, K., and McDowall, A. (2003). T-cell integrins: more than just sticking points. J Cell Sci *116*, 4695–4705. 10.1242/jcs.00876.
118. Schollhorn, A., Schuhmacher, J., Besedovsky, L., Fendel, R., Jensen, A.T.R., Stevanovic, S., Lange, T., Rammensee, H.G., Born, J., Gouttefangeas, C., and Dimitrov, S. (2021). Integrin Activation Enables Sensitive Detection of Functional CD4(+) and CD8(+) T Cells: Application to Characterize SARS-CoV-2 Immunity. Front Immunol *12*, 626308. 10.3389/fimmu.2021.626308.
119. Tabasum, S., Thapa, D., Giobbie-Hurder, A., Weirather, J.L., Campisi, M., Schol, P.J., Li, X., Li, J., Yoon, C.H., Manos, M.P., et al. (2023). EDIL3 as an Angiogenic Target of Immune Exclusion Following Checkpoint Blockade. Cancer Immunol Res *11*, 1493–1507. 10.1158/2326-6066.Cir-23-0171.
120. McEver, R.P., and Zhu, C. (2010). Rolling cell adhesion. Annu Rev Cell Dev Biol *26*, 363–396. 10.1146/annurev.cellbio.042308.113238.
121. Goldman, A.J., Cox, R.G., and Brenner, H. (1967). Slow viscous motion of a sphere parallel to a plane wall-II couette flow. Chemical Engineering Science *22*, 653–660. https://doi.org/10.1016/0009-2509(67)80048-4.
122. Hocde, S.A., Hyrien, O., and Waugh, R.E. (2009). Molecular accessibility in relation to cell surface topography and compression against a flat substrate. Biophys J *97*, 369–378. 10.1016/j.bpj.2009.04.034.
123. Hocde, S.A., Hyrien, O., and Waugh, R.E. (2009). Cell adhesion molecule distribution relative to neutrophil surface topography assessed by TIRFM. Biophys J *97*, 379–387. 10.1016/j.bpj.2009.04.035.
124. Nordenfelt, P., Elliott, H.L., and Springer, T.A. (2016). Coordinated integrin activation by actin-dependent force during T-cell migration. Nat Commun *7*, 13119. 10.1038/ncomms13119.
125. Yoshida, M., Westlin, W.F., Wang, N., Ingber, D.E., Rosenzweig, A., Resnick, N., and Gimbrone, M.A., Jr. (1996). Leukocyte adhesion to vascular endothelium induces E-selectin linkage to the actin cytoskeleton. J Cell Biol *133*, 445–455. 10.1083/jcb.133.2.445.

126. Marki, A., Gutierrez, E., Mikulski, Z., Groisman, A., and Ley, K. (2016). Microfluidics-based side view flow chamber reveals tether-to-sling transition in rolling neutrophils. Sci Rep *6*, 28870. 10.1038/srep28870.
127. Shao, J., Ging-Beall, H.P., and Hochmuth, R.M. (1998). Static and dynamic lengths of neutrophil microvilli. Proc Natl Acad Sci U S A *95*, 6797–6802.
128. Shao, J., and Hochmuth, R.M. (1996). Micropipette Suction for Measuring Piconewton Forces of Adhesion and tether formation from neutrophil membranse. Biophysical Journal *71*, 2892–2901.
129. Korn, C.B., and Schwarz, U.S. (2008). Dynamic states of cells adhering in shear flow: From slipping to rolling. Physical Review E *77*, 041904. 10.1103/PhysRevE.77.041904.
130. Angulo-Urarte, A., van der Wal, T., and Huveneers, S. (2020). Cell-cell junctions as sensors and transducers of mechanical forces. Biochim Biophys Acta Biomembr *1862*, 183316. 10.1016/j.bbamem.2020.183316.
131. Janssen, V., and Huveneers, S. (2024). Cell-cell junctions in focus - imaging junctional architectures and dynamics at high resolution. J Cell Sci *137*. 10.1242/jcs.262041.
132. Barry, A.K., Wang, N., and Leckband, D.E. (2015). Local VE-cadherin mechanotransduction triggers long-ranged remodeling of endothelial monolayers. J Cell Sci *128*, 1341–1351. 10.1242/jcs.159954.
133. Kutys, M.L., and Chen, C.S. (2016). Forces and mechanotransduction in 3D vascular biology. Curr Opin Cell Biol *42*, 73–79. 10.1016/j.ceb.2016.04.011.
134. Jackson, D.G. (2019). Leucocyte Trafficking via the Lymphatic Vasculature- Mechanisms and Consequences. Front Immunol *10*, 471. 10.3389/fimmu.2019.00471.
135. Duong, C.N., Nottebaum, A.F., Butz, S., Volkery, S., Zeuschner, D., Stehling, M., and Vestweber, D. (2020). Interference With ESAM (Endothelial Cell-Selective Adhesion Molecule) Plus Vascular Endothelial-Cadherin Causes Immediate Lethality and Lung-Specific Blood Coagulation. Arterioscler Thromb Vasc Biol *40*, 378–393. 10.1161/atvbaha.119.313545.
136. Bhat, A.A., Uppada, S., Achkar, I.W., Hashem, S., Yadav, S.K., Shanmugakonar, M., Al-Naemi, H.A., Haris, M., and Uddin, S. (2018). Tight Junction Proteins and Signaling Pathways in Cancer and Inflammation: A Functional Crosstalk. Front Physiol *9*, 1942. 10.3389/fphys.2018.01942.
137. Burns, A.R., Bowden, R.A., MacDonell, S.D., Walker, D.C., Odebunmi, T.O., Donnachie, E.M., Simon, S.I., Entman, M.L., and Wayne Smith, C. (2000`). Analysis of tight junctions during neutrophil transendothelial migration. Journal of Cell Science *113*, 45–57.
138. Abu Taha, A., and Schnittler, H.J. (2014). Dynamics between actin and the VE-cadherin/catenin complex: novel aspects of the ARP2/3 complex in regulation of endothelial junctions. Cell Adh Migr *8*, 125–135. 10.4161/cam.28243.
139. Garrett, J.P., Lowery, A.M., Adam, A.P., Kowalczyk, A.P., and Vincent, P.A. (2017). Regulation of endothelial barrier function by p120-catenin·VE-cadherin interaction. Mol Biol Cell *28*, 85–97. 10.1091/mbc.E16-08-0616.
140. Zhao, Y., Li, J., Ting, K.K., Chen, J., Coleman, P., Liu, K., Wan, L., Moller, T., Vadas, M.A., and Gamble, J.R. (2021). The VE-Cadherin/beta-catenin signalling axis regulates immune cell infiltration into tumours. Cancer Lett *496*, 1–15. 10.1016/j.canlet.2020.09.026.
141. Conway, D.E., Coon, B.G., Budatha, M., Arsenovic, P.T., Orsenigo, F., Wessel, F., Zhang, J., Zhuang, Z., Dejana, E., Vestweber, D., and Schwartz, M.A. (2017). VE-Cadherin Phosphorylation Regulates Endothelial Fluid Shear Stress Responses through the Polarity Protein LGN. Curr Biol *27*, 2219–2225.e2215. 10.1016/j.cub.2017.06.020.
142. Conway, D.E., Breckenridge, M.T., Hinde, E., Gratton, E., Chen, C.S., and Schwartz, M.A. (2013). Fluid shear stress on endothelial cells modulates mechanical tension across VE-cadherin and PECAM-1. Curr Biol *23*, 1024–1030. 10.1016/j.cub.2013.04.049.
143. van Nieuw Amerongen, G.P., Draijer, R., Vermeer, M.A., and Van Hinsbergh, V.W.M. (1998). Transient and Prolonged Increase in Endothelial Permeability Induced by Histamine and Thrombin. Circulation Research, 1115–1123.
144. Lal, B.K., Varma, S., Pappas, P.J., Hobson, R.W., 2nd, and Duran, W.N. (2001). VEGF increases permeability of the endothelial cell monolayer by activation of PKB/akt, endothelial nitric-oxide synthase, and MAP kinase pathways. Microvasc Res *62*, 252–262. 10.1006/mvre.2001.2338.
145. Kim, Y.M., Krantz, S., Jambusaria, A., Toth, P.T., Moon, H.G., Gunarathna, I., Park, G.Y., and Rehman, J. (2021). Mitofusin-2 stabilizes adherens junctions and suppresses endothelial inflammation via modulation of beta-catenin signaling. Nat Commun *12*, 2736. 10.1038/s41467-021-23047-6.
146. Colas-Algora, N., Garcia-Weber, D., Cacho-Navas, C., Barroso, S., Caballero, A., Ribas, C., Correas, I., and Millan, J. (2020). Compensatory increase of VE-cadherin expression through ETS1 regulates endothelial barrier function in response to TNFalpha. Cell Mol Life Sci *77*, 2125–2140. 10.1007/s00018-019-03260-9.
147. Cerutti, C., and Ridley, A.J. (2017). Endothelial cell-cell adhesion and signaling. Exp Cell Res *358*, 31–38. 10.1016/j.yexcr.2017.06.003.
148. McDonald, D.M. (1994). Endothelial gaps and permeability of venules in rat tracheas exposed to inflammatory stimuli. Am J Physiol *266*, L61–83. 10.1152/ajplung.1994.266.1.L61.
149. Xiao, K., Garner, J., Buckley, K.M., Vincent, P.A., Chiasson, C.M., Dejana, E., Faundez, V., and Kowalczyk, A.P. (2005). p120-Catenin regulates clathrin-dependent endocytosis of VE-cadherin. Mol Biol Cell *16*, 5141–5151. 10.1091/mbc.e05-05-0440.
150. Semina, E.V., Rubina, K.A., Sysoeva, V.Y., Rutkevich, P.N., Kashirina, N.M., and Tkachuk, V.A. (2014). Novel mechanism regulating endothelial permeability via T-cadherin-dependent VE-cadherin phosphorylation and clathrin-mediated endocytosis. Molecular and Cellular Biochemistry *387*, 39–53. 10.1007/s11010-013-1867-4.

151. Allport, J.R., Muller, W.A., and Luscinskas, F.W. (2000). Monocytes induce reversible focal changes in vascular endothelial cadherin complex during transendothelial migration under flow. J Cell Biol *148*, 203–216. 10.1083/jcb.148.1.203.
152. Rabodzey, A., Alcaide, P., Luscinskas, F.W., and Ladoux, B. (2008). Mechanical forces induced by the transendothelial migration of human neutrophils. Biophys J *95*, 1428–1438. 10.1529/biophysj.107.119156.
153. Schulte, D., Kuppers, V., Dartsch, N., Broermann, A., Li, H., Zarbock, A., Kamenyeva, O., Kiefer, F., Khandoga, A., Massberg, S., and Vestweber, D. (2011). Stabilizing the VE-cadherin-catenin complex blocks leukocyte extravasation and vascular permeability. EMBO J *30*, 4157–4170. 10.1038/emboj.2011.304.
154. Barzilai, S., Yadav, S.K., Morrell, S., Roncato, F., Klein, E., Stoler-Barak, L., Golani, O., Feigelson, S.W., Zemel, A., Nourshargh, S., and Alon, R. (2017). Leukocytes Breach Endothelial Barriers by Insertion of Nuclear Lobes and Disassembly of Endothelial Actin Filaments. Cell Rep *18*, 685–699. 10.1016/j.celrep.2016.12.076.
155. Coon, B.G., Baeyens, N., Han, J., Budatha, M., Ross, T.D., Fang, J.S., Yun, S., Thomas, J.L., and Schwartz, M.A. (2015). Intramembrane binding of VE-cadherin to VEGFR2 and VEGFR3 assembles the endothelial mechanosensory complex. J Cell Biol *208*, 975–986. 10.1083/jcb.201408103.
156. Verma, D., Bajpai, V.K., Ye, N., Maneshi, M.M., Jetta, D., Andreadis, S.T., Sachs, F., and Hua, S.Z. (2017). Flow induced adherens junction remodeling driven by cytoskeletal forces. Exp Cell Res *359*, 327–336. 10.1016/j.yexcr.2017.08.009.
157. Privratsky, J.R., Newman, D.K., and Newman, P.J. (2010). PECAM-1: conflicts of interest in inflammation. Life Sci *87*, 69–82. 10.1016/j.lfs.2010.06.001.
158. Hashimoto, K., Kataoka, N., Nakamura, E., Hagihara, K., Hatano, M., Okamoto, T., Kanouchi, H., Minatogawa, Y., Mohri, S., Tsujioka, K., and Kajiya, F. (2011). Monocyte trans-endothelial migration augments subsequent transmigratory activity with increased PECAM-1 and decreased VE-cadherin at endothelial junctions. Int J Cardiol *149*, 232–239. 10.1016/j.ijcard.2010.12.018.
159. Wimmer, I., Tietz, S., Nishihara, H., Deutsch, U., Sallusto, F., Gosselet, F., Lyck, R., Muller, W.A., Lassmann, H., and Engelhardt, B. (2019). PECAM-1 Stabilizes Blood-Brain Barrier Integrity and Favors Paracellular T-Cell Diapedesis Across the Blood-Brain Barrier During Neuroinflammation. Front Immunol *10*, 711. 10.3389/fimmu.2019.00711.
160. Liao, D., Mei, H., Hu, Y., Newman, D.K., and Newman, P.J. (2018). CRISPR-mediated deletion of the PECAM-1 cytoplasmic domain increases receptor lateral mobility and strengthens endothelial cell junctional integrity. Life Sci *193*, 186–193. 10.1016/j.lfs.2017.11.002.
161. van der Meer, W.J., van Steen, A.C.I., Mahlandt, E., Rolas, L., Wang, H., Arts, J.J.G., Kempers, L., Grönloh, M.L.B., Schoon, R.M., Driessen, A., et al. (2025). Leukocytes use endothelial membrane tunnels to extravasate the vasculature. Cell Rep *44*, 116242. 10.1016/j.celrep.2025.116242.
162. Fujiwara, K. (2006). Platelet endothelial cell adhesion molecule-1 and mechanotransduction in vascular endothelial cells. J Intern Med *259*, 373–380. 10.1111/j.1365-2796.2006.01623.x.
163. Alexander, J.S., Dayton, T., Davis, C., Hill, S., Haller Jackson, T., Blaschuk, O., Symonds, M., Okayama, N., Kevil, C.G., Laroux, F.S., et al. (1998). Activated T-lymphocytes express occludin, a component of tight junctions. Inflammation *22*, 573–582.
164. Watson, R.L., Buck, J., Levin, L.R., Winger, R.C., Wang, J., Arase, H., and Muller, W.A. (2015). Endothelial CD99 signals through soluble adenylyl cyclase and PKA to regulate leukocyte transendothelial migration. J Exp Med *212*, 1021–1041. 10.1084/jem.20150354.
165. Carman, C.V., and Springer, T.A. (2004). A transmigratory cup in leukocyte diapedesis both through individual vascular endothelial cells and between them. J Cell Biol *167*, 377–388. 10.1083/jcb.200404129.
166. Woodfin, A., Voisin, M.B., Beyrau, M., Colom, B., Caille, D., Diapouli, F.M., Nash, G.B., Chavakis, T., Albelda, S.M., Rainger, G.E., et al. (2011). The junctional adhesion molecule JAM-C regulates polarized transendothelial migration of neutrophils in vivo. Nat Immunol *12*, 761–769. 10.1038/ni.2062.
167. Rademakers, T., Goedhart, M., Hoogenboezem, M., Garcia Ponce, A., van Rijssel, J., Samus, M., Schnoor, M., Butz, S., Huveneers, S., Vestweber, D., et al. (2020). Hematopoietic stem and progenitor cells use podosomes to transcellularly cross the bone marrow endothelium. Haematologica *105*, 2746–2756. 10.3324/haematol.2018.196329.
168. Alon, R., and Feigelson, S.W. (2012). Chemokine-triggered leukocyte arrest: force-regulated bi-directional integrin activation in quantal adhesive contacts. Curr Opin Cell Biol *24*, 670–676. 10.1016/j.ceb.2012.06.001.
169. Alon, R., and Shulman, Z. (2011). Chemokine triggered integrin activation and actin remodeling events guiding lymphocyte migration across vascular barriers. Exp Cell Res *317*, 632–641. 10.1016/j.yexcr.2010.12.007.
170. Martinelli, R., Kamei, M., Sage, P.T., Massol, R., Varghese, L., Sciuto, T., Toporsian, M., Dvorak, A.M., Kirchhausen, T., Springer, T.A., and Carman, C.V. (2013). Release of cellular tension signals self-restorative ventral lamellipodia to heal barrier micro-wounds. J Cell Biol *201*, 449–465. 10.1083/jcb.201209077.
171. Turowski, P., Martinelli, R., Crawford, R., Wateridge, D., Papageorgiou, A.P., Lampugnani, M.G., Gamp, A.C., Vestweber, D., Adamson, P., Dejana, E., and Greenwood, J. (2008). Phosphorylation of vascular endothelial cadherin controls lymphocyte emigration. J Cell Sci *121*, 29–37. 10.1242/jcs.022681.
172. Linder, S., Cervero, P., Eddy, R., and Condeelis, J. (2023). Mechanisms and roles of podosomes and invadopodia. Nat Rev Mol Cell Biol *24*, 86–106. 10.1038/s41580-022-00530-6.
173. Sundd, P., Pospieszalska, M.K., and Ley, K. (2013). Neutrophil rolling at high shear: flattening, catch bond behavior, tethers and slings. Mol Immunol *55*, 59–69. 10.1016/j.molimm.2012.10.025.

174. Niemiec, M.J., De Samber, B., Garrevoet, J., Vergucht, E., Vekemans, B., De Rycke, R., Bjorn, E., Sandblad, L., Wellenreuther, G., Falkenberg, G., et al. (2015). Trace element landscape of resting and activated human neutrophils on the sub-micrometer level. Metallomics *7*, 996–1010. 10.1039/c4mt00346b.
175. Andersen, A.S., Aslan, H., Dong, M., Jiang, X., and Sutherland, D.S. (2016). Podosome Formation and Development in Monocytes Restricted by the Nanoscale Spatial Distribution of ICAM1. Nano Lett *16*, 2114–2121. 10.1021/acs.nanolett.6b00519.
176. Labernadie, A., Bouissou, A., Delobelle, P., Balor, S., Voituriez, R., Proag, A., Fourquaux, I., Thibault, C., Vieu, C., Poincloux, R., et al. (2014). Protrusion force microscopy reveals oscillatory force generation and mechanosensing activity of human macrophage podosomes. Nat Commun *5*, 5343. 10.1038/ncomms6343.
177. Wang, L., Wang, B., Jia, L., Yu, H., Wang, Z., Wei, F., and Jiang, A. (2023). Shear stress leads to the dysfunction of endothelial cells through the Cav-1-mediated KLF2/eNOS/ERK signaling pathway under physiological conditions. Open Life Sci *18*, 20220587. 10.1515/biol-2022-0587.
178. Parazynski, S.E., Tucker, B.J., Aratow, M., Crenshaw, A., and Hargens, A.R. (1993). Direct measurement of capillary blood pressure in the human lip. J Appl Physiol (1985) *74*, 946–950. 10.1152/jappl.1993.74.2.946.
179. Blumenthal, D., Chandra, V., Avery, L., and Burkhardt, J.K. (2020). Mouse T cell priming is enhanced by maturation-dependent stiffening of the dendritic cell cortex. Elife *9*. 10.7554/eLife.55995.
180. Vargas-Pinto, R., Gong, H., Vahabikashi, A., and Johnson, M. (2013). The effect of the endothelial cell cortex on atomic force microscopy measurements. Biophys J *105*, 300–309. 10.1016/j.bpj.2013.05.034.
181. Rosenbluth, M.J., Lam, W.A., and Fletcher, D.A. (2006). Force microscopy of nonadherent cells: a comparison of leukemia cell deformability. Biophys J *90*, 2994–3003. 10.1529/biophysj.105.067496.
182. Hu, M., Wang, J., Zhao, H., Dong, S., and Cai, J. (2009). Nanostructure and nanomechanics analysis of lymphocyte using AFM: From resting, activated to apoptosis. Journal of Biomechanics *42*, 1513–1519. https://doi.org/10.1016/j.jbiomech.2009.03.051.
183. Liu, Z., Sniadecki, N.J., and Chen, C.S. (2010). Mechanical Forces in Endothelial Cells during Firm Adhesion and Early Transmigration of Human Monocytes. Cell Mol Bioeng *3*, 50–59. 10.1007/s12195-010-0105-3.
184. Al-Aghbar, M.A., Jainarayanan, A.K., Dustin, M.L., and Roffler, S.R. (2022). The interplay between membrane topology and mechanical forces in regulating T cell receptor activity. Communications Biology *5*, 40. 10.1038/s42003-021-02995-1.
185. Zarnitsyna, V.I., and Zhu, C. (2011). Adhesion frequency assay for in situ kinetics analysis of cross-junctional molecular interactions at the cell-cell interface. J Vis Exp, e3519. 10.3791/3519.
186. Li, N., Yang, H., Wang, M., Lü, S., Zhang, Y., and Long, M. (2018). Ligand-specific binding forces of LFA-1 and Mac-1 in neutrophil adhesion and crawling. Molecular Biology of the Cell *29*, 408–418. 10.1091/mbc.E16-12-0827.
187. Snook, J.H., and Guilford, W.H. (2010). The Effects of Load on E-Selectin Bond Rupture and Bond Formation. Cell Mol Bioeng *3*, 128–138. 10.1007/s12195-010-0110-6.
188. Lai, A., Thurgood, P., Cox, C.D., Chheang, C., Peter, K., Jaworowski, A., Khoshmanesh, K., and Baratchi, S. (2022). Piezo1 Response to Shear Stress Is Controlled by the Components of the Extracellular Matrix. ACS Applied Materials & Interfaces *14*, 40559–40568. 10.1021/acsami.2c09169.
189. Harada, N., Masuda, M., and Fujiwara, K. (1995). Fluid flow and osmotic stress induce tyrosine phosphorylation of an endothelial cell 128 kDa surface glycoprotein. Biochem Biophys Res Commun *214*, 69–74. 10.1006/bbrc.1995.2257.
190. Osawa, M., Masuda, M., Kusano, K., and Fujiwara, K. (2002). Evidence for a role of platelet endothelial cell adhesion molecule-1 in endothelial cell mechanosignal transduction: is it a mechanoresponsive molecule? J Cell Biol *158*, 773–785. 10.1083/jcb.200205049.



Chapter 7

General discussion

General Discussion

Adherens junctions (AJs) are dynamic structures that bridge neighboring endothelial cells in the vessel wall, balancing mechanical stability in diverse hemodynamic environments with the capacity to adapt to homeostatic and inflammatory cues. This thesis set out to determine how vascular endothelial (VE)-cadherin, the core adhesion receptor of AJs, orchestrates molecular organization, intracellular signaling, and mechanotransduction at endothelial junctions to control vascular integrity. By uncovering new VE-cadherin-binding partners and their regulatory principles, the work presented here moves beyond the classical view of VE-cadherin as a static adhesive link and instead positions it as a responsive, multifunctional, scaffold that defines endothelial behavior. The roles of these junctional interactions were studied across hierarchical scales, from protein structure to cellular dynamics and ultimately tissue-level force adaptation.

At the molecular scale, we showed that VE-cadherin's extracellular domain forms a structurally intact adhesive interface that can function independently of its arginine-glycine-aspartate (RGD) integrin-binding motifs **(chapter 4)**, even though these RGD motifs are highly conserved for VE-cadherin across species. Within the cell, the VE-cadherin complex associates with a versatile set of catenins and regulatory factors, including PKP4 and the newly identified interacting proteins ARVCF, ARHGAP23, and KEAP1. These interacting proteins modulate junction organization, cytoskeletal tension, and redox balance **(chapters 2&3)**. At the mechanical level, we investigated the importance of the mechanosensitive α-catenin-vinculin module, which converts actomyosin activity into reinforced cell-to-cell adhesion. Our findings showed that intracellular tension is linked to enhanced barrier resilience in developing vessels **(chapter 5)**.

The significance of mechanotransduction becomes especially apparent during leukocyte transmigration **(chapter 6)**, where endothelial surface and junction receptors are challenged by highly localized and rapidly changing mechanical loads. As overviewed in **chapter 6**, arresting and transmigrating leukocytes exert pushing, pulling, and shear-related rolling forces onto the apical endothelial surface, which are interpreted by mechanosensitive receptors which, in turn, trigger signaling pathways that reorganize the junctions and actin cytoskeleton. During this process, the AJs function within a broader biomechanical framework in which external stress, receptor mechanics, and cellular compliance collectively determine whether the vascular barrier resists or remodels.

Together, the findings presented in this thesis uncover previously unrecognized mechanisms governing endothelial junction stability and remodeling in vascular homeostasis, development and inflammation.

Junctions as signaling bridges

By further exploring the molecular diversity of the VE-cadherin adhesion complex, this thesis identified several novel intracellular proteins that interact with VE-cadherin and may contribute to AJ compositions that are tailored to various environmental demands. We have focused on characterization of the roles of ARVCF, ARHGAP23, KEAP1 and PKP4 in endothelial junctions. PKP4 belongs to the same armadillo-repeat family as ARVCF and p120-catenin [1]. This raised the question whether these proteins may have redundant roles or whether they have specialized tasks. As shown in chapter 2, ARVCF binds to a pool of VE-cadherin protein that is distinct from those bound to p120-catenin, indicating that multiple armadillo proteins can interact with the VE-cadherin cytoplasmic domain in parallel or sequential manners. From these findings, combined with the notion that the domains within ARVCF that bind to VE-cadherin are sequentially distinct from those of p120-catenin [2], despite them binding to the same part of VE-cadherin [3,4], we hypothesize that ARVCF and p120-catenin may diversify how VE-cadherin links with the actin cytoskeleton and/or associated signaling machinery. In addition, PKP4 (chapter 3) can also influence the organization of the actin cytoskeleton via RhoA [5]. The diversity of armadillo-repeat proteins able to interact with VE-cadherin suggests the existence of a broad spectrum of AJ conformations, acting in parallel or sequentially, fit to deal with spatiotemporal demands.

Redundancy and buffering

Differences in the relative abundance of ARVCF, p120-catenin, and PKP4 protein levels across tissues [6] suggest that members of the armadillo family provide a buffering system that safeguards cadherin function in diverse cellular and mechanical environments. In endothelium, the predominant abundance of p120-catenin maintains VE-cadherin basal surface retention [6], whereas ARVCF levels increase when junctions transition towards a mature state (chapter 2). Importantly, of the armadillo containing proteins ARVCF and p120-catenin have the greatest structural similarities [1,7]. Studies have demonstrated that armadillo proteins compete for overlapping binding sequences within the juxtamembrane domain of classical cadherins: direct competition has been documented between p120-catenin and PKP4, and between p120-catenin and ARVCF [3,4,8,9]. Whether ARVCF and PKP4 also directly compete for cadherin binding remains unresolved and warrants future investigation. Interestingly, ARVCF and p120-catenin can compensate for each other's expression [10], while this is not the case between p120-catenin and PKP4 [5]. In endothelial cells, we find that the pool of p120-catenin-bound VE-cadherin suffices to maintain cell surface levels even in the absence of ARVCF (chapter 2) while overall barrier integrity is compromised. Differences in spatiotemporal recruitment of the armadillo family might enable a certain division of labor between them, which could explain why VE-cadherin remains on the endothelial surface upon ARVCF or PKP4 depletion (chapter 2).

The moderate junctional defects that we observed upon depletion of individual proteins PKP4 and ARVCF, rather than complete loss of barrier function, points to a model in which these proteins form an adaptable network around VE-cadherin rather than acting as essential determinants for endothelial junctions. Within such a network, I suspect that ARVCF primarily tunes mechanical coupling, while PKP4 organizes local RhoA signaling through the recruitment of GEFs and GAPs [5]. Of note, in other cell types ARVCF has been reported to control Rho activity levels [10], which may potentially contribute to junction maturation in the endothelium as well. The presence of multiple, parallel VE-cadherin complex assemblies could explain why endothelial junctions remain remarkably resilient when individual AJ complex components are removed in experimental settings: compensatory pathways may absorb perturbations while preserving overall tissue integrity.

The biochemical association between VE-cadherin and KEAP1 (chapter 2) that does not take place at the cell border (chapter 3) further expands this view by suggesting that VE-cadherin participates in signaling beyond the AJ. Through binding partners involved in redox control and stress response pathways such as KEAP-Nrf2, VE-cadherin may therefore integrate mechanical with metabolic and inflammatory cues, as these factors are usually present upon inflammation and immune cell transmigration [11,12].

Versatile control of force

ARVCF recruitment to AJs increases as they mature, and the depletion of ARVCF results in intercellular gaps and impaired collective migration (chapter 2). These processes are inherently force dependent [13,14]. These results indicate that AJs can adjust their molecular composition to accommodate changes in mechanical load. Although ARVCF is not a proven mechanotransducer, like for instance α-catenin is, ARVCF's selective association with VE-cadherin pools in mature junctions expands the repertoire of protein complexes available to resist cytoskeletal-derived stress across the junctions. Through its intrinsically disordered regions [15-17], ARVCF is suited to act as a flexible scaffold that enables adjustment of protein interactions, thereby allowing junctions to match structural AJ organization to mechanical demand.

Regulation of junction maturation and plasticity

The requirement of ARVCF for junction stabilization and coordinated collective behavior places endothelial cells in line with epithelial cells, where ARVCF is known to support tension generation and cadherin organization during development [13,18]. Moreover, epithelial ARVCF has been shown to interact with other junctional structures though linkage with the tight junction component ZO-1 [19]. Based on this, we hypothesize that the presence of ARVCF in mature junctions allows not only scaffolding for AJs, but also coupling of AJs to other junctional systems such as tight junctions. The

stabilizing role of ARVCF happens in parallel to reinforcement of endothelial intercellular adhesion through vinculin recruitment (chapter 5). Whether endothelial ARVCF is needed for barrier function in perfused blood vessels remains to be investigated.

While both ARVCF and vinculin correlate with mechanically demanding junction states, they operate at different stages of force-dependent remodeling. ARVCF promotes the organization of mature junctional complexes that are competent to bear load (chapter 5). Vinculin, in contrast, is specifically recruited only *after* tension across the AJ complex has unfolded α-catenin, and subsequently acts to strengthen and stabilize adhesion in response to that load [20]. Thus, we assume that ARVCF primarily contributes to enabling force transmission between cells, whereas vinculin consolidates the effect of tension across the remodeling AJs.

The depletion of ARVCF and vinculin disrupts collective endothelial behavior and compromises barrier integrity. We showed that the loss of ARVCF *in vitro* introduces gaps in the endothelial monolayer and disrupts collective cell migration in wound healing (chapter 2), while the loss of vinculin leads to vascular leakage *in vivo* and impaired sprouting angiogenesis (chapter 5). I postulate that ARVCF functions upstream of junctional mechanotransduction by organizing which VE-cadherin complexes are available for mechanical engagement, in parallel with its described scaffolding function in epithelial tissue. In such a model, ARVCF-mediated maturation of VE-cadherin assemblies at the membrane may establish a junctional architecture that is mechanically competent and poised for subsequent tension-dependent reinforcement by vinculin. Future research could address the prediction that in the absence of ARVCF, endothelial cells would fail to properly assemble force-bearing focal adherens junctions and exhibit impaired vinculin recruitment under tension. Together, this model suggests complementary layers of control within endothelial AJs: mechanisms that promote tension at junctions, and mechanisms that reinforce adhesion once tension is present. In this context, ARVCF as a scaffold might serve to organize an appropriate junctional composition, after which vinculin locks the strong junction to bear load.

The identification of ARHGAP23 as a VE-cadherin-associated RhoGAP introduces a regulatory signaling layer (chapter 3). The recruitment of ARHGAP23 to AJs, once activated, may inhibit near junctional actomyosin contractility, which may dampen the production of tension across the junctions. By monitoring effects on force generation and force-dependent reinforcement, this thesis gives new leads to assess AJ mechanobiology and illustrates how molecular diversity within the VE-cadherin complex translates into tissue-level vascular stability.

Extracellular regulation of VE-cadherin

Contrary to expectations based on the widespread role of RGD motifs in integrin-mediated adhesion for monocytes [21], our data showed that mutation of the extracellular RGD sequences in VE-cadherin has no discernible influence on monocyte transmigration (chapter 4). Perturbing the RGD motifs in the extracellular VE-cadherin domain also did not compromise junction integrity. The dispensability of the RGD motifs may reflect the architectural reality of adherens junctions, where dense clustering and cis/trans interactions restrict access to sequences in VE-cadherin's extracellular domain. It would be interesting to investigate whether cytoplasmic junction components such as ARVCF or p120-catenin might affect the extracellular conformation of the VE-cadherin.

Future perspectives

The research in this thesis positions VE-cadherin at the center of an adaptable interaction network that safeguards endothelial integrity across changing mechanical and inflammatory environments. This thesis complemented the AJ complex molecular landscape by identifying and characterizing several new interactors ARVCF, ARHGAP23, KEAP1, and NGLY1. Having shown that ARVCF is essential for junction stabilization and maturation, the depletion of other individual components such as PKP4 or ARHGAP23 resulted in milder phenotypes. These outcomes emphasize the presence of overlapping and cooperative regulatory layers. Understanding how these layers are coordinated remains a central challenge.

One promising direction is to dissect how armadillo proteins distribute within the heterogeneous landscape of the AJ. The preferential association of ARVCF with VE-cadherin pools that lack p120-catenin suggests the existence of molecularly distinct clusters. Future live imaging studies should further investigate the exchange kinetics between armadillo proteins and what environmental or chemical cues determine switching between AJ pools. Advanced microscopy approaches, including super-resolution imaging or single-molecule tracking, could determine whether ARVCF defines specialized nanoclusters with unique mechanical or signaling properties, and whether ARVCF is causal for VE-cadherin clustering or merely correlated with it. Mapping this organization would provide insight into how endothelial cells tune adhesion strength while maintaining plasticity.

Another future research direction is to resolve how junctional composition relates to local force generation. ARHGAP23 and PKP4 are likely to influence the amplitude and spatial confinement of RhoA activity. Combining optogenetic or FRET-based GTPase sensors with live imaging of VE-cadherin complexes could reveal how changes in contractility translate into specific adaptor recruitment. Such strategies would allow temporal ordering of events and define how signaling and mechanics reinforce one another during junction maturation, remodeling, or leukocyte passage.

The interaction between VE-cadherin and KEAP1 further raises questions regarding communication between junctions and cellular stress pathways. It will be important to determine under which physiological conditions this association is modified and whether oxidative or inflammatory challenges, which are linked to KEAP1's role in inflammation [11,12], alter its spatial distribution. Integrating redox reporters with junctional imaging may clarify how metabolic state and barrier stability are coupled.

Extending these analyses to *in vivo* systems represents an exciting step toward physiological relevance. Models such as zebrafish, where vascular development and leakage can be visualized in real time, provide opportunities to link molecular exchange within junctions to tissue-level outcomes. Approaches that combine intravital imaging with force or activity sensors could reveal how buffering mechanisms operate under hemodynamic stress. By resolving how VE-cadherin organizes mechanical, cytoskeletal, and stress-response pathways across scales, future studies may uncover strategies to selectively stabilize or loosen the endothelial barrier. Such knowledge could inform therapeutic approaches for inflammatory disease, edema, and tumor vascular dysfunction.

Concluding summary

Taken together, this thesis provides new insights into how VE-cadherin-based junctions safeguard endothelial cohesion through interconnected structural and mechanosignaling principles. **Chapters 2 and 3** explored the molecular diversity of the VE-cadherin interactome, identifying ARVCF, PKP4, ARHGAP23, and KEAP1 as context-dependent regulators that couple junctional organization to cytoskeletal control and cellular stress pathways. **Chapter 4** refined this molecular picture by demonstrating that the extracellular RGD motifs of VE-cadherin are structurally dispensable for barrier formation and leukocyte transmigration, underscoring that VE-cadherin's adhesive function relies primarily on cadherin homophilic binding rather than crosstalk with junctional integrins. **Chapter 5** translated molecular insights into a mechanical framework, showing that vinculin recruitment via α-catenin fortifies the endothelial barrier under physiological load. **Chapter 6** overviews more of such forces at the endothelial-leukocyte interface. Together, the lines of research spanning from molecular composition to multicellular- and tissue-scale mechanotransduction elucidate the versatility of VE-cadherin-based AJs.

References

1. Carnahan, R.H., Rokas, A., Gaucher, E.A., and Reynolds, A.B. (2010). The molecular evolution of the p120-catenin subfamily and its functional associations. PLoS One *5*, e15747. 10.1371/journal.pone.0015747.
2. Keirsebilck, A., Bonné, S., Staes, K., van Hengel, J., Nollet, F., Reynolds, A., and van Roy, F. (1998). Molecular cloning of the human p120ctn catenin gene (CTNND1): expression of multiple alternatively spliced isoforms. Genomics *50*, 129–146. 10.1006/geno.1998.5325.
3. Xiao, K., Garner, J., Buckley, K.M., Vincent, P.A., Chiasson, C.M., Dejana, E., Faundez, V., and Kowalczyk, A.P. (2005). p120-Catenin regulates clathrin-dependent endocytosis of VE-cadherin. Mol Biol Cell *16*, 5141–5151. 10.1091/mbc.e05-05-0440.
4. Chiasson, C.M., Wittich, K.B., Vincent, P.A., Faundez, V., and Kowalczyk, A.P. (2009). p120-catenin inhibits VE-cadherin internalization through a Rho-independent mechanism. Mol Biol Cell *20*, 1970–1980. 10.1091/mbc.e08-07-0735.
5. Müller, L., Keil, R., Glaß, M., and Hatzfeld, M. (2024). Plakophilin 4 controls the spatio-temporal activity of RhoA at adherens junctions to promote cortical actin ring formation and tissue tension. Cell Mol Life Sci *81*, 291. 10.1007/s00018-024-05329-6.
6. Garrett, J.P., Lowery, A.M., Adam, A.P., Kowalczyk, A.P., and Vincent, P.A. (2017). Regulation of endothelial barrier function by p120-catenin·VE-cadherin interaction. Mol Biol Cell *28*, 85–97. 10.1091/mbc.E16-08-0616.
7. Sirotkin, H., O'Donnell, H., DasGupta, R., Halford, S., St Jore, B., Puech, A., Parimoo, S., Morrow, B., Skoultchi, A., Weissman, S.M., et al. (1997). Identification of a new human catenin gene family member (ARVCF) from the region deleted in velo-cardio-facial syndrome. Genomics *41*, 75–83. 10.1006/geno.1997.4627.
8. Mariner, D.J., Wang, J., and Reynolds, A.B. (2000). ARVCF localizes to the nucleus and adherens junction and is mutually exclusive with p120(ctn) in E-cadherin complexes. J Cell Sci *113 (Pt 8)*, 1481–1490. 10.1242/jcs.113.8.1481.
9. Kourtidis, A., Ngok, S.P., and Anastasiadis, P.Z. (2013). p120 catenin: an essential regulator of cadherin stability, adhesion-induced signaling, and cancer progression. Prog Mol Biol Transl Sci *116*, 409–432. 10.1016/B978-0-12-394311-8.00018-2.
10. Fang, X., Ji, H., Kim, S.W., Park, J.I., Vaught, T.G., Anastasiadis, P.Z., Ciesiolka, M., and McCrea, P.D. (2004). Vertebrate development requires ARVCF and p120 catenins and their interplay with RhoA and Rac. J Cell Biol *165*, 87–98. 10.1083/jcb.200307109.
11. Saha, S., Buttari, B., Panieri, E., Profumo, E., and Saso, L. (2020). An Overview of Nrf2 Signaling Pathway and Its Role in Inflammation. Molecules *25*. 10.3390/molecules25225474.
12. Zhang, L., Xu, L.Y., Tang, F., Liu, D., Zhao, X.L., Zhang, J.N., Xia, J., Wu, J.J., Yang, Y., Peng, C., and Ao, H. (2024). New perspectives on the therapeutic potential of quercetin in non-communicable diseases: Targeting Nrf2 to counteract oxidative stress and inflammation. J Pharm Anal *14*, 100930. 10.1016/j.jpha.2023.12.020.
13. Weng, S., Huebner, R.J., and Wallingford, J.B. (2022). Convergent extension requires adhesion-dependent biomechanical integration of cell crawling and junction contraction. Cell Rep *39*, 110666. 10.1016/j.celrep.2022.110666.
14. Hayer, A., Shao, L., Chung, M., Joubert, L.M., Yang, H.W., Tsai, F.C., Bisaria, A., Betzig, E., and Meyer, T. (2016). Engulfed cadherin fingers are polarized junctional structures between collectively migrating endothelial cells. Nat Cell Biol *18*, 1311–1323. 10.1038/ncb3438.
15. Morris, O.M., Torpey, J.H., and Isaacson, R.L. (2021). Intrinsically disordered proteins: modes of binding with emphasis on disordered domains. Open Biol *11*, 210222. 10.1098/rsob.210222.
16. Chakrabarti, P., and Chakravarty, D. (2022). Intrinsically disordered proteins/regions and insight into their biomolecular interactions. Biophys Chem *283*, 106769. 10.1016/j.bpc.2022.106769.
17. Struhl, K. (2024). Intrinsically disordered regions (IDRs): A vague and confusing concept for protein function. Mol Cell *84*, 1186–1187. 10.1016/j.molcel.2024.02.023.
18. Huebner, R.J., Weng, S., Lee, C., Sarikaya, S., Papoulas, O., Cox, R.M., Marcotte, E.M., and Wallingford, J.B. (2022). ARVCF catenin controls force production during vertebrate convergent extension. Dev Cell *57*, 1119–1131 e1115. 10.1016/j.devcel.2022.04.001.
19. Kausalya, P.J., Phua, D.C., and Hunziker, W. (2004). Association of ARVCF with zonula occludens (ZO)-1 and ZO-2: binding to PDZ-domain proteins and cell-cell adhesion regulate plasma membrane and nuclear localization of ARVCF. Mol Biol Cell *15*, 5503–5515. 10.1091/mbc.e04-04-0350.
20. Huveneers, S., Oldenburg, J., Spanjaard, E., van der Krogt, G., Grigoriev, I., Akhmanova, A., Rehmann, H., and de Rooij, J. (2012). Vinculin associates with endothelial VE-cadherin junctions to control force-dependent remodeling. J Cell Biol *196*, 641–652. 10.1083/jcb.201108120.
21. Benelli, R., Mortarini, R., Anichini, A., Giunciuglio, D., Noonan, D.M., Montalti, S., Tacchetti, C., and Albini, A. (1998). Monocyte-derived dendritic cells and monocytes migrate to HIV-Tat RGD and basic peptides. Aids *12*, 261–268. 10.1097/00002030-199803000-00003.



Appendices

English summary
Nederlandse lekenintroductie en inhoud
Nederlandse samenvatting
List of publications
PhD portfolio
Curriculum vitae
Closing credits

English summary

Adherens junctions (AJs) are dynamic structures that bridge neighboring endothelial cells (ECs) in the vessel wall that must simultaneously preserve tissue integrity and permit the controlled passage of fluid and immune cells. The central adhesion receptor of AJs is vascular endothelial (VE)-cadherin, a transmembrane protein that mediates homophilic adhesion between neighboring ECs and anchors a cytoplasmic protein network to the actin cytoskeleton. Although the molecular composition of this AJ complex has been extensively studied, the full range of VE-cadherin-associated AJ signaling remains incompletely understood. This thesis set out to investigate the composition and functional organization of VE-cadherin complexes and define how intracellular protein organization contributes to AJ stabilization, signaling, and mechanotransduction, to control vascular integrity.

The canonical endothelial AJ complex consists of three main proteins: p120- and β-catenin bind directly to VE-cadherin and function, respectively, to ensure VE-cadherin membrane localization and to connect to α-catenin, which in turn links the AJ structure to the actin cytoskeleton. VE-cadherin's cytoplasmic region contains three key tyrosine residues that are subject to phosphorylation and modulate interactions with catenins and downstream effectors. To further define the VE-cadherin interactome, we employed a proteomics strategy in ECs expressing GFP-tagged VE-cadherin or non-phosphorylatable variants in which tyrosines 658, 685, and 731 were substituted by phenylalanine. Mass-spectrometry on VE-cadherin pull-downs identified 37 interacting proteins, among which a core interactome of 9 proteins was consistently detected regardless of tyrosine phosphorylation. This group included established partners such as α -, β-, p120-catenin, validating our approach, but several previously unreported VE-cadherin-associated proteins were identified, including ARVCF, ARHGAP23, KEAP1, and NGLY1. These findings defined a phosphorylation-resilient VE-cadherin interaction network that formed the basis for functional characterization.

Among the novel interactors, ARVCF emerged as a prominent binding partner. ARVCF, a member of the catenin family structurally related to p120-catenin, associates with the VE-cadherin juxtamembrane domain but engages in a distinct junctional pool that is unbound from p120-catenin. ARVCF localization to AJs is VE-cadherin-dependent and their colocalization is enhanced in mature, confluent monolayers, consistent with a role in junction maturation. Although ARVCF depletion did not alter surface levels of VE-cadherin, it disrupted AJ organization, increased intercellular gap formation, reduced barrier resistance, and impaired coordinated cell migration. Live imaging demonstrated unstable junction dynamics in the absence of ARVCF, whereas treatment with an EPAC1 agonist that tightens the endothelial barrier through Rap1-mediated junctional reinforcement restored barrier integrity, supporting a role for ARVCF in tension-dependent AJ stabilization. Together, these findings identify ARVCF as a maturation-associated stabilizer of the VE-cadherin complex.

Our proteomic dataset further identified ARHGAP23, KEAP1, and PKP4 as VE-cadherin-associated proteins. These partners extend AJ function beyond structural adhesion: ARHGAP23 links VE-cadherin complexes to RhoGTPase signaling, connecting adhesion to cytoskeletal dynamics, KEAP1 introduces a potential interface between cell-cell contacts and redox signaling, and PKP4 contributes to junctional scaffolding and cytoskeletal organization important for cell-matrix adhesions. The identification and characterization of these partners show that VE-cadherin integrates mechanical, cytoskeletal, and stress-responsive pathways, expanding the available network to enable dynamic and precise AJ adaptation from vascular homeostasis to remodeling and inflammation.

This thesis also examined the functional relevance of two extracellular RGD motifs in VE-cadherin. Although RGD sequences are typically associated with integrin binding, our ECs in which we replaced endogenous VE-cadherin with variants in which the RGD motifs were mutated to nonfunctional RGE sequences showed that these motifs are dispensable for junction formation, barrier integrity, and monocyte transmigration, with VE-cadherin localization and function preserved. These findings refine the understanding of VE-cadherin adhesion and the specific recruitment of leukocytes, indicating that these processes do not rely on the extracellular RGD domain.

Mechanical AJ reinforcement was further investigated *in vivo* through the role of vinculin, a force-sensitive adaptor recruited to α-catenin. In vinculin-knockout zebrafish, the endothelial cells still generated functionally perfused blood vessels, which surprisingly were more permeable for small dextran molecules, whereas large dextran did not extravasate. These findings demonstrate physiological relevance for AJ-associated proteins and underscore the importance of intracellular force transmission for maintaining barrier function.

Lastly, the specific biomechanical forces were overviewed for the T-cell-endothelial interface, outlining how shear stress and forces with a dragging, twisting, or peeling direction shape reciprocal signaling during leukocyte transmigration through the vessel wall. Integrating endothelial mechanosensitive pathways with T-cell force responsiveness, immune synapse formation, and force-dependent activation, a biomechanical framework is provided for understanding how inflammation and vascular function intersect at sites of leukocyte recruitment.

Altogether, by linking molecular architecture to biomechanical performance, this thesis bridges fundamental cell biological mechanisms with physiological outcomes at the level of vascular stability and permeability.

Nederlandse introductie voor leken

Het vaatstelsel reikt overal in je lichaam

Het bloedvatenstelsel is een belangrijk transportsysteem dat elk lichaamsdeel, orgaan, en weefsel bereikt van gewervelde dieren. Het bestaat uit een goed verbonden netwerk van bloedvaten: grote slagaders brengen bloed rijk aan zuurstof en voedingsstoffen naar de organen, waar kleine haarvaten de lading naar de verschillende weefselcellen transporteren en afvalstoffen verzamelen, waarna het bloed vervolgens via aderen wordt teruggevoerd naar het hart om de bloedsomloop te voltooien. Deze continue stroom zorgt ervoor dat alle weefsels ontvangen wat ze nodig hebben en dat afvalstoffen efficiënt worden afgevoerd. Naast deze transportfunctie speelt het vaatstelsel een cruciale rol in het immuunsysteem, tijdens de ontwikkeling van weefsels en organen, en bij het behouden van weefselhomeostase (evenwicht van het inwendig milieu en alle celprocessen).

Bloedvaten zijn binnenin bekleed met endotheel

De binnenkant van elk vat in de bloedsomloop is bekleed met endotheel: een dunne, enkele laag endotheelcellen die in direct contact staan met het bloed en dit scheiden van het omringende weefsel. Deze cellulaire bekleding wordt de endotheelmonolaag genoemd en is opmerkelijk dynamisch: niet slechts een passieve, fysieke barrière, maar een actieve regelaar van wat er de bloedbaan in- en uitgaat. Als poortwachters beheren de endotheelcellen actief de uitwisseling tussen bloed en weefsel van immuuncellen, van moleculen zoals zuurstof, en van opgeloste stoffen zoals glucose. Daarom zijn de verbindingen tussen endotheelcellen – de cel-celcontacten – een fascinerende plek waar vorm en functie stabiel edoch flexibel gecoördineerd moeten worden. Wanneer deze contacten niet goed functioneren, kunnen problemen voorkomen zoals oedeem (vochtophoping wanneer vloeistoffen uit de bloedbaan in andere weefsels lekken, vaak leidend tot gezwollen benen en voeten), of chronische ontsteking (wanneer het lichaam immuuncellen blijft sturen om een infectie op te lossen die er niet is, wat kan leiden tot pijn en vermoeidheid).

VE-cadherin vormt de cel-celbrug

De structurele verbindingen tussen endotheelcellen worden voornamelijk gevormd door een familie van calciumafhankelijke adhesiemoleculen genaamd cadherins. Endotheelcellen produceren verschillende types van deze cadherins, waarvan vasculaire endotheliale cadherin (VE-cadherin), zoals de naam al doet vermoeden, de meest karakteristieke en specifieke is. VE-cadherin is een transmembraan eiwit, wat betekent dat het uit de endotheelcellen naar buiten steekt. Twee VE-cadherinmoleculen op aangrenzende cellen koppelen hun ‘hoofdjes’ in de ruimte tussen de cellen, terwijl hun staarten binnenin de cel aan het celskelet worden gekoppeld. Deze staart kan ook aan andere eiwitten binden en zo deelnemen aan allerlei signaleringsprocessen in de cel. Simpel gezegd

vormt VE-cadherin dus de moleculaire brug tussen endotheelcellen die signalen tussen buiten en binnen overbrengt zodat cellen zich kunnen aanpassen aan hun omgeving.

VE-cadherin als centraal signaalknooppunt

VE-cadherin speelt een sleutelrol in een breed scala aan endotheelfuncties. Het helpt de integriteit van de vaatwandbarrière te behouden in verschillende soorten bloedvaten, waar de lokale mechanische omgevingen sterk kunnen verschillen (stel je voor dat cellen in de aortawand meer bloeddruk van je hart ervaren, dan de cellen in een distaal adertje in je voet). VE-cadherinbruggen (ook wel adherens juncties genoemd, vaak afgekort tot AJ) moeten ook veranderen wanneer de vaatwand reageert op ontstekingssignalen, zodat immuuncellen die uit de bloedbaan worden gerekruteerd door het endotheel kunnen passeren en het aangetaste weefsel kunnen bereiken. Daarnaast ondersteunt VE-cadherin de groei en hervorming van bloedvaten tijdens de ontwikkeling, maar ook in een volwassen lichaam, zowel in gezondheid als in ziekte. In al deze situaties moet VE-cadherin strikt worden gereguleerd, waarbij adhesie (het hechten van eiwitten en cellen) wordt aan- of uitgezet om cel-celcontacten te versterken of te versoepelen. Dit wisselen wordt geregeld door specifieke moleculaire partners te rekruteren wanneer nodig. De afgelopen jaren is er uitgebreid onderzoek gedaan naar de eiwitten die VE-cadherin zelf reguleren, evenals naar de eiwitten die worden aangetrokken naar de plek waar endotheelcellen via VE-cadherin met elkaar in contact staan. De wetenschappelijke methoden voor biochemische analyse en beeldvormingstechnieken geven een steeds beter beeld van waar en wanneer de cellulaire processen gebeuren. Toch weten we nog steeds niet precies welke eiwitten allemaal betrokken zijn bij de verbindingen rond VE-cadherin. Vooral hoe deze verbindingen zich aanpassen aan veranderingen, zoals mechanische krachten op de bloedvatwandcellen of aan de signalen die tijdens de ontwikkeling of tijdens afweerreacties worden gestuurd, wordt nog volop onderzocht.

Opzet en inhoud van dit proefschrift

De onvolledigheid van kennis over welke eiwitten VE-cadherin precies reguleren, vormde de aanleiding voor het onderzoek in dit proefschrift. In dit promotieproject onderzochten we met welke eiwitten VE-cadherin samenwerkt en wat deze interacties betekenen voor de werking van bloedvaten. Onze hypothese was dat VE-cadherin specifieke eiwitpartners heeft en dat deze interacties afhankelijk van de biologische context kunnen veranderen. Met een combinatie van biochemische experimenten, mechanobiologisch onderzoek (naar fysieke krachten), en beeldvorming met hoge ruimtelijke en tijdsresolutie identificeerden we nieuwe bindingspartners ARVCF, KEAP1, ARHGAP23, en NGLY1. Van een aantal eiwitten karakteriseerden we de invloed op VE-cadherin en de AJ. Daarnaast onderzochten we of VE-cadherin mogelijk aan immuuncellen hecht en bestudeerden we de rol van een eiwit dat VE-cadherin stabiliseert bij de vorming van nieuwe bloedvaten tijdens de ontwikkeling. Dit proefschrift presenteert nieuwe inzichten die helpen om beter te begrijpen hoe verbindingen tussen endotheelcellen worden aangestuurd tijdens processen zoals bloedvatvorming, immuuncelmigratie, en mechanotransductie.

Hoofdstuk 1 gaf een algemeen overzicht van het vaatstelsel, waarbij VE-cadherin werd geïntroduceerd als een moleculaire brug die de hechting tussen endotheelcellen in de vaatwand bemiddelt. Ook werd een overzicht gegeven van de moleculaire organisatie van het AJ-complex en de mechanismen die het reguleren in context van vasculaire integriteit. Hiermee legt dit hoofdstuk de basis om VE-cadherin te begrijpen als signaalknooppunt bij endotheelverbindingen, zodat we een context hebben voor de nieuwe interacterende eiwitten die in de volgende experimentele hoofdstukken worden onderzocht.

Hoofdstuk 2 presenteert de experimentele ontdekking en karakterisering van nieuwe VE-cadherin-bindende eiwitten. We gebruikten proteomics om een kern-VE-cadherin-interactienetwerk te definiëren dat verschillende bekende celcontactcomponenten bevat (zoals worden geïntroduceerd in de Engelse specialistenintroductie), maar bovendien presenteren we vier nieuwe bindingspartners: ARVCF, KEAP1, ARHGAP23 en NGLY1. Eén van deze eiwitten, ARVCF, wordt in dit hoofdstuk verder bestudeerd: we laten zien hoe ARVCF specifiek bindt aan een bepaalde groep VE-cadherin-eiwitten, en welke rol het speelt bij de ‘rijping’ van celverbindingen, de stabiliteit van de endotheelbarrière, en de gezamenlijke verplaatsing van cellen. Deze resultaten voegen een nieuwe regulatielaag toe aan ons begrip van het VE-cadherin-complex.

Hoofdstuk 3 gaat verder met de analyse van de nieuw ontdekte VE-cadherin-bindende eiwitten: we duiken dieper in de regulatie van VE-cadherin door de rol van ARHGAP23, PKP4, en KEAP1 voor endotheelcellen te onderzoeken. Hoewel deze eiwitten zich minder goed tot in detail lieten bestuderen, toonden de experimenten aan dat ze wel degelijk bijdragen aan de stabiliteit en

organisatie van VE-cadherin-gebaseerde cel-celcontacten. Samen met hoofdstuk 2 geven deze resultaten een breder beeld van het eiwitnetwerk dat betrokken is bij het VE-cadherin-complex.

Hoofdstuk 4 verlegt de aandacht van eiwitten die binnen de cel VE-cadherin binden naar het extracellulaire domein. Dit deel va het eiwit dat buiten het celmembraan uitsteekt, bevat twee zogenoemde RGD-motieven: korte sequenties die bekendstaan als bindingsplaatsen voor integrines (een ander type celhechtingsmoleculen dan VE-cadherin). Tot nu toe waren deze RGD-motieven nog nooit onderzocht op het VE-cadherin molecuul. In onze experimenten hebben we niet-functionele varianten van deze motieven gemaakt om te testen of ze nodig zijn voor verbindingen tussen cellen, barrière-integriteit, en het passeren van afweercellen door de vaatwand. We ontdekten echter dat deze motieven voor géén van deze belangrijke processen nodig zijn. Daarmee sluiten we een open vraag en kunnen toekomstige studies zich richten op de functioneel relevante delen van VE-cadherin.

Hoofdstuk 5 gaat verder in op de rol van krachtgevoelige eiwitten bij het in stand houden van een goed werkend bloedvatenstelsel. We onderzoeken hier het eiwit vinculin, dat niet direct aan VE-cadherin bindt, maar wel wordt aangetrokken naar celverbindingen wanneer hierop mechanische spanning staat. Met behulp van zowel celkweek als een zebravismodel laten we zien dat vinculin helpt om stabiele verbindingen tussen endotheelcellen te behouden en lekkage te voorkomen tijdens de vorming van nieuwe vaten. Deze resultaten benadrukken het belang van mechanische versterking bij celcontacten en voegen een ontwikkelingsperspectief toe aan de regulatie van de endotheelbarrièrefunctie.

Hoofdstuk 6 zoomt uit en biedt een breder perspectief op de mechanische regulatie van endotheelverbindingen. Hier wordt verder verkend hoe endotheelcellen reageren op mechanische prikkels tijdens ontsteking, vooral in interactie met afweercellen. We presenteren kwantitatieve gegevens over hoe endotheel- en T-cellen kracht op elkaar uitoefenen tijdens de reis van immuuncellen vanuit het bloed, door de cel-celcontacten, naar het weefsel, en hoe de eiwitten die deze krachten waarnemen en doorgeven dit proces vormgeven. Door huidige concepten en moleculaire spelers te onderzoeken, biedt dit hoofdstuk een geïntegreerd beeld van de dynamische mechanische interactie tussen immuuncellen en de vaatwand.

Hoofdstuk 7 vat de belangrijkste bevindingen van dit proefschrift samen en plaatst ze terug in de bredere context van het vakgebied. Ook komen in dit hoofdstuk de nieuwe vragen en ideeën aan bod die uit ons onderzoek zijn voortgekomen. Kortom: dit proefschrift heeft veel nieuwe kennis opgeleverd, maar er blijven genoeg spannende richtingen over om verder te verkennen, te onderzoeken en over te discussiëren.

Nederlandse Samenvatting

De adherens junctions (AJ) is een dynamische structuur die aangrenzende endotheelcellen (EC's) in de vaatwand met elkaar verbindt. AJ's moeten tegelijkertijd de weefselintegriteit waarborgen en de gecontroleerde doorgang van vocht en immuuncellen mogelijk maken. De centrale adhesiereceptor van AJ's is vasculaire endotheliale cadherin (VE-cadherin), een transmembraan eiwit dat homofiele adhesie tussen naburige EC's medieert en een cytoplasmatisch eiwitnetwerk verankert aan het actine cytoskelet. Hoewel de moleculaire samenstelling van dit AJ-complex uitgebreid is bestudeerd, is het volledige spectrum aan VE-cadherin-geassocieerde signaalprocessen nog niet volledig opgehelderd. Dit proefschrift beoogde de samenstelling en functionele organisatie van VE-cadherincomplexen te onderzoeken en te definiëren hoe de intracellulaire organisatie van eiwitten bijdraagt aan AJ-stabilisatie, signalering en mechanotransductie, teneinde de vasculaire integriteit te reguleren.

Het standaard endotheliale AJ-complex bestaat uit drie hoofdeiwitten: p120- en β-catenine binden direct aan VE-cadherin en zorgen respectievelijk voor VE-cadherin's membraanlocalisatie en voor de koppeling aan α-catenine, dat op zijn beurt de AJ-structuur verbindt met het actine cytoskelet. VE-cadherin's cytoplasmatische deel bevat drie relevante tyrosineresiduen die gefosforyleerd kunnen worden en zo interacties met catenines en effectoren verderop moduleren. Om het VE-cadherin-interactoom verder in kaart te brengen, volgden wij een proteomicsstrategie in EC's die GFP-gelabeld VE-cadherin tot expressie brachten of niet-fosforyleerbare varianten waarin tyrosines 658, 685 en 731 waren vervangen door fenylalanine. Massaspectrometrie van VE-cadherin pull-downs identificeerde 37 interacterende eiwitten, waaronder een kerninteractoom van 9 eiwitten dat consistent werd aangetroffen, onafhankelijk van tyrosinefosforylatie. Deze groep omvatte bekende partners zoals α-, β- en p120-catenin, wat onze aanpak valideerde, maar ook verschillende niet eerder beschreven VE-cadherin-geassocieerde eiwitten, waaronder ARVCF, ARHGAP23, KEAP1 en NGLY1. Deze bevindingen definieerden een forsforylatie-onafhankelijk VE-cadherin-interactienetwerk dat de basis vormde voor verdere functionele karakterisering.

Onder de nieuw geïdentificeerde interactoren kwam ARVCF naar voren als een prominente bindingspartner. ARVCF, een lid van de cateninefamilie dat structureel verwant is aan p120-catenin, associeert met het juxtamembraandomein van VE-cadherin, maar bevindt zich in een afzonderlijke junctionele subgroep die niet gebonden is aan p120-catenine. Lokalisatie van ARVCF naar AJ's is afhankelijk van VE-cadherin, en hun colocalisatie neemt toe in stabiele, confluente monolagen, passend bij een rol in junctionele maturatie. Hoewel depletie van ARVCF de membraan-expressie van VE-cadherin niet veranderde, verstoorde dit de organisatie van AJ's, leidde tot meer

intercellulaire spleetvorming, verminderde de barrièreresistentie en belemmerde gecoördineerde celmigratie. Microscopie van levende cellen toonde instabiele junctionele dynamiek in afwezigheid van ARVCF, terwijl behandeling met een EPAC1-agonist, die via Rap1-gemedieerde junctionele versterking de endotheelbarrière verstevigt, de barrière-integriteit herstelde. Deze resultaten suggereren een rol voor ARVCF in spanningsafhankelijke stabilisatie van AJ's. Gezamenlijk identificeren deze bevindingen ARVCF als een met maturatie geassocieerde stabilisator van het VE-cadherincomplex.

Onze proteomicsdataset identificeerde daarnaast ARHGAP23, KEAP1 en PKP4 als VE-cadherin-geassocieerde eiwitten. Deze partners breiden de functie van AJ's uit voorbij structurele adhesie: ARHGAP23 koppelt VE-cadherin complexen aan RhoGTPase-signalering en verbindt zo adhesie met cytoskeletdynamiek; KEAP1 introduceert een potentiële koppeling tussen cel-celcontacten en redoxsignalering; en PKP4 draagt bij aan junctionele- en cytoskeletorganisatie met belang voor cel-matrixadhesies. De identificatie en karakterisering van deze partners tonen aan dat VE-cadherin mechanische, cytoskeletale, en stress-responsieve routes integreert. Daarmee wordt het beschikbare netwerk uitgebreid en kunnen AJ's zich dynamisch en nauwkeurig aanpassen, variërend van vasculaire homeostase tot structurele veranderingen en inflammatie.

In dit proefschrift werd tevens de functionele relevantie onderzocht van twee extracellulaire RGD-motieven in VE-cadherin. Hoewel RGD-sequenties doorgaans geassocieerd worden met integrinebinding, toonden onze EC's, waarin endogeen VE-cadherin was vervangen door varianten met gemuteerde RGD-motieven (omgezet naar niet-functionele RGE-sequenties), aan dat deze motieven niet essentieel zijn voor AJ vorming, barrière-integriteit, of transmigratie van monocyten. Lokalisatie en functie van VE-cadherin bleven behouden. Deze bevindingen verfijnen het inzicht in VE-cadherin-gemedieerde adhesie en de specifieke rekrutering van leukocyten, en geven aan dat deze processen niet afhankelijk zijn van het extracellulaire RGD-domein.

Mechanische versterking van AJ's werd verder *in vivo* onderzocht door de rol van vinculin, een krachtgevoelige adaptor, die wordt gerekruteerd naar α-catenin. In vinculin-knockout zebravissen vormden endotheelcellen nog steeds functionele bloedvaten, die echter verrassend permeabeler waren voor kleine dextraanmoleculen, terwijl grote dextranen niet extravaseerden. Deze bevindingen tonen de fysiologische relevantie van AJ-geassocieerde eiwitten en onderstrepen het belang van een juiste krachtoverdracht tussen endotheelcellen voor een goede barrièrefunctie.

Ten slotte werden de specifieke biomechanische krachten op raakvlak tussen het endotheel en T-cellen besproken. Tijdens leukocyttransmigratie door de vaatwand zijn er frictie van het

langsstromende bloed en krachten die de leukocyt van de vaatwand af kunnen rollen, die tezamen wederzijdse signalering vormgeven. Door endotheliale mechanosensitieve routes te integreren met de krachtresponsiviteit van T-cellen, immuunsynapsvorming, en krachtafhankelijke activatie, wordt een biomechanisch raamwerk gegeven om te begrijpen hoe inflammatie en vasculaire functie samenkomen op plaatsen van leukocytenrekrutering.

Alles bij elkaar genomen, door moleculaire architectuur en aan biomechanische uitkomsten te linken, slaat dit proefschrift de brug tussen fundamentele celbiologische mechanismen naar fysiologische uitkomsten op het niveau van vasculaire stabiliteit en permeabiliteit.

List of publications

This thesis

Schoon RM, van Krimpen-Malinova TS, de Heer I, Hoogendijk AJ, van Alphen FPJ, de Haan A, van Stalborch AD, Tol S, van Buul JD, van den Biggelaar M, Huveneers S. VE-cadherin interaction proteomics identifies ARVCF as stabilizer of endothelial adherens junctions. iScience. 2026 Mar 21;29(4):115450. doi:10.1016/j.isci.2026.115450. eCollection 2026 Apr 17. PMID: 42006337; PMCID: PMC13089046.

Schoon RM *, van der Meer WJ *, van Stalborch AD, van Buul JD, Huveneers S. VE-cadherin RGD motifs are dispensable for cell-cell junctions, endothelial barrier function and monocyte extravasation. Tissue Barriers. 2025;13(4):2478349. doi: 10.1080/21688370.2025.2478349. Epub 2025 Mar 18. PMID: 40099517; PMCID: PMC12667659.

van der Stoel MM *, Kotini MP *, **Schoon RM**, Affolter M, Belting HG, Huveneers S. Vinculin strengthens the endothelial barrier during vascular development. Vasc Biol. 2023 Jan 27;5(1):e220012. doi: 10.1530/VB-22-0012. PMID: 36260739; PMCID: PMC9986378.

Other publications

Rubio-Beltrán E, **Schoon RM**, van den Berg J, Schuiling-Veninga CCM, Koch BCP, Villalón CM, Versmissen J, Danser AHJ, van den Meiracker AH, Ibrahimi K, MaassenVanDenBrink A. Trigeminovascular effects of propranolol in men and women, role for sex steroids. Ann Clin Transl Neurol. 2022 Sep;9(9):1405-1416. doi: 10.1002/acn3.51640. Epub 2022 Aug 27. PMID: 36029132; PMCID: PMC9463958.

van der Meer WJ, van Steen ACI, Mahlandt E, Rolas L, Wang H, Arts JJG, Kempers L, Grönloh MLB, **Schoon RM**, Driessen A, van Rijssel J, Klaassen I, Schlingemann RO, Manavski Y, Hoogenboezem M, Boon RA, Khuon S, Wait E, Heddleston J, Chew TL, Nolte MA, Nourshargh S, Goedhart J, van Buul JD. Leukocytes use endothelial membrane tunnels to extravasate the vasculature. Cell Rep. 2025 Sep 23;44(9):116242. doi: 10.1016/j.celrep.2025.116242. Epub 2025 Sep 4. PMID: 40913770.

PhD portfolio

Courses	Year	ECTS
Amsterdam UMC World of Science	2020	0.5
e-learnings Basic laboratory safety (yearly)	2020-2024	0.5
e-learnings Privacy rules (AVG)	2022	0.2
e-learnings Fire	2022	0.3
Confocal live imaging training	2021	0.5
Techniques: FRET, FLIM, LSS		
Machines: Leica SP5/8/Thunder/Falcon/Stellaris8; Zeis DLS/Airyscan		
Wide-field live imaging training	2021	0.2
Nikon Eclipse TI with FRET and TIRF options		
Electron microscopy traning (cryo-sectioning, SEM, TEM, CLEM)	2021	0.3
Advanced microscopy course - AUMC facility	2021	1.0
Research data management additional module data processing, AUMC	2021	0.2
Research data management online course, AUMC	2021	0.3
Cytoflex training	2021	0.2
FACS training	2022	0.3
	Total:	**4.5**

Scientific collaboration meetings	Year	ECTS
Weekly Medical Biochemistry department meeting	2020-2024	5.0
Weekly Huveneers group meeting AMC	2020-2024	6.0
Bi-weekly Vascular Biology Lab meeting AMC	2020-2024	2.0
Bi-weekly Medical Biochemistry journal club	2020-2024	2.5
Bi-weekly European Vascular Biology Seminar (+technical support)	2020-2024	1.5
Monthly Huveneers group journal club	2020-2024	1.5
Monthly Rembrandt work discussion	2020-2024	2.0
Monthly ACS symposium	2020-2024	1.0
	Total:	**21.5**

Other meetings	Year	ECTS
PhD representative Medical Biochemistry Department	2022-2044	0.6
Medical Biochemistry Green Team	2022-2024	0.4
	Total	**2**

Conferences	Year	ECTS
Rembrandt Annual symposia (10^{th}, 11^{th}, 12^{th}, 13^{th}, 14^{th})	2020-2024	2.5
Rembrandt Laureates symposium	2023	0.5
EVBO/ESM Vascular Biology summer school	2021	1.0
Meeting Gesellschaft für Mikrozirkulation und Vaskuläre Biologie	2021	1.0
International Vascular Biology Meeting (San Francisco, Amsterdam)	2022, 2024	3.0
Netherlands Vascular Biology Organization (NeVBO) Biezenmortel	2022	1.0
ACS Annual symposia	2022-2024	1.0
ACS PhD retreat	2022, 2023	2.0
North American Vascular Biology Organization seminars	2023	0.5
	Total	**13**

Supervision	Year	ECTS
Master internship E. Kinloch (8 months)	2022	1.5
Master internship M. Heijmans (9 months)	2023	2.0
Bachelor internship S. Poppen (3 months)	2023	0.5
Master internship M. Smit (9 months)	2024	2.0
	Total	**6.0**

Honors and awards	Year
NaVBO InFocus - selected abstract invited speaker	2023
Amsterdam Cardiovascular Sciences - best talk	2022
International Vascular Biology Organisation - plenary talk	2024

International collaboration	Year
EMBL Heidelberg Advanced Imaging Center - EuroBioImaging	2024

Curriculum Vitae

Research experience

PhD candidate 2020 – 2025
Lab of S. Huveneers, PhD
Dept. Medical Biochemistry
Amsterdam University Medical Center,
Faculteit der Geneeskunde
University of Amsterdam

Research intern 2019 – 2020
Lab of prof. J.D. van Buul
Dept. Molecular cell biology
Sanquin research Amsterdam

Research intern 2018 - 2019
Lab of prof. R. van Amerongen
Dept. Developmental, Stem Cell and Cancer Biology
Swammerdam Institute of Life Sciences Amsterdam

Research intern 2017 – 2017
Lab of prof. A. Maassen-van den Brink
Dept. Internal Medicine – Pharmacology and Vascular Disease
Erasmus Medical Center Rotterdam

Education

MSc. Cell Biology and Advanced Microscopy 2018 – 2020
University of Amsterdam

BSc. Neurobiology 2014 – 2017
University of Amsterdam
Minor: Programming and Data Processing, Harvard University 2017 – 2018
Year 1: double BSc. Psychologie, University of Amsterdam 2014 – 2015

Closing credits

The work in this thesis would not be possible without the support of a lot of people. I would like to express my gratitude to all of you.

Firstly, I want to thank my promotor dr. **Stephan Huveneers**. Within the department and throughout changes of the cast, your lab has been a close-knit, inspiring, and safe home-base for me. Your door was always open and you aimed to cultivate an atmosphere where scientific ideas can be coined and discussed critically yet safely. Thank you for celebrating with me when the microscopy was just beautiful, I could run to your office or text an image and you would share my amazement at the cells. Thank you for your patience, guidance, and involvement at every step of the way towards the final result of this book.

Secondly, I want to thank my co-promotor prof. dr. **Jaap van Buul** for originally taking me on as a master student at Sanquin and for later introducing me to Stephan. Your enthusiasm about microscopy imaging of transmigration has inspired me greatly and I am happy we got to publish the tunnels and the RGD story together.

I want to sincerely thank the members of my PhD committee for taking the time to read, assess, and discuss this thesis: prof. dr. **Carlie de Vries**, prof dr. **Ed van Bavel**, dr. **Jeffrey Kroon**, prof. dr. **Paul Quax**, and dr. ing. **Charissa van den Brom**. It will be a privilege to discuss this work with you at the defense. Special thanks to Carlie: as the head of the Medical Biochemistry department, you take notice of everyone; I appreciated your regular check-ins when I was alone in the office. Special thanks as well to Paul, for the collaborative and inspiring Rembrandt meetings together with **Thijs** and **Margreet**.

Now, a lot of thanks to my paranymphs: dr. **Vera Janssen** and dr. **Werner van der Meer**. Both of you have been such key parts of my daily life at the AMC.

Vera, we started in Stephans group just weeks apart, sat within five meters of each other both in the office and in the lab, and *also* chose to spend parties, festivals, and holidays together. I still mean what I first said in the Marktkantine <3. Thank you for being my friend, and for being a social initiator and glue - because of you I have met so many people and done so many activities - I am really proud of you for the scientist and person that you are.

Werner, both at Sanquin and at the AMC our morning coffee rituals were the best part of my day, where we would talk about nothing and laugh about everything (or vice versa?). Thank you for the California road trip, for the parties, for taking my call in the middle of the night about a bench, for the only thing filtered about you being your coffee, and for being my friend, despite (~~because of?~~) the RGD story we did together. I am proud of you, doctor!

I want to thank the past and current staff of the Medical Biochemistry department for all the help and gezelligheid over the years. The PIs **Vivian**, **Carlie**, **Menno**, **Marten**, **Annette**, **Koen**, **Noam**, **Dave**; and the analysts **Annett**, **Iris**, **Anne-Marieke**, **Inge**, **Claudia**, **Cindy**, **Jenina**, **Roelof**, **Marlene**: thank you all for brainstorming, critical questions, and practical input. Special thanks to Marten for bouldering; to Annett for lab support and chats since my start; to Iris for joining the ARVCF story; and to Anne-Marieke for cloning and organization.

The past and current members of lab Huveneers: **Tsveta**, thank you for the ARVCF story (these thanks extend to **Maartje**, **Floris**, **Arjan**, **Simon**). **Miesje**, for answering many questions when I started. **Ana** for encouragement. **Vanessa**, for the KEAP1 story. **Aukie**, thank you for so much: bouldering, coffee, chats during endless cell-culturing, road tripping, partying, rooting, for being my friend, and for introducing me to more of your climbing friends like **Floris**. **Johanna**, thank you for your energy. **Tong**, for being an excellent and friendly addition to the lab. **Anouk**, for working together during my last months at the AMC. Thanks to **Emma**, **Sytske**, **Matthijs**, **Marisa**, and **Fenne** for being eager and fast-learning students. **Lilian**, **Sekar**, **Dimitris**, **Hannah**: good luck to you as the next cohort!

The past and current members of lab Van Buul: **Bram**, **Lanette**, **Sofia**, **Merel**, **Jeffrey**, **Marianthi**, **Natalia**, **Marije**, **Andreas**, **Anouk**. Special thanks to **Eike**: we met at SILS and you introduced me to Jaap for an internship, effectively starting off the academic cascade leading to this thesis - thank you! And special thanks to **Max**, you make science look so natural and easy; thank you for the daily morning coffees, for the road trip, for rooting, for the screaming, for your honesty, and for being my friend.

Thanks to all past and current MBIOC members for the scientific input, drinks, outings, and activities: **Myrthe**; **Laura**; **Winnie** for facsing, camping, bouldering, introducing me to the Sterk gang, and for coffee + chatting also with **Bram** and **Ricky**. **Bea** thanks for everything; **Carmen** for chats and friendship. **Sanne** for climbing together. **Lobke**; **Guillermo** for the dancing at wees jezelf. **Oliver** for friendship, climbing, abs, and your endless science motivation. **Rosalie** for PhD retreats. **Alexandra**; **Femke**; **Mees**; **Maartje**; **Josje**; **Amber**; **Andrej**; **Jayron**; **Suzanne**; **Kristina**; **Ilaria**; **Claudia**; **Karen**; **Panos**; **Thirza**. **Klevis** for bike talk, kudos, friendship. **Sebastian** for friendship, concerts, honest talks, and bouldering.

I want to thank the Amsterdam United Mob of Climbers for the weekly destressment sessions and for the gains: **Sebastian**, **Marten**, **Oliver**, **Aukie**, **Floris**, **Eike**, **Winnie**, *et al.*

Almost done: much love to friends and family: **Tegan**, for your friendship and support since the first day at uni. **Steven**, for supports and sports since the bachelor. **Bas** & **Mieke**, heerlijke auties. **Tanne**, for career guidance. **Victor**, for being my windshield. Dikke knuffels voor **Rineke**, **Martin**, **Eric**, **Jeroen**, **Lisa**, **Gerrit**, **Lia**. En nu zet ik er echt een punt achter.

